

**U.S. Department of Commerce  
National Technical Information Service**



**N74 75522**

**LONGITUDINAL AND LATERAL STABILITY AND  
CONTROL CHARACTERISTICS OF A LARGE-SCALE  
MODEL WITH A SWEPT WING AND AUGMENTED  
JET FLAP**

**U.S. ARMY AIR MOBILITY R&D LABORATORY  
MOFFETT FIELD, CA**

**APR 72**

**NASA TECHNICAL  
MEMORANDUM**

**NASA TM X-62,145**

**NASA TM X-62,145**

**LONGITUDINAL AND LATERAL STABILITY AND CONTROL  
CHARACTERISTICS OF A LARGE-SCALE MODEL WITH A  
SWEPT WING AND AUGMENTED JET FLAP**

**Michael D. Falarski and David G. Koenig**

**Ames Research Center  
and  
U.S. Army Air Mobility R&D Laboratory  
Moffett Field, Calif. 94035**

**April 1972**

**REPRODUCED BY  
NATIONAL TECHNICAL  
INFORMATION SERVICE  
U.S. DEPARTMENT OF COMMERCE  
SPRINGFIELD, VA. 22161**

**(NASA-TM-X-62145) LONGITUDINAL AND  
LATERAL STABILITY AND CONTROL  
CHARACTERISTICS OF A LARGE-SCALE MODEL  
WITH A SWEPT WING AND AUGMENTED JET FLAP ,  
(NASA) 160 p**

**N74-75522**

**00/99 40981  
Unclas**

# NOTATION

A	thrust augmentation ratio of jet augmentor, $J_A/J_I$
b	wing span, m(ft)
BLC	boundary layer control
c	chord, m(ft)
$\bar{c}$	mean aerodynamic chord, m(ft)
$C_D$	drag coefficient, $\frac{\text{drag}}{qS}$
$C_{D_m}$	total momentum drag coefficient due to gas generator and compressor gas flow
$C_{J_{AI}}$	isentropic augmentor jet force coefficient, (see text) $\frac{\text{isentropic force}}{qS}$
$C_{J_I}$	total isentropic jet thrust coefficient, $C_{J_{AI}} + C_{\mu_{AI}} + C_{\mu_{FI}}$
$C_f, C_R$	rolling moment coefficient, $\frac{\text{rolling moment}}{qSb}$
$C_L$	lift coefficient, $\frac{\text{lift}}{qS}$
$C_m$	pitching moment coefficient, $\frac{\text{pitching moment}}{qS\bar{c}}$
$C_n$	yawing moment coefficient, $\frac{\text{yawing moment}}{qSb}$
$C_{T_{JP}}$	jet pipe thrust coefficient, $\frac{\text{thrust}}{qS}$
$C_Y$	side force coefficient, $\frac{\text{side force}}{qS}$
$C_{\mu_{AI}}$	isentropic aileron BLC coefficient, $\frac{\text{isentropic BLC force}}{qS}$
$C_{\mu_{FI}}$	isentropic fuselage BLC coefficient, $\frac{\text{isentropic BLC force}}{qS}$
d	distance between trailing edge of flap and shroud, m(ft) (see fig. 2(e))
$i_t$	horizontal tail incidence, positive with trailing edge down, deg

$J_A$	augmentor jet force at $q = 0$ , $n/m^2$ (psf)
$J_I$	isentropic jet force at $q = 0$ , $n/m^2$ (psf)
$q$	free-stream dynamic pressure, $n/m^2$ (psf)
$S$	wing area, sq m(sq ft)
$t$	airfoil thickness, m(ft)
$x$	chordwise station, m(ft)
$y$	airfoil ordinate, m(ft)
$Z_{JP}$	distance between moment center and line of action of Jet-pipe residual thrust, m(ft)
$\alpha, AL$	model angle of attack, deg
$\beta$	angle of sideslip of plane of symmetry, deg
$\delta_a$	aileron deflection ( $\delta_a = 45/60$ means left aileron at $45^\circ$ , right aileron at $60^\circ$ ) positive with trailing edge down, deg
$\delta_e$	elevator deflection, positive with trailing edge down, deg
$\delta_f$	augmentor flap deflection, positive with trailing edge down, deg (see figure 2(e))
$\delta_{ID}$	augmentor intake door deflection, positive with leading edge down, deg (see figure 2(e))
$\delta_{JP}$	deflection of jet pipes relative to fuselage datum plane, deg
$\delta_s$	slat deflection, positive with leading edge down, deg (see figure 2(c))
$\delta_{SP}$	spoiler deflection, trailing edge up, deg (see figure 2(k))
$\Delta_d$	augmentor throttling, reduction in distance between trailing edge of flap and shroud in percent of $d$ .
$\theta$	augmentor jet angle relative to wing chord plane, deg



## SUBSCRIPTS

a	aileron
A	augmentor
f	flap
F	fuselage
JP	jet-pipe
I	isentropic
L	left
R	right
s	slat
u	uncorrected
V	Viper
w	wing
1	forward elevator element
2	aft elevator element

## SUMMARY

This report presents data of an investigation of the lateral-directional stability and control characteristics of large-scale swept augmentor wing model in the Ames 40-by 80- foot wind tunnel. Also included are the results of a study to determine the static efficiency of the augmentor flap. As a preliminary investigation of engine nacelle interferences, flow-through nacelles were mounted on the model for a short series of tests. The results of the investigation are included in this report. Studies were made for augmentor primary thrust coefficient of 0 to 1.50. The Reynolds Numbers range based on the wing mean aerodynamic chord was  $2.43 \times 10^6$  to  $4.1 \times 10^6$ .

## INTRODUCTION

The augmentor wing concept is being studied as one means of attaining STOL performance in turbofan powered aircraft. Wind tunnel tests on a large-scale unswept augmentor wing model are reported in references 1 and 2. An initial investigation of a swept augmentor wing model was reported in reference 3. These tests indicate that the lift and drag characteristics were comparable to those of the unswept wing. The investigation also indicated no serious longitudinal or lateral stability and control problems.

The aerodynamics of the swept wing were subsequently investigated more extensively and these results are reported herein. The primary emphasis of the test program was on the longitudinal and lateral stability and control characteristics. Also included are the results of tests to determine the static augmentation of this configuration. As a preliminary study of engine nacelle interferences, flow-through nacelles were mounted under the wing for a short series of runs. The results of this study are also presented in this report.

This research program was undertaken in cooperation with the Defense Research Board of Canada and DeHavilland Aircraft of Canada, Limited.

## MODEL AND APPARATUS

### Basic Model

The model is shown installed in the wind tunnel in figures 1(a) and 1(b). Figure 1(c) shows the model mounted on the static test support. The basic geometric details of the model are shown in figure 2 and the model reference dimensions and airfoil coordinates are listed in Tables I to III. The air for the augmentor and BLC systems was supplied by a pump consisting of a J-85 coupled pneumatically to two turbocompressors, which are modified Viper engines. The turbocompressor supplied air for the augmentor and aileron BLC (see figure 3).

The wing planform and leading edge slat geometry are shown in figures 4(a) and 4(b). Slat gaps of  $.5\%c_w$ ,  $1.0\%c_w$  and  $1.5\%c_w$  were investigated.

The horizontal tail planform geometry is described in figure 5(a) and Table II. For this series of tests the tail was equipped with the leading edge slat shown in figure 5(b). The slotted, double-hinged elevator, shown in figure 5(c), provided longitudinal control. The horizontal tail was mounted in either a high or low position as shown in figures 2 and 5(d). When the tail was in the high position it was set at an incidence of  $-8.7^\circ$ . The incidence of the tail in the low position was  $0.3^\circ$ .

### Augmentor Flap

The geometry of the augmentor flap cross section is shown in figure 6(a). The augmentor is an ejector system consisting of a trailing edge primary nozzle (figure 6(b)) through which the compressed air is delivered, (lower) flap, (upper) shroud, and intake door. The secondary air is entrained from the wing upper surface, the slot between the intake door and shroud, and the tertiary gap between the wing lower surface and flap. The mixed jet is ejected downward between the flap and the shroud. The angle of the intake door was optimized for each flap deflection. The diffusion angle for this report is  $4^{\circ}50'$ ; for the investigation of reference 3, it was  $6^{\circ}37'$ .

The ducting for the primary air and aileron BLC is shown in figures 6(c) and 6(d). Figure 6(d) shows the variation of duct diameter with wing span which was designed to maintain a duct Mach number of .36.

### Fuselage BLC

The fuselage BLC installation is shown in figure 7. It was located just aft of the wing leading edge in the part of the wing spanning the fuselage for the purpose of preventing airflow separation at the wing fuselage juncture by energizing the fuselage boundary layer. The BLC air was provided by J-85 compressor bleed air.

### Aileron BLC

The geometry of the aileron BLC system is shown in figure 8. The system was fed through an extension of the augmentor primary air duct. Aileron blowing was therefore coupled with the augmentor output. Airflow to the aileron was approximately 5% of the total turbo-compressor output.

A short series of tests were made with a slotted aileron as shown in figure 9. For these tests the aileron BLC duct and nozzle were removed. The augmentor duct was sealed at its tip and the augmentor primary nozzle area was increased over the outer 25% span to maintain the same nozzle area. In an attempt to improve the slotted aileron performance, a few tests were made with the lower slot inlet radius removed and the slot overlap increased.

### Lateral Control System

The model was equipped with several methods for lateral control: Ailerons.- Lift requirements for landing and take-off resulted in symmetrical drooping of the BLC aileron by as much as  $45^\circ$ . They were normally drooped to  $30^\circ$ . Lateral control was obtained by differentially deflecting the ailerons.

Spoilers.- Upper wing panel type spoilers were installed on the left wing for lateral control as shown in figure 8. The spoilers were 11.2% of wing chord, located ahead of the aileron.

Augmentor Throttling.- A flat plate was installed

on the lower portion of the flap of the outer 50% of the port wing augmentor as shown in figure 6(a). This simulates a deflected aft portion of the flap to reduce the augmentor exit area and affect a local throttling of the augmentor efflux to create a rolling moment.

#### Flow-Through Nacelles

The flow-through nacelle used for the engine nacelle interference study is shown in figure 10(a). The flow through the left inboard nacelle was measured with a pressure rake mounted vertically at the duct exit. A typical exit pressure distribution is presented in figure 10(b). Unless otherwise specified, the flow-through nacelles were not mounted on the wing.

## TESTS

### Wind Tunnel

The test procedure consisted primarily of varying either angle of attack or sideslip at constant thrust coefficient. The angle of attack range was  $-8^\circ$  to  $30^\circ$  and the sideslip range was  $-19^\circ$  to  $8^\circ$ . Thrust coefficient was varied from 0 to 1.5. The dynamic pressure and augmentor plenum total pressure for each nominal  $C_{J_I}$  are listed below.

$C_{J_I}$ nominal	$q$ $n/m^2$ (psf)	$P_{TAUG}$ cm. of Hg (in. of Hg)
1.5	201(4.2)	61.0(24)
1.1	240(5)	53.4(21)
0.8	383(8)	61.0(24)
0.4	383(8)	25.4(10)
0.2	670(14)	20.3(8)
0.0	383(8)	00.0(0)

The position of the augmentor intake door was set at its optimum angle for each flap deflection, as determined in reference 3. Longitudinal characteristics of the model with the slotted aileron were investigated during the first several runs of the program. For the duration of the program the aileron BLC was installed. The ailerons were symmetrically deflected to  $30^\circ$  unless otherwise specified. The effect of wing leading edge slot gap on longitudinal characteristics was also investigated during the first part of the test program. For the remainder of the investigation the slot gap was set at  $1.0\% c_w$ .



The longitudinal characteristics of the wing with intake door-shroud assembly removed, simulating a slotted jet flap, were studied. The tertiary slot was sealed for part of the investigation to simulate a plain jet flap. The slot was sealed with a flat plate attached from the bottom surface of the wing to the bottom surface of the flap. Longitudinal characteristics with flow-through nacelles were measured with the complete augmentor flap and the shroud removed.

### Static Augmentor Performance

The static performance of the model was obtained outside the wind tunnel with the model installed on the test stand shown in figure 1(c). The forces were measured by three 2-axis load cells. The following augmentor configurations were investigated:

Configuration	Augmentor Diffuser Angle	Aileron
1	6° 37'	BLC
2	6° 37'	Slotted
3	4° 50'	Slotted

Configuration 1 is the augmentor arrangement reported in reference 3, while arrangement 3 was studied in the present investigation.

## DATA REDUCTION

For all force and moment data, the effects of compressor residual jet thrust, and the intake momentum drag of the fuselage mounted J85 and Viper engines, have been subtracted from the measured values. Forces and moments are referred to the stability axes. The corrections made for thrust and ram drag are as follows:

$$C_L = C_{L_u} - C_{TJP} \sin (\alpha_u - \delta_{JP})$$

$$C_{D_{net}} = C_{D_u} + C_{TJP} \cos (\alpha_u - \delta_{JP}) - C_{D_{MJ85}} - C_{D_{MV}}$$

$$C_{m_{net}} = C_{m_u} - C_{TJP} \frac{z_{JP}}{\bar{c}}$$

Wind tunnel boundary corrections were based upon the "aerodynamic  $C_L$ ", computed as follows:

$$C_{L_{AERO}} = C_{L_u} - C_{JA} (A_{net}) \sin (\theta + \alpha_u) \quad (\text{Augmentor})$$

$$-C_{\mu_{aL}} \sin (\delta_{aL} + \alpha_u) \frac{S_a}{S} \quad (\text{Aileron BLC, left})$$

$$-C_{\mu_{aR}} \sin (\delta_{aR} + \alpha_u) \frac{S_a}{S} \quad (\text{Aileron BLC, right})$$

$$-C_{\mu_F} \sin \alpha_u \left( \frac{S_F}{S} \right) \quad (\text{Fuselage BLC})$$

Thus the following boundary corrections were made:

$$C_a = C_{a_u} + .458 C_{L_{AERO}}$$

$$C_D = C_{D_u} + .00799 C_{L_{AERO}}^2$$

$$C_m = C_{m_u} + .023 C_{L_{AERO}} \quad (\text{tail on only})$$

The moment center used for data computation was located longitudinally at 0.25  $\bar{c}$  and vertically 0.20  $\bar{c}$  below the wing chord datum.

The  $C_{J_{AI}}$  is the force coefficient computed on the basis of the measured mass flow and total pressure in the duct prior to discharge.

## DATA PRESENTATION

Results of the static tests are presented in figure 11. The longitudinal aerodynamic characteristics of the model are presented in figures 12 to 23. This data is summarized in figures 24 to 26. An index to the longitudinal data figures is presented in Table IV. The lateral stability and control characteristics are presented in figures 27 to 37. Table V is an index to these figures.

Table VI is presented as a run by run index of the wind tunnel tests.

## REFERENCES

1. Koenig, D. G.; Corsiglia, V. R.; Morelli, J. P.; Aerodynamic Characteristics of a Large Scale Model with an Unswept Wing and Augmented Jet Flap. NASA TN D-4610, 1968.
2. Cook, A. M.; Aiken, T. N.: Low Speed Aerodynamic Characteristics of a Large Scale STOL Transport Model with an Augmented Jet Flap. NASA TM X-62017, 1971.
3. Palarski, M. D.; Koenig, D. G.: Aerodynamic Characteristics of a Large Scale Model with a Swept Wing and Augmented Jet Flap. NASA TM X-62029, 1971.

TABLE I. - WING REFERENCE DIMENSIONS

Wing area, sq m(sq ft)	21.36(230.0)
Aspect ratio	8.0
Span, m(ft)	13.08(42.895)
Taper ratio	0.30
Sweep at 1/4 chord, deg	27.5
Airfoil section	RAE 104
Root chord, m(ft)	2.515(8.25)
Tip chord, m(ft)	0.755(2.475)
Root thickness, percent	12 1/2
Tip thickness, percent	10 1/2
Augmentor span limits, Inner, m(ft) (percent)	1.111(3.645) (12.34)
Augmentor span limits, Outer, m(ft) (percent)	4.575(15.01) (70.0)
Wing area spanned by one augmentor, sq m(sq ft)	6.75(72.62)
Wing area spanned by one aileron, sq m(sq ft)	1.997(21.50)
Wing area spanned by fuselage, sq m(sq ft)	3.88(41.77)
Flap hinge axis, percent chord	68.543
Aileron hinge axis, percent chord	68.0
Incidence, camber, twist	0
Mean aerodynamic chord, m(ft)	1.793(5.880)

NOTE: All chords are measured in streamwise direction.

TABLE II. - TAIL REFERENCE DIMENSION

Horizontal Tail	
Gross area, sq m(sq ft)	55.77(60.0)
Aspect ratio	4.5
Span, m(ft)	5.005(16.432)
Taper ratio	0.40
Sweep at 1/4 chord, deg	25
Airfoil section	RAE 104 with modified l.e.
Thickness/Chord ratio, percent	10
Root chord, m(ft)	1.591(5.22)
Tip chord, m(ft)	0.635(2.082)
Elevator hinge axis, percent chord	<del>6.35</del> see fig. 5c
Elevator travel, deg	±30
Tailplane incidence, deg	±12
Tailplane arm, m(ft)	6.804(22.32)
Tailplane volume coefficient, HIGH Pos.	0.990
" " " " LOW Pos.	0.816
Mean aerodynamic chord, m(ft)	1.114(3.654)

Vertical Fin	
Fin arm, m(ft)	5.361(17.603)
Fin volume coefficient	0.07476

TABLE III. - COORDINATES OF R.A.E. 104 AIRFOIL( $t/c$  max.=.10)

X/C	Y/C 100	X/C	Y/C 100
0	0	0.35	4.9300
0.001	0.3441	0.36	4.9488
0.002	0.4863	0.38	4.9775
0.003	0.5953	0.4	4.9946
0.004	0.6870	0.42	5.0000
0.005	0.7676	0.44	4.9937
0.006	0.8404	0.45	4.9862
0.007	0.9072	0.46	4.9756
0.0075	0.9387	0.48	4.9454
0.008	0.9692	0.5	4.9027
0.009	1.0274	0.52	4.8468
0.01	1.0824	0.54	4.7769
0.012	1.1842	0.55	4.7363
0.0125	1.2083	0.56	4.6917
0.014	1.2776	0.58	4.5802
0.016	1.3642	0.6	4.4650
0.018	1.4452	0.62	4.3113
0.02	1.5215	0.64	4.1370
0.025	1.6960	0.65	4.0438
0.03	1.8522	0.66	3.9473
0.035	1.9945	0.68	3.7452
0.04	2.1256	0.7	3.5331
0.05	2.3617	0.72	3.3128
0.06	2.5709	0.74	3.0861
0.07	2.7592	0.75	2.9708
0.075	2.8468	0.76	2.8545
0.08	2.9307	0.78	2.6103
0.09	3.0881	0.8	2.3819
0.1	3.2336	0.82	2.1437
0.12	3.4945	0.84	1.9055
0.14	3.7222	0.85	1.7864
0.15	3.8254	0.86	1.6673
0.16	3.9224	0.88	1.4202
0.18	4.0992	0.9	1.1910
0.2	4.2556	0.92	0.9528
0.22	4.3936	0.925	0.8932
0.24	4.5149	0.94	0.7146
0.25	4.5697	0.95	0.5955
0.26	4.6208	0.96	0.4764
0.28	4.7124	0.975	0.2977
0.3	4.7905	0.98	0.2382
0.32	4.8556	0.9875	0.1489
0.34	4.9082	1.0	0



TABLE IV.- INDEX TO LONGITUDINAL DATA FIGURES

FIGURE	EFFECTS	$S_{\alpha}$	AILERON	HORIZ. TAIL	VERTICAL TAIL	NACELLES	SHROU.	REMARKS
12 a	$S_{\alpha}$	70	SLOT	OFF	OFF	OFF	ON	SLOTTED AILERON
b	$C_{J_2}$	↓						$S_{\alpha}=4$ , SLOT SEALED
c	↓	40						↓
d	$S_{\alpha R}$	70						
e	$S_{\alpha L}$	↓						
f	$S_{\alpha R}$		↓					
13 a	SLOT GAP		BLC					SLOT GAP STUDY
b	↓							↓
14	$S_{ID}$							
15 a	FUS. BLC							
b	↓	↓			↓			
16 a	$C_{J_2}$	30			ON			
b	↓	↓			↓		↓	
c					↓		OFF	
17 a		40			OFF		ON	
b				↓	ON			
c				HIGH		↓		
d				OFF		ON		
e	↓			LOW		↓		
f	$S_{\alpha}$			↓		↓		
g	$C_{J_2}$			OFF		OFF	OFF	
h						↓		
i						ON		TERTIARY SLOT SEALED
18		60			OFF	OFF	ON	
19 a		70						
b	↓							$S_{\alpha}=4^{\circ}$
c	$S_{\alpha}$				↓	↓		
d	$C_{J_2}$				ON	UN		
e						↓		
f						OFF	OFF	INB'D NACELLES ONLY
g	↓					ON	↓	
20 a				LOW		OFF	ON	
b	$S_{\alpha}$							
c	↓							$S_{\alpha}=0$
d								$S_{\alpha}=-15$
21 a	$C_{J_2}$			HIGH				
b	↓			↓				
c	$S_{\alpha}$			↓				$S_{\alpha}=0$

### TABLE IV.- CONCLUDED

FIGURE	EFFECTS	SC	ANEROID	HORIZ. TAIL	VERTICAL TAIL	NACELLES	SHROUD.	REMARKS
21 d	Se <sub>1</sub>	70	BLC	HIGH	ON	OFF	ON	Se <sub>2</sub> = +6
e		↓		↓	↓	↓		Se <sub>2</sub> = -21
f	Se <sub>2</sub>					↓		
22 a	C <sub>TX</sub>			LOW		ON		
b	Se			↓	↓	↓		
c	Se	↓		↓	↓	↓		
23 a	C <sub>DC</sub> = CONST	30-70		OFF	ON	OFF		SUMMARY FIGURES
b	C <sub>LX</sub> = 0	↓						
c	C <sub>DX</sub> = 0							
d	C <sub>L</sub> MAX						↓	
24 a	C <sub>DC</sub> = CONST						OFF	
b	C <sub>LX</sub> = 0						↓	
c	C <sub>DX</sub> = 0						↓	
d	C <sub>L</sub> MAX					↓	↓	
25 a	C <sub>DC</sub> = CONST					ON & OFF	ON & OFF	
b	C <sub>LX</sub> = 0	↓	↓	↓	↓	↓	↓	
c	C <sub>DX</sub> = 0							
d	C <sub>L</sub> MAX	↓	↓	↓	↓	↓	↓	↓

TABLE V. - INDEX TO LATERAL STABILITY AND CONTROL FIGURES.

FIGURE	EFFECTS	$\Sigma F$	ANERON	HORIZ. TAIL	VERTICAL TAIL	NACELLES	SHROUD	$\alpha$ , deg	$\beta$ , deg	NON. $C_{DZ}$	
26a	$C_{JZ}$	70	BLC	OFF	OFF	OFF	ON	0	~	~	
b	$C_{JZ}$	↓		↓	↓			12	↓	0	
27a		40		HIGH	ON			0	↓	~	
b		↓		↓				12	↓	↓	
28a		70		↓				12	↓	↓	
b		↓		↓		↓		0	↓	↓	
29a	$\alpha$	↓		LOW		ON		0, 12	↓	.77	
b	-	↓		↓		↓		0	↓	↓	
30a	$\delta_a$	40		HIGH		OFF		~	~	~	
b	↓	↓						~	-8	1.1	
c	$C_{JZ}$	↓						0	~	~	$\delta_a = 15/45$
d	↓	↓						12	↓	~	↓
e	$\delta_{aL}$	↓						0, 12	0	1.1	
f	$\delta_{aR}$	↓						↓	↓	↓	
31a	$\delta_a$	70						~	↓	~	
b	$C_{JZ}$	↓						0	~	~	$\delta_a = 15/45$
c	↓	↓						12	↓	~	↓
d	$\delta_a$	↓						~	0	1.12	
e	$\delta_a$	↓						4	0	1.1	
f	$\delta_{aR}$	↓						0	0	1.1	
32a	THROTTLING	40						~	0	1.1	
b	↓	↓						↓	↓	1.09	
c	↓	↓						↓	↓	.36	
d	↓	↓						↓	↓	↓	
e	$\beta$	↓						~	-8.0	1.1	$\Delta\beta = 60\%$
f	↓	↓						↓	↓	.36	↓
g	↓	↓						4	~	1.1	
33a	THROTTLING	70						~	0	1.09	
b	↓	↓						↓	↓	↓	
c	↓	↓						↓	↓	.36	
d	↓	↓						↓	↓	↓	
e	$\beta$	↓						↓	0, -8	↓	$\Delta\beta = 60\%$
f	↓	↓						↓	↓	1.1	↓
34a	$\delta_{SP}$	70						~	0	1.1	0.1 cu Vent
b	↓	↓						↓	↓	.36	↓
c	$\delta_{SP}, \delta_{aL}$	↓						4	↓	1.1	
d	↓	↓	↓	↓	↓	↓	↓	↓	↓	.4	↓

TABLE V. - CONCLUDED.

[illegible]

# TABLE VI. - SWEEP AUGMENTOR WING RUN INDEX

RUN		TUNNEL			Power			WING					TAIL			REMARKS	FIG NO
Run No		$q$ , psf	$\alpha$ , deg	$\beta$ , deg	AKWP, H <sub>g</sub>	FUS BLC, PSIG	$C_F$	$\delta_f$ , deg	$\delta_{10}$ , deg	$\delta_a$ , deg	$\delta_s$ , deg	SLAT GAP, %	POS.	$i_t$ , deg	$\delta_{\text{eff}}$ , %		
7		8	~	0	0	0	0	70	50	4	60	1.0	OFF	-	-	SLOTTED AILERON	12a
8		↓	↓	↓	↓	↓	↓	↓	↓	15	↓	↓	↓	↓	↓	↓	↓
9		↓	↓	↓	↓	↓	↓	↓	↓	30	↓	↓	↓	↓	↓	↓	↓
10		5	↓	↓	21	↓	1.1	↓	↓	15	↓	↓	↓	↓	↓	↓	↓
11		↓	↓	↓	↓	↓	↓	↓	↓	30	↓	↓	↓	↓	↓	↓	↓
12		↓	0.2, 12	↓	↓	↓	↓	↓	↓	~	↓	↓	↓	↓	↓	↓	12d, e, f
13		↓	0	↓	↓	↓	↓	↓	↓	~	↓	↓	↓	↓	↓	↓	↓
14		↓	0, ~	↓	↓	↓	↓	↓	↓	~	↓	↓	↓	↓	↓	ALL SLOT FAIRING OFF ALL SLOT FAIRING OFF AND OVERLAP EXTENDED	↓, e, f
15		4.2	~	↓	24	↓	1.5	↓	↓	4	↓	↓	↓	↓	↓	AILERON SLOT SEALED	12b
16		8	↓	↓	↓	↓	.8	↓	↓	↓	↓	↓	↓	↓	↓	↓	↓
17		↓	↓	↓	↓	↓	.8	40	↓	↓	↓	↓	↓	↓	↓	↓	12c
18		4.2	↓	↓	↓	↓	1.5	↓	↓	↓	↓	↓	↓	↓	↓	↓	↓
19		8	↓	↓	0	↓	0	↓	↓	↓	↓	↓	↓	↓	↓	↓	↓
20		4.2	↓	↓	24	↓	1.5	70	↓	↓	↓	↓	↓	↓	↓	BLOWN AILERON INSTALLED	19b
21		8	↓	↓	↓	↓	.8	↓	↓	↓	↓	↓	↓	↓	↓	↓	↓
22		5	↓	↓	21	↓	1.1	↓	↓	↓	↓	↓	↓	↓	↓	↓	↓
23		↓	↓	↓	↓	↓	↓	↓	↓	30	↓	1.5	↓	↓	↓	SLAT OPTIMIZATION	13a
24		↓	↓	↓	↓	↓	↓	↓	↓	15	↓	1.5	↓	↓	↓	↓	13b
25		↓	↓	↓	↓	↓	↓	↓	↓	30	↓	1.0	↓	↓	↓	↓	13a, 14, 19a
26		↓	↓	↓	↓	↓	↓	↓	↓	45	↓	↓	↓	↓	↓	↓	19c
27		↓	↓	↓	↓	↓	↓	↓	↓	15	↓	↓	↓	↓	↓	↓	13b, 19c
28		↓	0	↓	↓	↓	↓	↓	↓	4/~	↓	↓	↓	↓	↓	↓	31f

NOTE: VERTICAL FIN OFF RUNS 7-55

19

23

# TABLE VI.- SWEEP AUGMENTOR WING RUN INDEX

RUN		TUNNEL			POWER			WING					TAIL			REMARKS	FIG NO
Run No		$\alpha$ , deg	$\beta$ , deg	AKP, %	FUS BLC, pos	$G_T$	$\delta_f$ , deg	$\delta_{TD}$ , deg	$\delta_a$ , deg	$\delta_s$ , deg	SEAT GAP, %	POS.	$\delta_t$ , deg	$\delta_{\theta}$ , deg			
29		8	N	0	0	0	70		30	60	1.0	OFF	-	-		14a	
30		4.2	↓		24		1.5									14a	
31		5	0.12		↓		1.25		N								
32		5	N		↓		1.25		45								
33		5			21		1.1		45							14	
34		8			24		.8									15b, 14a	
35		8			10		.4									↓	
36		14			8	↓	.2										
37		5			21	30	1.1									15a	
38		8			24	20	.8				↓					15b	
39		8			10	0	.4				.5					13a	
40		5			21	30	1.1	↓			.5						
41		4.2			24	0	1.55	60			1.0					18	
42		5			21		1.1									↓	
43		8			24		.8									↓	
44		8			10		.4									↓	
45		8			0		0	↓								↓	
46		4.2			24		1.5	40									
47		5			21		1.1									17a	
48		8			24		.8									↓	
49		8			10		.4									↓	
50		14	↓		8		.2	↓		↓	↓	↓				↓	

20

21

# TABLE VI. - SWEEP AUGMENTOR WING RUN INDEX

RUN		TUNNEL			POWER			WING					TAIL			REMARKS	FIG NO
Run No		q, ft psf	$\alpha$ , deg	$\beta$ , deg	AUGP, "Hg	FUS BLK, PSIG	G <sub>T</sub>	$\delta_f$ , deg	$\delta_{10}$ , deg	$\delta_a$ , deg	$\delta_s$ , deg	SLAT GAP, %	POS.	Lt, deg	$\epsilon_{\alpha}/\epsilon_{\alpha_0}$		
51		8	~	0	0	0	0	40		30	60	1.0	OFF	-	-		17a
52		8	0	~	24		.8	70								VERTICAL TAIL OFF	27a
53		8	12	↓	24		.8									↓	27b
54		8	↓	↓	0		0										27a
55		8	0	↓	0		0										20a
56		4.2	~	0	24		1.5						Low	.3	0		↓, b, c
57		5	-8, 0, 12	↓	21		1.1								~0		20 b
58		5	~	↓	21		1.1								-25		20a
59		8	↓	↓	24		.8								0		↓
60		8	↓	↓	10		.4								0		20d
61		5	-8, 0	↓	21		1.1								~15		22b, c
62		5	~	↓	21		1.1								~25	4 NACELLES ON	22a
63		4.2	↓	↓	24		1.5								0		↓, b
64		4.2	↓	↓	24		1.5										↓
65		5	↓	↓	21		1.1										29a
66		8	↓	↓	24		.8										29a
67		8	0	~	↓		↓										22a
68		8	12	↓	↓		↓										22a
69		8	~	0	10		.4										↓
70		8	↓	↓	0		0	↓							↓		17e, f
71		5	↓	↓	21		1.1	40							~25		↓
72		4.2	↓	↓	24		1.5	↓		↓	↓	↓	↓	↓	0		↓

21

25

# TABLE VII. - SWEEP AUGMENTOR WING RUN INDEX

RUN		TUNNEL			Power			WING					TAIL			REMARKS	FIG NO
Run No		q, psf	$\alpha$ , deg	$\beta$ , deg	AWGP, %	FUS BLC, psig	$C_{T5}$	$\delta_f$ , deg	$\delta_{10}$ , deg	$\delta_a$ , deg	$\delta_s$ , deg	SLAT CAP, %	POS.	$i_t$ , deg	$S_{e/f}$ , %		
73		5	~	0	21	0	1.1	40		30	60	1.0	LOW	.3	0	4 NACELLES ON	17c
74		8	↓	0	24		.8	↓		↓	↓	↓	↓	↓	↓	↓	↓
75		↓	0	~	↓		↓	↓		↓	↓	↓	↓	↓	↓	↓	↓
76		↓	12	~	↓		↓	↓		↓	↓	↓	↓	↓	↓	↓	↓
77		4.2	~	0	24		1.5	70					OFF	-	-	VERTICAL FW OFF - 4 NACELLES ON	17c
78		5	↓	0	21		1.1	↓		↓	↓	↓	↓	↓	↓	↓	↓
79		8	0	~	24		.8	↓		↓	↓	↓	↓	↓	↓	↓	↓
80		8	12	~	24		↓	↓		↓	↓	↓	↓	↓	↓	↓	↓
81		4.2	~	0	24		1.5	40					↓	↓	↓	↓	↓
82		5			21		1.1						↓	↓	↓	↓	↓
83		8			24		.8						↓	↓	↓	↓	↓
84		8			0		0	↓					↓	↓	↓	↓	↓
85		4.2			24		1.5	70					↓	↓	↓	↓	↓
86		5			21		1.1						↓	↓	↓	↓	↓
87		8			24		.8						↓	↓	↓	↓	↓
88		8			0		0						↓	↓	↓	↓	↓
89		5	↓		21		1.1						HIGH	-8.7	0		21a, 31a
90		↓	-8, 0, 12		↓		↓	↓		↓	↓	↓	↓	↓	~		21c
91		↓	~		↓		↓	↓		↓	↓	↓	↓	↓	-25		21b
92		↓	~		↓		↓	↓		↓	↓	↓	↓	↓	-25/16		21b
93		↓	-8, 0, 12		↓		↓	↓		↓	↓	↓	↓	↓	1/16		21d
94		↓	~		↓		↓	↓		↓	↓	↓	↓	↓	-25/21		21b

22

26



# TABLE VI. - SWEEP AUGMENTOR WING RUN INDEX

RUN		TUNNEL			POWER			WING					TAIL			REMARKS	FIG NO
RUN NO		g, ft/sec	$\alpha$ , deg	$\beta$ , deg	AKCP, "Hg	FUS BLC, psig	$C_{T2}$	$\delta_f$ , deg	$\delta_{SD}$ , deg	$\delta_a$ , deg	$\delta_s$ , deg	SLAT GAP, %	POS.	$i_t$ , deg	$\epsilon_{ex}/\epsilon_{in}$		
95		S	0, 12	0	21	0	1.1	70		30	60	1.0	HIGH	-8.7	$\sim 1/21$		21e
96		S	$\sim$	$\downarrow$	21		1.1								$-25/17.8$		21b
97		4.2	$\downarrow$	$\downarrow$	24		1.5								0		21a
98		S	$\downarrow$	$\downarrow$	21		1.1										$\downarrow$
99		8	$\downarrow$	$\downarrow$	24		.8										
100		8	$\downarrow$	$\downarrow$	10		.4										31a
101		8	$\downarrow$	$\downarrow$	0		0										$\downarrow$
102		S	0	$\sim$	21		1.1										28d
103		S	12	$\downarrow$	21		1.1										28c
104		8	0	$\downarrow$	10		.4										28d
105		8	12	$\downarrow$	10		.4										28c
106		4.2	$\sim$	0	24		1.5	40									17c
107		S	$\downarrow$	$\downarrow$	21		1.1										30a
108		8	$\downarrow$	$\downarrow$	24		.8										$\downarrow$
109		8	$\downarrow$	$\downarrow$	10		.4										30a
110		$\downarrow$	0	$\sim$	$\downarrow$		$\downarrow$										28a
111		$\downarrow$	12	$\sim$	$\downarrow$		$\downarrow$										28b
112		S	12	$\downarrow$	21		1.1										28b
113		S	0	$\downarrow$	21		1.1										28a
114		8	$\sim$	0	10		.4			15/45							30a
115		S	$\downarrow$	$\downarrow$	21		1.1			$\downarrow$							30a
116		S	0	$\sim$	21		1.1			$\downarrow$							30c

23

27

# TABLE VI. - SWEEP AUGMENTOR WING RUN INDEX

RUN		TUNNEL			Power			WING					TAIL			REMARKS	FIG NO
Run No		q, psi	$\alpha$ , deg	$\beta$ , deg	AirP, "H <sub>2</sub>	FUS BLE, PSIG	C <sub>T</sub>	$\delta_f$ , deg	$\delta_{to}$ , deg	$\delta_a$ , deg	$\delta_s$ , deg	SLAT GAP, %	POS.	Lt, deg	$\delta_{ex}$ , deg		
117		8	~	0	0	0	0	40		30	60	1.0	HIGH	-9.7	0		17c
118		5	0	↓	21		1.1	↓		~	↓	↓	↓	↓	↓		31e,f
119		↓	4	↓	↓	↓	↓	↓		↓	↓	↓	↓	↓	↓		↓, 35d
120		↓	12	↓	↓	↓	↓	↓		↓	↓	↓	↓	↓	↓		↓
121		↓	12	~	↓	↓	↓	↓		15/45	↓	↓	↓	↓	↓		30d
122		↓	~	-8	↓	↓	↓	↓		↓	↓	↓	↓	↓	↓		30b
123		↓	↓	-8	↓	↓	↓	↓		30	↓	↓	↓	↓	↓		30b
124		8	0	~	10		.4	↓		15/45	↓	↓	↓	↓	↓		30c
125		↓	12	↓	↓	↓	↓	↓		↓	↓	↓	↓	↓	↓		30d
126		5	~	0	21		1.1	70		↓	↓	↓	↓	↓	↓		31a
127		8	↓	↓	10		.4	↓		↓	↓	↓	↓	↓	↓		↓
128		5	↓	↓	21		1.1	↓		45/15	↓	↓	↓	↓	↓		↓, 36d
129		↓	4	↓	↓	↓	↓	↓		~	↓	↓	↓	↓	↓		31e, 31c
130		↓	0	~	↓	↓	↓	↓		15/45	↓	↓	↓	↓	↓		31b
131		↓	12	↓	↓	↓	↓	↓		↓	↓	↓	↓	↓	↓		31c
132		8	12	↓	10		.4	↓		↓	↓	↓	↓	↓	↓		31c
133		↓	0	↓	↓	↓	↓	↓		↓	↓	↓	↓	↓	↓		31b
134		5	~	-8	21		1.1	↓		↓	↓	↓	↓	↓	↓		31d
135		↓	↓	-8	↓	↓	↓	↓		30	↓	↓	↓	↓	↓		31d
136		↓	↓	0	↓	↓	↓	↓		↓	↓	↓	↓	↓	↓	20% THROTTLE	33a,b
137		8	↓	↓	10		.4	↓		↓	↓	↓	↓	↓	↓	↓	33c,d
138		5	↓	↓	21	↓	1.1	↓		↓	↓	↓	↓	↓	↓	60% THROTTLE	33a,b,f

24

28

# TABLE VI. - SWEEP AUGMENTOR WING RUN INDEX

RUN		TUNNEL			POWER			WING					TAIL			REMARKS	FIG NO
RUN NO		g, deg	$\alpha$ , deg	$\beta$ , deg	AKCP, "Hg	FUS BLC, PSIG	$C_T$	$\delta_f$ , deg	$\delta_{ID}$ , deg	$\delta_a$ , deg	$\delta_s$ , deg	SAT GAP, %	POS.	$L_t$ , deg	$\epsilon_e$ , %		
139		8	~	0	10	0	4	70		30	60	1.0	HIGH	-8.7	0	60% THROTTLING	33c,d,e
140		↓	↓	-8	↓		4									↓	33e
141		S	↓	-8	21		1.1										33f
142		↓	4	~	↓		↓									↓	
143		↓	~	0	↓		↓									40% THROTTLING	
144		8			10		4	↓								↓	
145		S			21		1.1	40									32a,b
146		8			10		4									↓	32c,d
147		S			21		1.1									60% THROTTLING	32a,b,e
148		8		↓	10		4									↓	32c,d,f
149		↓		-8	↓		↓										32f
150		S	↓	-8	21		1.1									↓	32e
151		↓	4	~	↓		↓									↓	32g
152		↓	~	0	↓		↓									20% THROTTLING	32a,b
153		8			10		4									↓	32c,d
154		S			21		1.1										32a,b,35a
155		8			10		4	↓									32c,d,35b
156		S			21		1.1	70									34a,36a
157		8			10		4										34b,36b
158		S	↓		21		1.1			↓						$\delta_{30} = 22^\circ$ ( ) VENT	34a
159		↓	4		↓		↓			~30						↓	34c
160		8	~	↓	10	↓	4			30	↓		↓			↓	34b

25

29

# TABLE VI. - SWEEP AUGMENTOR WING RUN INDEX

RUN		TUNNEL			POWER			WING					TAIL			REMARKS	FIG NO
RUN NO		g, ft/sec	$\alpha$ , deg	$\beta$ , deg	AUGP, "Hg	FUS BLC, PSIG	$C_{Tj}$	$\delta_f$ , deg	$\delta_{SD}$ , deg	$\delta_a$ , deg	$\delta_s$ , deg	SLAT GAP, %	POS.	$L_t$ , deg	$E_{ex}/C_{Tj}$		
161		8	~	0	10	0	4	70		~30	60	1.0	HIGH	-8.7	0	$\delta_{SP} = 22^\circ$ ( ) VENT	34d
162		5	4		21		1.1									$\delta_{SP} = 38^\circ$ ↓	34c
163		↓	↓		↓		↓									( ) VENT	36d
164		↓	↓		↓		↓									$\delta_{SP} = 10^\circ$	36d
165		8	↓		10		4			↓						↓	36e
166		5	~		21		1.1			30							36c
167		8	↓		10		4			30						↓	36b
168		5	4		21		1.1			~30						$\delta_{SP} = 20^\circ$	36d
169		8	↓		10		4	↓								↓	36e
170		5	↓		21		1.1	40		↓							35d
171		↓	~		↓		↓			30							35a
172		8	↓		10		4			30							35b
173		↓	4		↓		↓			~30						↓	35d
174		5	~		21		1.1									$\delta_{SP} = 36^\circ$	35a, c
175		↓	4	↓	↓		↓									↓	35d
176		↓	↓	-8	↓		↓	↓		↓						↓	35c
177		↓	~	0	↓		↓	70		30						$\delta_{SP} = 50^\circ$	36a
178		↓	4	↓	↓		↓			~30						↓	36d
179		8	~		10		4			30							36b
180		↓	4	↓	↓		↓			~30							36e
181		5	↓	~	21		1.1			30						↓	36c
182		8	↓	0	10		4	↓		~30	↓	↓	↓				34d

26

30

# TABLE VI. - SWEEP AUGMENTOR WING RUN INDEX

RUN		TUNNEL			Power			WING					TAIL			REMARKS	FIG NO
Run No		g, ft	$\alpha$ , deg	$\beta$ , deg	AKP, "Hg	FUS BLC, psig	$C_F$	$\delta_f$ , deg	$\delta_{ID}$ , deg	$\delta_a$ , deg	$\delta_s$ , deg	SLAT GAP, %	POS.	$\delta_t$ , deg	$\delta_{e/c}$		
183		0	-8	0	21	0	$\infty$	70		4	60	1.0	OFF	-	-		
184		5	~				1.1	↓		30							19a
185		0					$\infty$	30		4							
186		5					1.1			30							16a
187		8			10		.4										
188		8			24		.8										
189		14			8		.2										
190		16			24		.4										16b
191		25			24		.3										16b
192		4.2			24		1.5										16a
193		8	↓		0		0	↓									16a
194		0	-8		21		$\infty$	40									
195		8	~		24		.8										17b
196		16					.4										
197		25	↓				.3			↓							
198		0	-8		21		$\infty$			4							
199		4.2	~		24		1.5			30							17g
200		5			21		1.1										
201		8			24		.8										
202		8			10		.4										
203		14	↓		8		.2										
204		14	14	↓	~	↓	~	↓		↓	↓	↓	↓				

SHROUD & INTAKE DOOR OFF

27

31

# TABLE VI. - SWEEP AUGMENTOR WING RUN INDEX

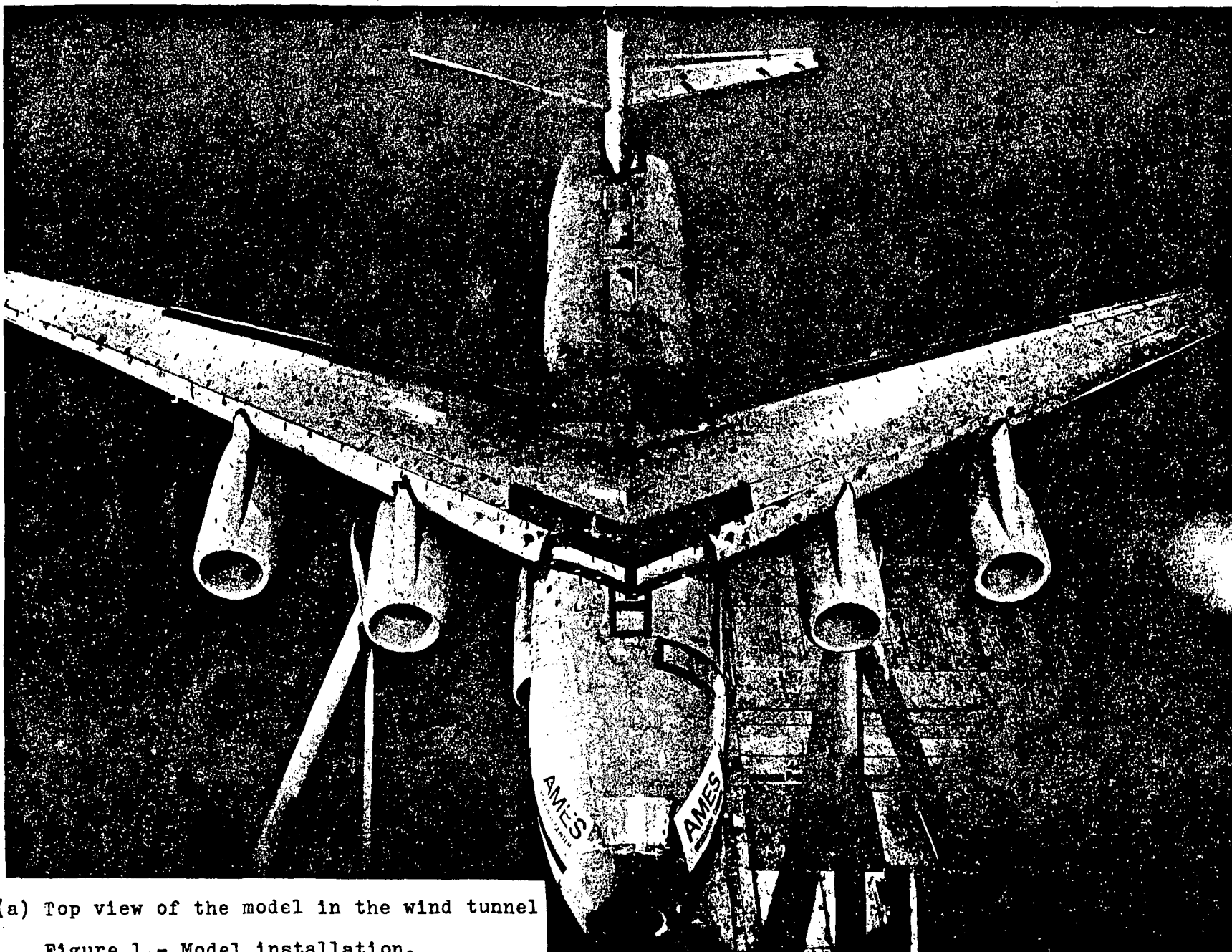
RUN		TUNNEL			Power			WING					TAIL			REMARKS	FIG NO
RUN NO		q, psi	$\alpha$ , deg	$\beta$ , deg	AUGP, "Hg	FUS BLC, PSIG	C <sub>T</sub>	$\delta_f$ , deg	$\delta_{ID}$ , deg	$\delta_a$ , deg	$\delta_s$ , deg	SLAT GAP, %	POS.	L, deg	S <sub>e</sub> /S <sub>w</sub>		
205		25	14	0	~	0	~	40		30	60	1.0	OFF	-	-	SHROUD & INTAKE DOOR OFF	17g
206		8	~		0		0			↓							
207		0	-8		21		∞	70		4							19e
208		4.2	~		24		1.5			30							
209		5			21		1.1										
110		8			24		.8										
211		8			10		.4										
212		14	↓		8		.2										
213		14	14		~		~										
214		25	14		~		~										
215		8	~		0		0	↓									19e
216		4.2			24		1.5	30									16c
217		5			21		1.1	↓									
218		8	↓		24		.8	↓		↓							
219		0	-8		21		∞	40		4						TERTIARY SLOT SEALED	
220		4.2	~		24		1.5			30							
221		5			21		1.1										
222		8			24		.8										
223		8			0		0	↓									
224		4.2			24		1.5	70								4 NACELLES ON	
225		5			21		1.1	↓									
226		8	↓	↓	24	↓	.8	↓		↓	↓	↓	↓				

28

32

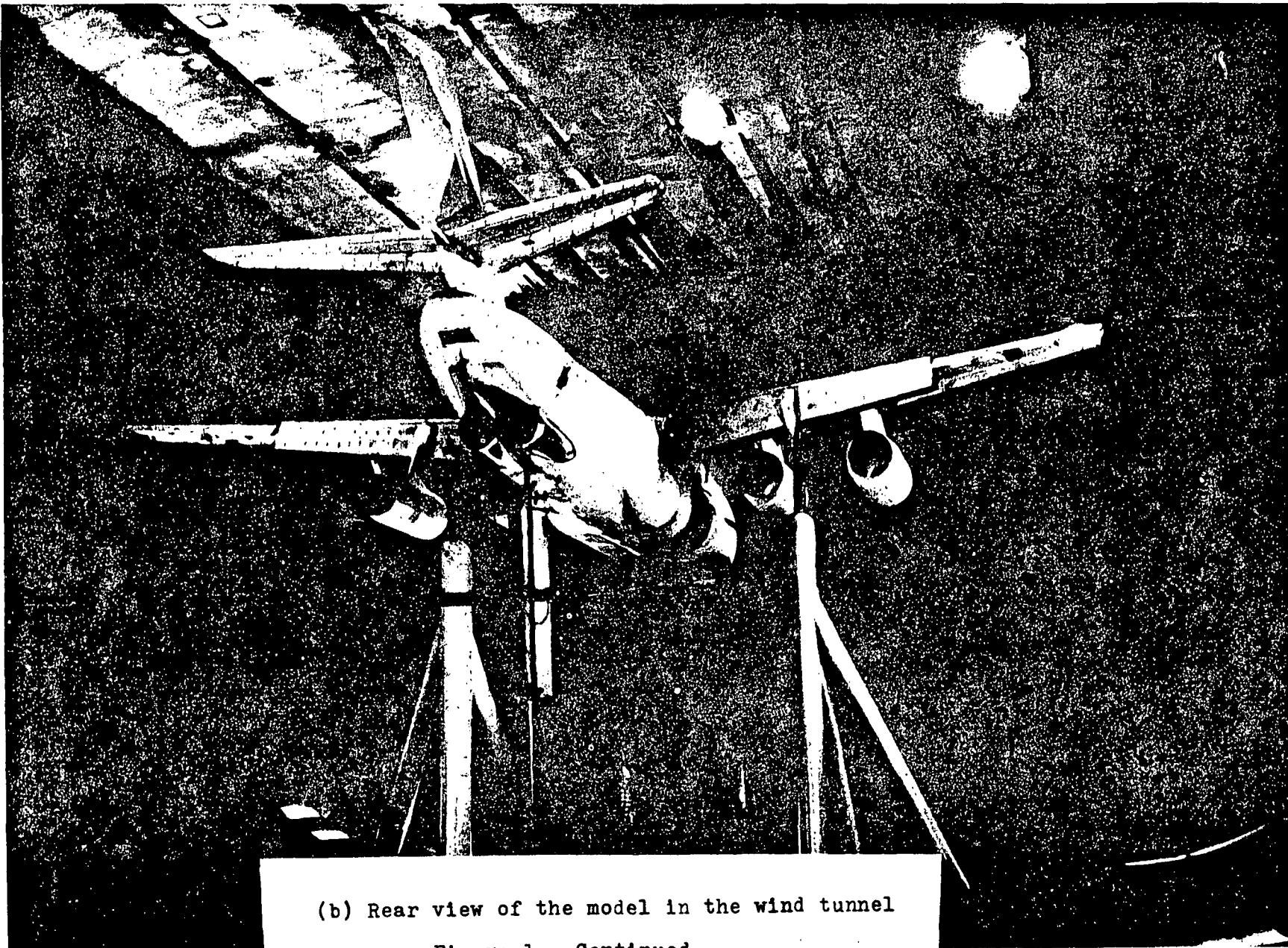
29

CC  
CC  
A



(a) Top view of the model in the wind tunnel  
Figure 1.- Model installation.





(b) Rear view of the model in the wind tunnel  
Figure 1.- Continued.



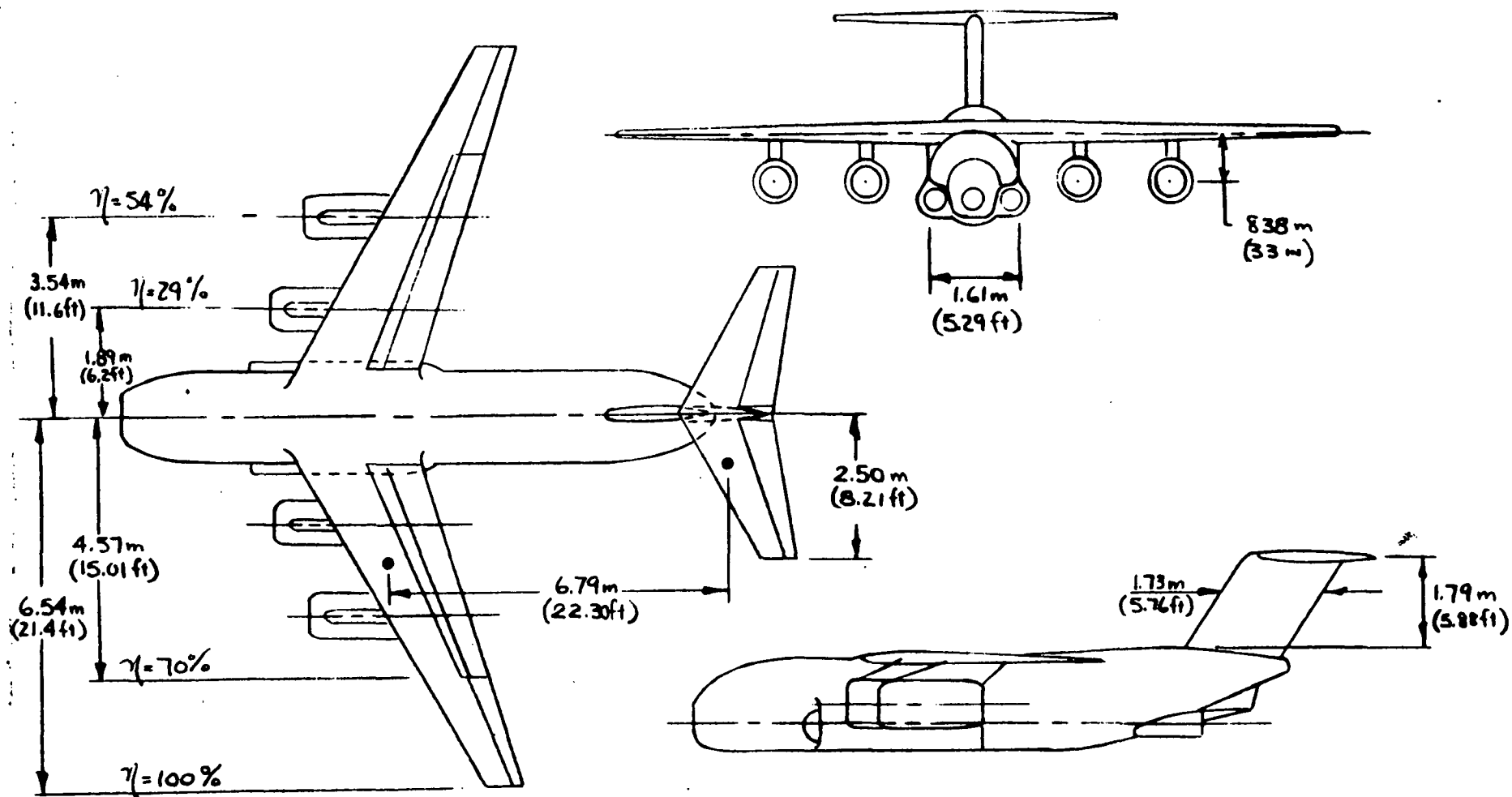


Figure 2.- Basic model geometry.

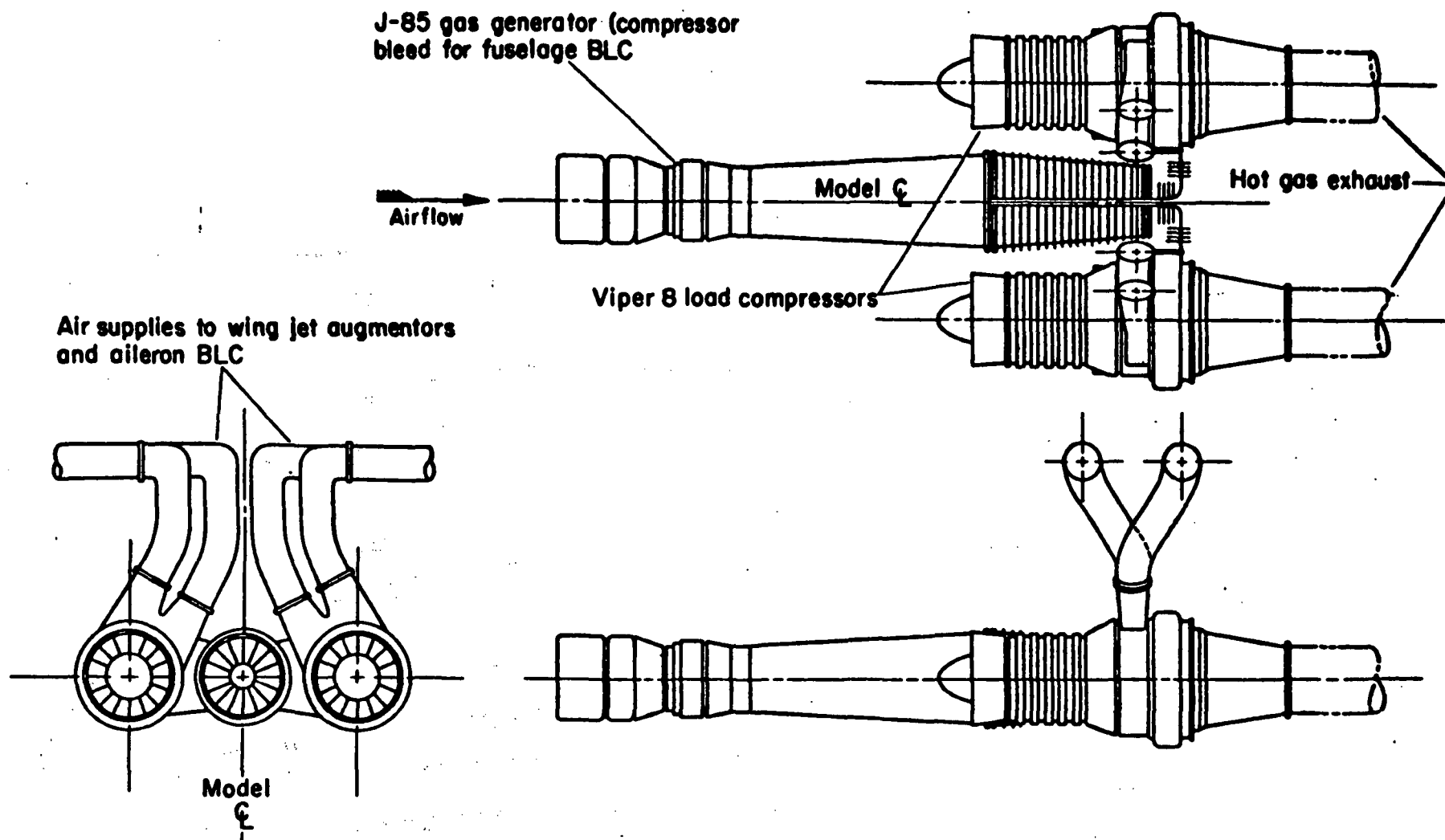


Figure 3.- Augmentor air compressor system.

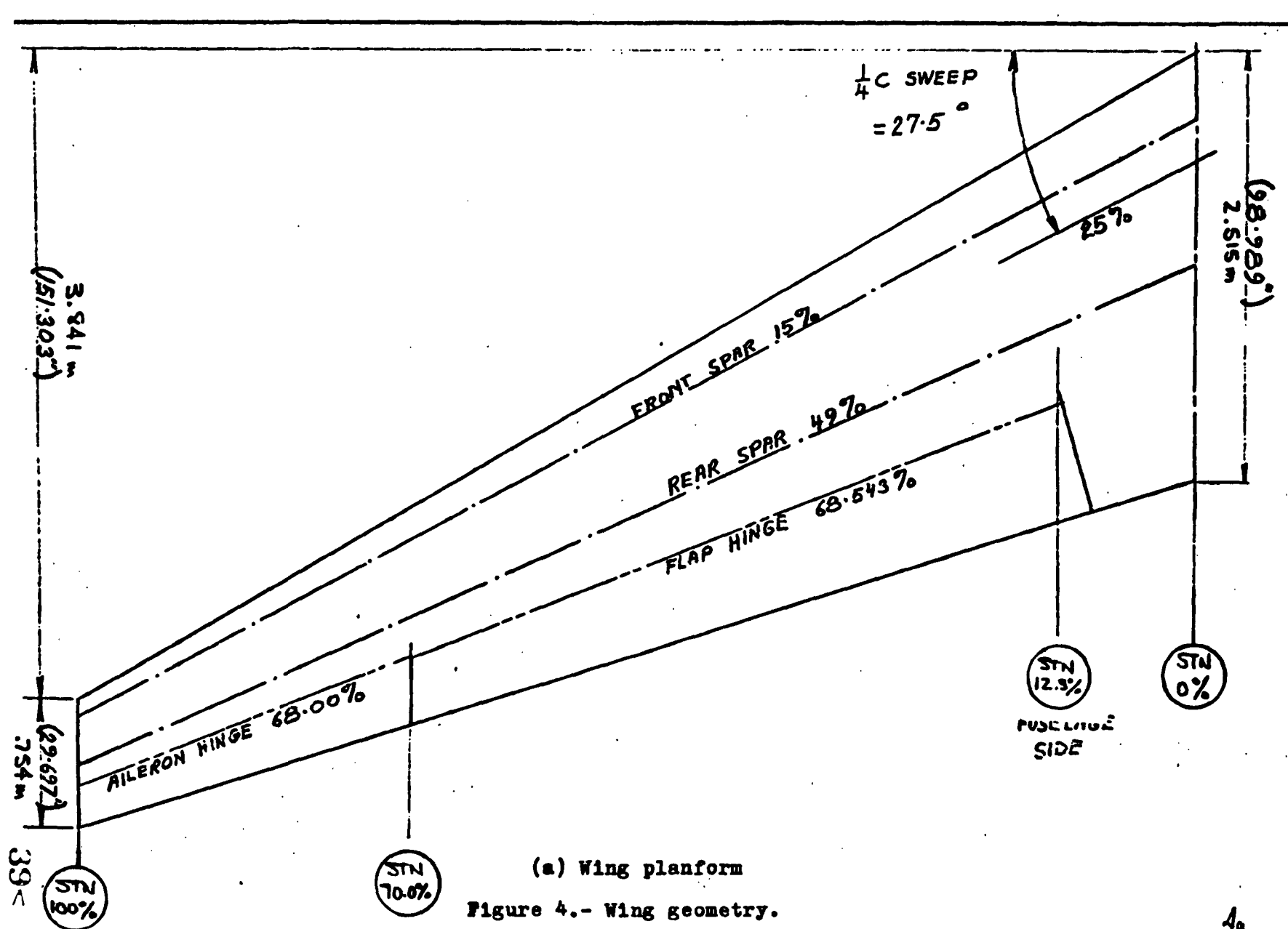
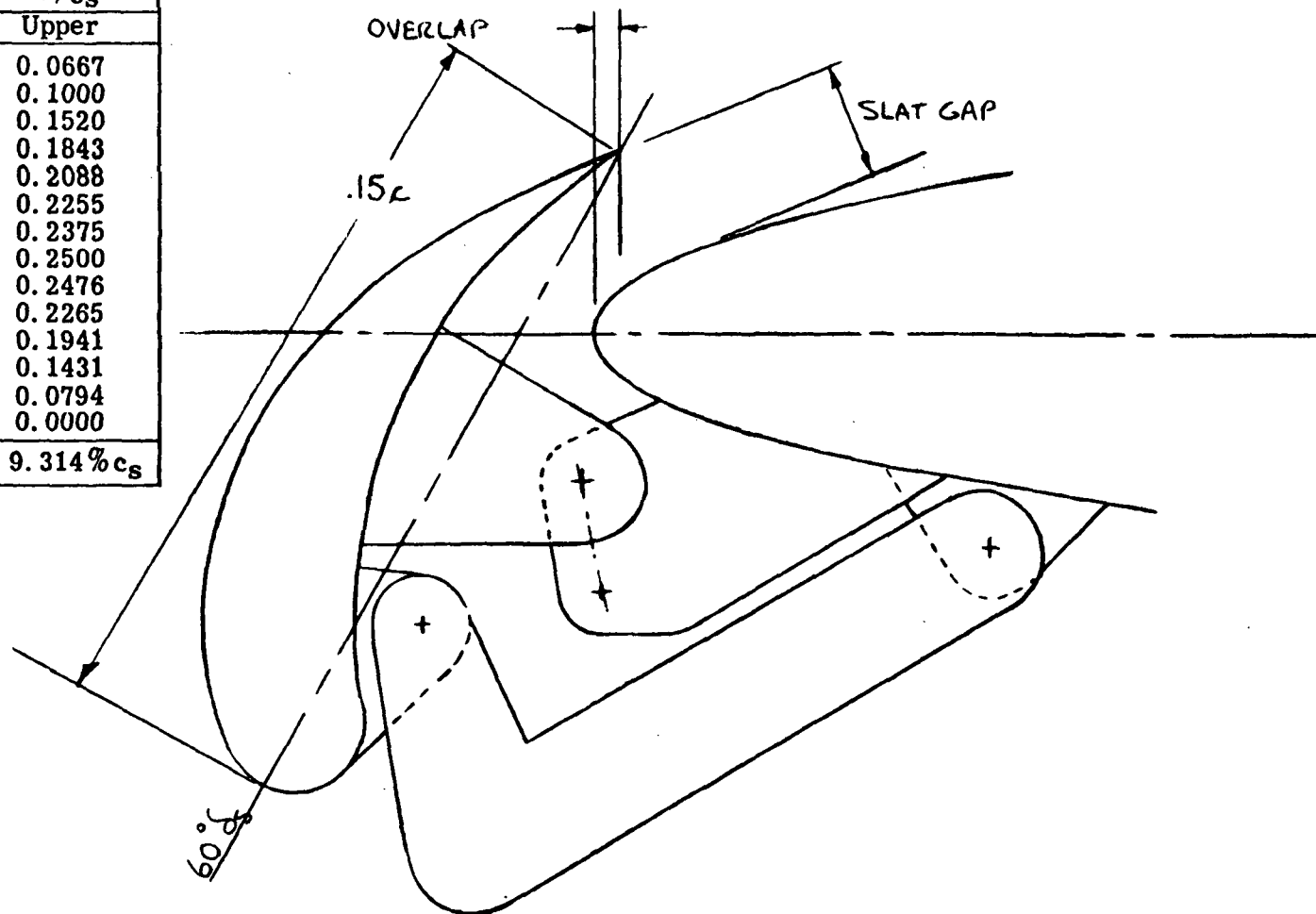


Figure 4.- Wing geometry.

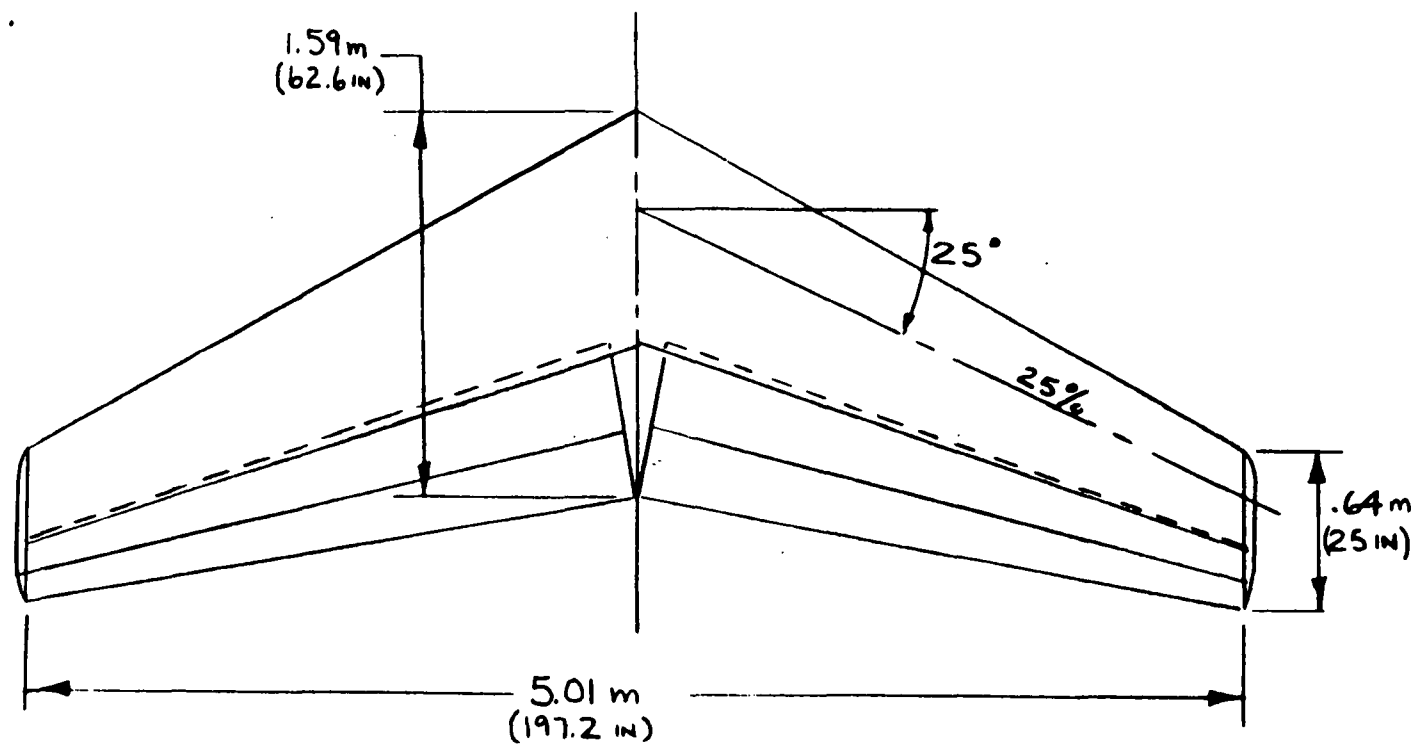
SLAT CO-ORDINATES	
$x/c_s$	$y/c_s$
	Upper
0.025	0.0667
0.05	0.1000
0.10	0.1520
0.15	0.1843
0.20	0.2088
0.25	0.2255
0.30	0.2375
0.40	0.2500
0.50	0.2476
0.60	0.2265
0.70	0.1941
0.80	0.1431
0.90	0.0794
1.00	0.0000
L/E RADIUS = 9.314% $c_s$	



(b) Wing leading edge slat

Figure 4.- Concluded.

RAE 104 10% $\frac{1}{2}$   
WITH MODIFIED L. E.

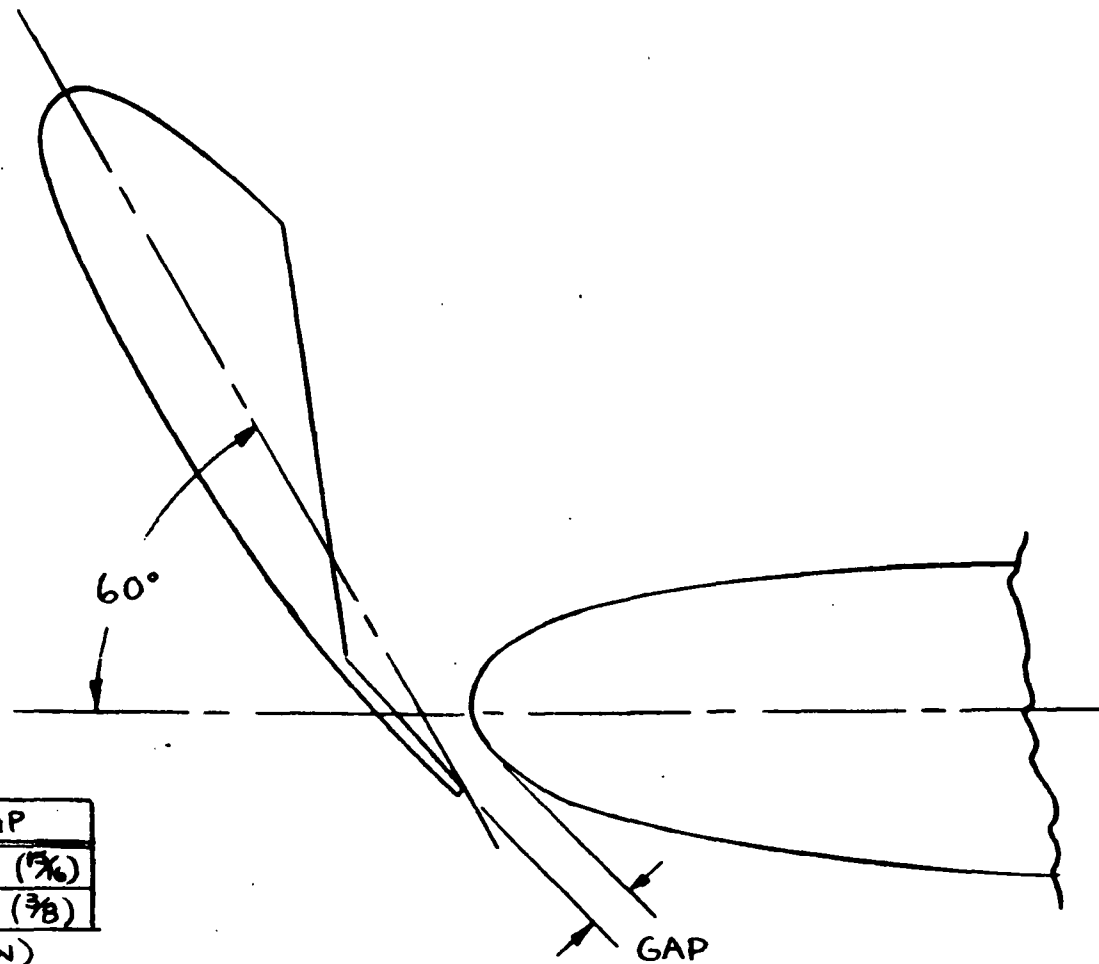


(a) Basic geometry

Figure 5.- Horizontal tail geometry.

	CHORD	GAP
ROOT	20.3 (8)	2.4 ( $\frac{5}{8}$ )
TIP	10.2 (4)	1.0 ( $\frac{3}{8}$ )

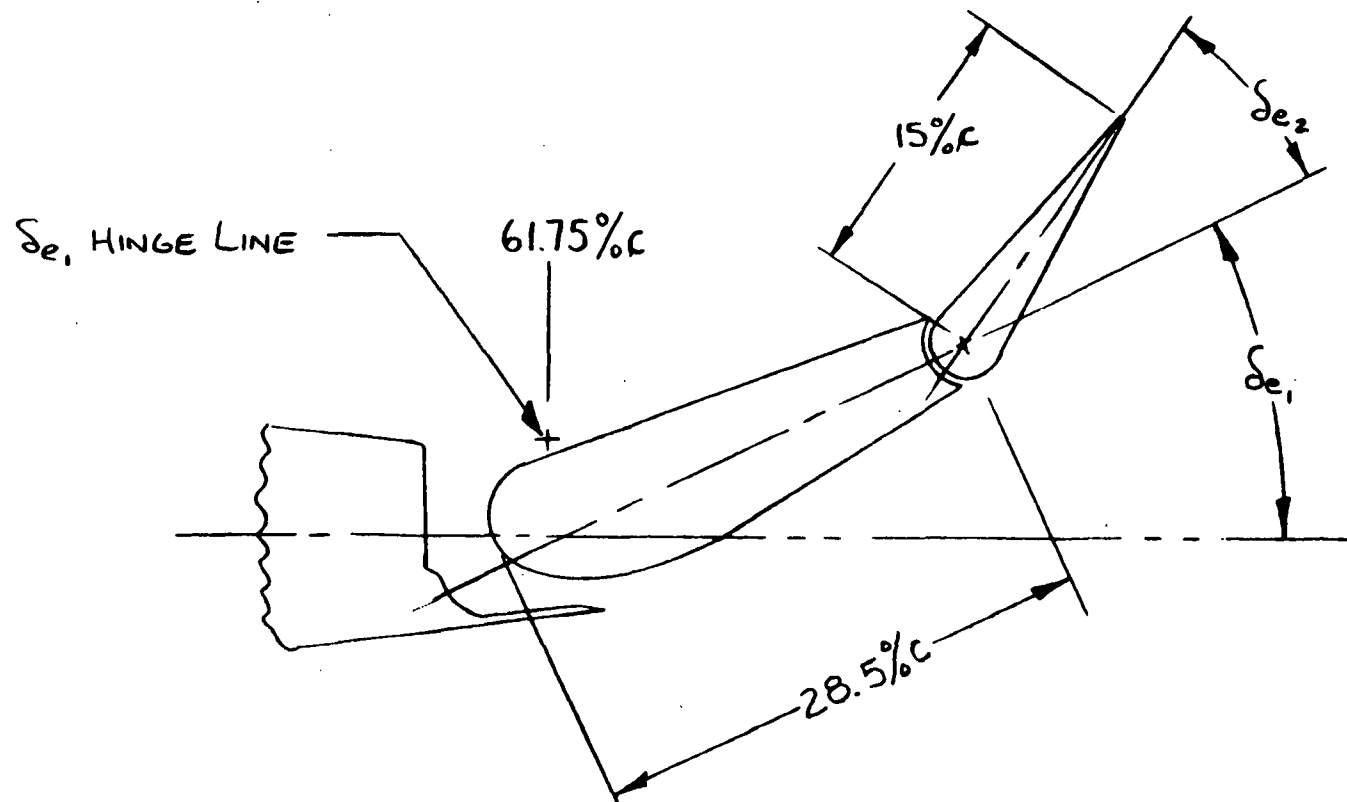
DIMENSIONS IN CM(IN)



(b) Leading edge slat

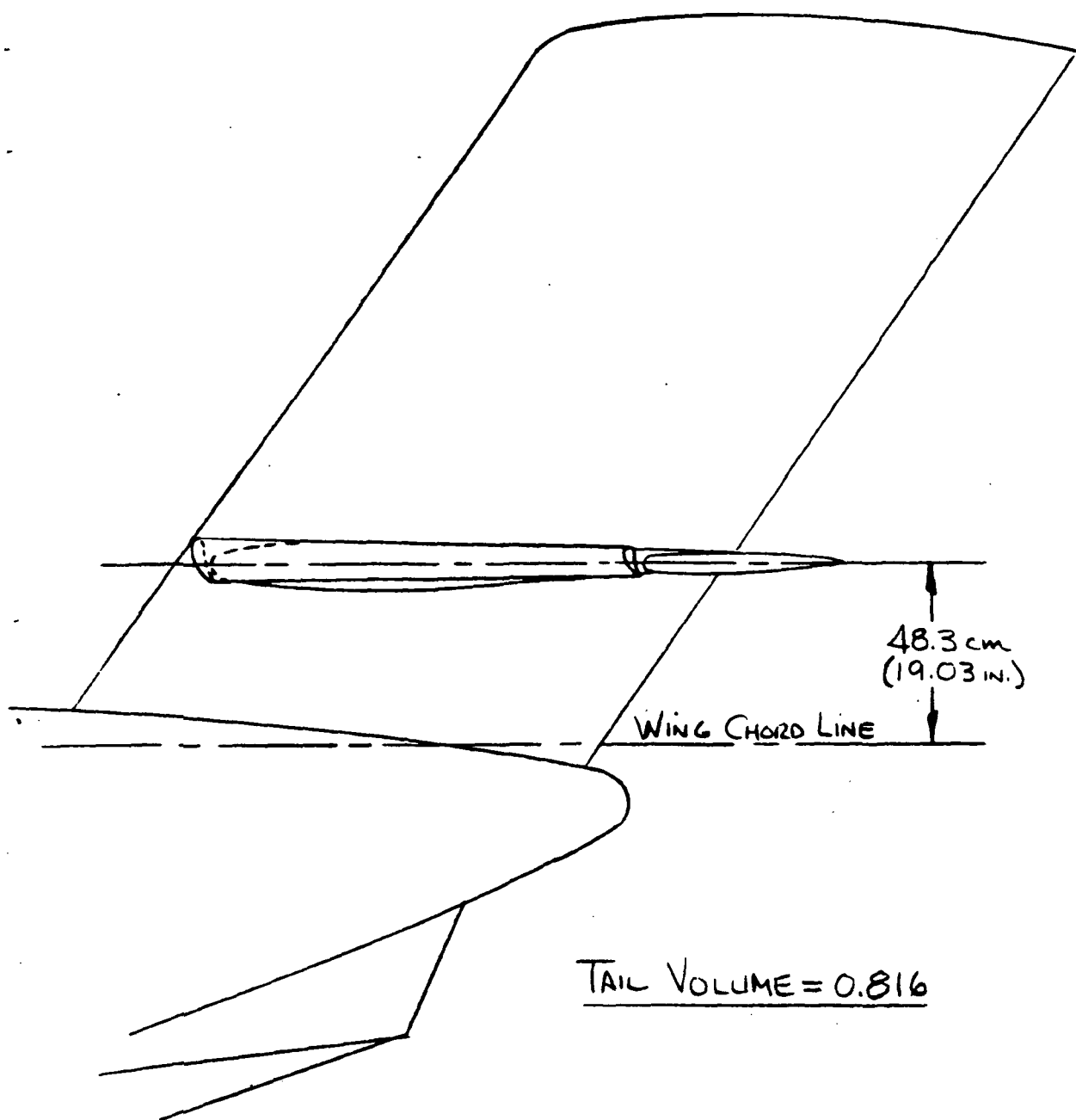
Figure 5.- Continued.



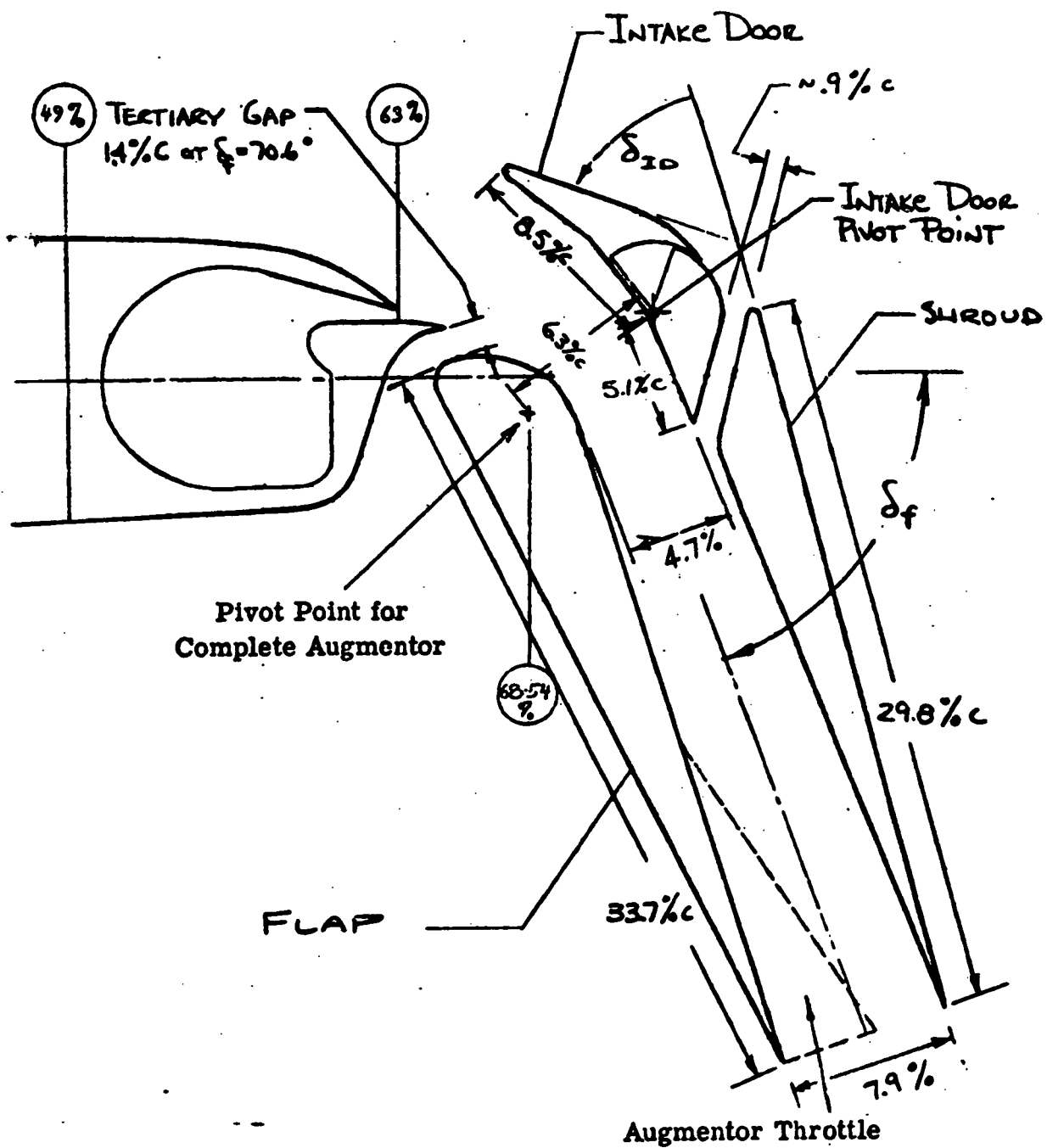


(c) Slotted, double-hinged elevator

Figure 5.- Continued.

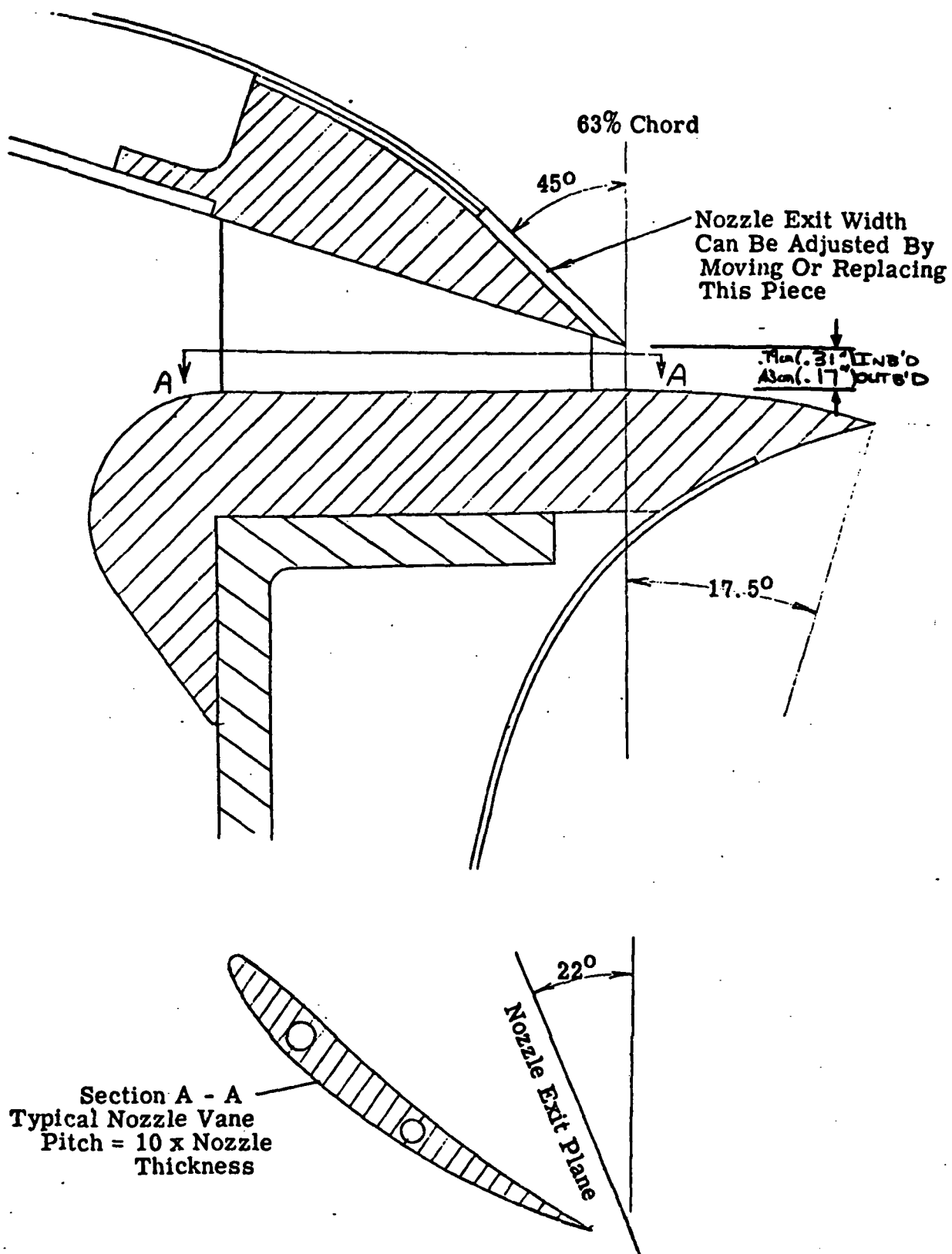


(d) Low tail position  
Figure 5.- Concluded.



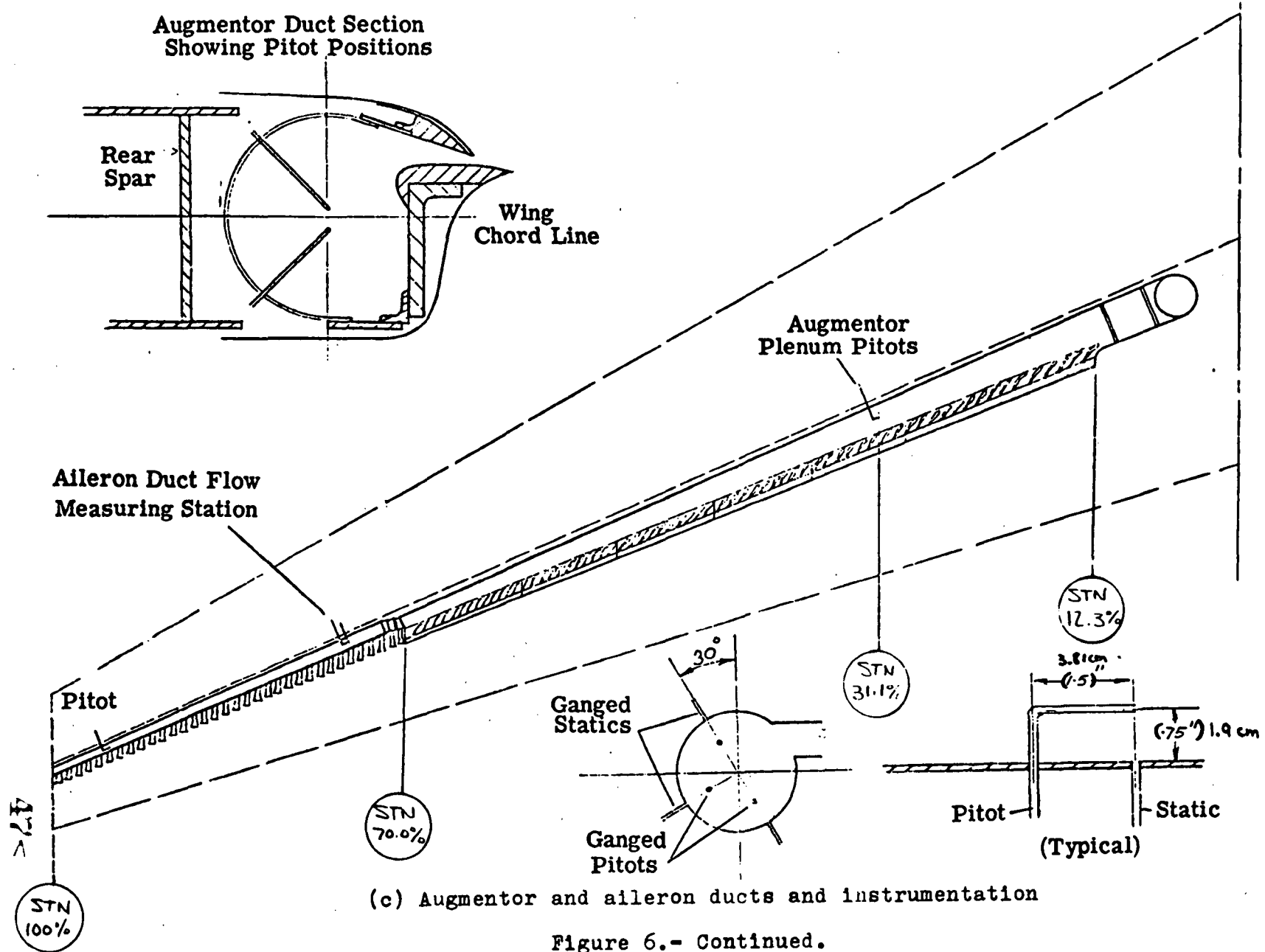
(a) Basic geometry

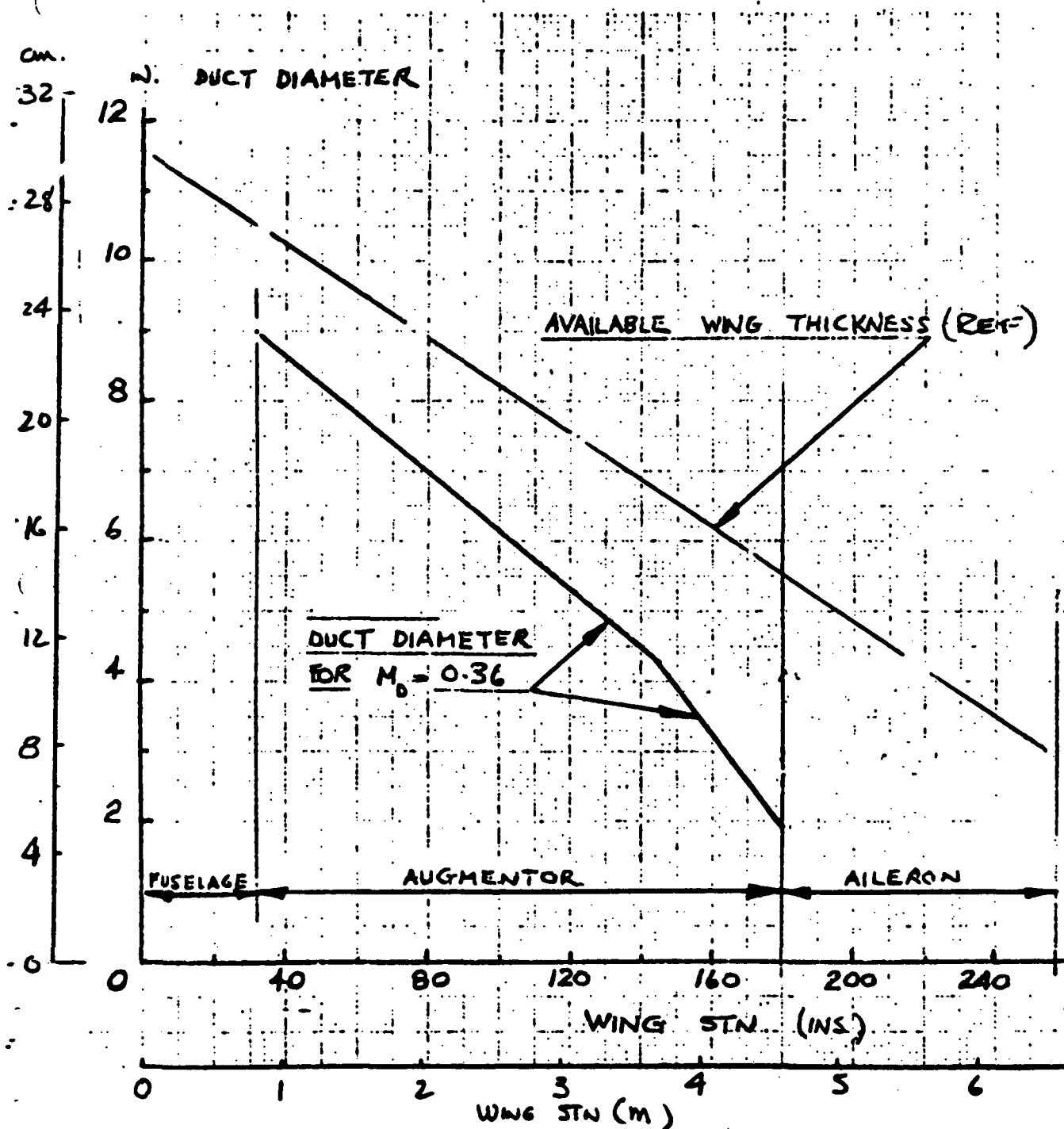
Figure 6.- Augmentor geometry.



(b) Primary nozzle geometry

Figure 6.- Continued.





(d) Augmentor duct diameter as a function of wing span

Figure 6.- Concluded.

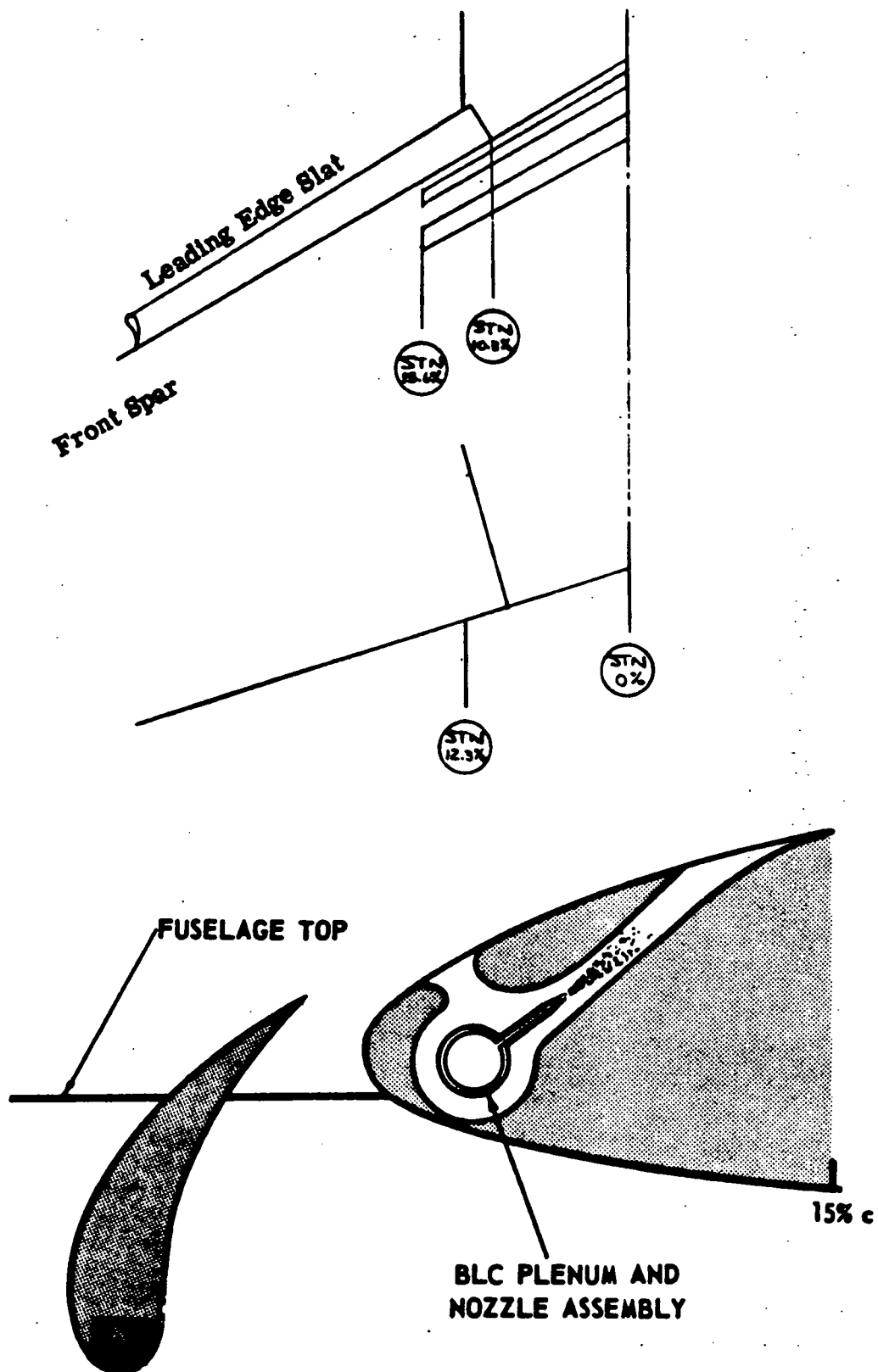
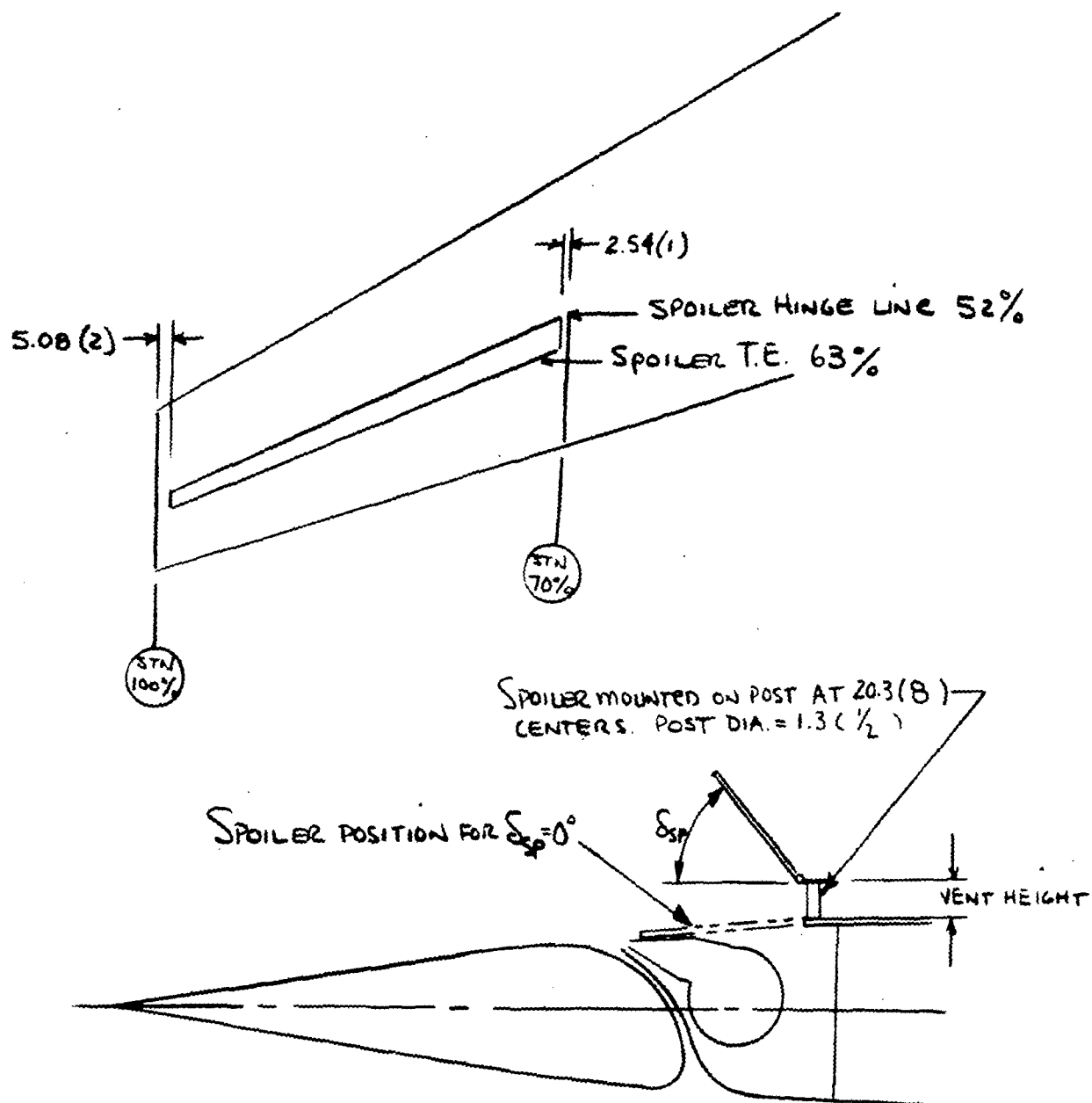


Figure 7.- Fuselage BLC geometry.



ALL DIMENSIONS IN CM (IN)

Figure 8.- Geometry of aileron BLC and vented spoiler.



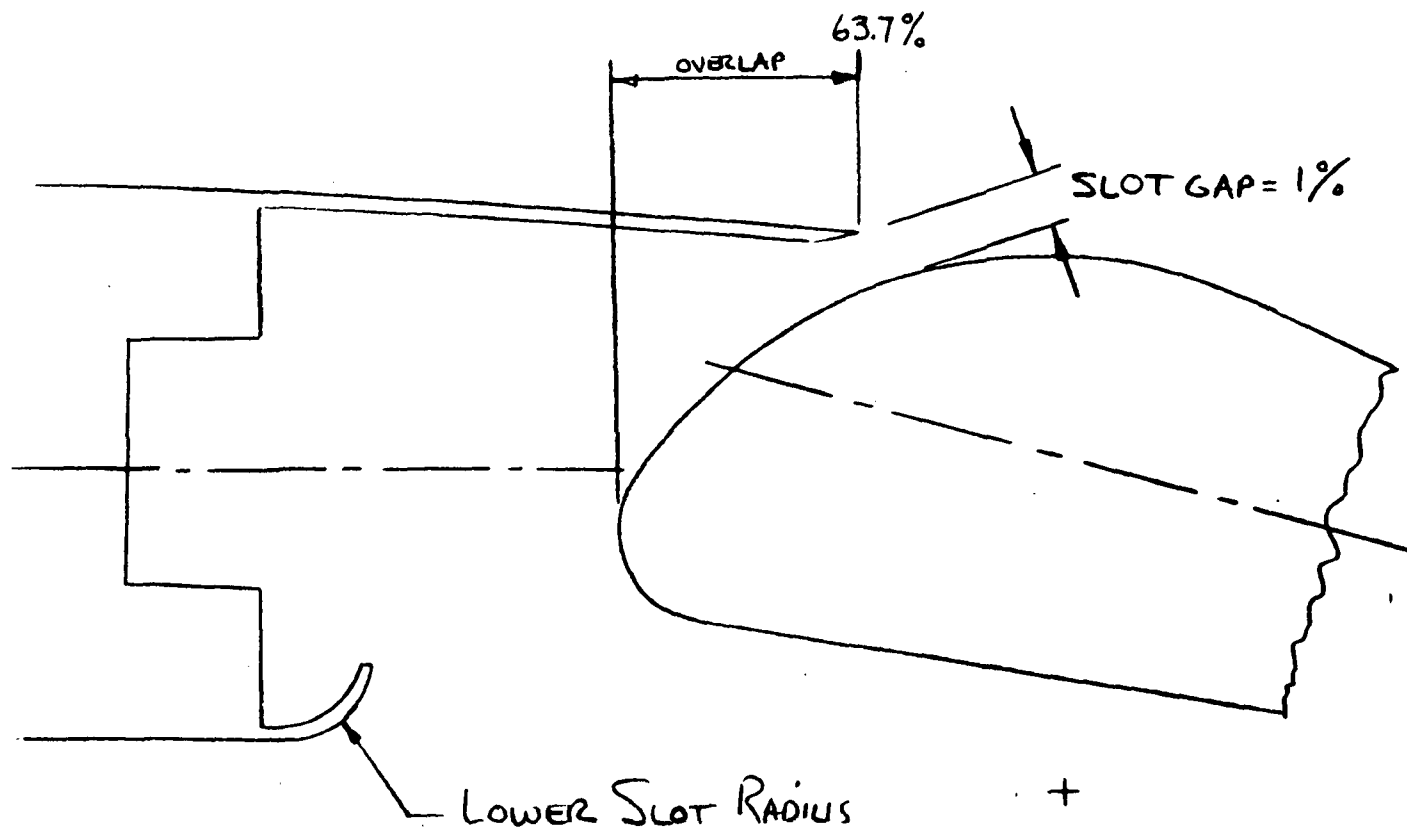
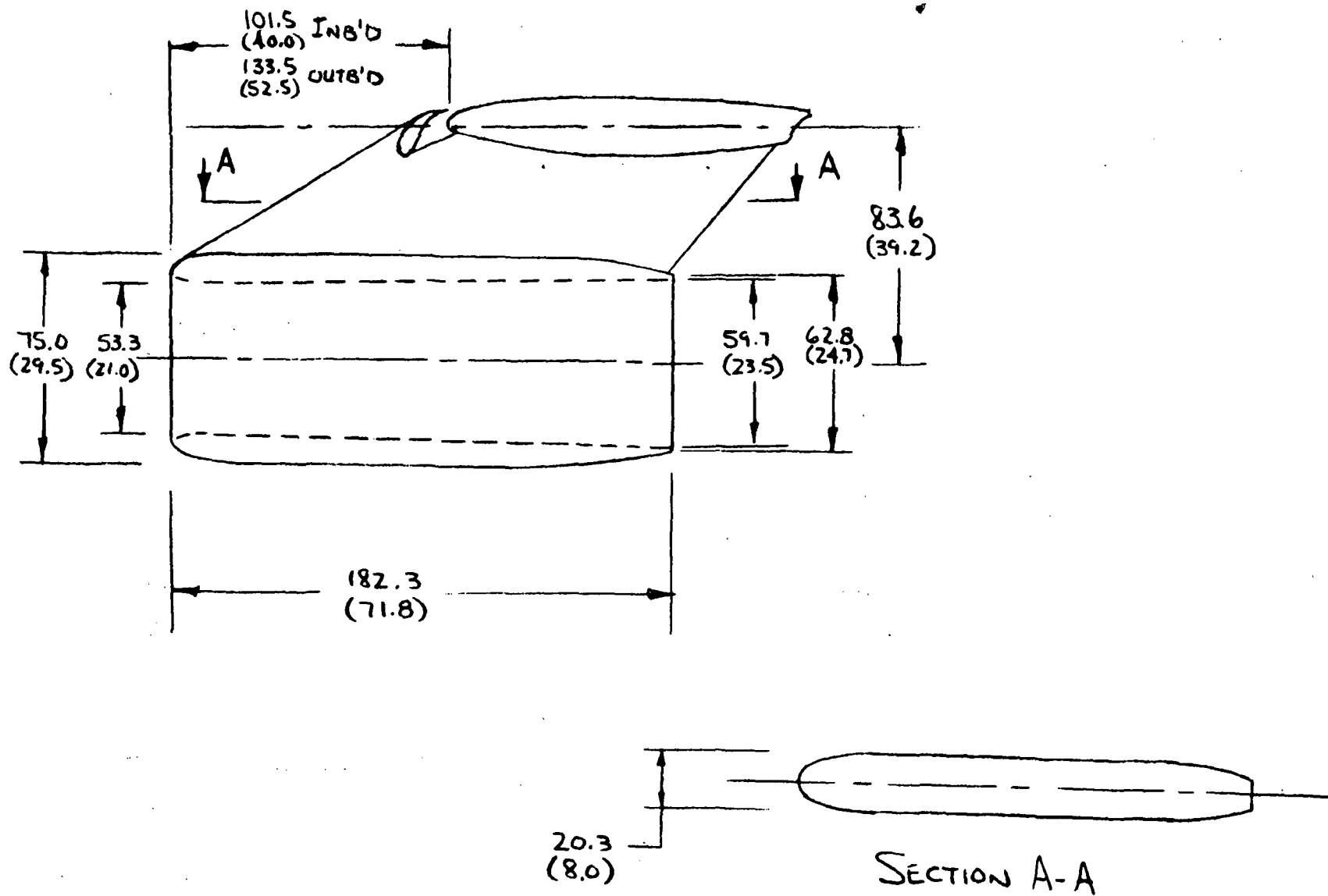
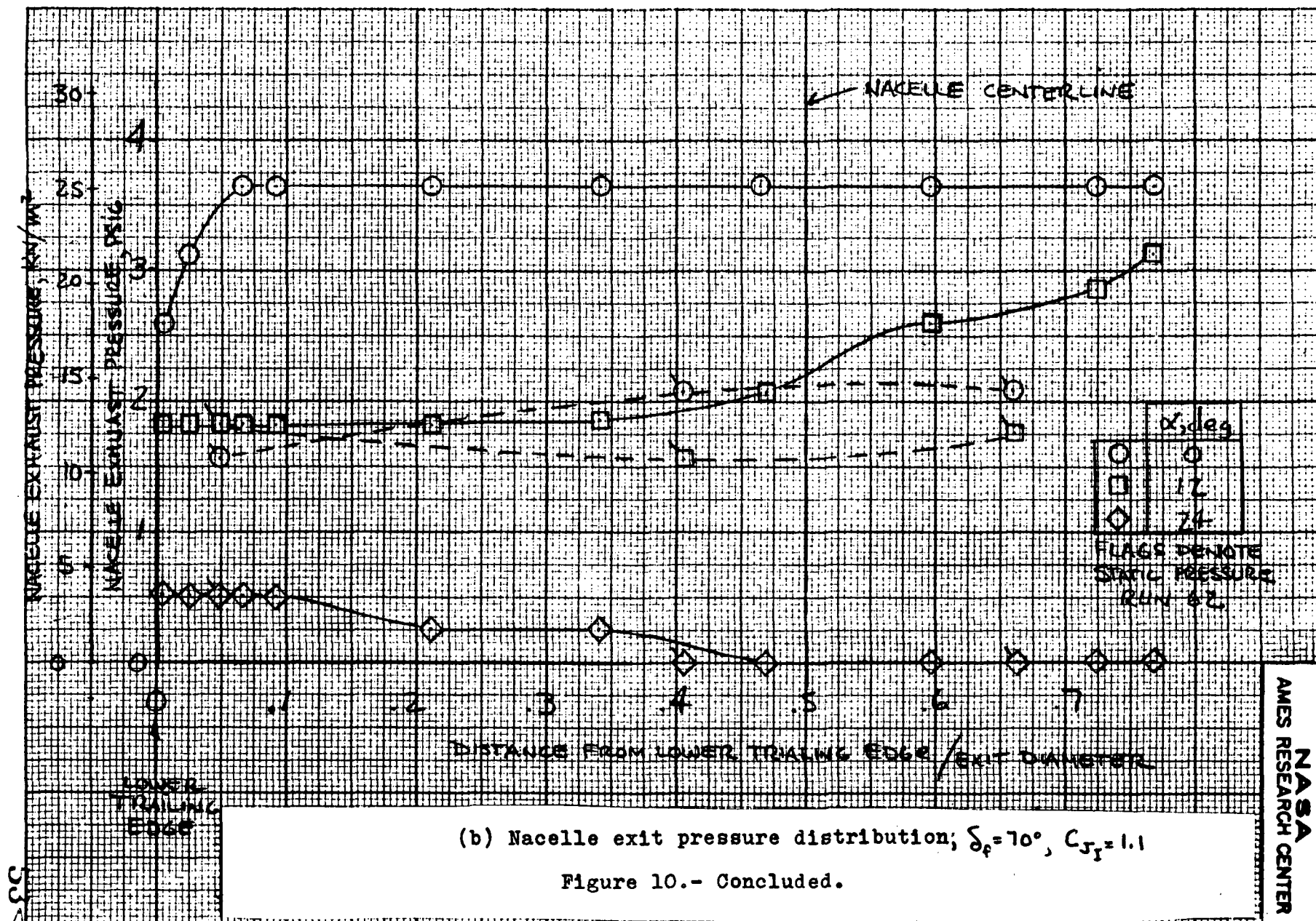


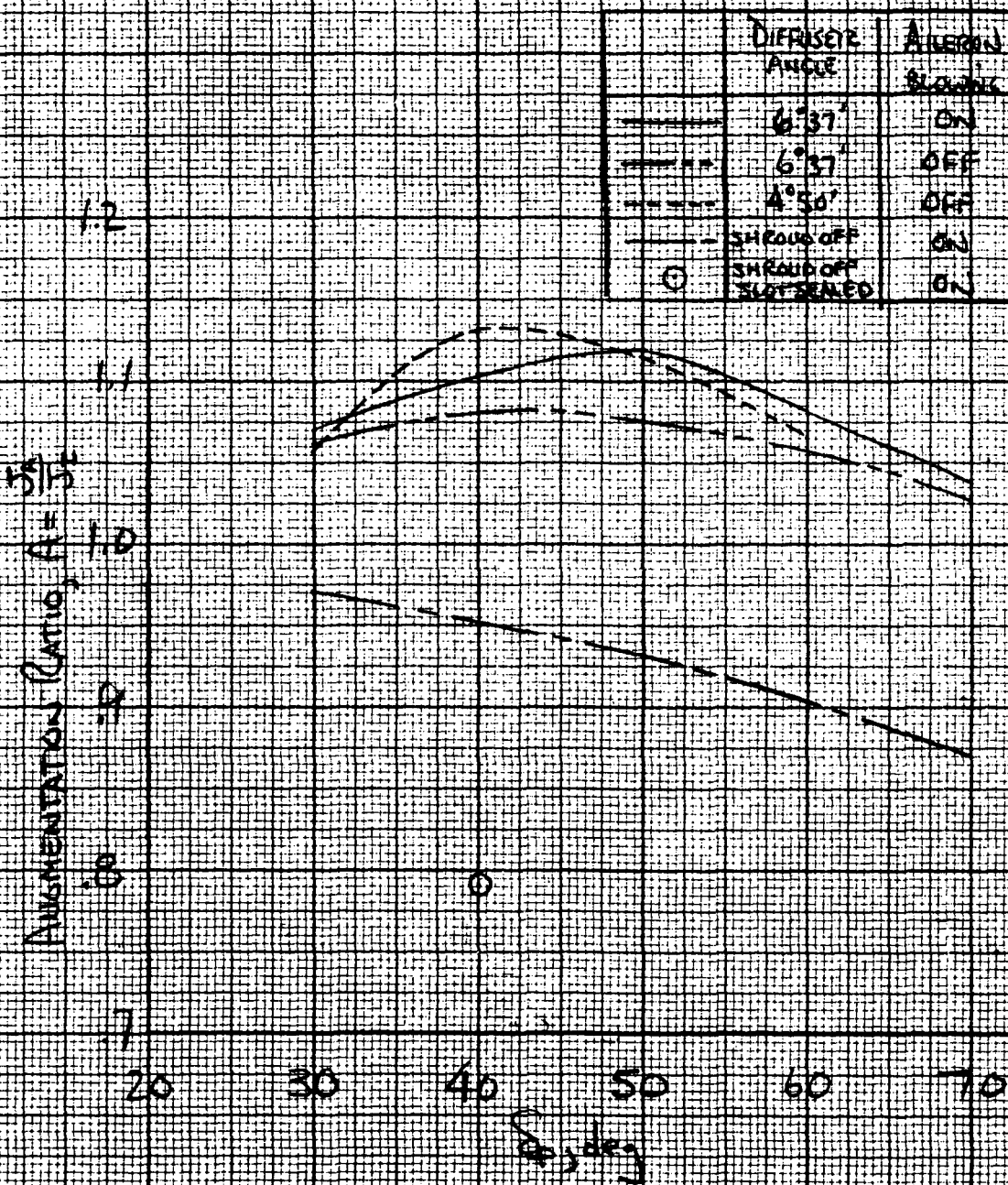
Figure 9.- Slotted aileron geometry.



(a) Basic geometry

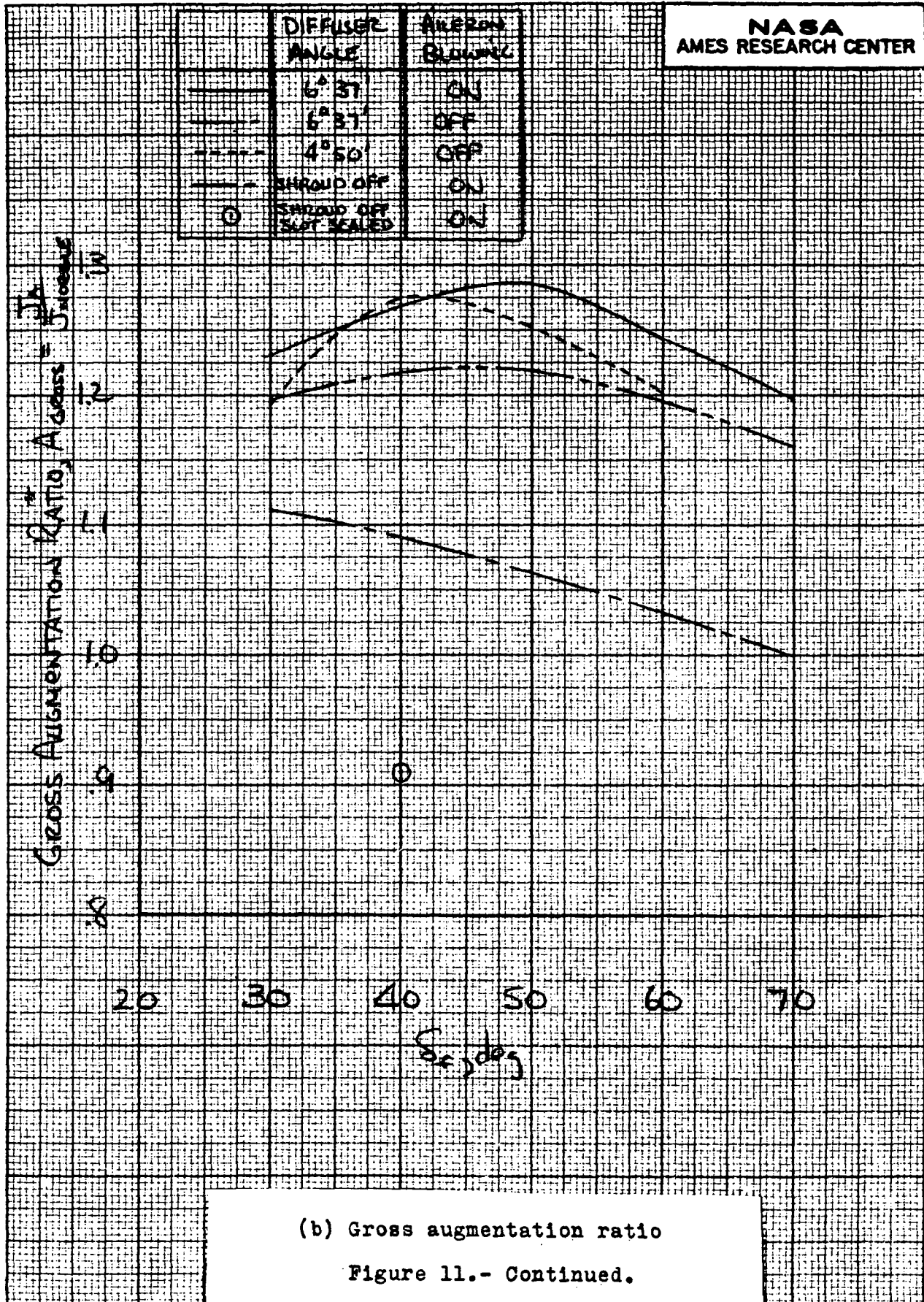
Figure 10.- Flow-thru nacelle geometry and flow characteristic.





(a) Net augmentation ratio

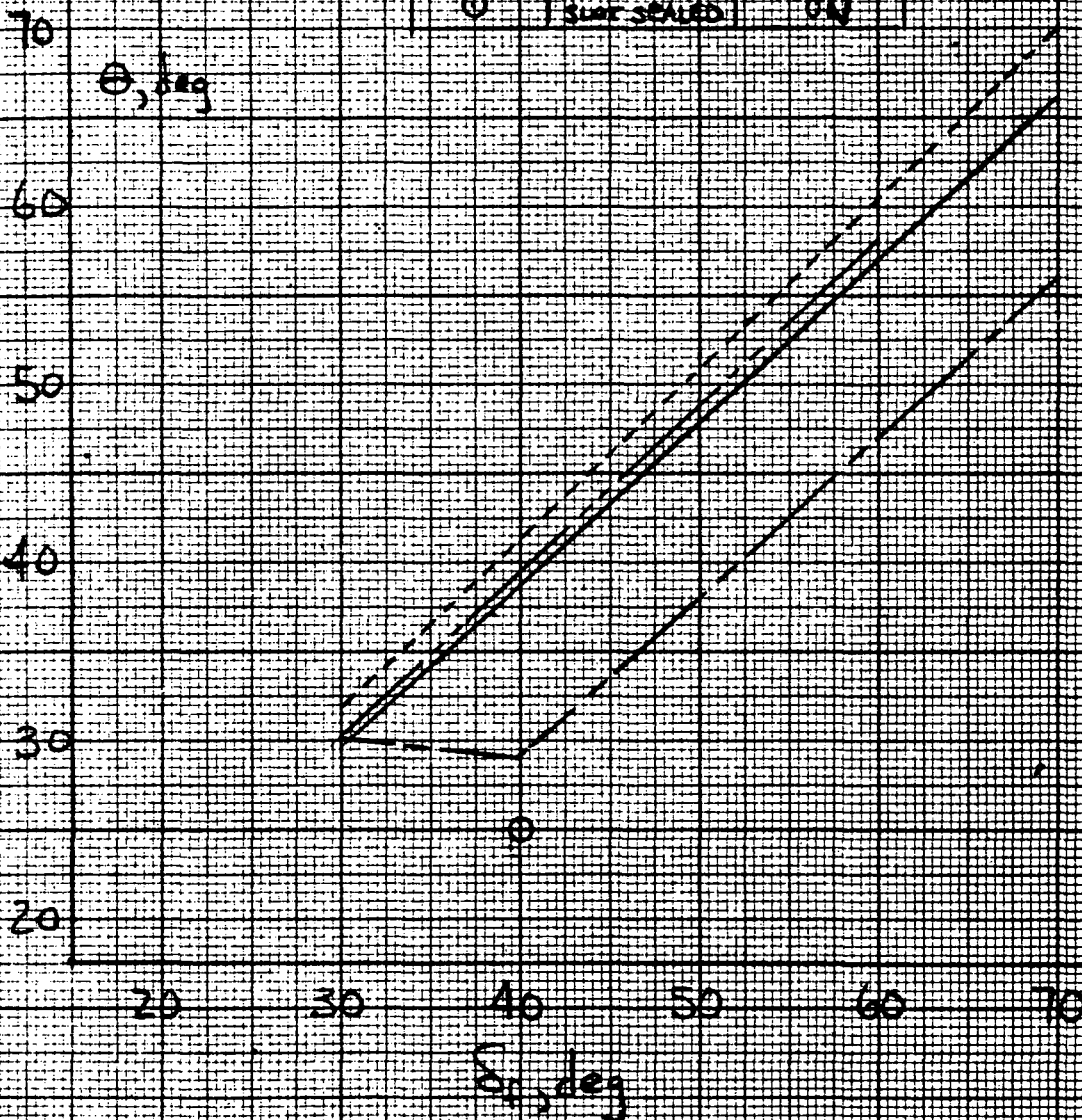
Figure 11.- Static augmentor wing performance.



(b) Gross augmentation ratio

Figure 11.- Continued.

	DIFFUSER ANGLE	AUXILIARY BLOWING
—	6°37'	ON
—	6°37'	OFF
—	4°50'	OFF
—	SHROUD OFF	ON
○	SHROUD OFF SHROUD OFF SURF SEALED	ON



(c) Jet turning

Figure 11.- Concluded.



FIRST RUN IS 7.

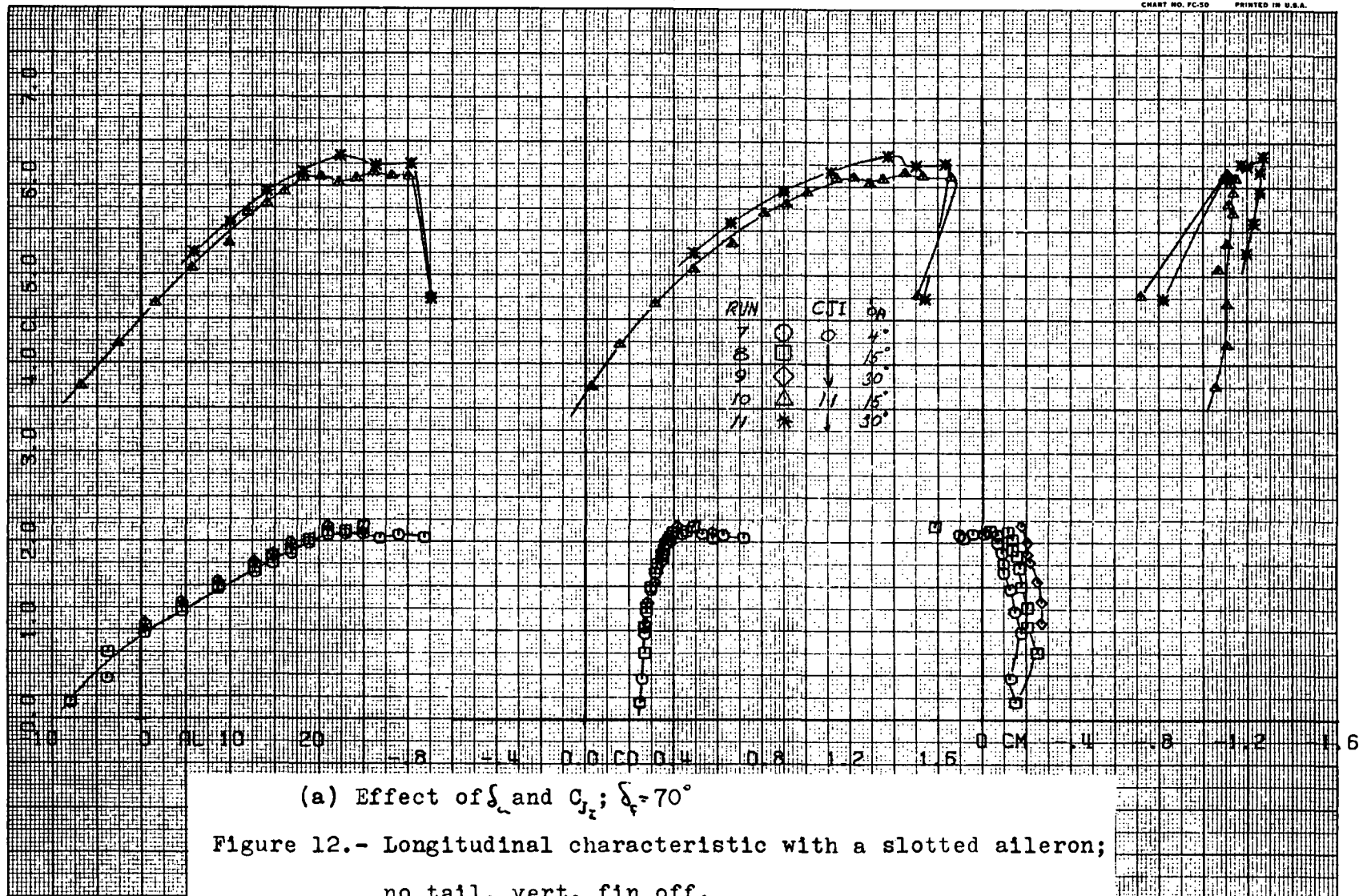
COMPLØT®

OMNIGRAPHIC®

HOUSTON INSTRUMENT

BELL LAIRE, TEXAS

CHART NO. FC-50 PRINTED IN U.S.A.



(a) Effect of  $\delta_a$  and  $C_{j_z}$ ;  $\delta_f = 70^\circ$

Figure 12.- Longitudinal characteristic with a slotted aileron;  
no tail, vert. fin off.

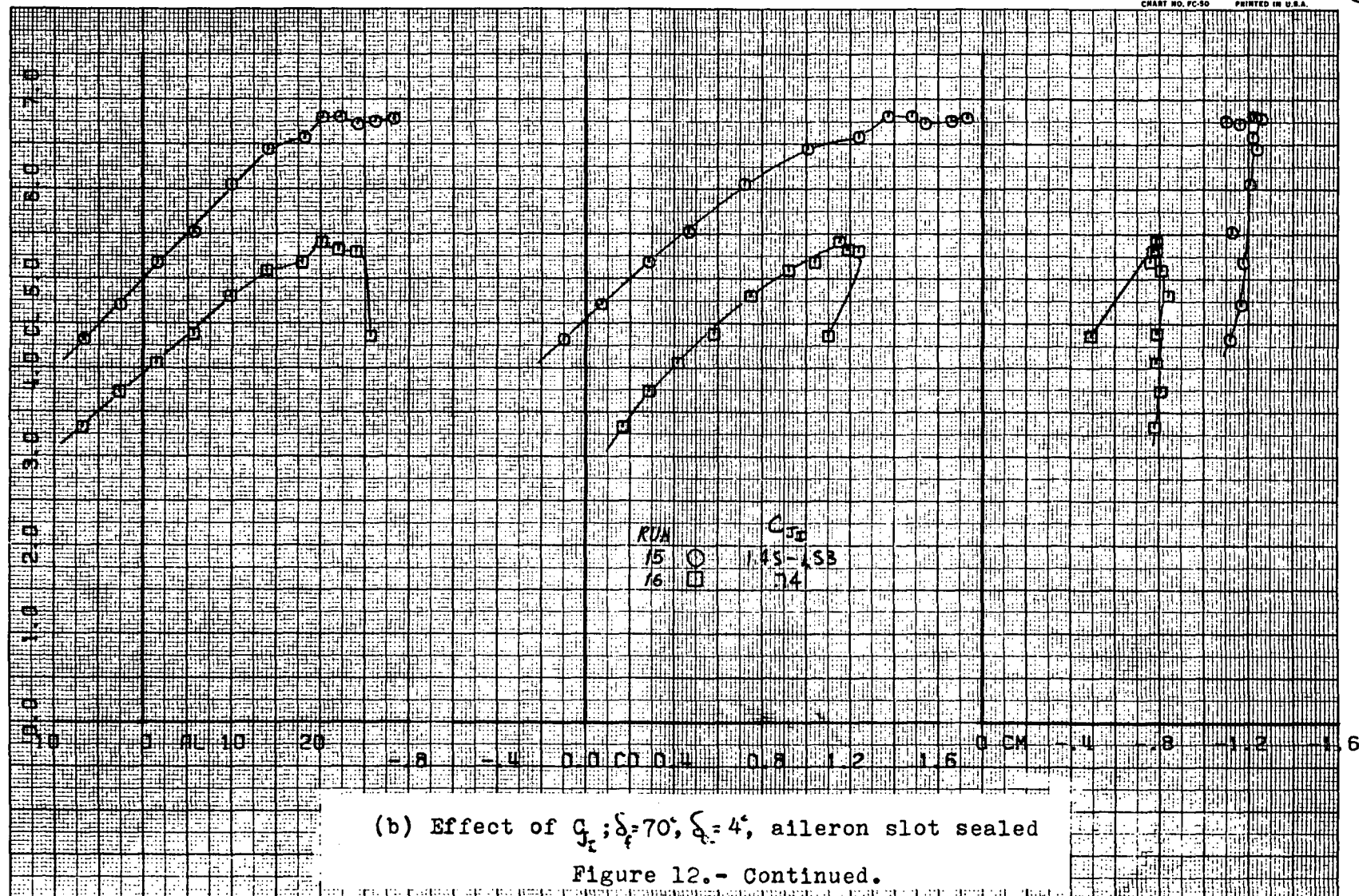
57<

FIRST RUN 15 15.

COMPLØT®

OMNIGRAPHIC®

HOUSTON INSTRUMENT  
BELLARE, TEXAS  
CHART NO. FC-50 PRINTED IN U.S.A.



126

30

126



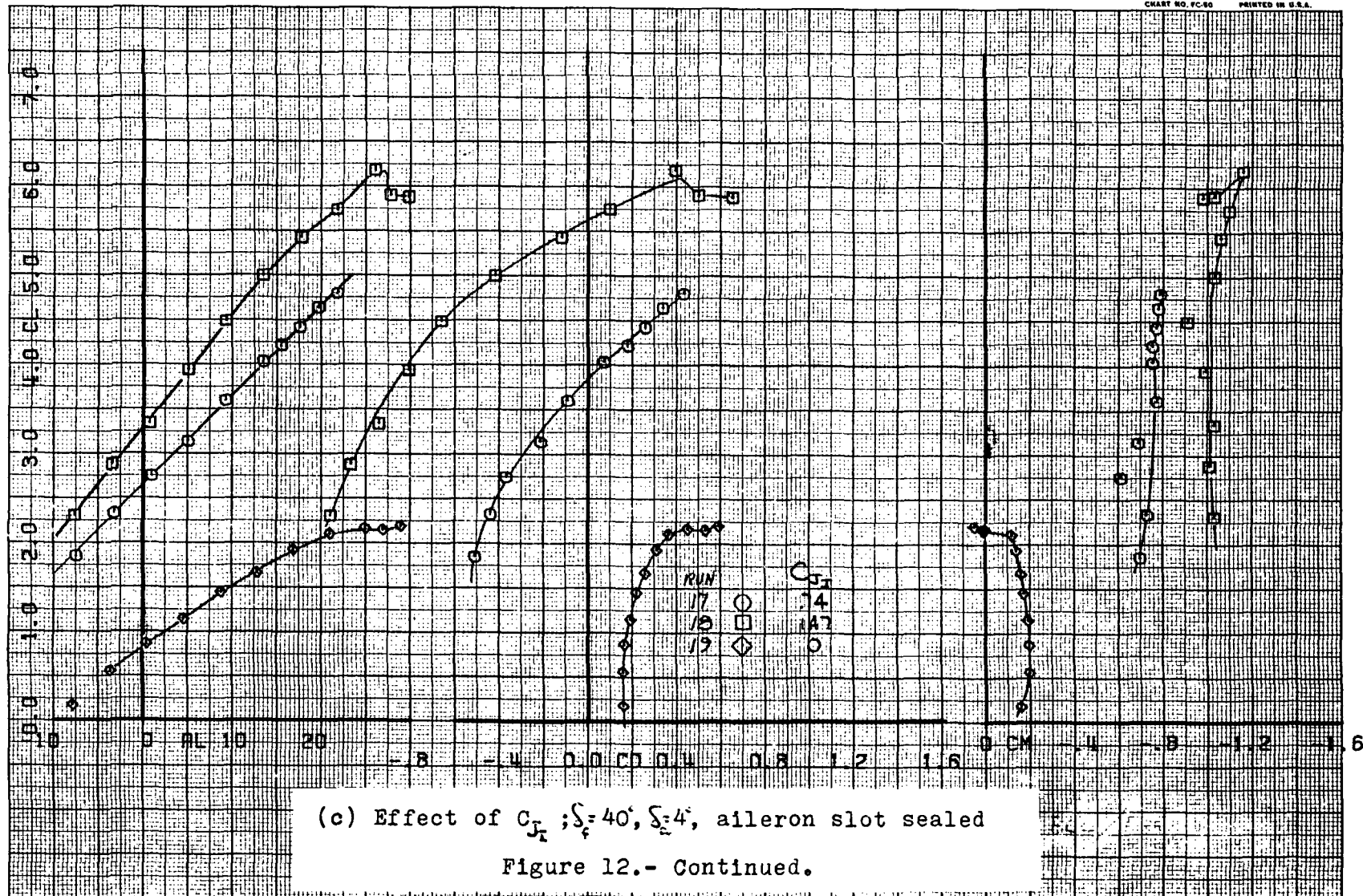
FIRST RUN IS 17.

COMPLØT®

OMNIGRAPHIC®

HOUSTON INSTRUMENT  
BELLARE, TEXAS  
CHART NO. FC-50 PRINTED IN U.S.A.

3



(c) Effect of  $C_L$ ;  $\delta_f = 40^\circ$ ,  $\delta_e = 4^\circ$ , aileron slot sealed

Figure 12.- Continued.

59 >

31

12c

Run	Configuration
12	ORIGINAL
13	LOWER SLAT RADIIUS REMOVED
14	LOWER SLAT RAD. CRP AND OVERLAP EXTENDED

$C_L$

0.08

0.04

0.00

-0.04

-0.08

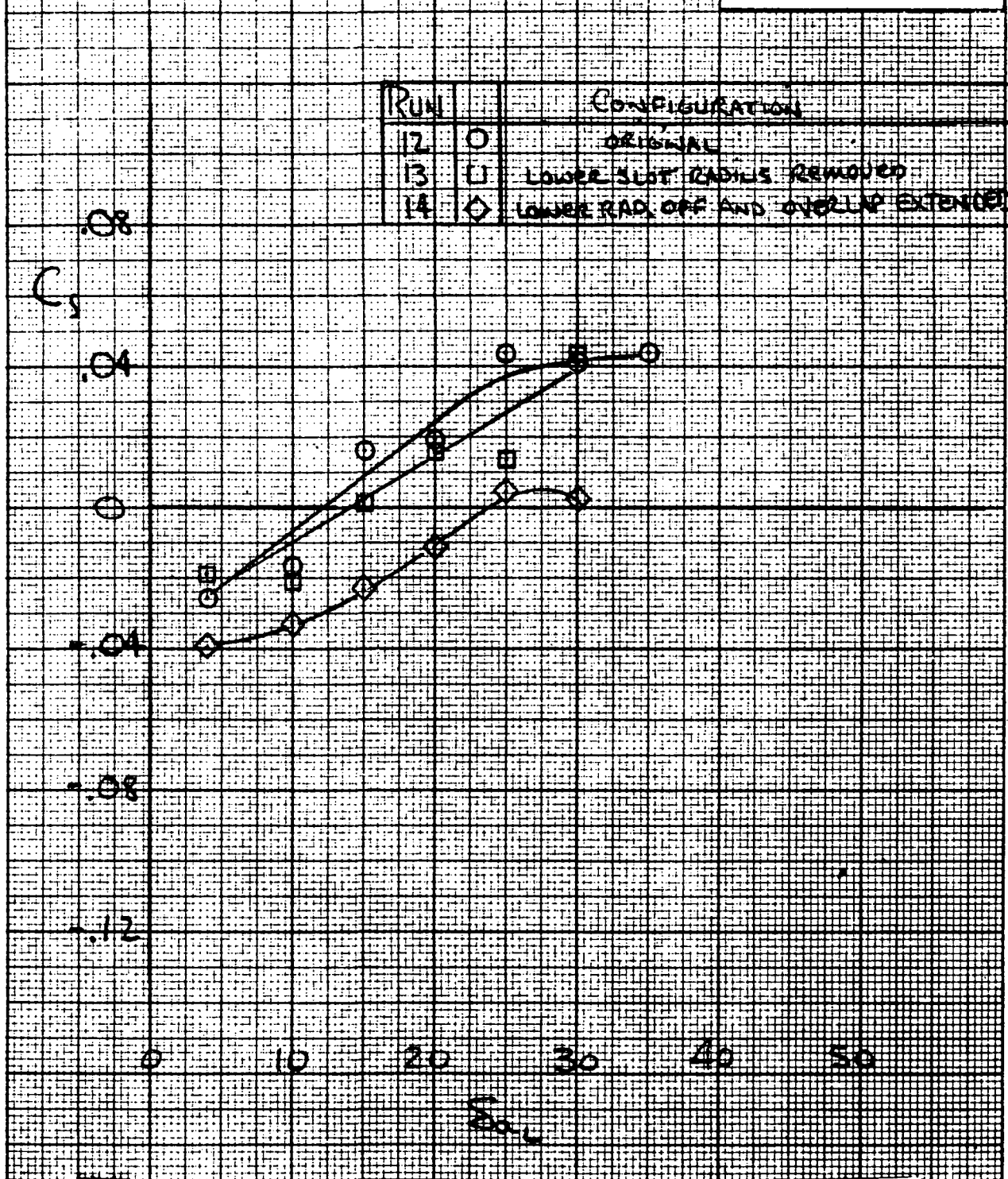
-0.12

0 10 20 30 40 50

$\delta_a$

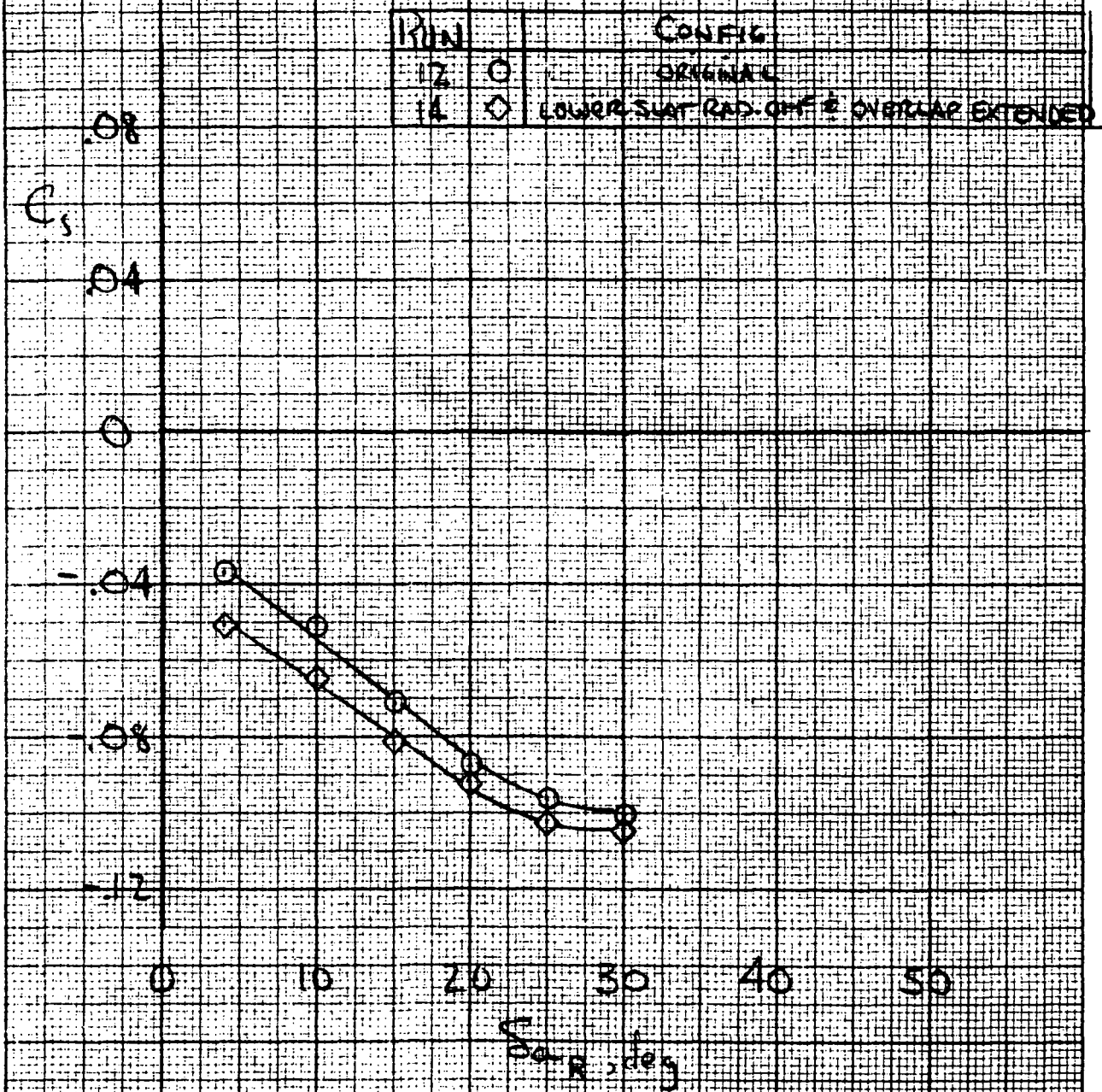
(d) Aileron control effectiveness;  $\delta_f 70^\circ$ ,  $C_L 1.1$ ,  $\alpha 0^\circ$

Figure 12.- Continued.



(e) Aileron control effectiveness;  $\delta_f = 70^\circ$ ,  $C_{J_1} = 1.1$ ,  $\alpha = 0^\circ$

Figure 12.- Continued.



(f) Aileron control effectiveness;  $S_f=70^\circ$ ,  $C_{L_T}=1.1$ ,  $\alpha=12^\circ$

Figure 12.- Concluded.



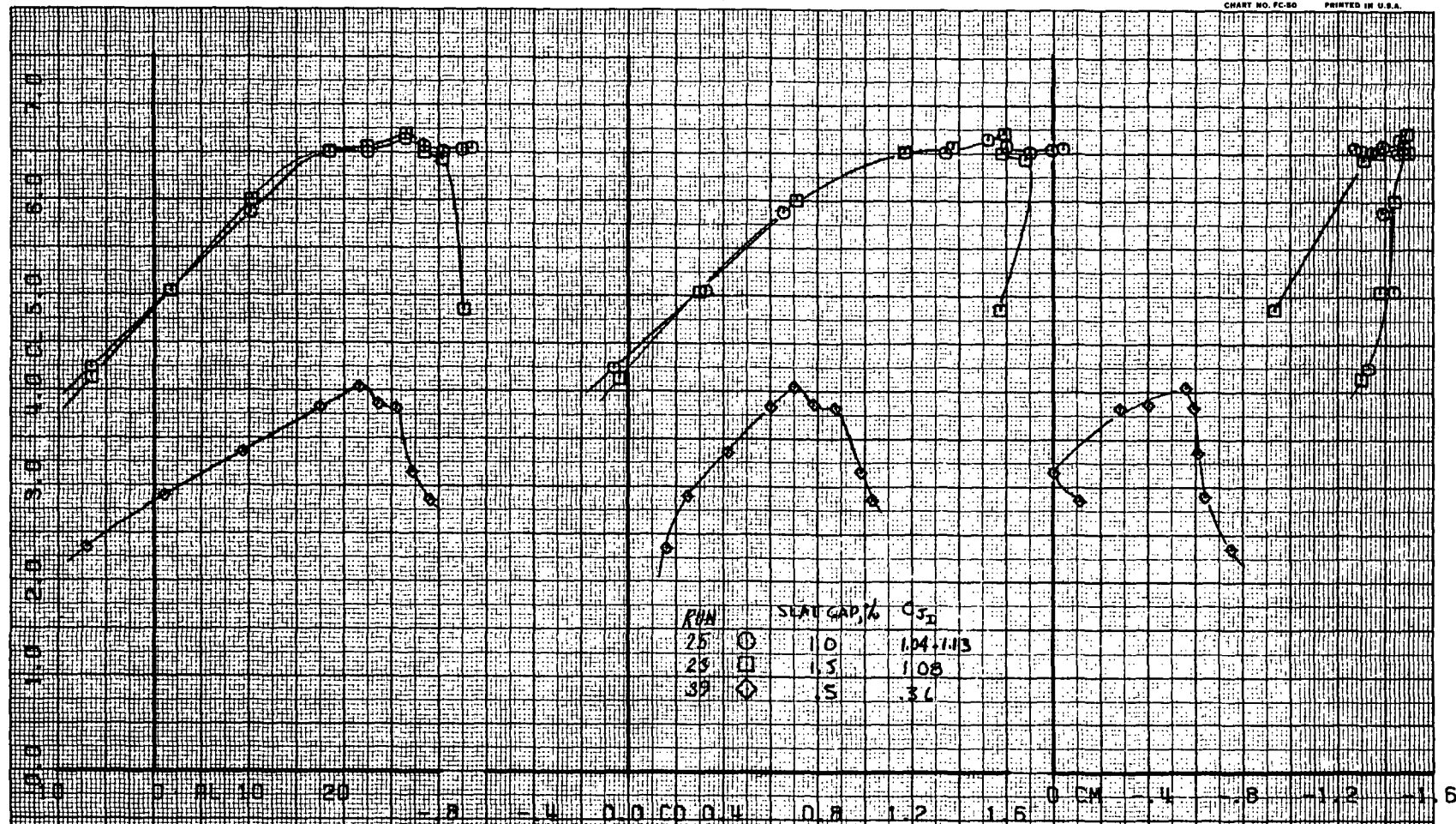
FIRST RUN IS 25.

COMPLLOT

OMNIGRAPHIC

HOUSTON INSTRUMENT  
BELLARE, TEXAS  
CHART NO. FC-80 PRINTED IN U.S.A.

4



(a) Effect of slat gap

Figure 13.- Longitudinal characteristic for various wing leading edge slat gaps;  $\delta_f = 70^\circ$ ; no tail, vert. fin off.

63  
^

32

13a

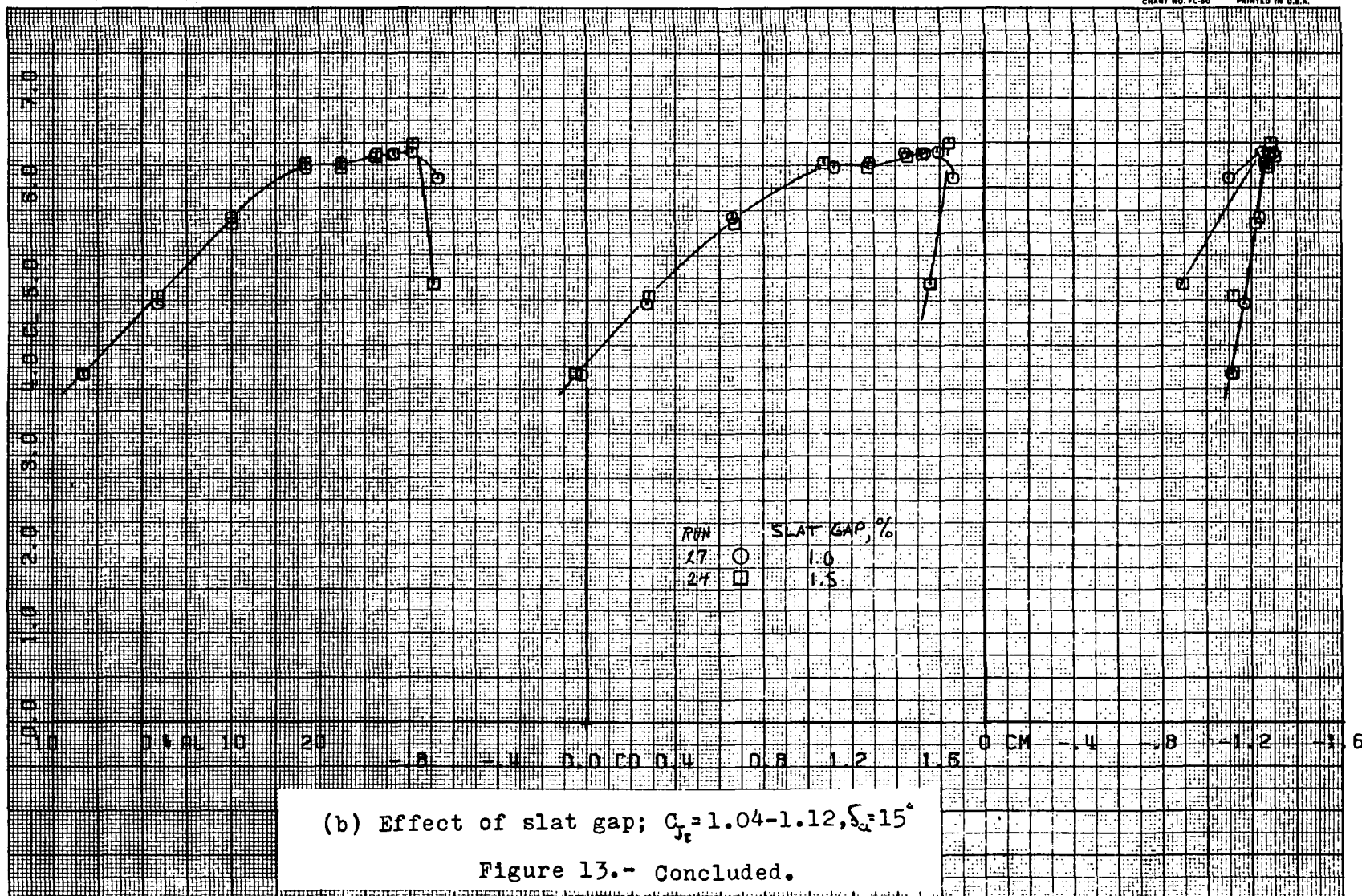
FIRST RUN IS 27.

COMPL0T\*

OMNIGRAPHIC\*

HOUSTON INSTRUMENT  
BELL LAIRE, TEXAS

CHART NO. PC-50 PRINTED IN U.S.A.



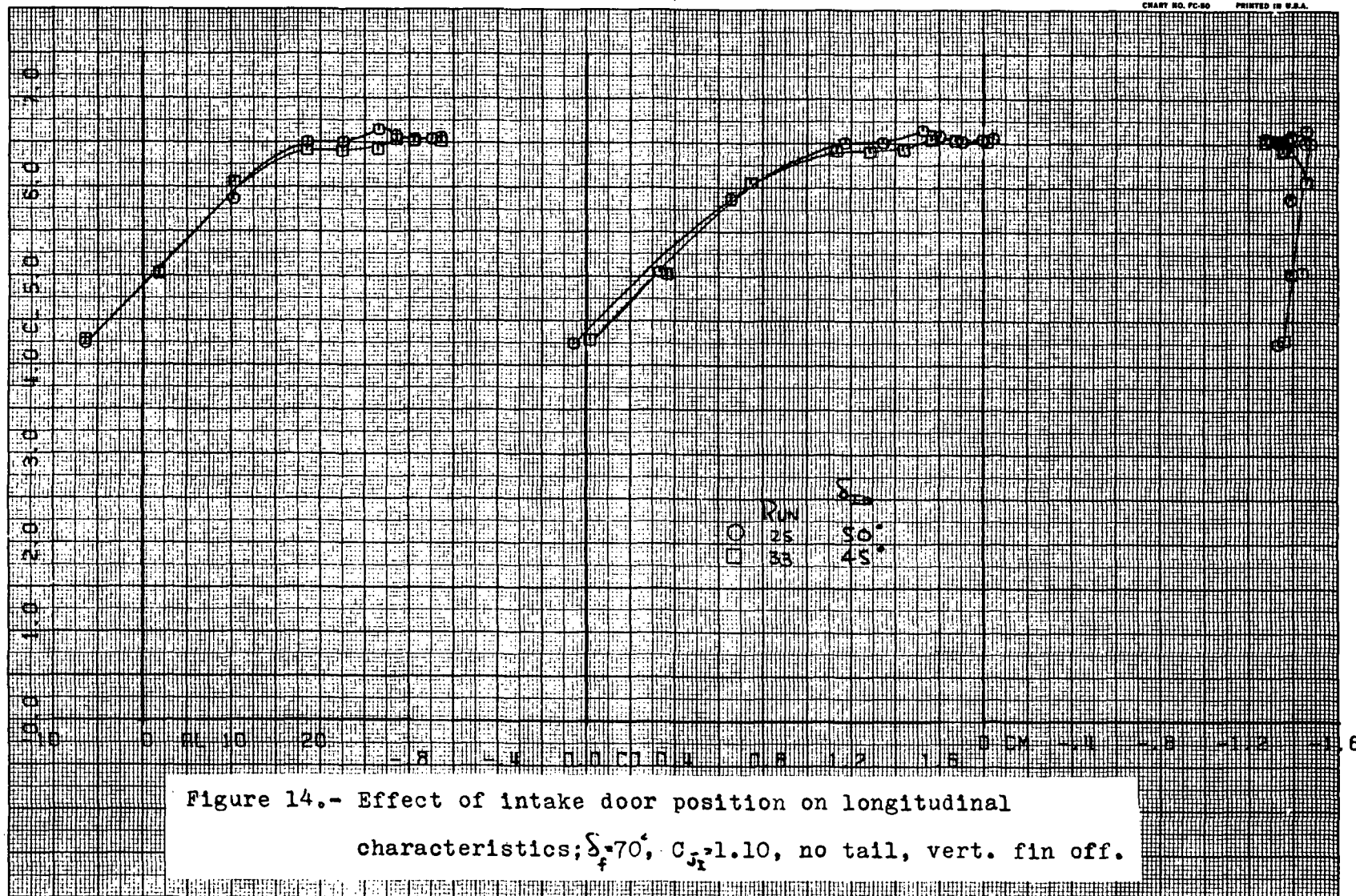
FIRST RUN IS 25.

COMPL0T®

OMNIGRAPHIC®

HOUSTON INSTRUMENT  
DIVISION OF HOUSTON INSTRUMENTS  
HOUSTON, TEXAS

CHART NO. PC-50 PRINTED IN U.S.A.

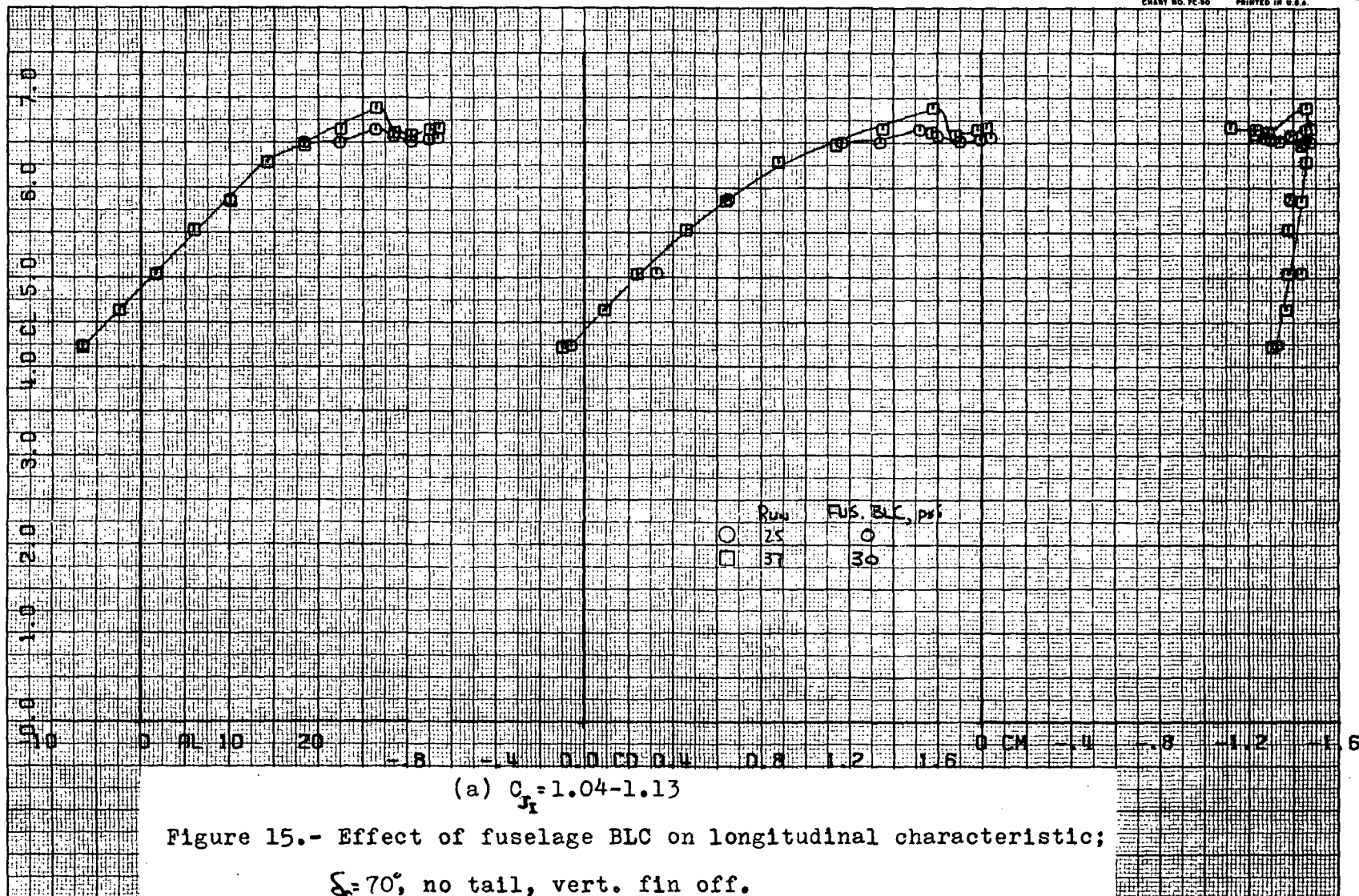


FIRST RUN IS 25.

COMPLØT

OMNIGRAPHIC

HOUSTON INSTRUMENT  
DIVISION OF CHRYSLER CORPORATION  
BELLAIR, TEXAS  
CHART NO. FC-50 PRINTED IN U.S.A.



(a)  $C_{p_i} = 1.04-1.13$

Figure 15.- Effect of fuselage BLC on longitudinal characteristic;

$\xi_f = 70^\circ$ , no tail, vert. fin off.



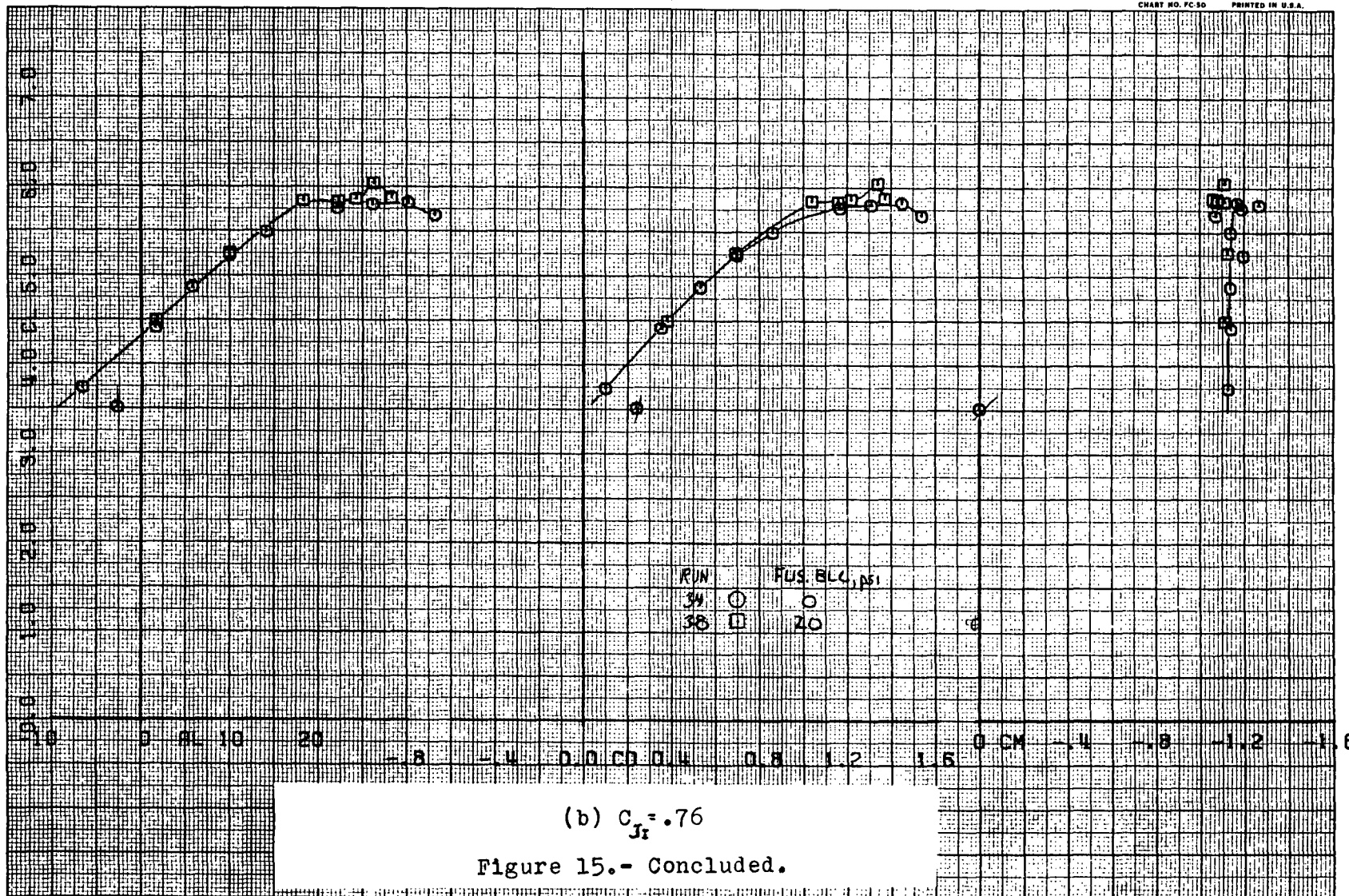
FIRST RUN IS 34.

COMPLLOT

OMNIGRAPHIC

HOUSTON INSTRUMENT  
DIVISION OF SOUTHWESTERN  
BELLAIRE, TEXAS  
CHART NO. FC-50 PRINTED IN U.S.A.

9



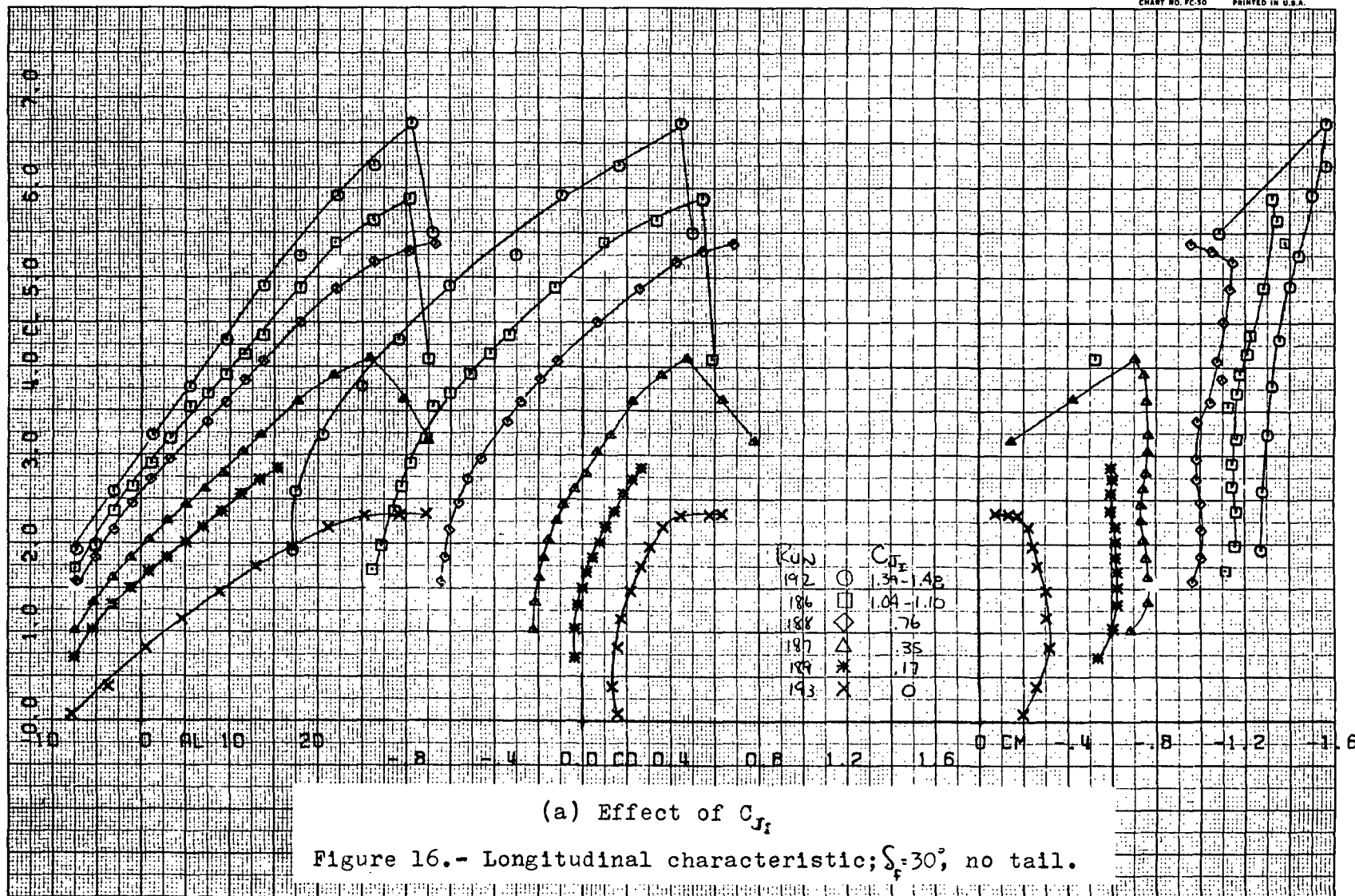
(b)  $C_{Jr} = .76$

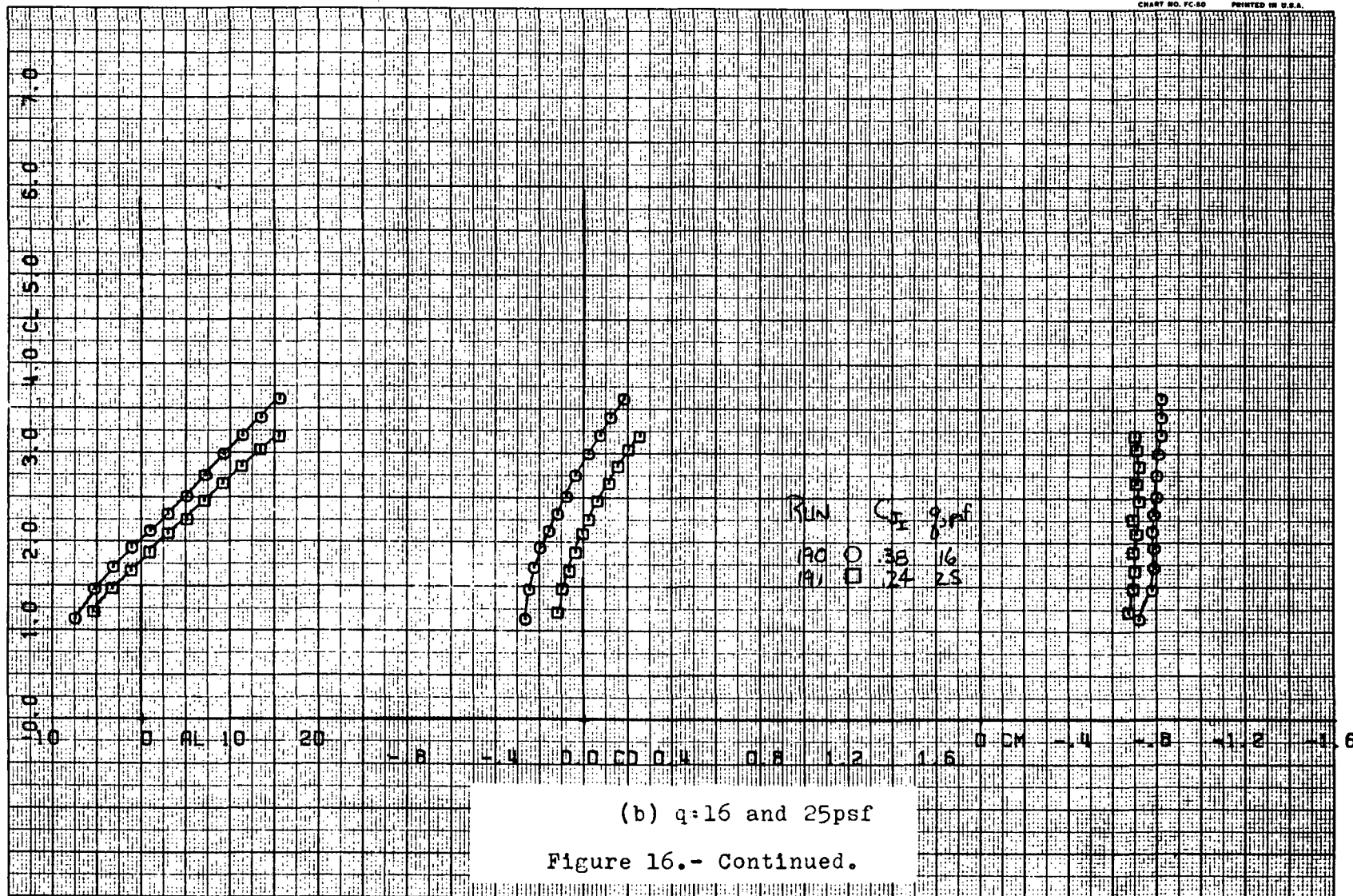
Figure 15.- Concluded.

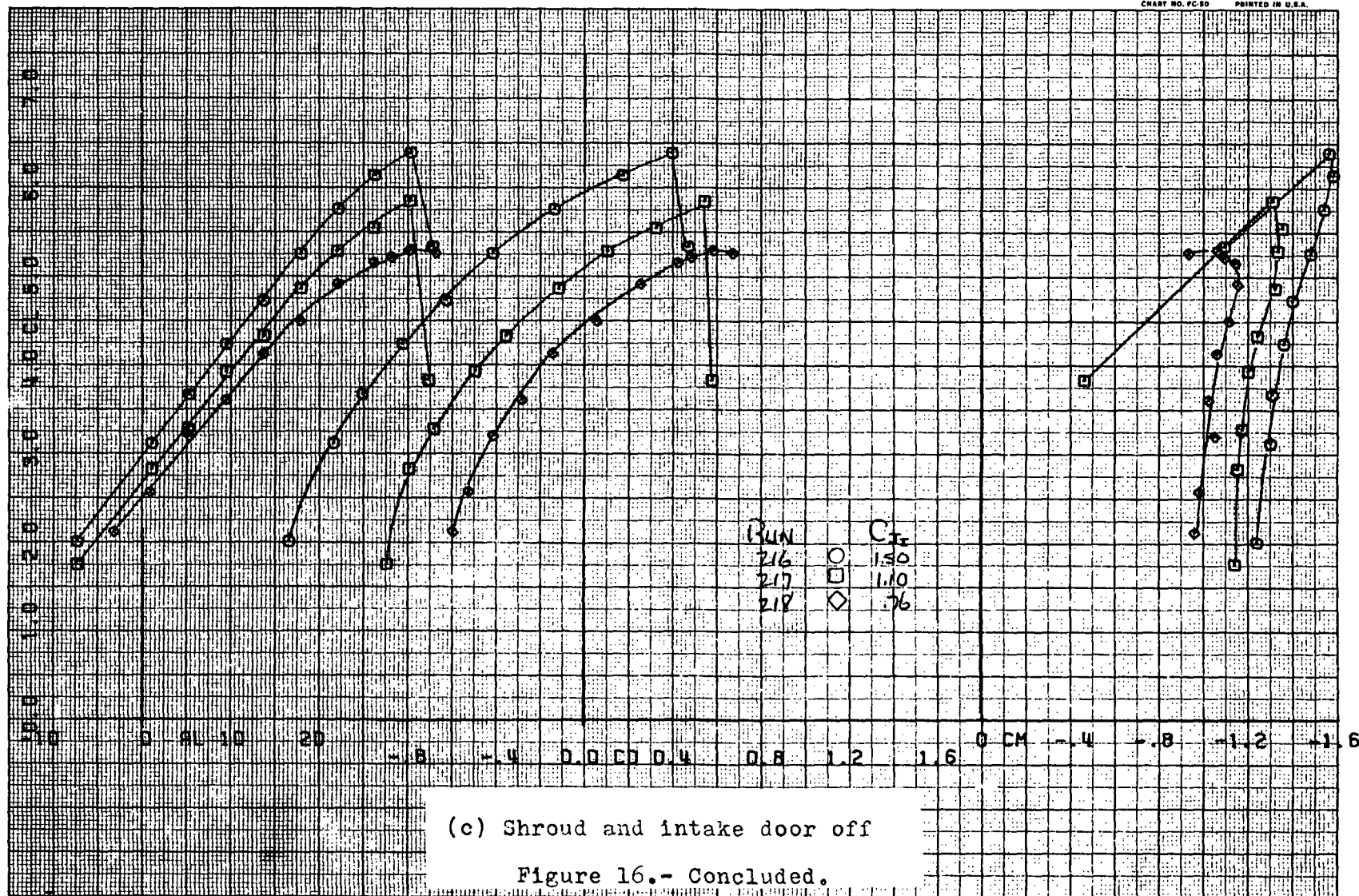
677

37

156







20

19

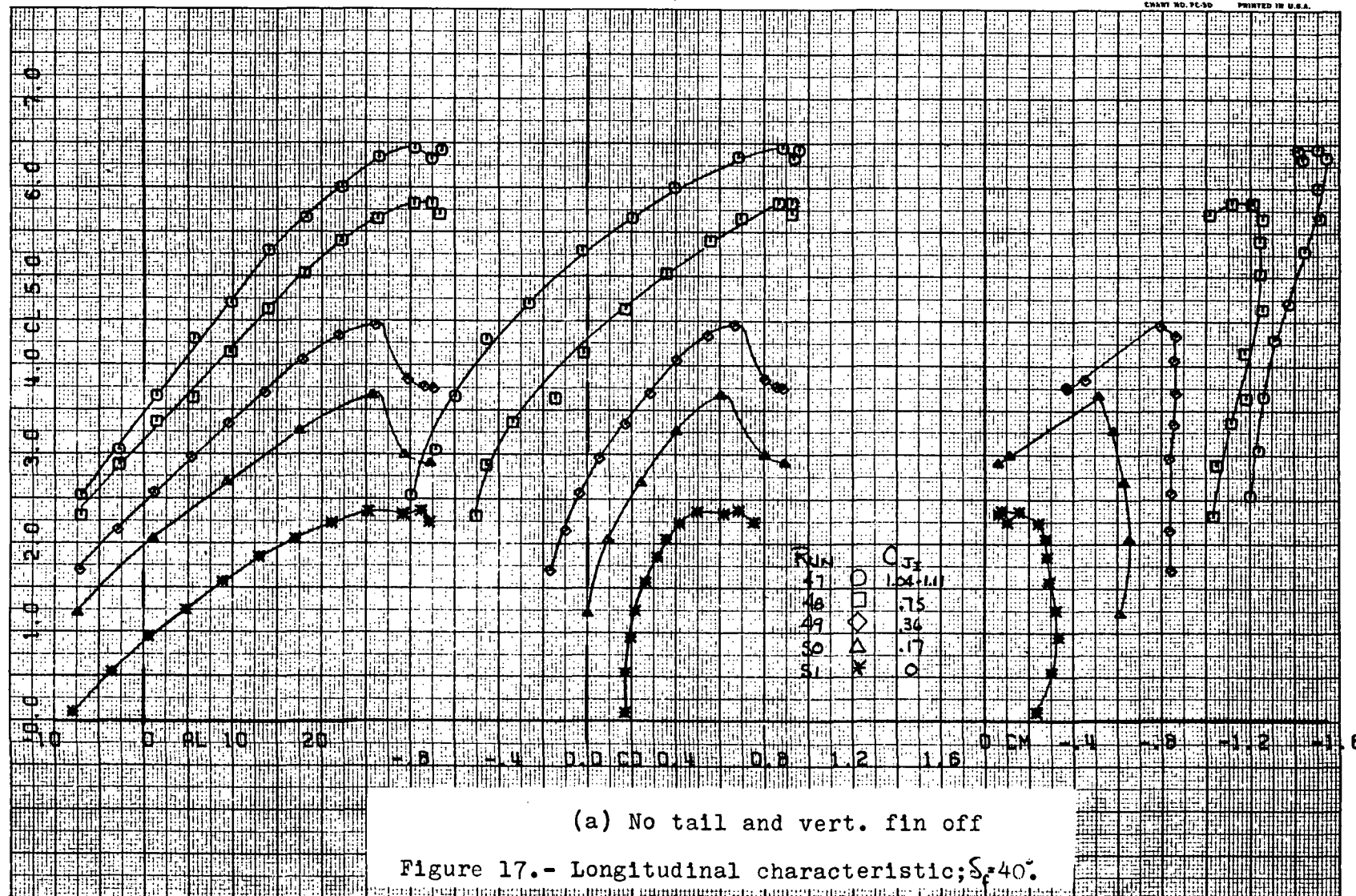
16c

FIRST RUN 13 47.

COMPL0T

OMNIGRAPHIC

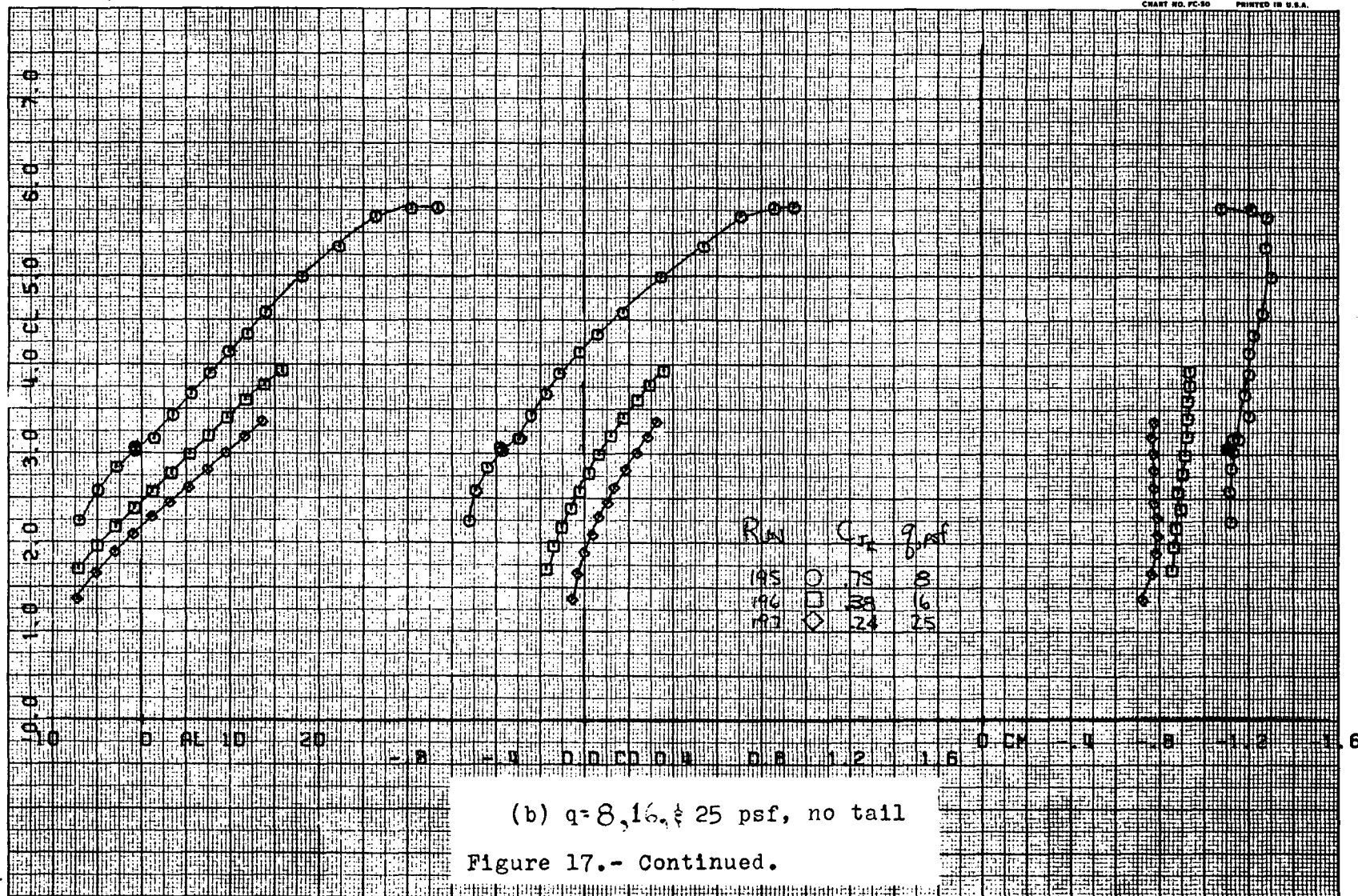
HOUSTON INSTRUMENT  
DIVISION OF HOUSTON LUBRICANTS  
BELLAIRE, TEXAS  
CHART NO. 7C-50 PRINTED IN U.S.A.



(a) No tail and vert. fin off

Figure 17.- Longitudinal characteristic;  $\delta_1 40^\circ$ .





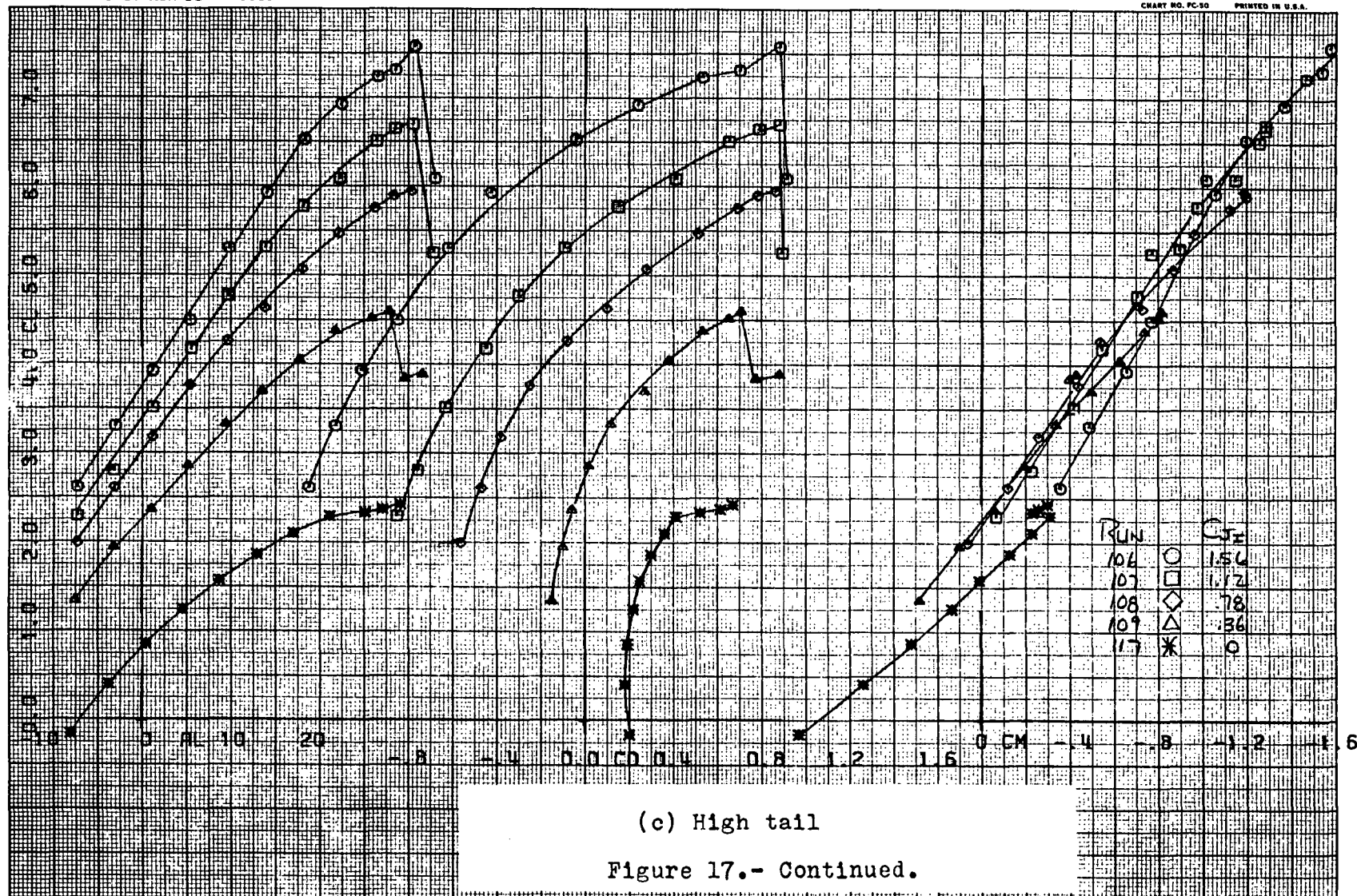
(b)  $q=8, 16, \& 25$  psf, no tail  
Figure 17.- Continued.

FIRST RUN 15 106.

COMPLØT®

OMNIGRAPHIC®

HOUSTON INSTRUMENT  
BELL LAINE, TEXAS  
CHART NO. PC-50 PRINTED IN U.S.A.

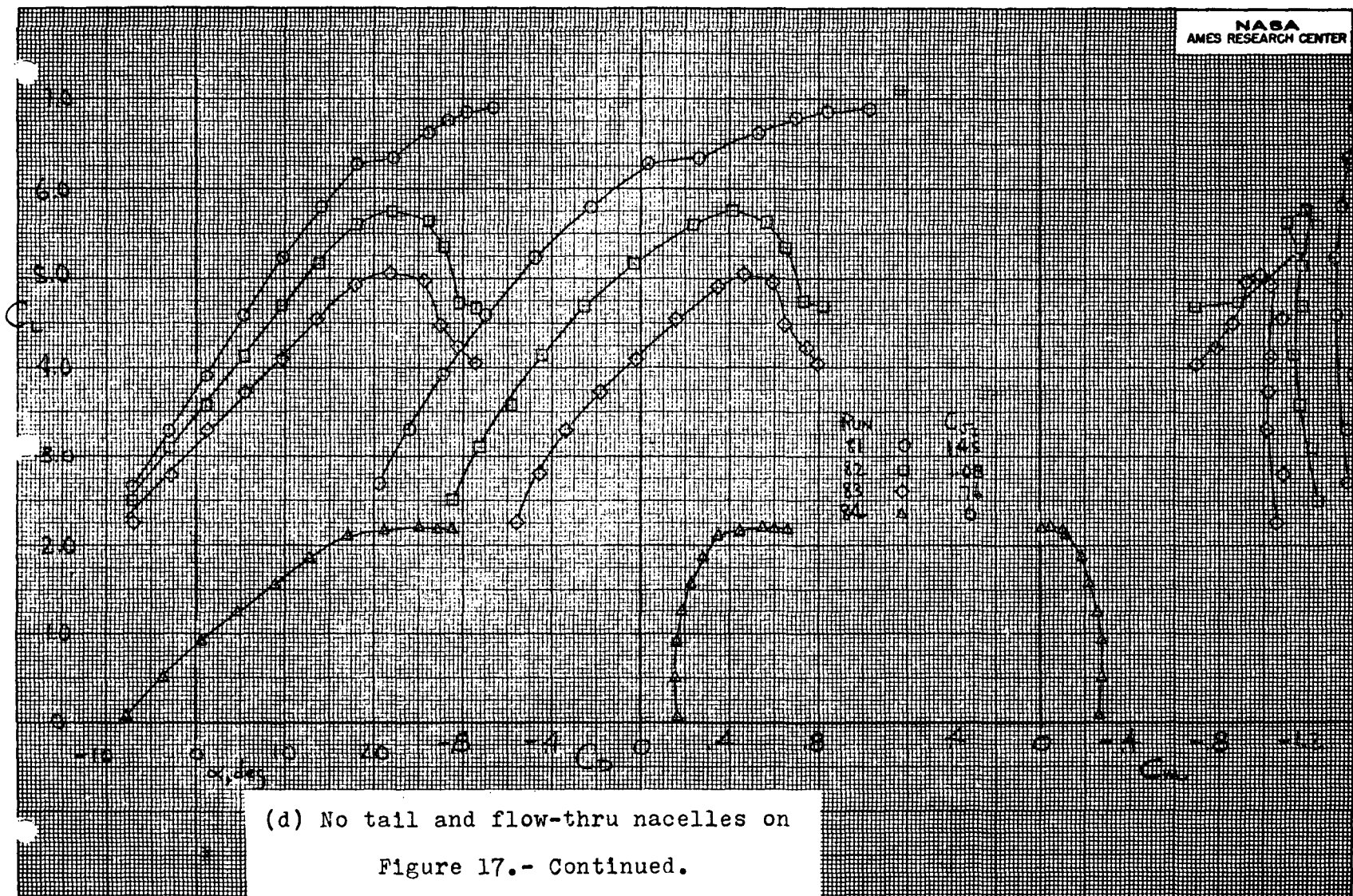


22

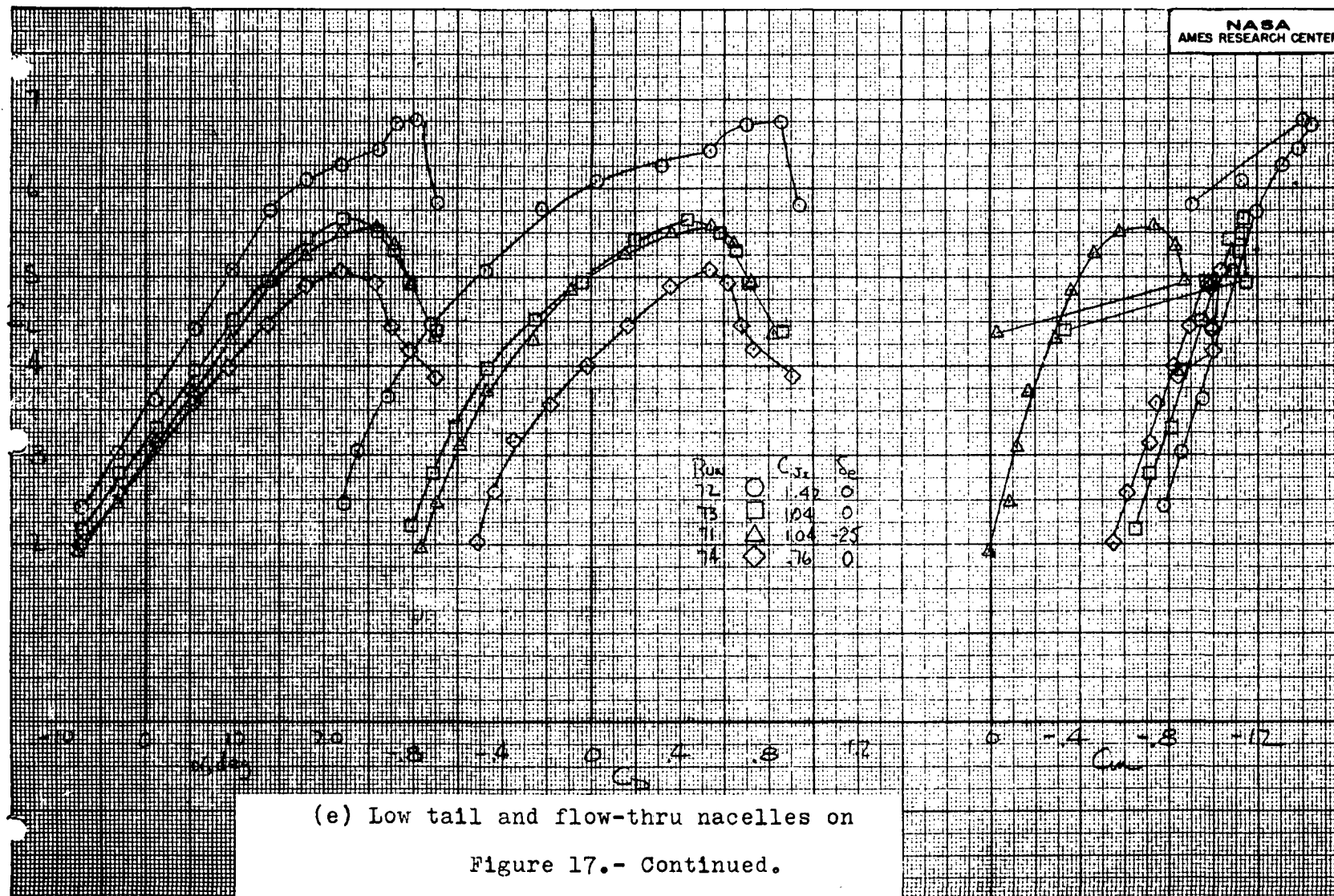
10

17c

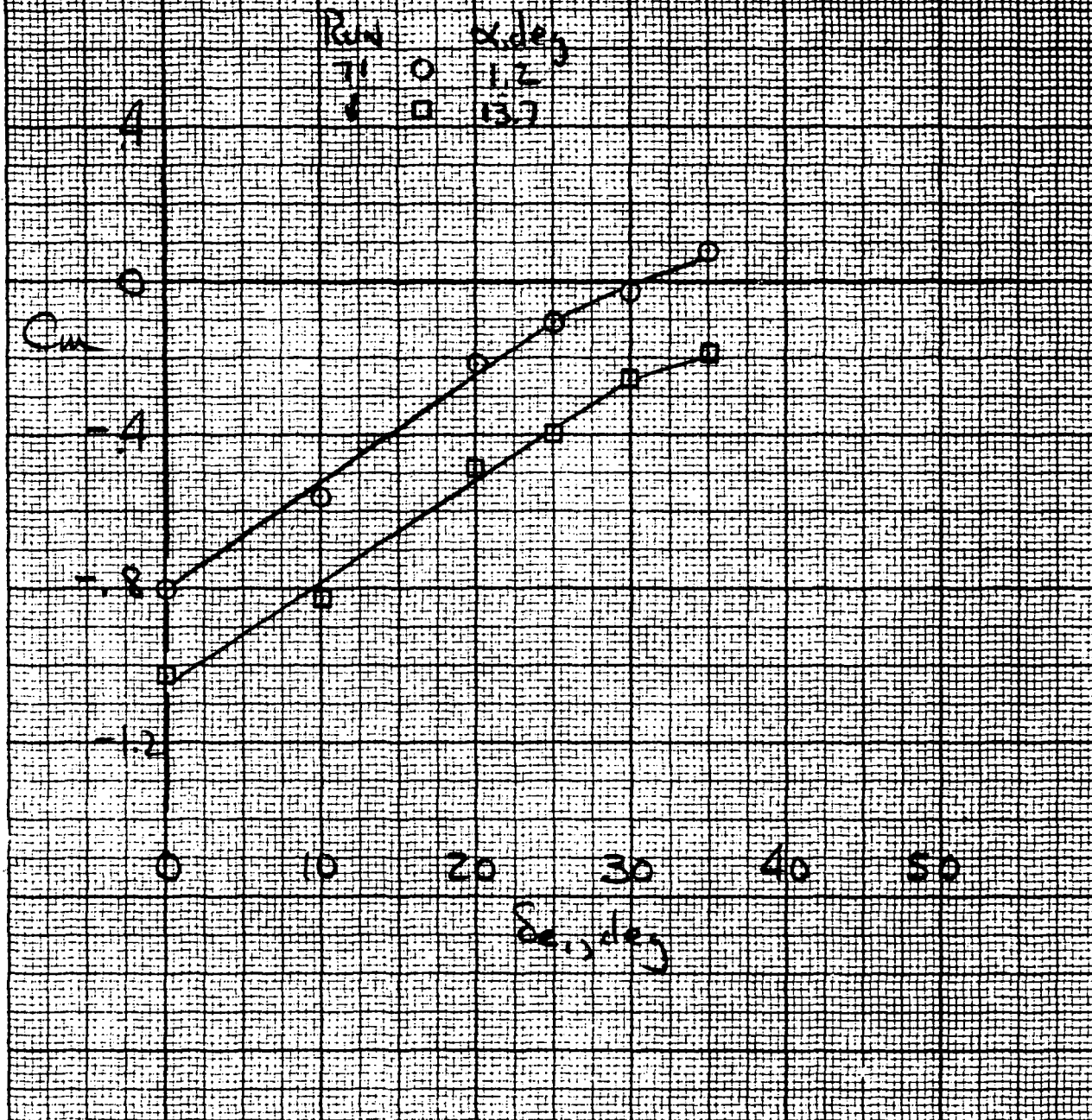
73







(e) Low tail and flow-thru nacelles on  
Figure 17.- Continued.



(f) Elevator control effectiveness; low tail and flow-thru nacelles on,  $C_{D_T} = 1.1$ ,  $\delta_{e_1} = 0^\circ$

Figure 17.- Continued.

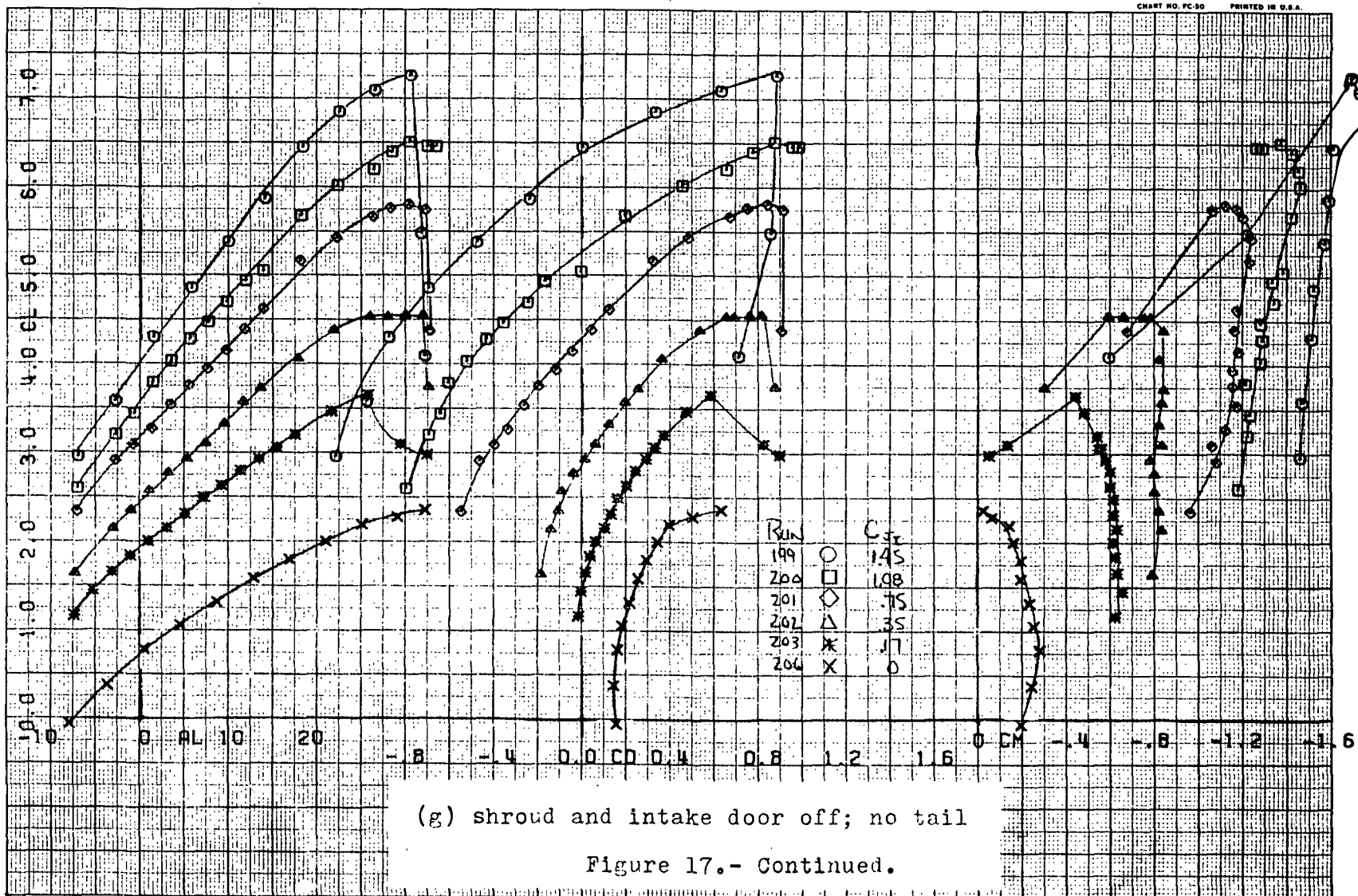
FIRST RUN 15 198.

COMPLØT®

OMNIGRAPHIC®

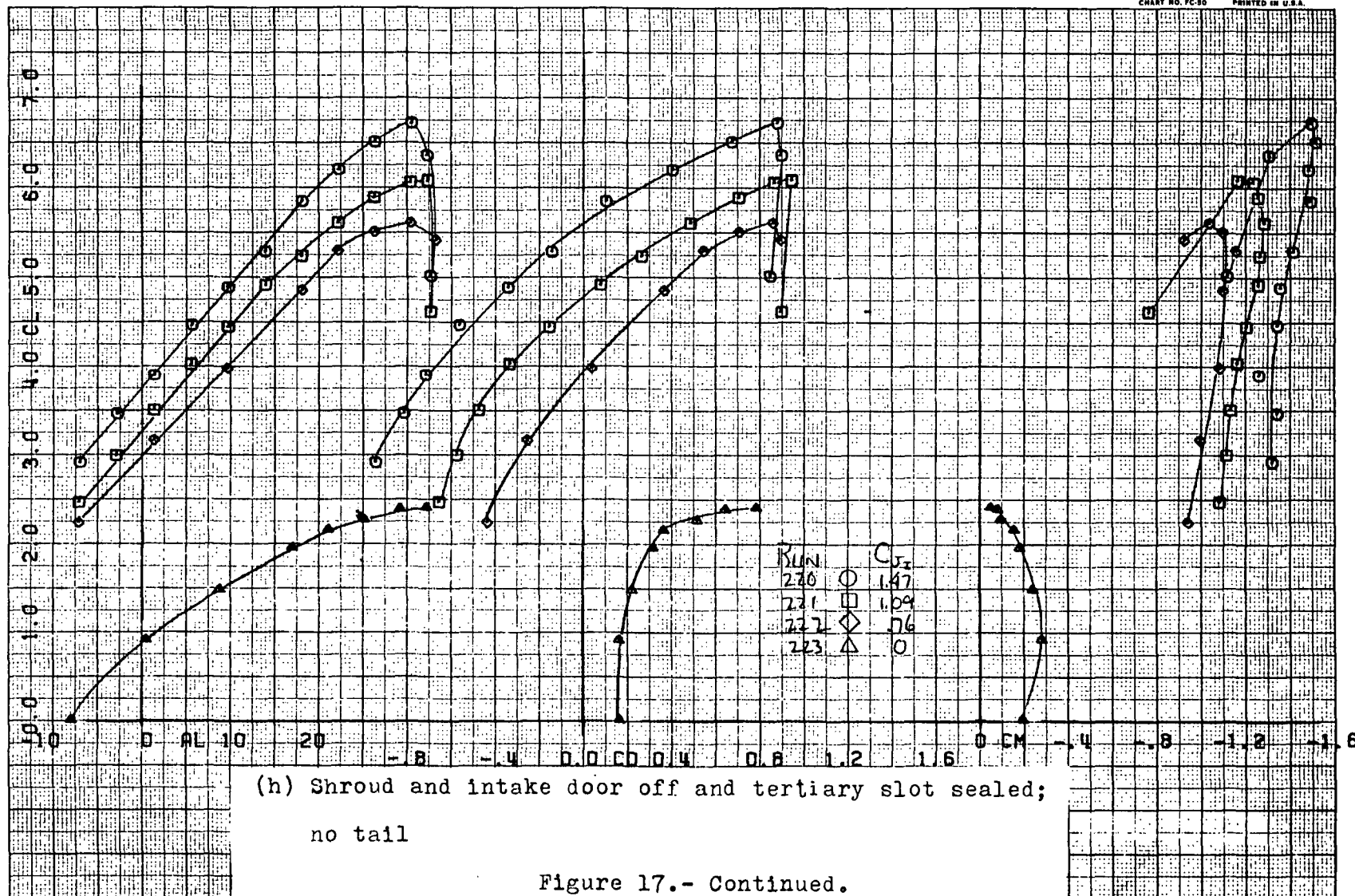
HOUSTON INSTRUMENT  
DALLAS, TEXAS  
CHART NO. FC-50 PRINTED IN U.S.A.

31



17

179



(h) Shroud and intake door off and tertiary slot sealed;  
no tail

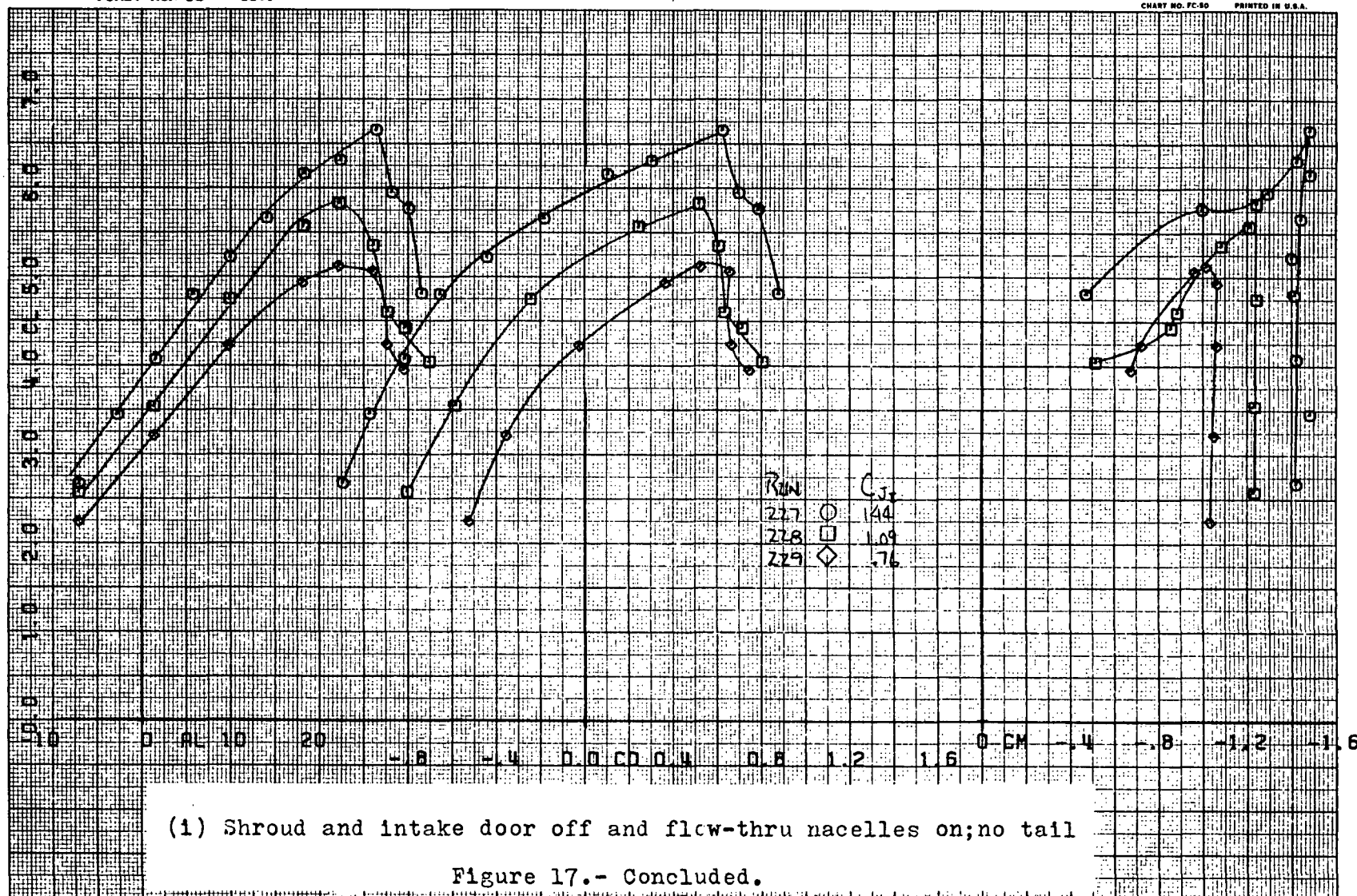
Figure 17.- Continued.

FIRST RUN IS 227.

COMPLØT

OMNIGRAPHIC

HOUSTON INSTRUMENT  
DIVISION OF HONEYWELL  
BELL LAIR, TEXAS  
CHART NO. FC-50 PRINTED IN U.S.A.



(1) Shroud and intake door off and flow-thru nacelles on; no tail

Figure 17.- Concluded.



FIRST RUN IS 41.

COMPLLOT®

OMNIGRAPHIC®

HOUSTON INSTRUMENT  
DIVISION OF HARRIS CORPORATION  
BELLARE, TEXAS  
CHART NO. FC-50 PRINTED IN U.S.A.

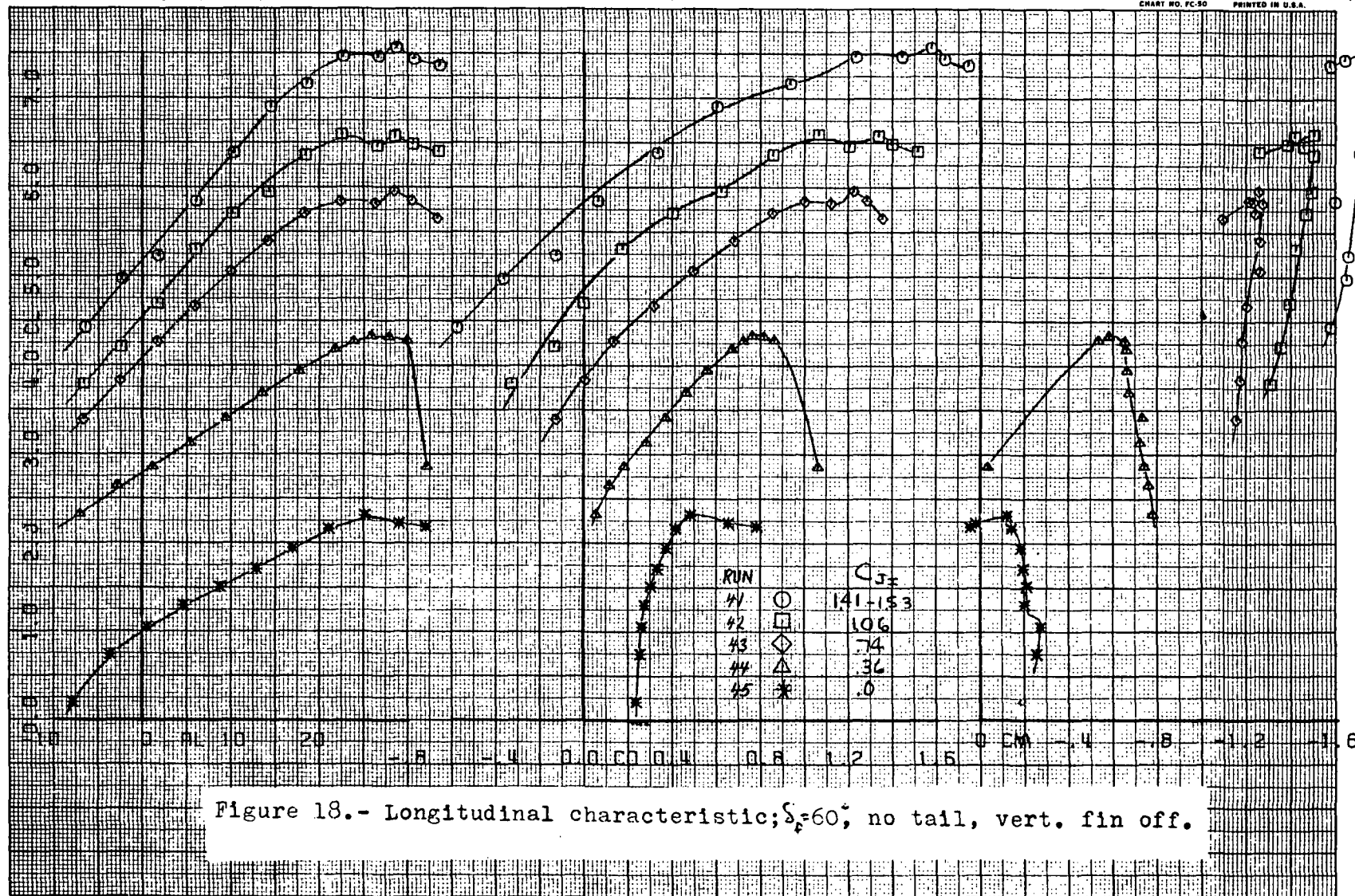


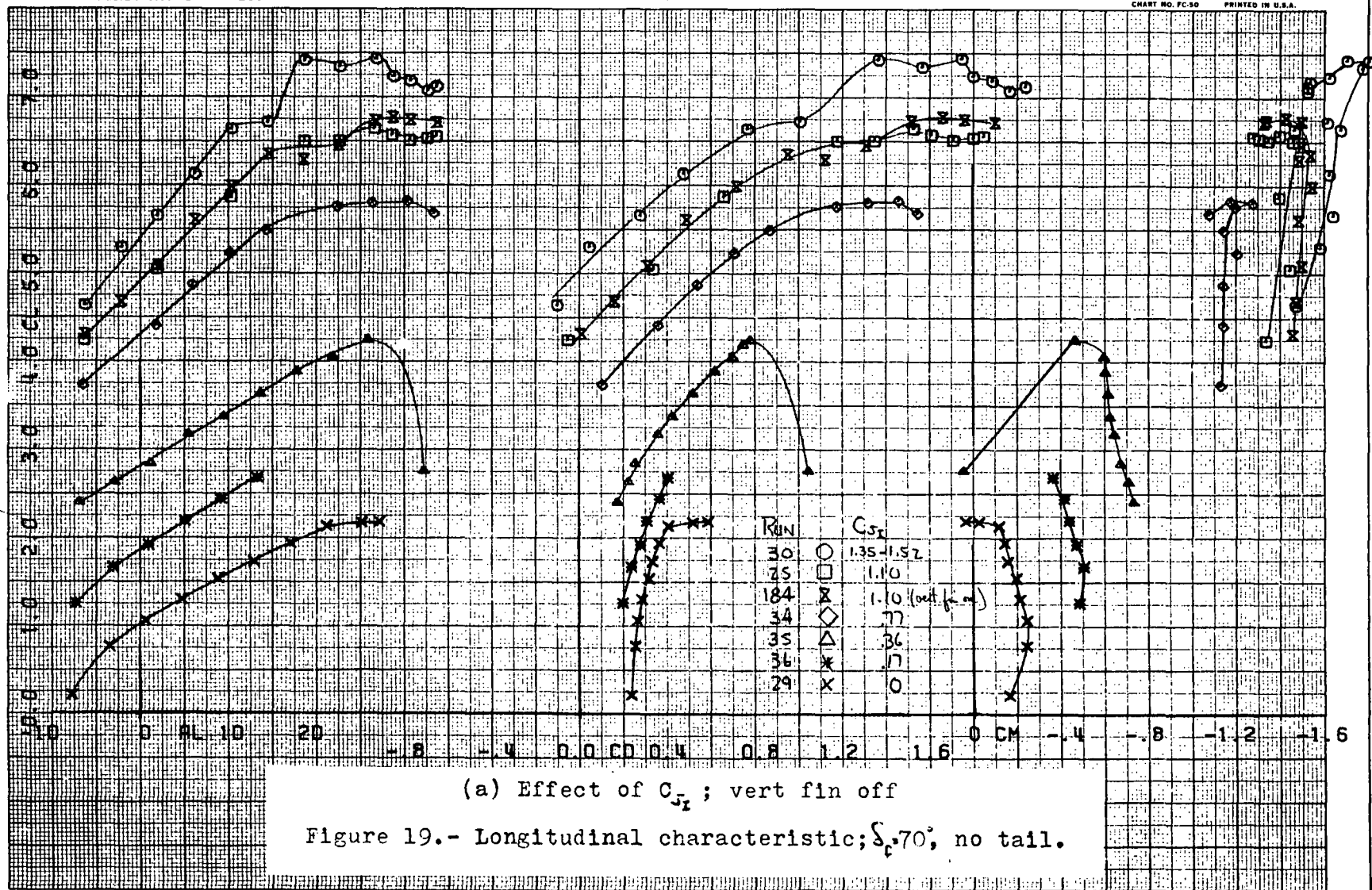
Figure 18.- Longitudinal characteristic;  $\delta_f=60^\circ$ ; no tail, vert. fin off.

FIRST RUN 15 30.

COMPLØT®

OMNIGRAPHIC®

HOUSTON INSTRUMENT  
DIVISION OF COMPELLING®  
BELLAIRE, TEXAS  
CHART NO. FC-50 PRINTED IN U.S.A.



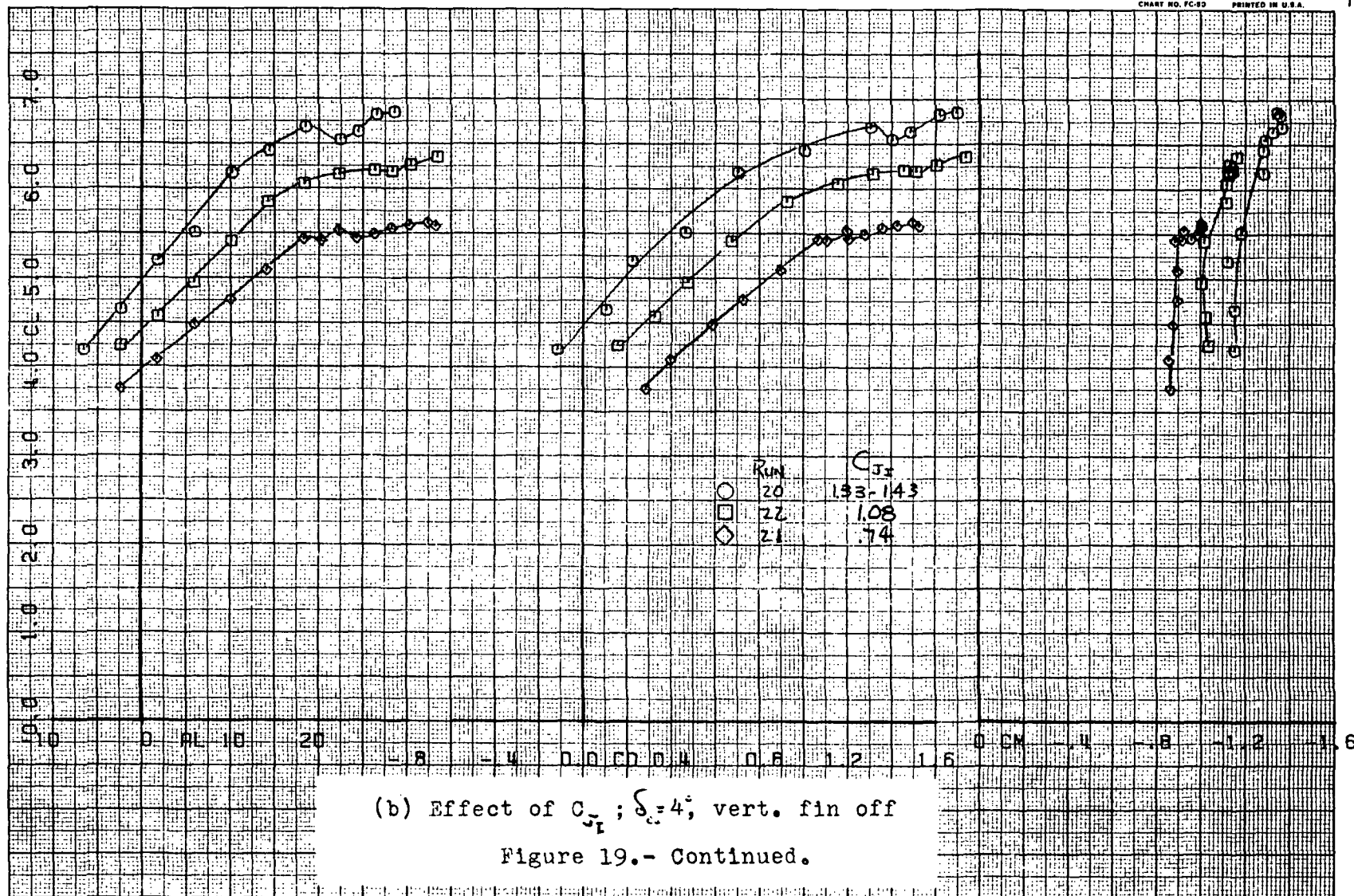
FIRST RUN IS 20.

COMPLØT®

OMNIGRAPHIC®

HOUSTON INSTRUMENT  
DIVISION OF GENERAL ELECTRIC  
BELLAIRE, TEXAS  
CHART NO. FC-92 PRINTED IN U.S.A.

12



822

43

196



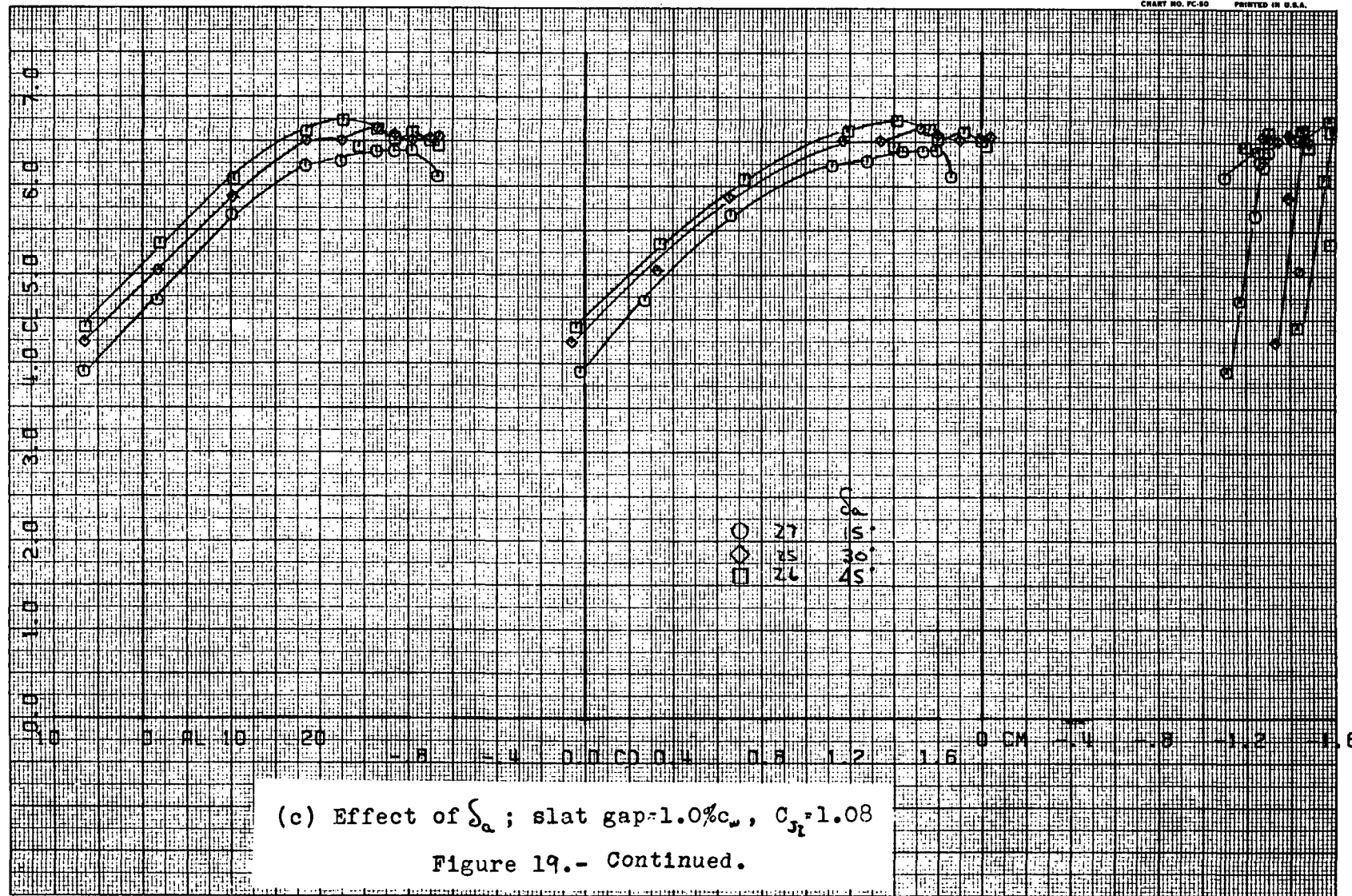
FIRST RUN IS 27.

COMPLLOT

OMNIGRAPHIC

HOUSTON INSTRUMENT  
BELLAIRE, TEXAS  
CHART NO. FC-60 PRINTED IN U.S.A.

6



33

34

19c

FIRST RUN IS 77.

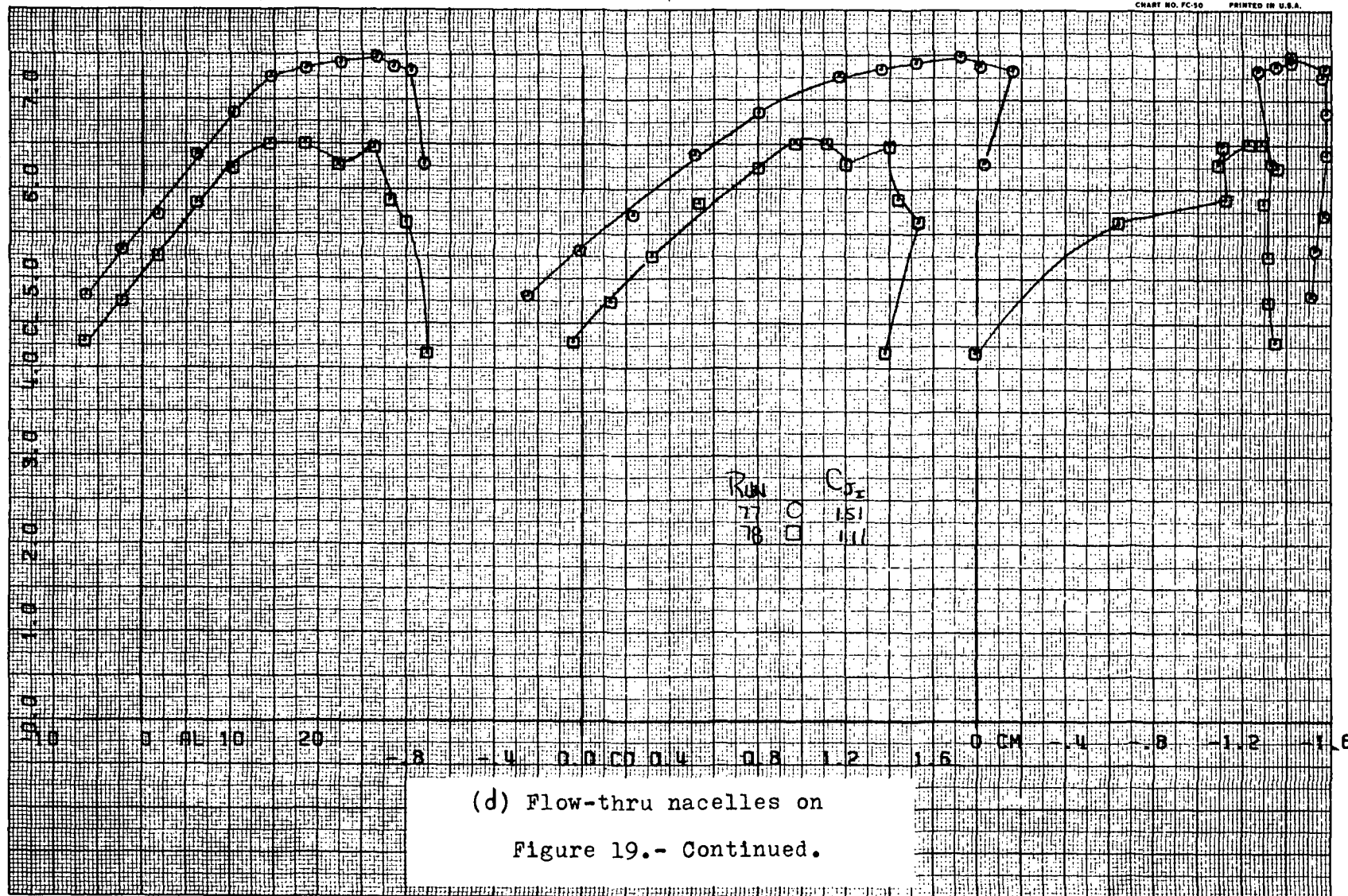
COMPLØT®

OMNIGRAPHIC®

HOUSTON INSTRUMENT  
BELL LAIRE, TEXAS

CHART NO. FC-50 PRINTED IN U.S.A.

27



(d) Flow-thru nacelles on  
Figure 19.- Continued.

84-

14

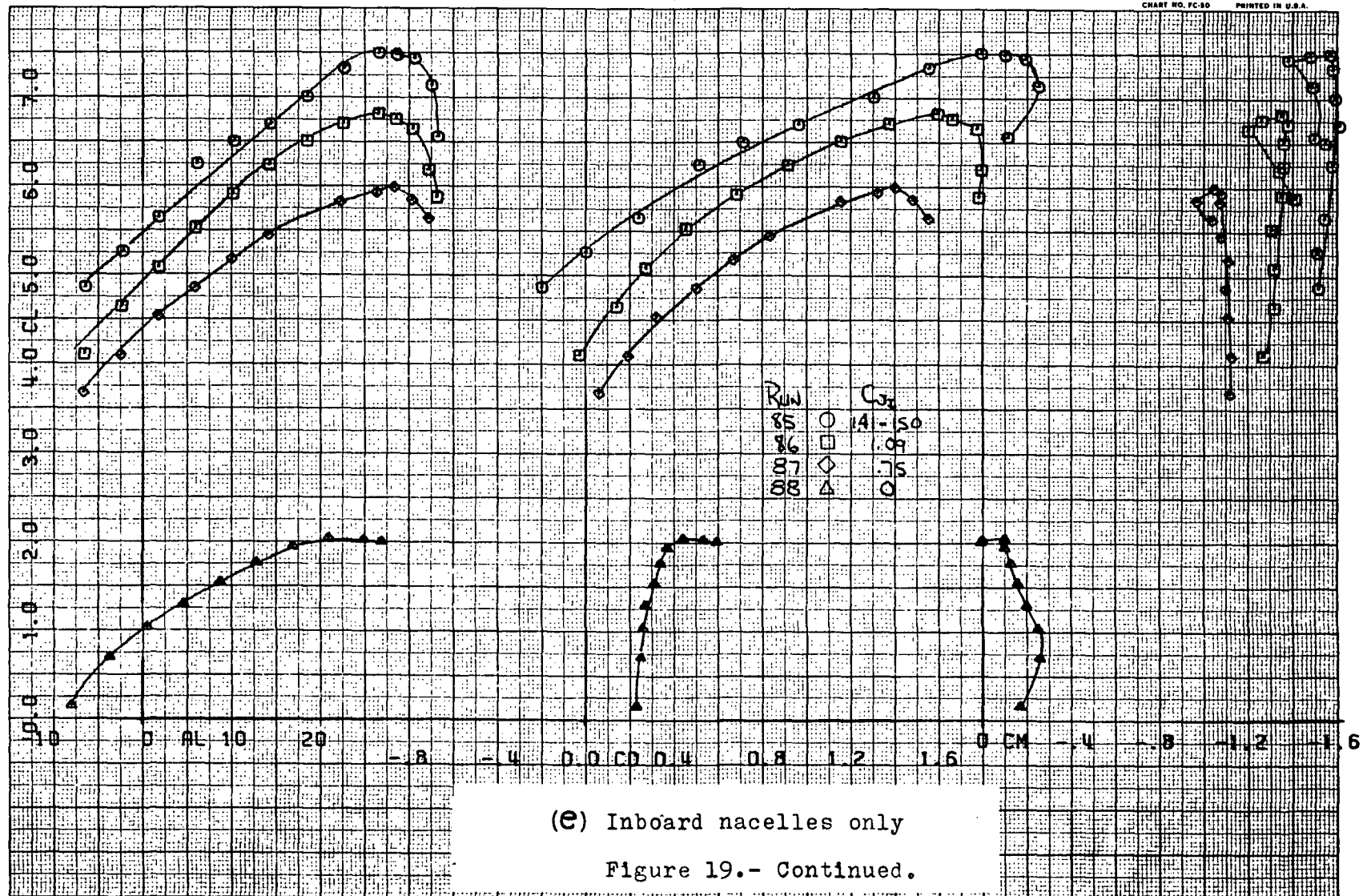
19d

FIRST RUN JS 85.

COMPL0T\*

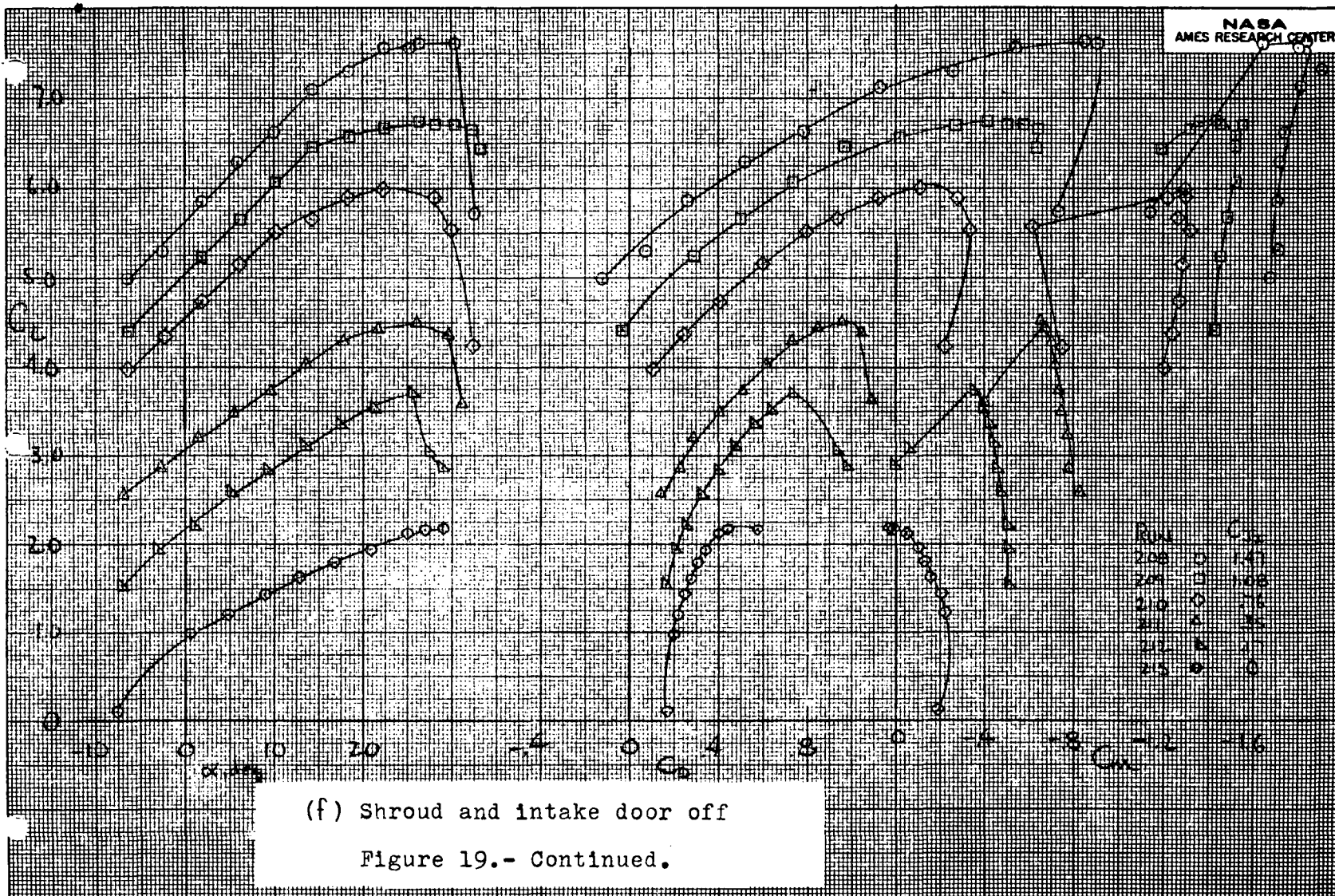
OMNIGRAPHIC\*

HOUSTON INSTRUMENT  
BELLARE, TEXAS  
CHART NO. FC-80 PRINTED IN U.S.A.



(e) Inboard nacelles only

Figure 19.- Continued.



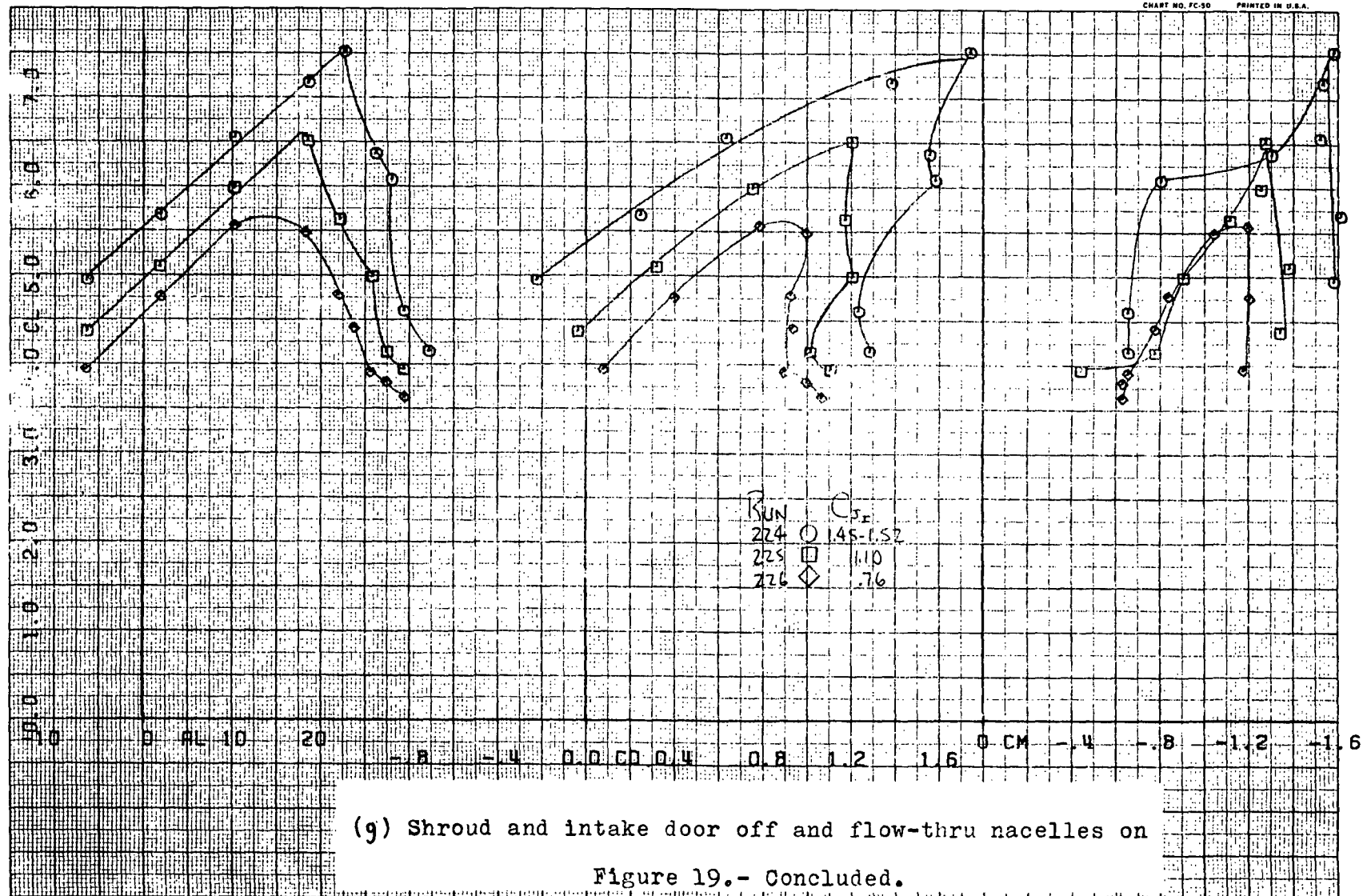


FIRST RUN IS 224.

COMPL0T

OMNIGRAPHIC

HOUSTON INSTRUMENT  
DIVISION OF HOUSTON INSTRUMENTS  
BELLAIRE, TEXAS  
CHART NO. FC-50 PRINTED IN U.S.A.



(g) Shroud and intake door off and flow-thru nacelles on  
Figure 19.- Concluded.

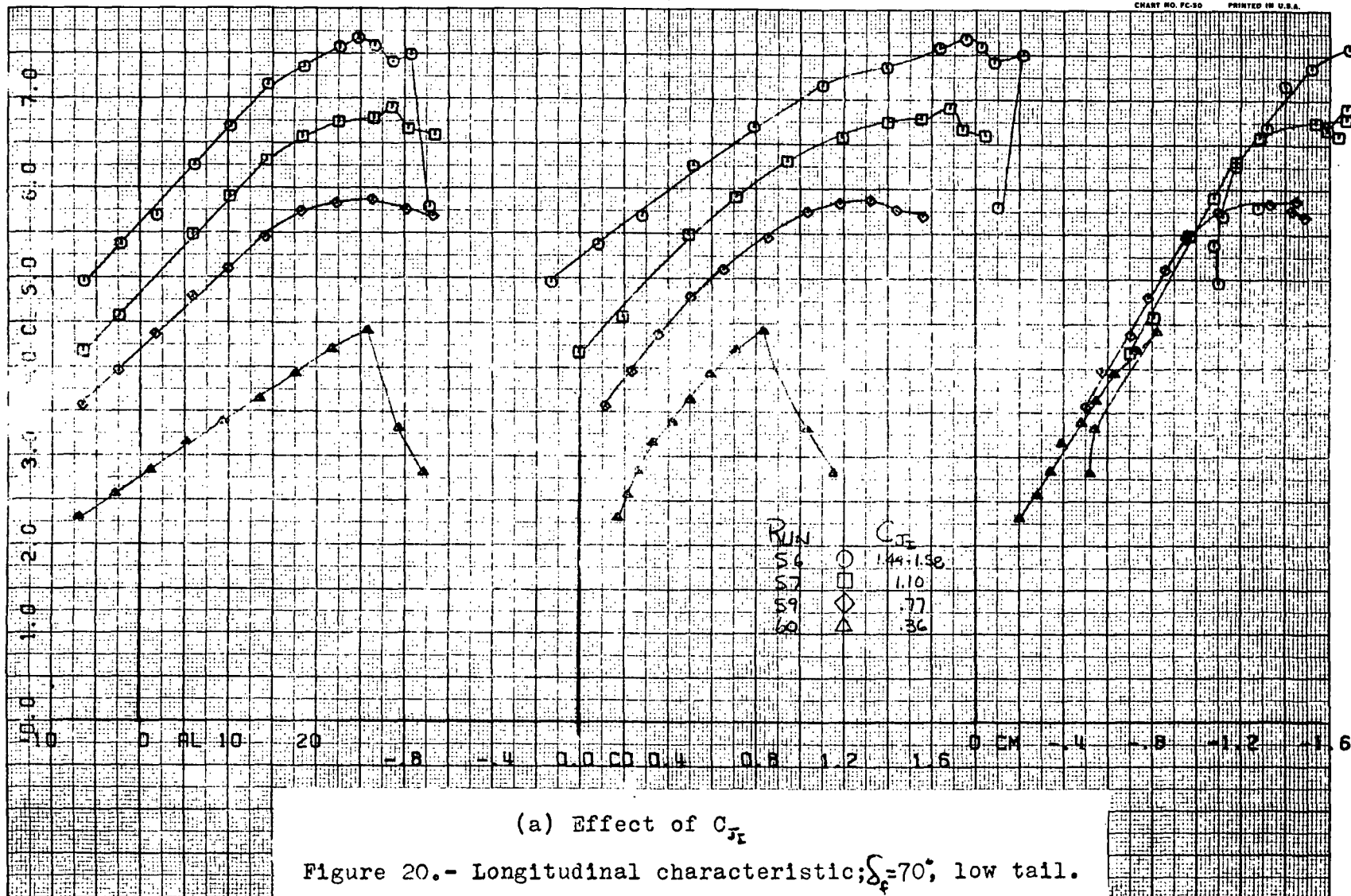
FIRST RUN IS S6.

COMPLOT®

OMNIGRAPHIC®

HOUSTON INSTRUMENT  
DIVISION OF AMERICAN LAMARCO  
DALLAS, TEXAS  
CHART NO. FC-50 PRINTED IN U.S.A.

18



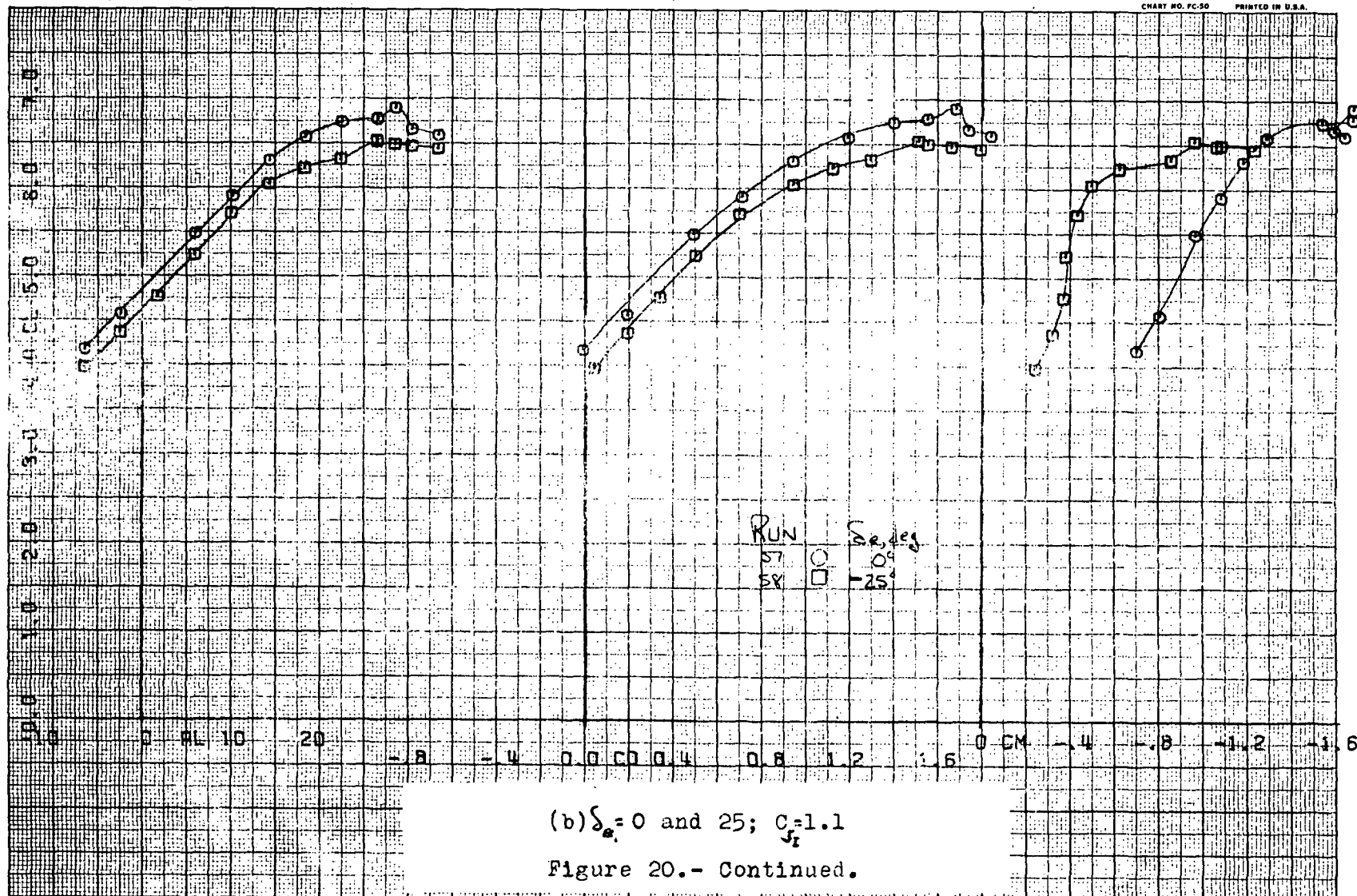
(a) Effect of  $C_T$

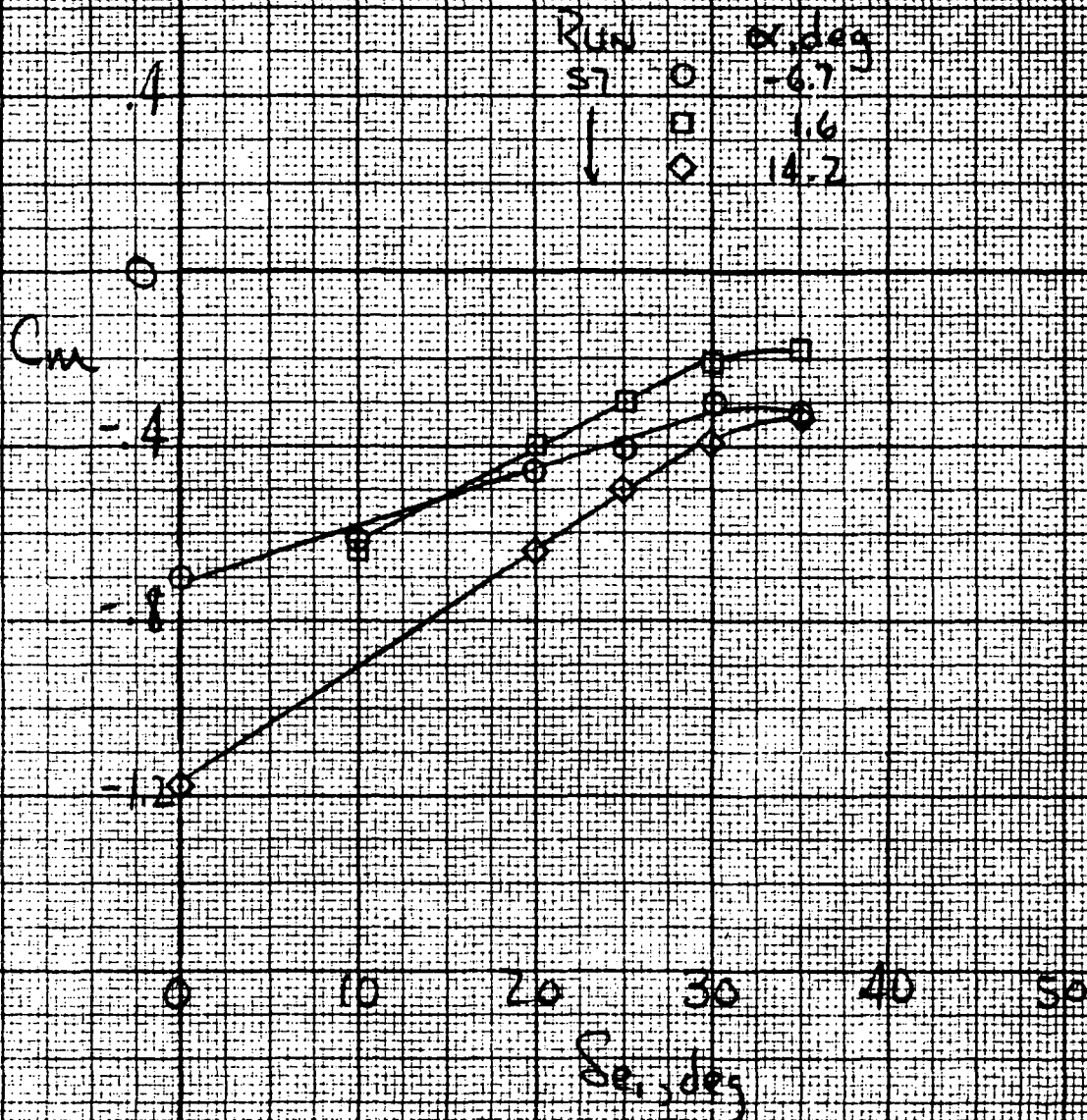
Figure 20.- Longitudinal characteristic;  $\delta_f = 70^\circ$ ; low tail.

20a.

89

93

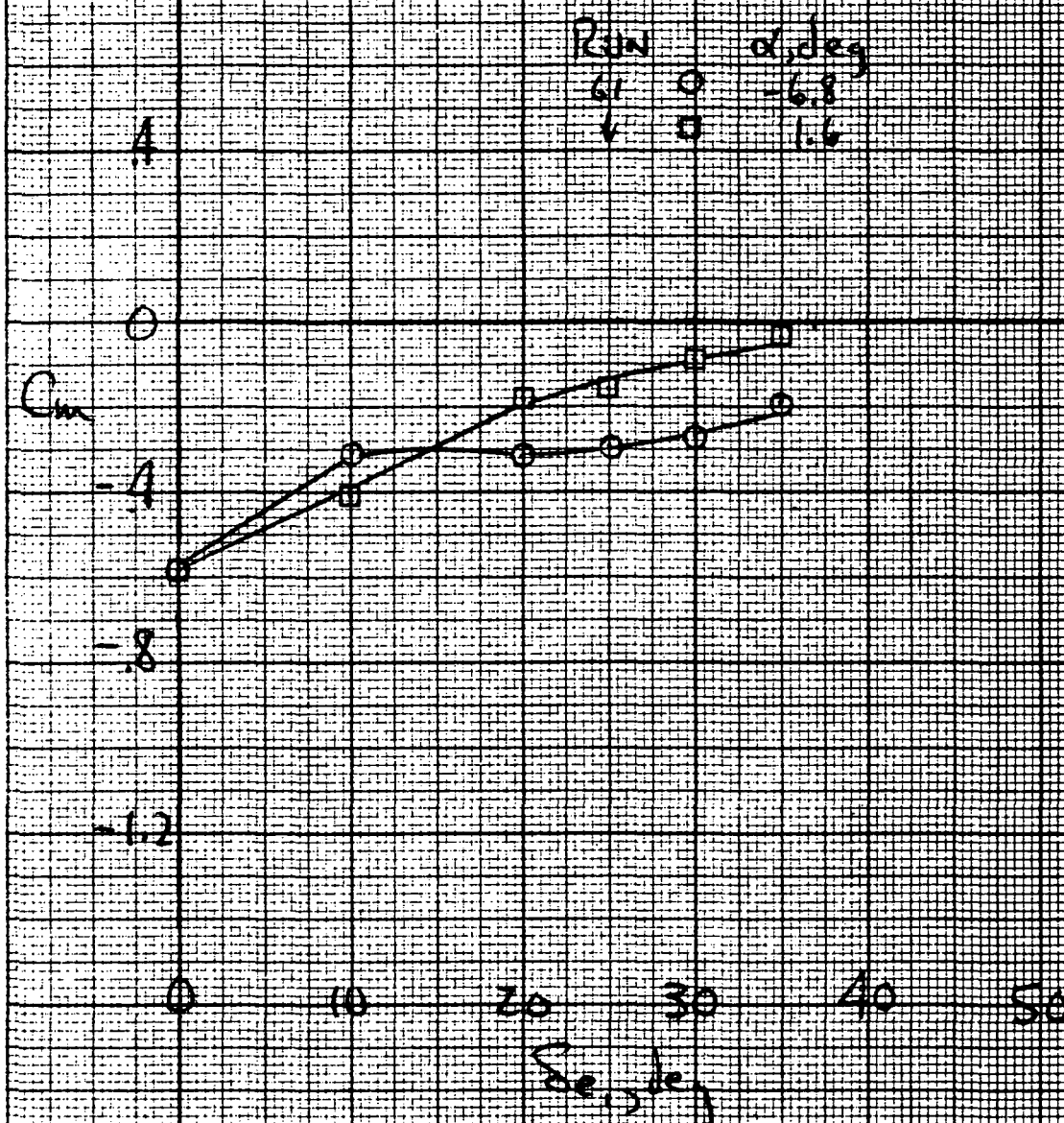




(c) Elevator effectiveness;  $\delta_e = 0^\circ$ ,  $C_{x_f} = 1.1$

Figure 20.- Continued.





(d) Elevator effectiveness;  $\delta_e = -15^\circ$ ,  $C_{x_1} = 1.1$

Figure 20.- Concluded.

FIRST RUN IS 97.

COMPL0T®

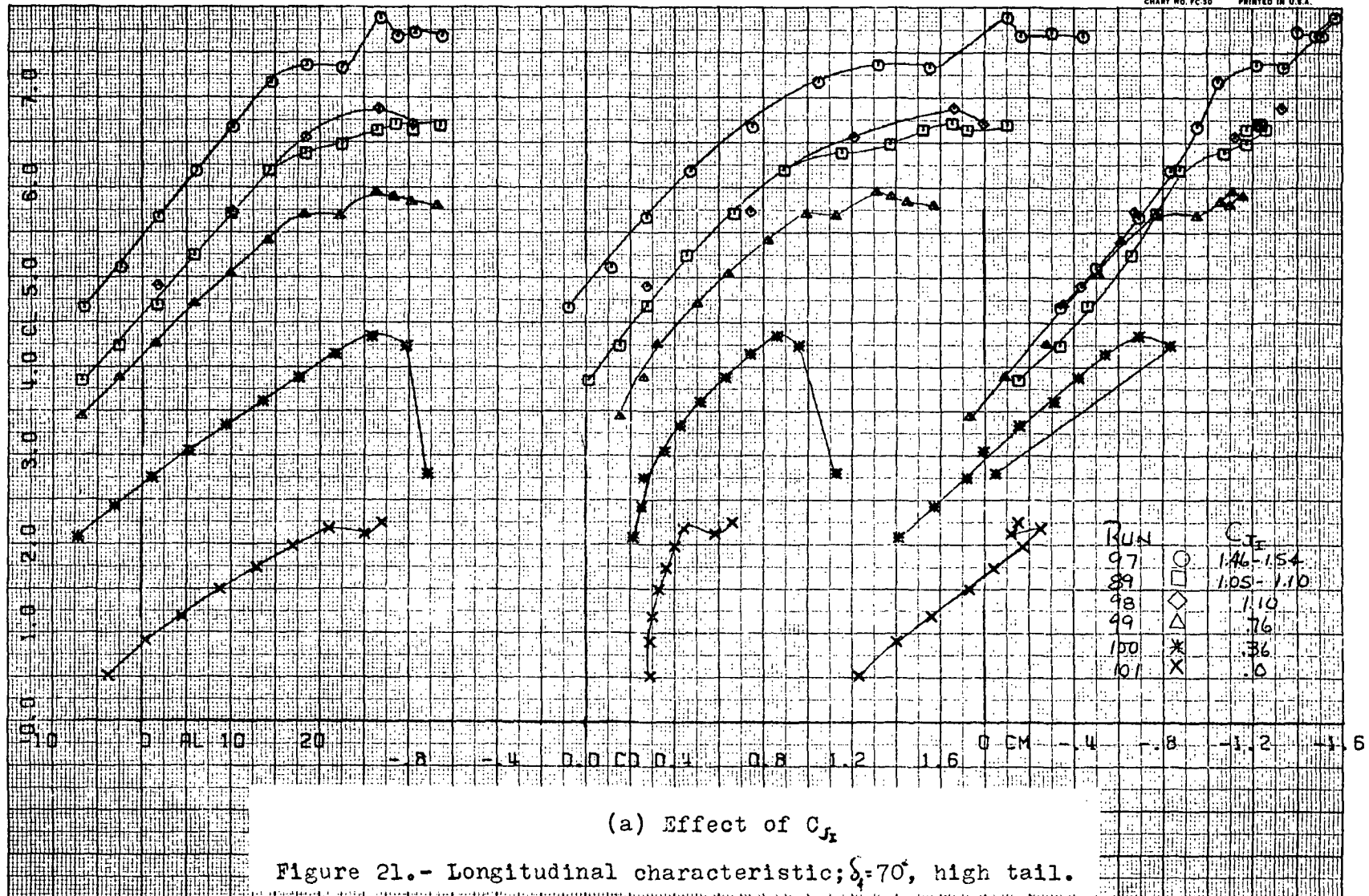
OMNIGRAPHIC®

HOUSTON INSTRUMENT

Divide of Houston Instrument

BELLINGHAM, TEXAS

CHART NO. FC-30 PRINTED IN U.S.A.



(a) Effect of  $C_{J_2}$

Figure 21.- Longitudinal characteristic;  $\delta_1=70^\circ$ , high tail.

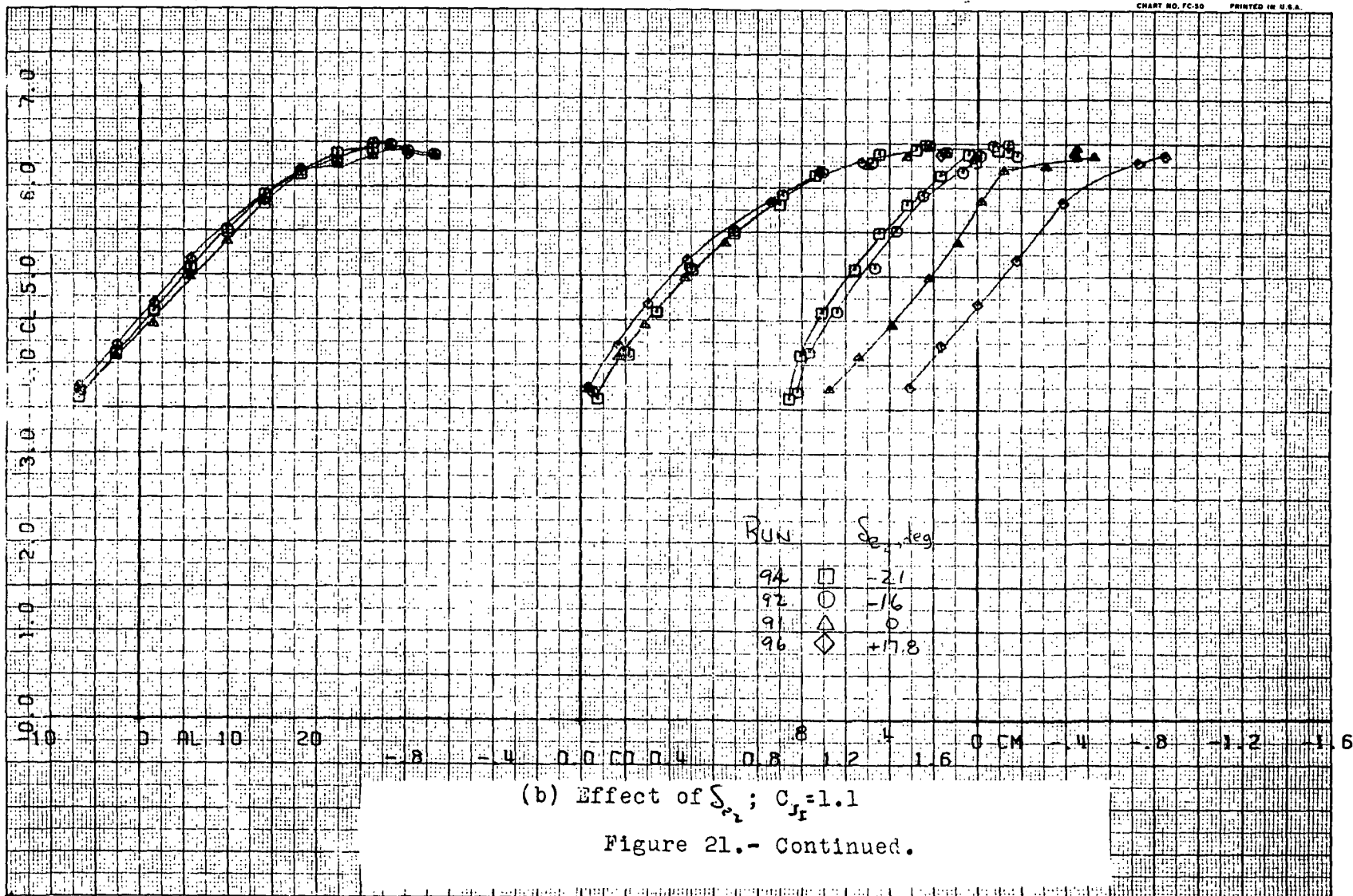
FIRST RUN 15 92.

COMPLØT®

OMNIGRAPHIC®

HOUSTON INSTRUMENT  
DIVISION OF HUGHES-ANDREW  
BELLARE, TEXAS

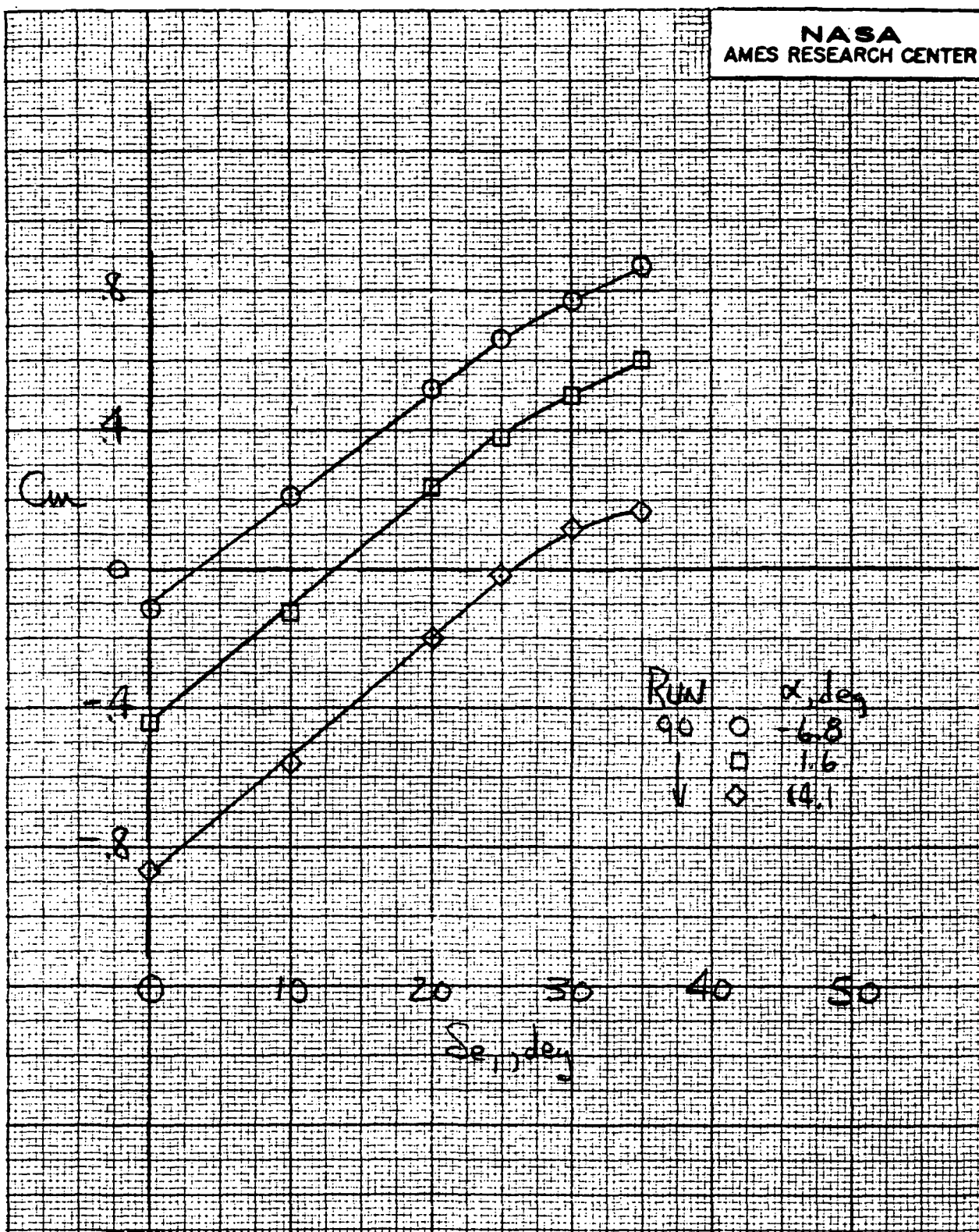
CHART NO. FC-30 PRINTED IN U.S.A.



21

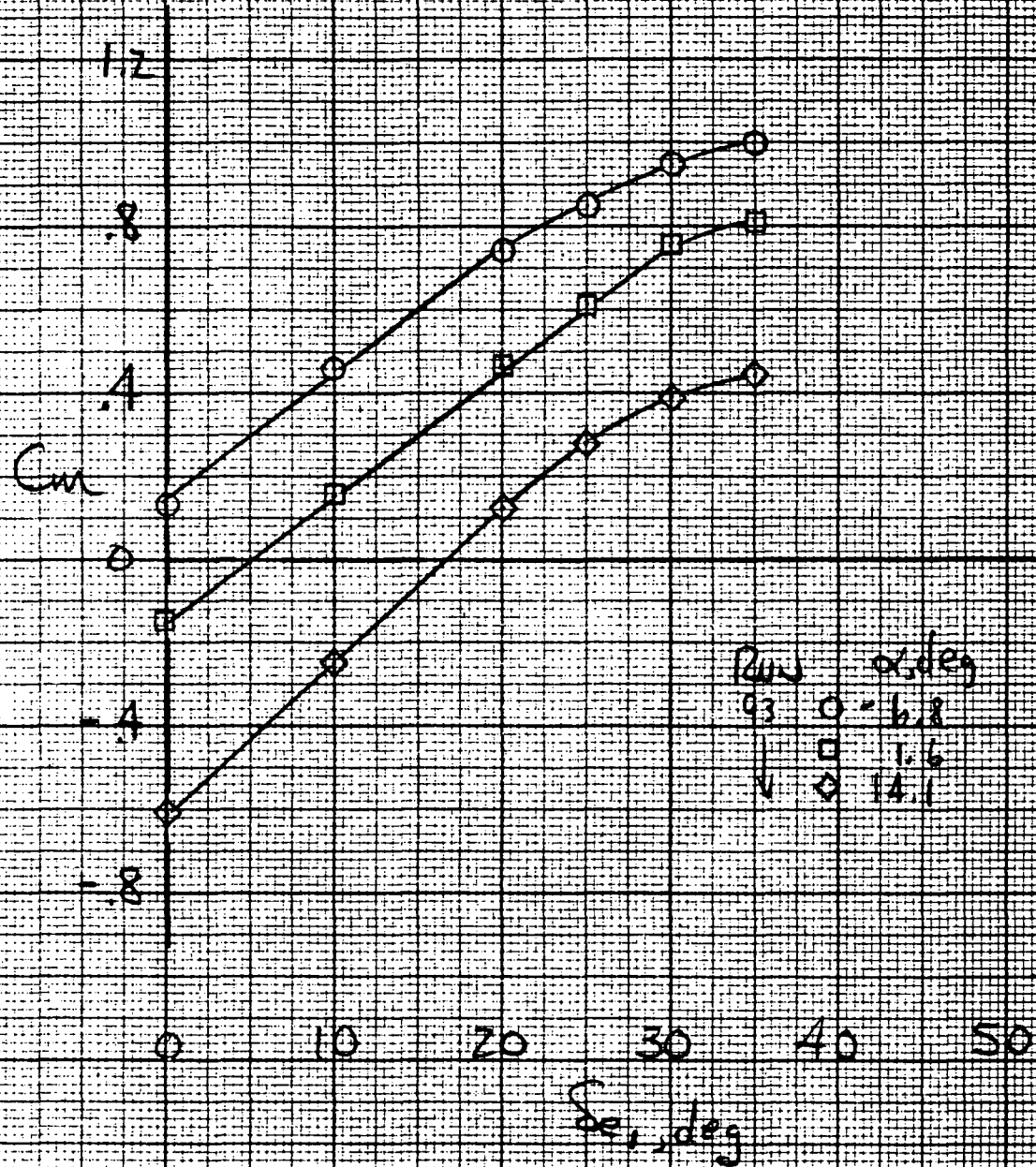
6

216



(c) Elevator effectiveness;  $S_{e1}=0^\circ$ ,  $C_{x1}=1.1$

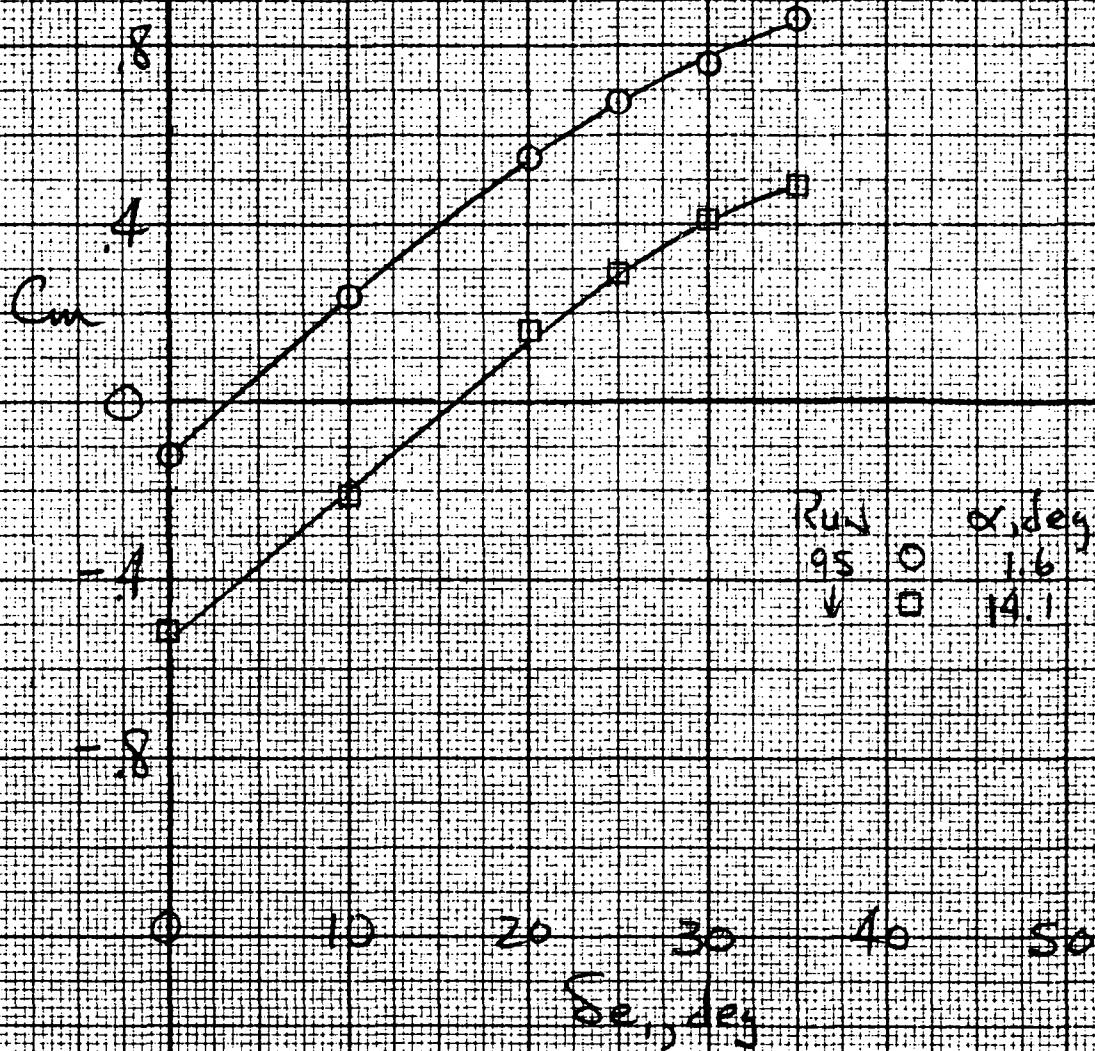
Figure 21.- Continued.



(d) Elevator effectiveness;  $\delta_e = -16^\circ$ ;  $C_{L_i} = 1.1$

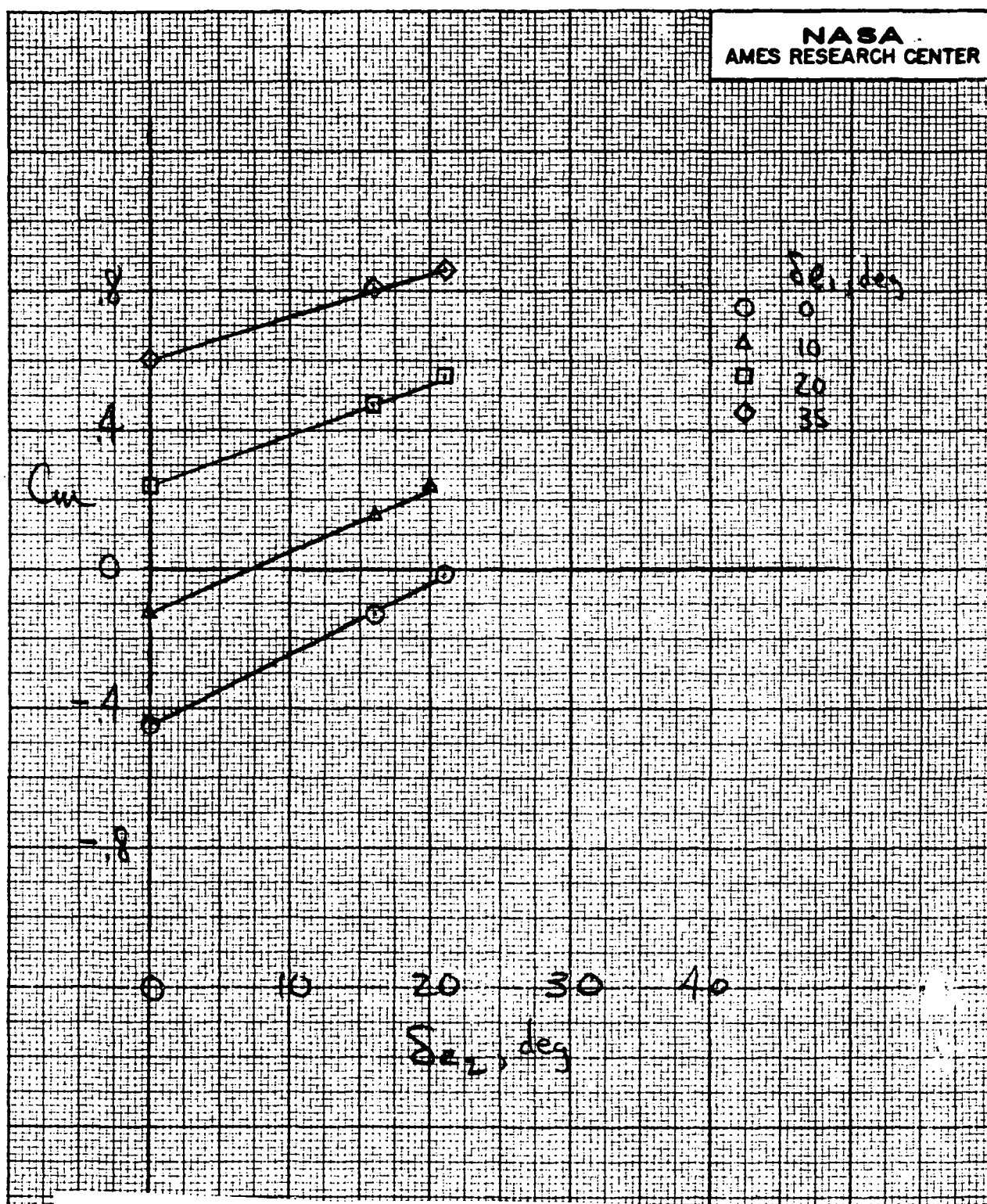
Figure 21.- Continued.





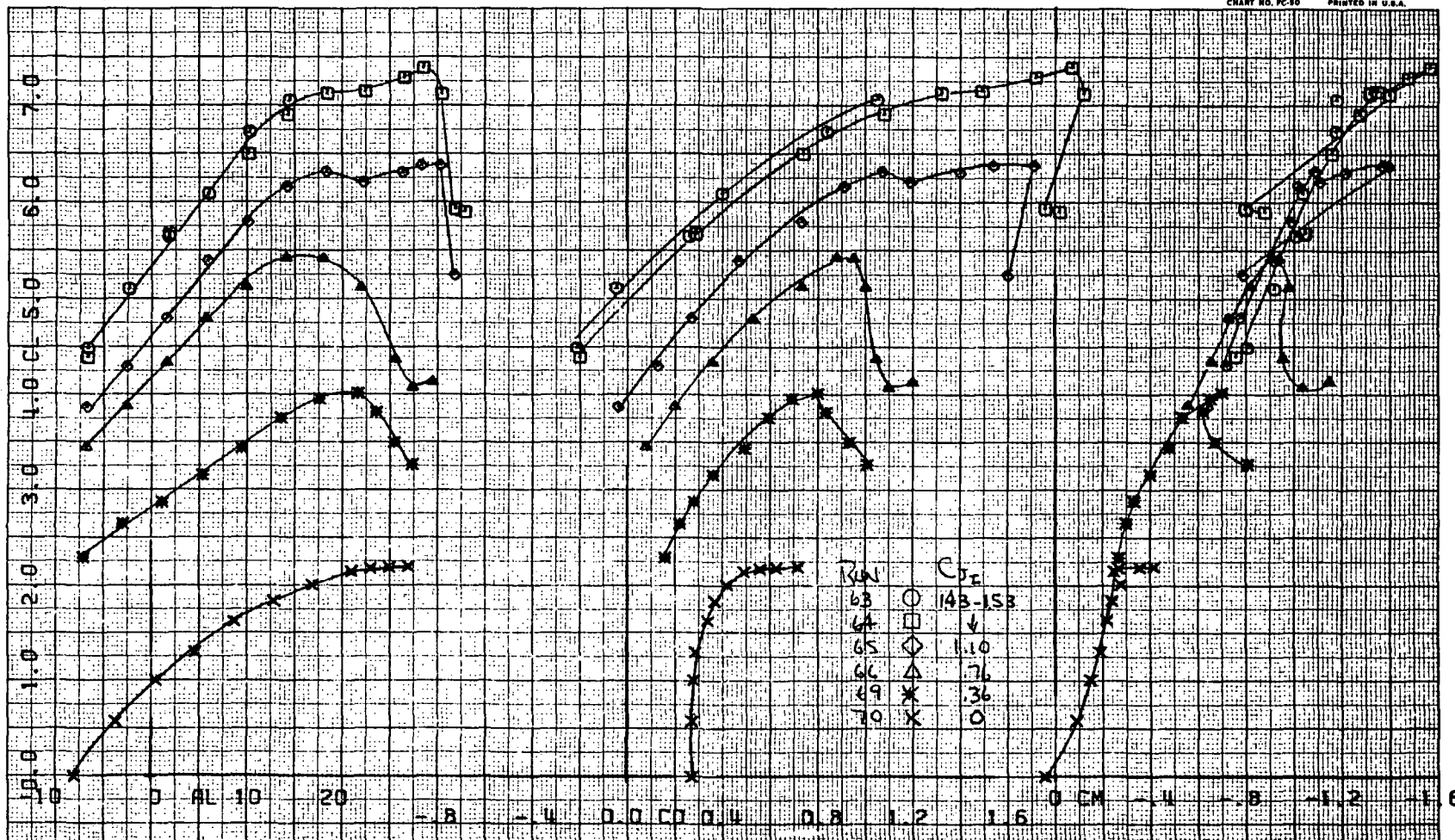
(e) Elevator effectiveness;  $\delta_z = -21^\circ$ ,  $C_{x_1} = 1.1$

Figure 21.- Continued.



(f) Aft elevator element effectiveness;  $\alpha = 0^\circ$ ,  $C_L = 1.1$

Figure 21.- Concluded.



(a) Effect of  $C_{Jr}$

Figure 22.- Longitudinal characteristic;  $S_f=70^\circ$ , low tail, flow-thru nacelles on.

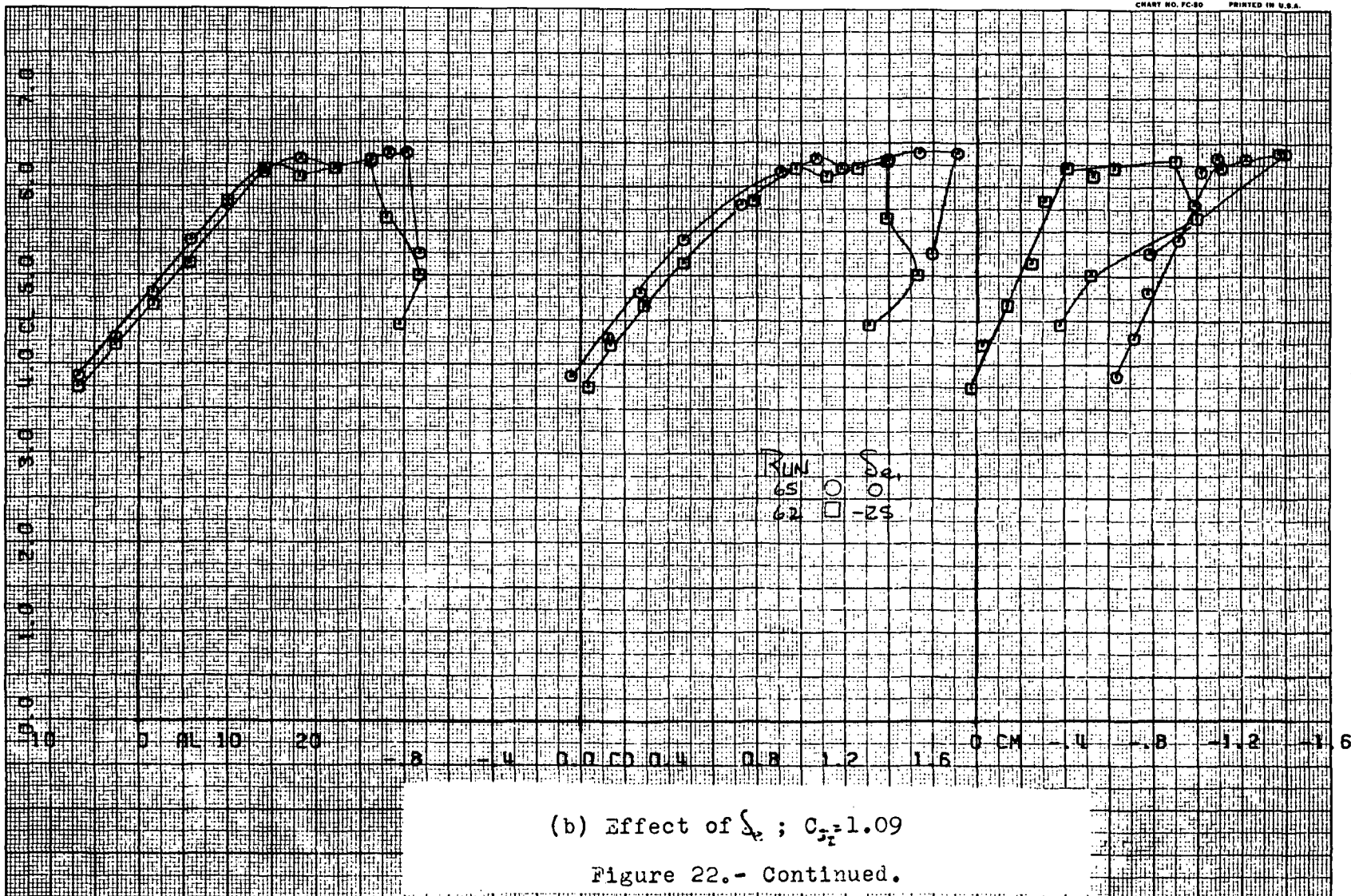


FIRST RUN 15 65.

COMPL0T

OMNIGRAPHIC

HOUSTON INSTRUMENT  
DIVISION OF BELL & HOWELL  
BELL LAIRE, TEXAS  
CHART NO. FC-60 PRINTED IN U.S.A.



(b) Effect of  $S_d$ ;  $C_{Fz}=1.09$

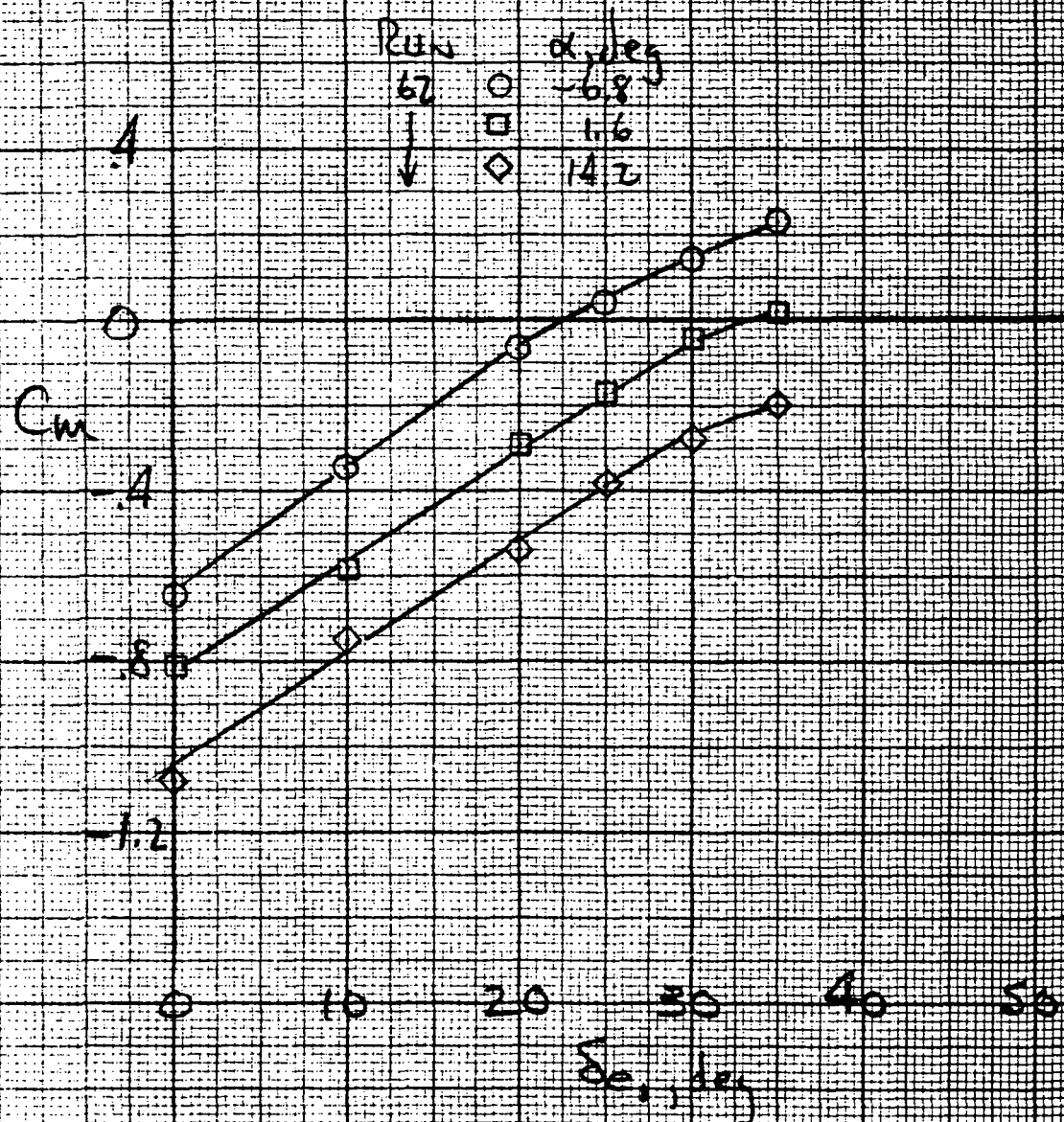
Figure 22.- Continued.

66

13

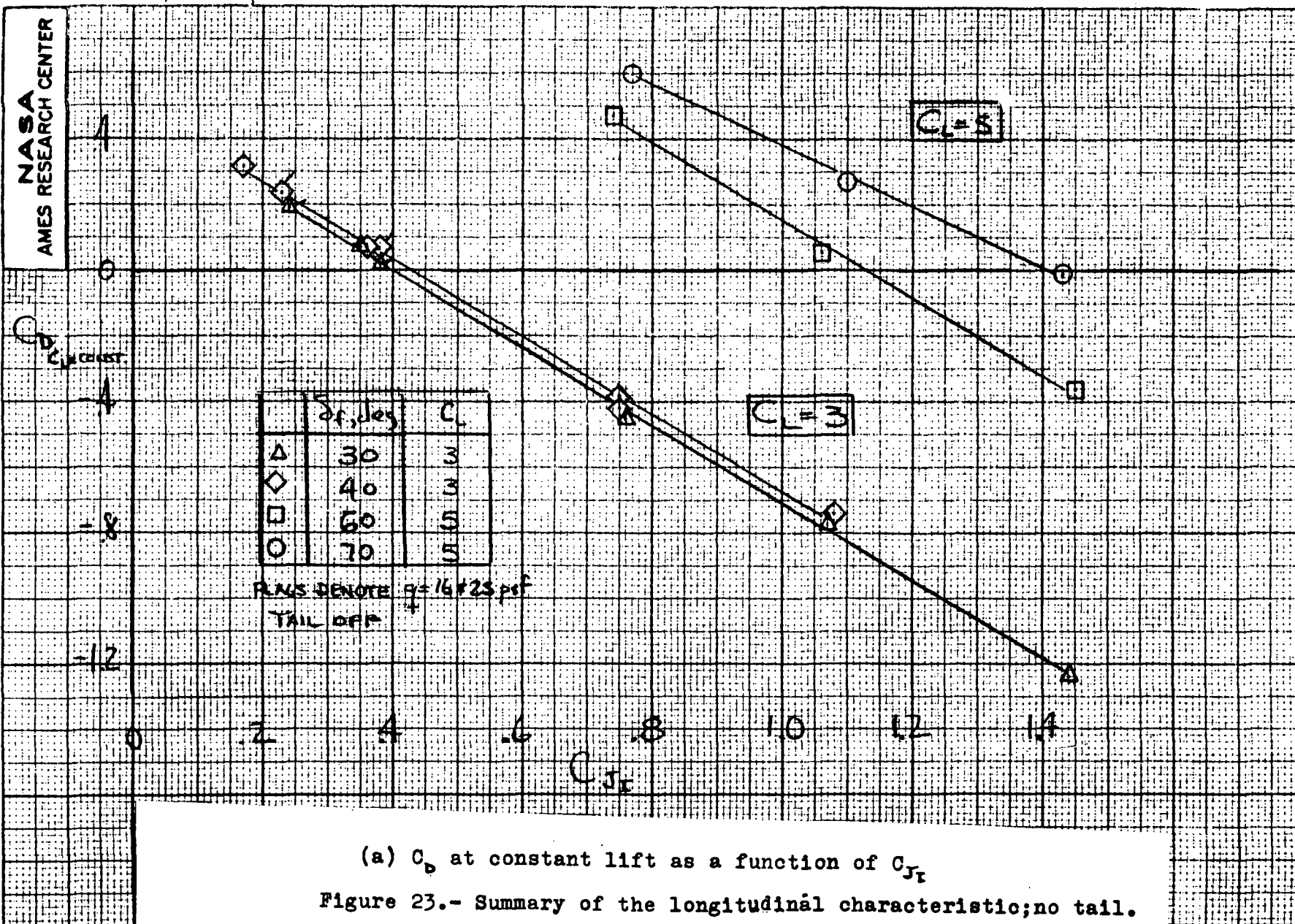
24

226



(c) Elevator effectiveness;  $\delta_{e_i} = 0^\circ$ ;  $C_{J_i} = 1.1$

Figure 22.- Concluded.



(a)  $C_D$  at constant lift as a function of  $C_{JT}$   
Figure 23.- Summary of the longitudinal characteristic; no tail.

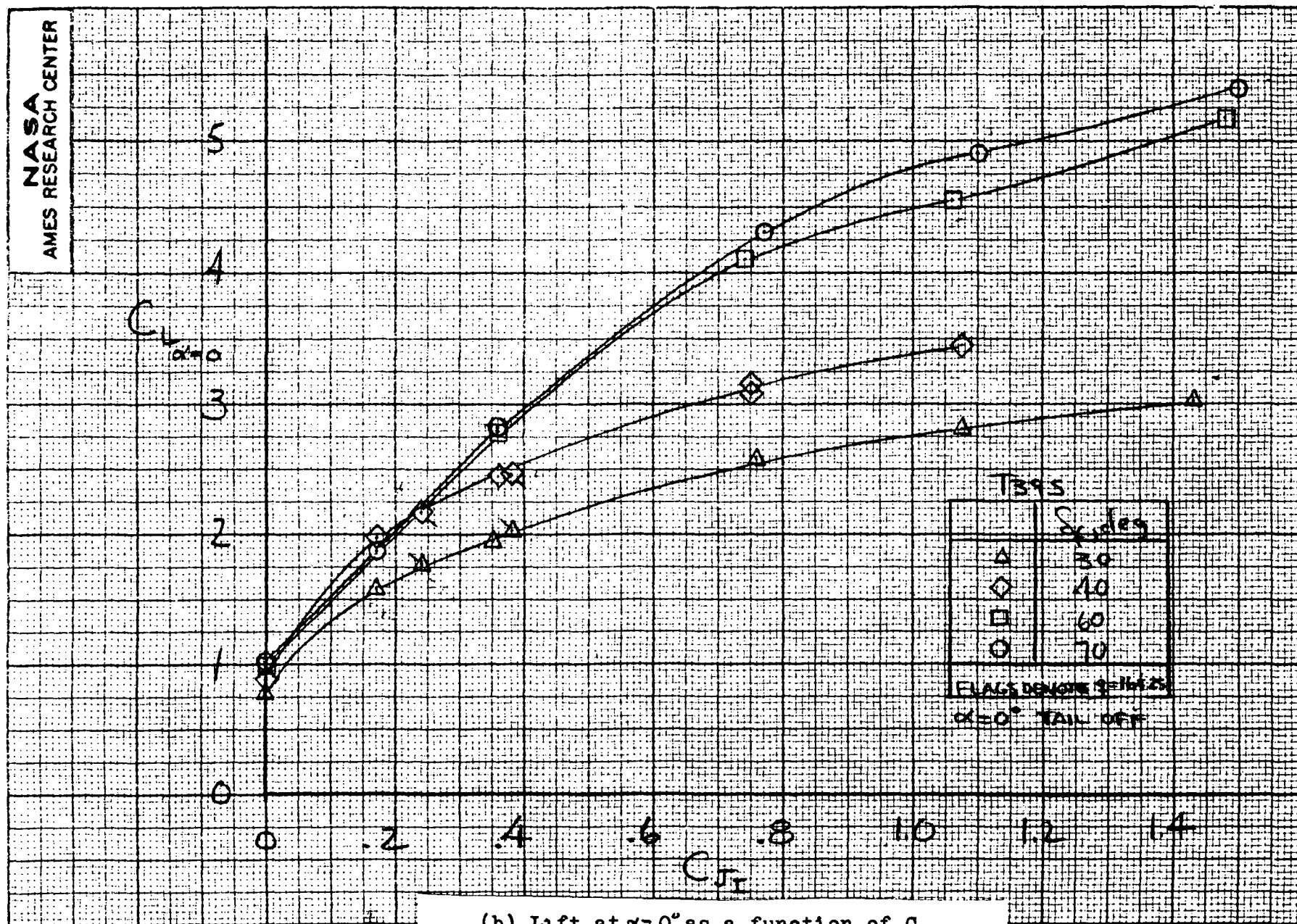
(b) Lift at  $\alpha = 0^\circ$  as a function of  $C_{D_i}$ 

Figure 23.- Continued.

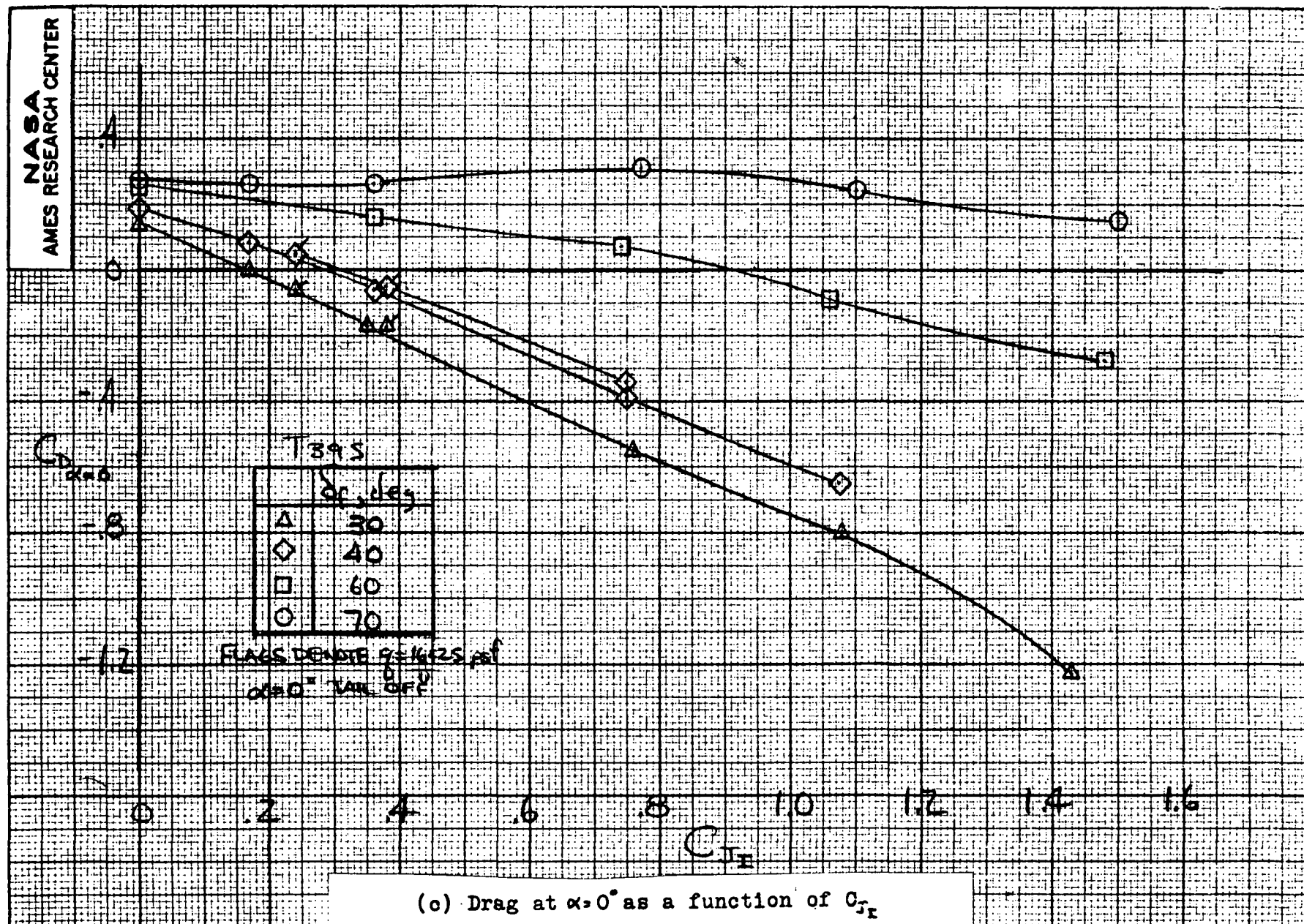


Figure 23.- Continued.



$C_{L_{max}}$

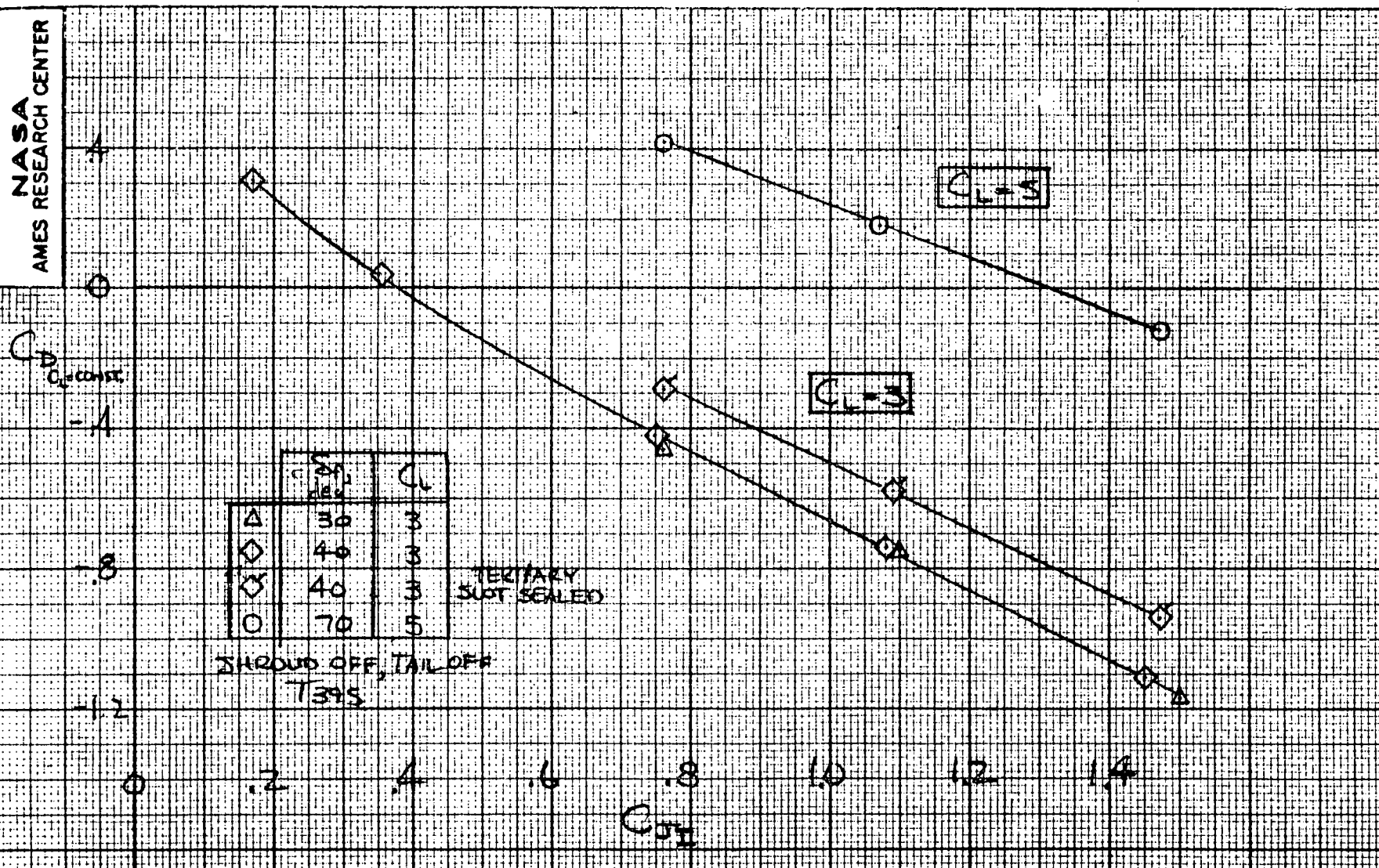
T395

	$\delta_f, \text{deg}$
$\triangle$	30
$\diamond$	40
$\square$	60
$\circ$	70

$C_{J_I}$

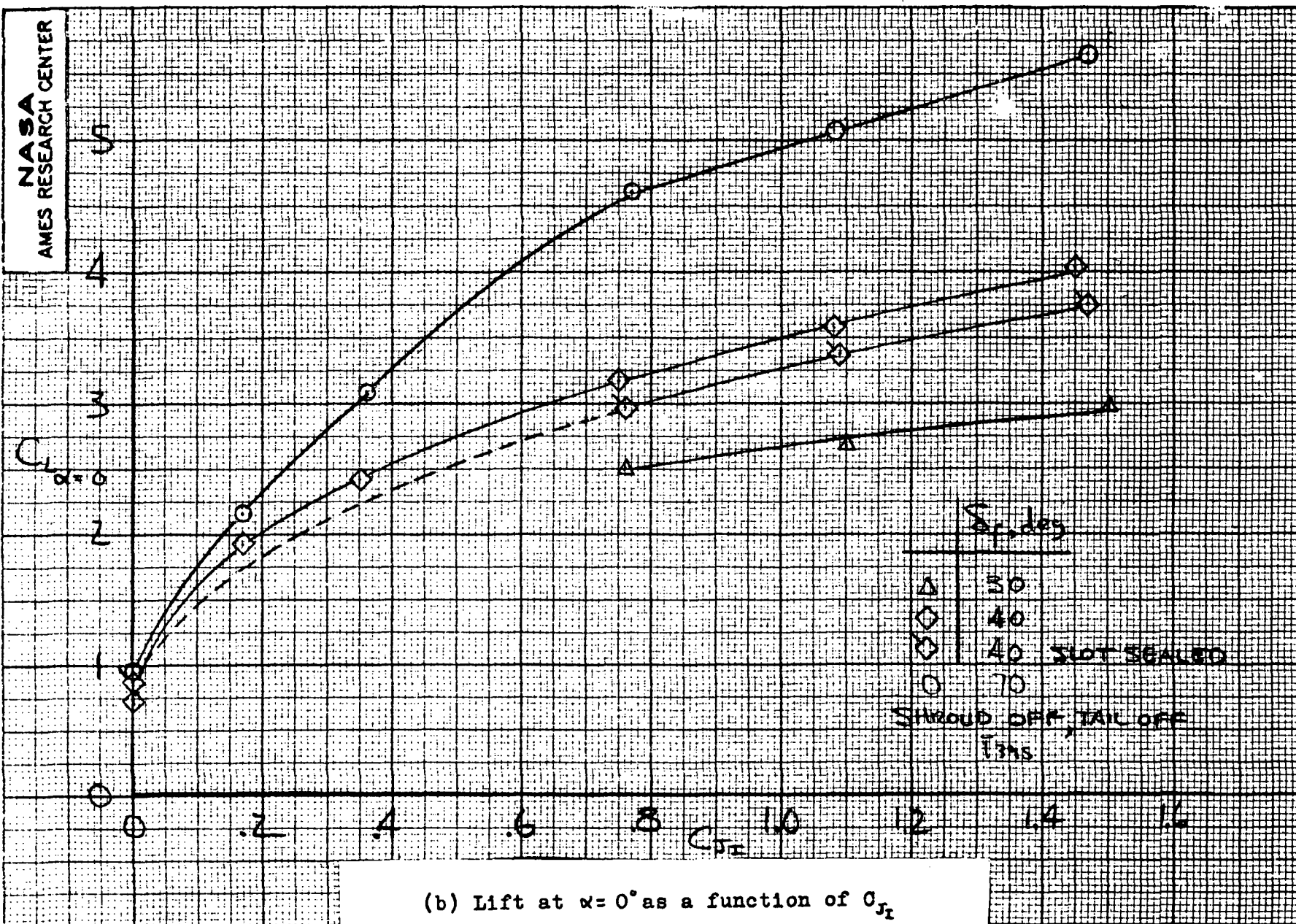
(d) Maximum lift as a function of  $C_{J_I}$

Figure 23.- Concluded.



(a) Drag at constant lift as a function of  $C_{T1}$

Figure 24.- Summary of the longitudinal characteristic; shroud and intake door off.



(b) Lift at  $\alpha = 0^\circ$  as a function of  $C_{D_i}$

Figure 24.- Continued.



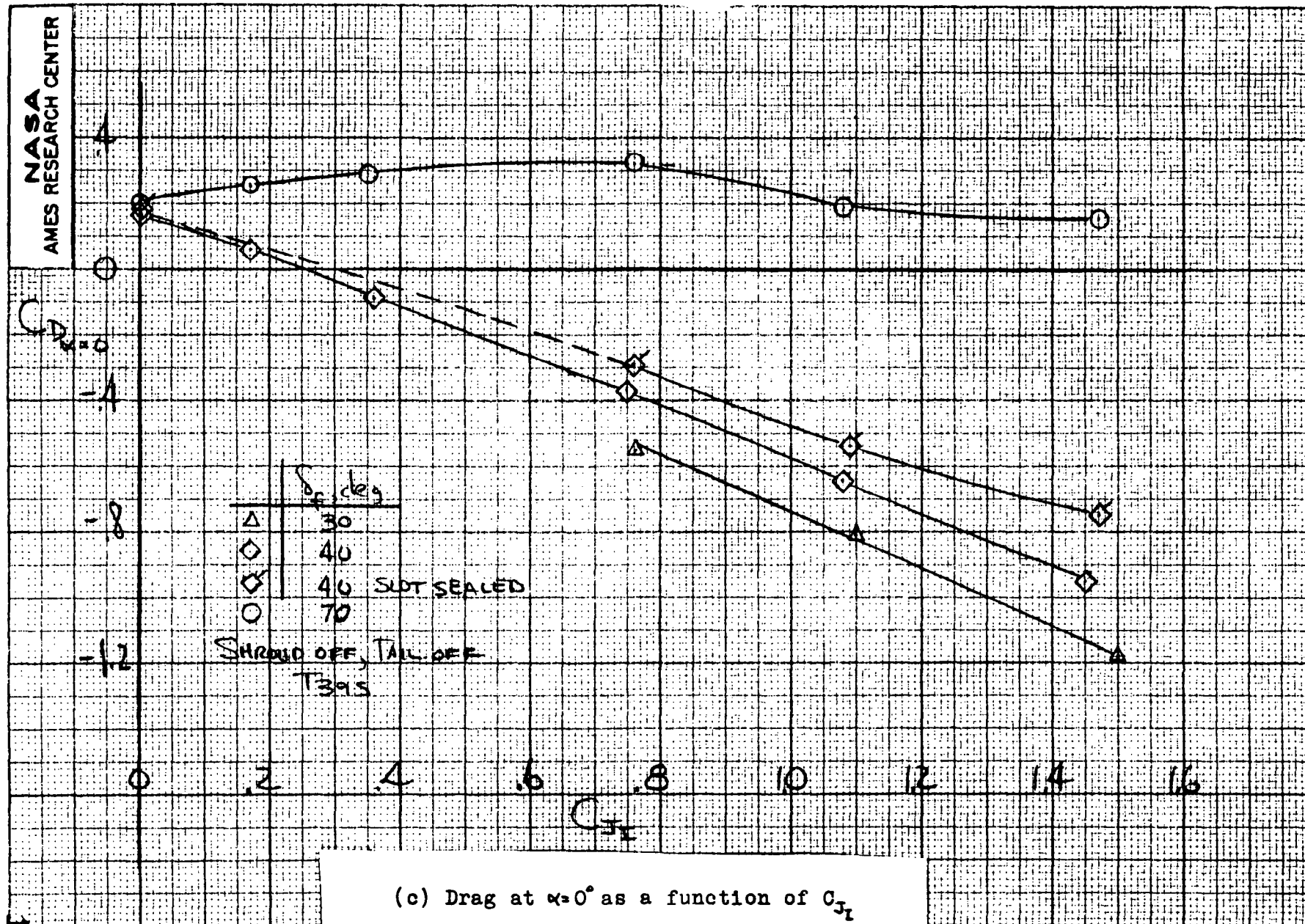
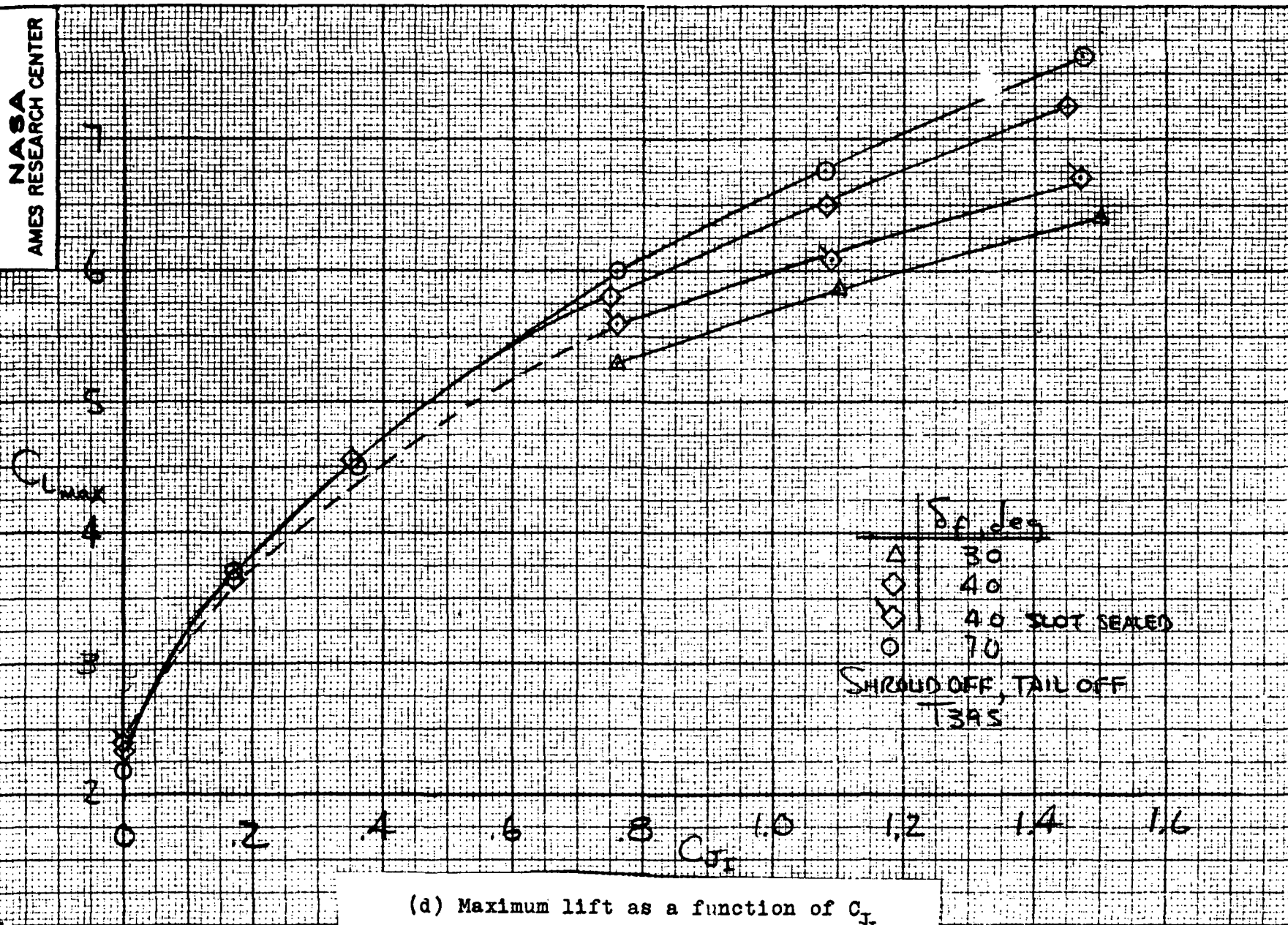
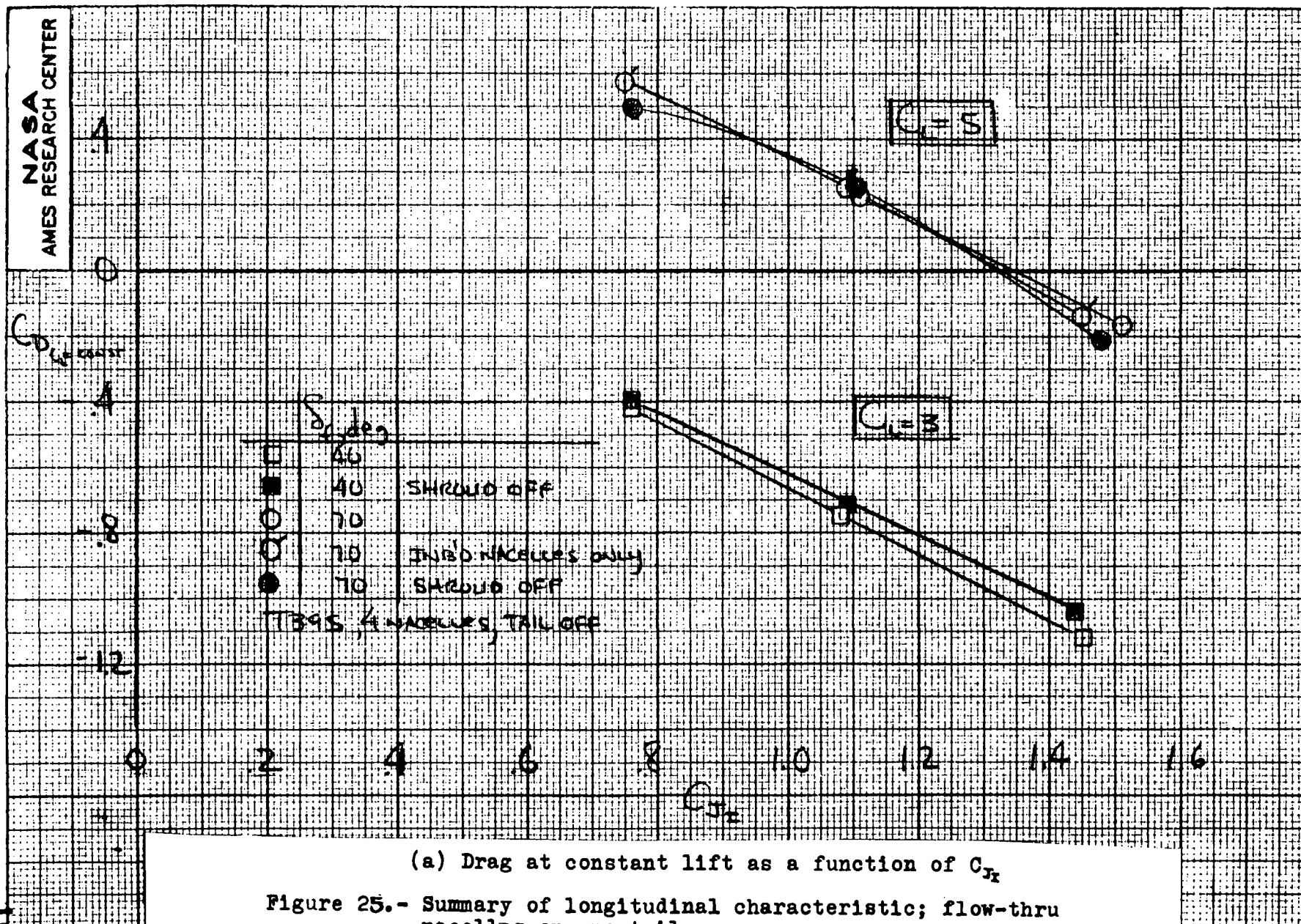


Figure 24.- Continued.



(d) Maximum lift as a function of  $C_L$

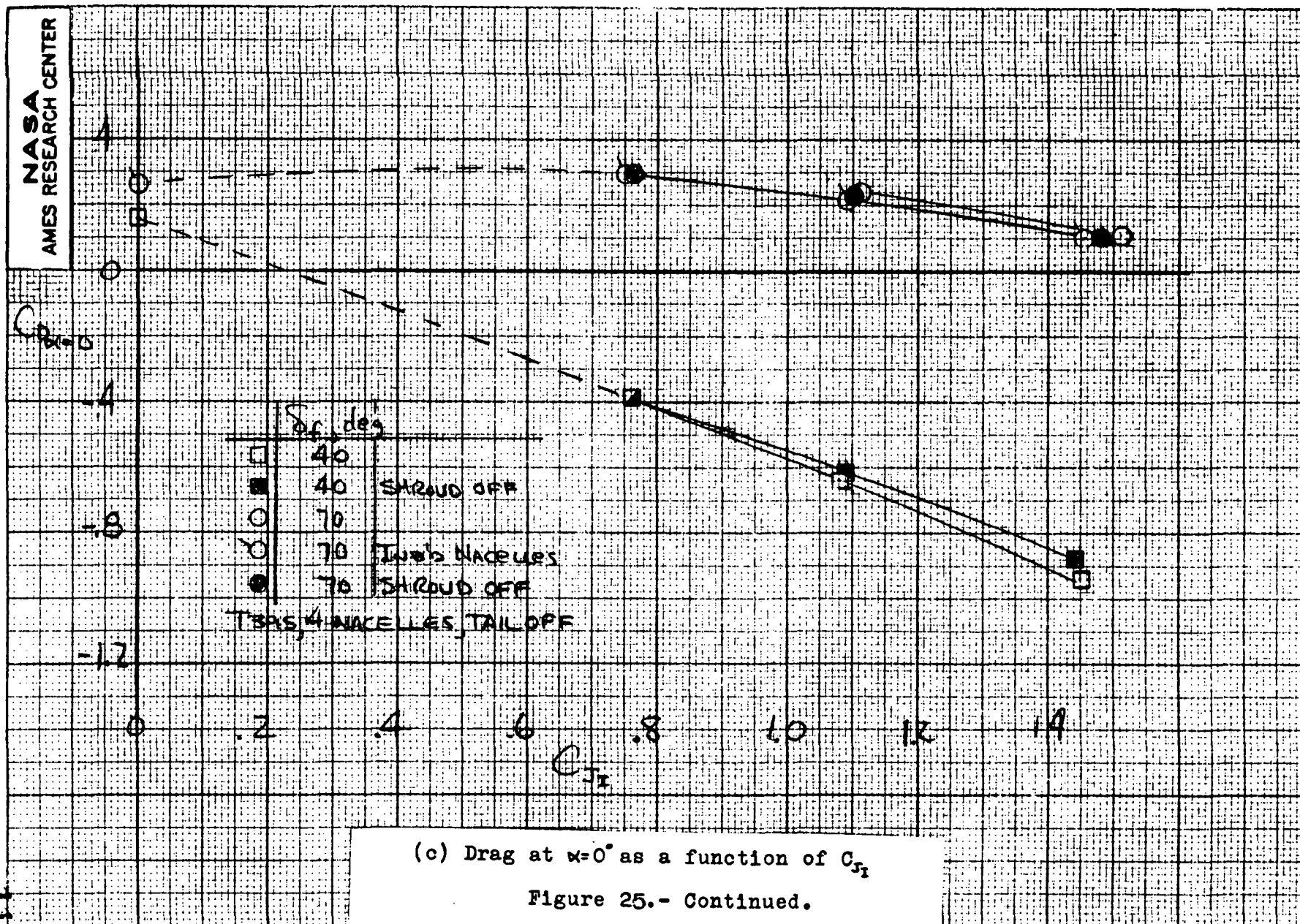
Figure 24.- Concluded.



(a) Drag at constant lift as a function of  $C_T$

Figure 25.- Summary of longitudinal characteristic; flow-thru nacelles on, no tail.





(c) Drag at  $\alpha=0^\circ$  as a function of  $C_{D1}$

Figure 25.- Continued.



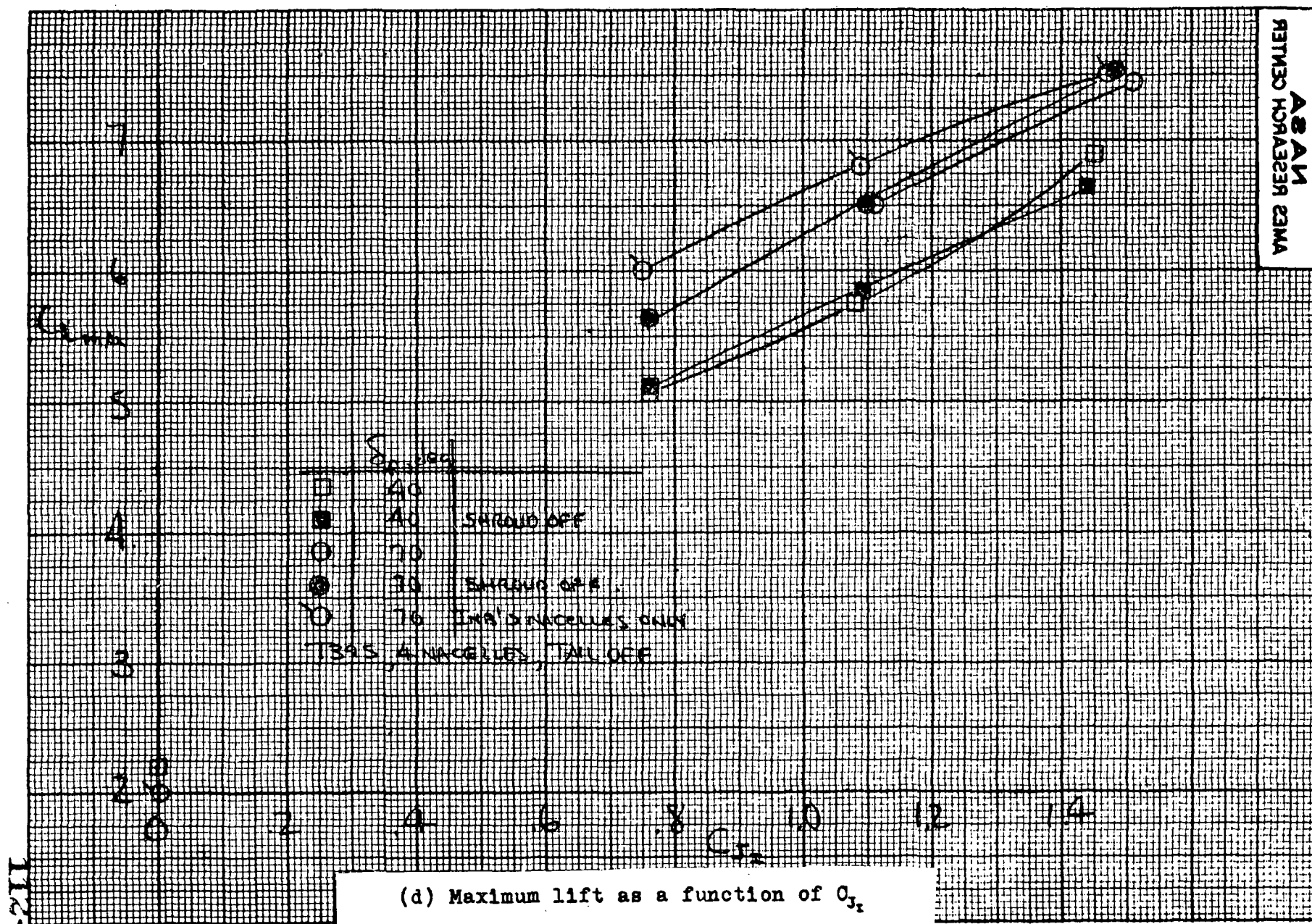


Figure 25.- Concluded.

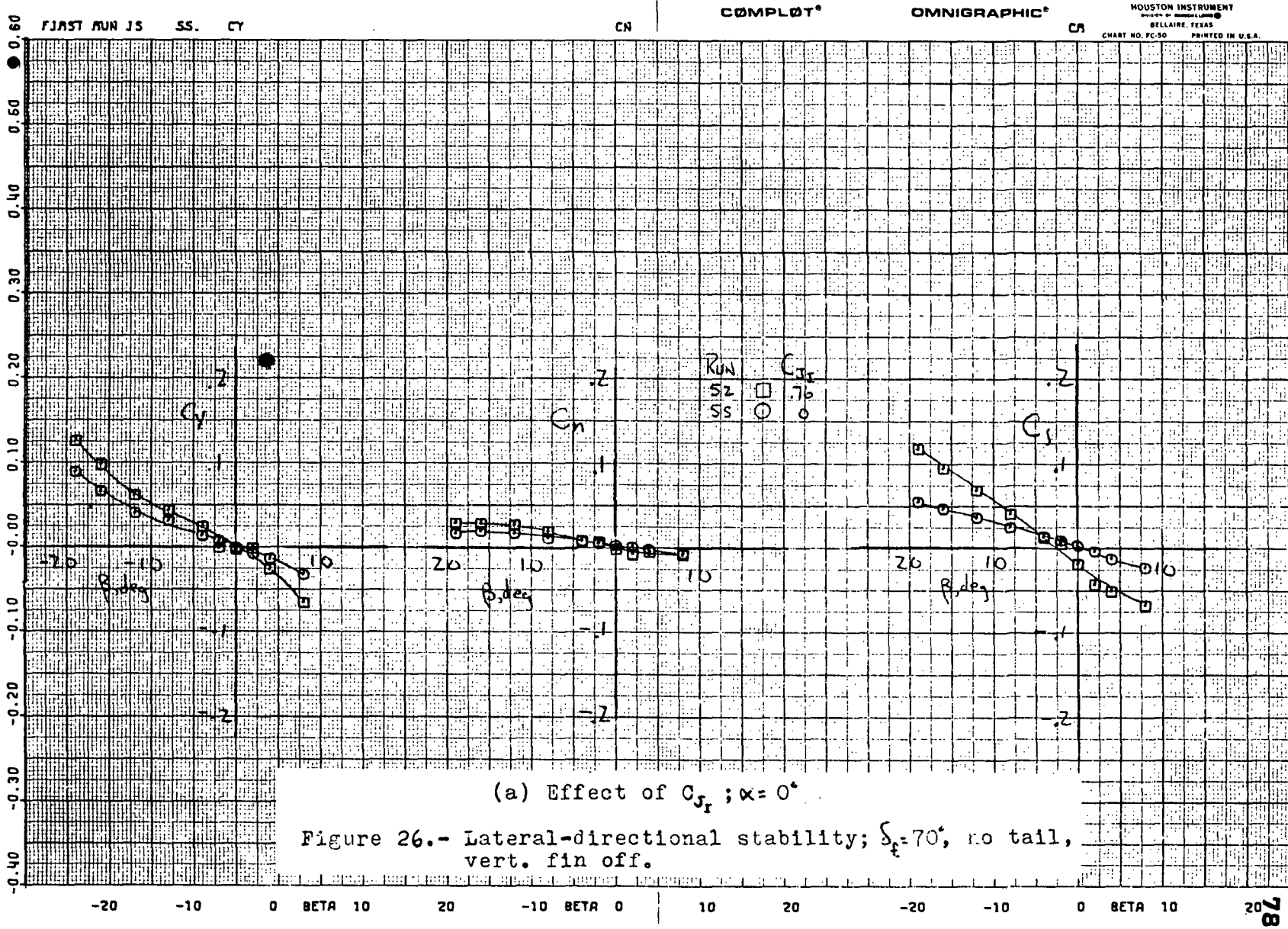
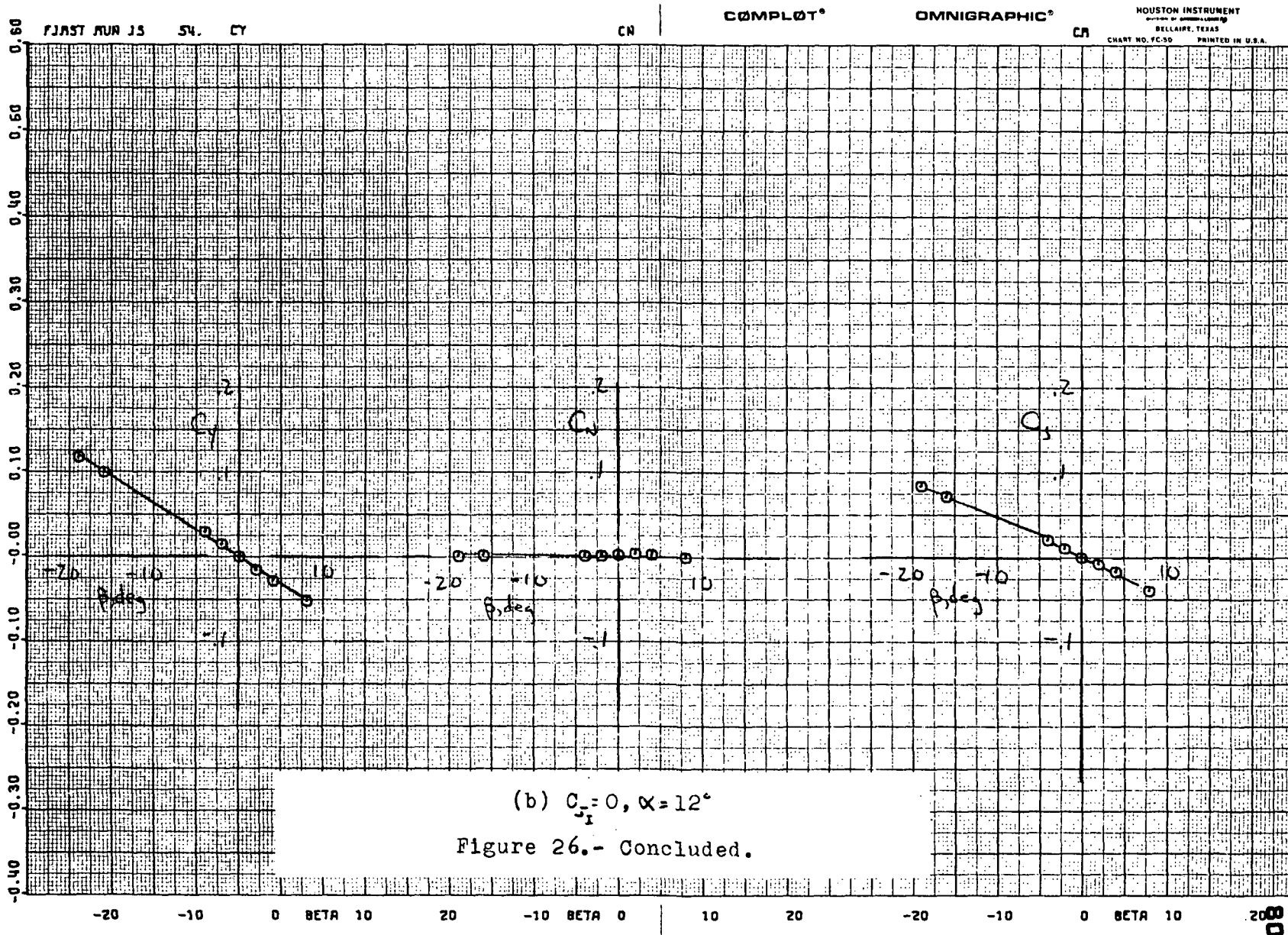


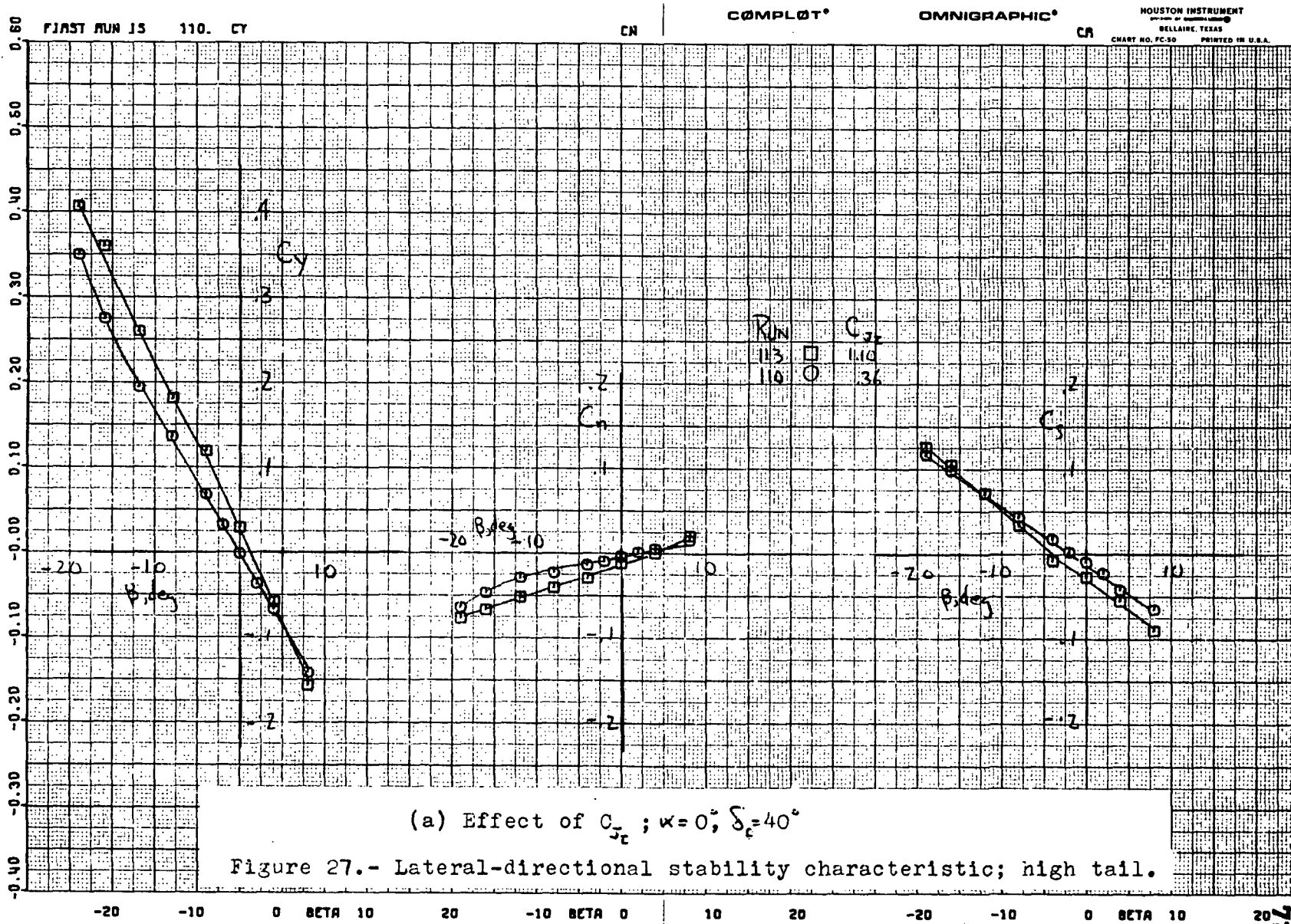
Figure 26.- Lateral-directional stability;  $\delta_f = 70^\circ$ , no tail, vert. fin off.

133



111





FAST RUN JS 111. CY

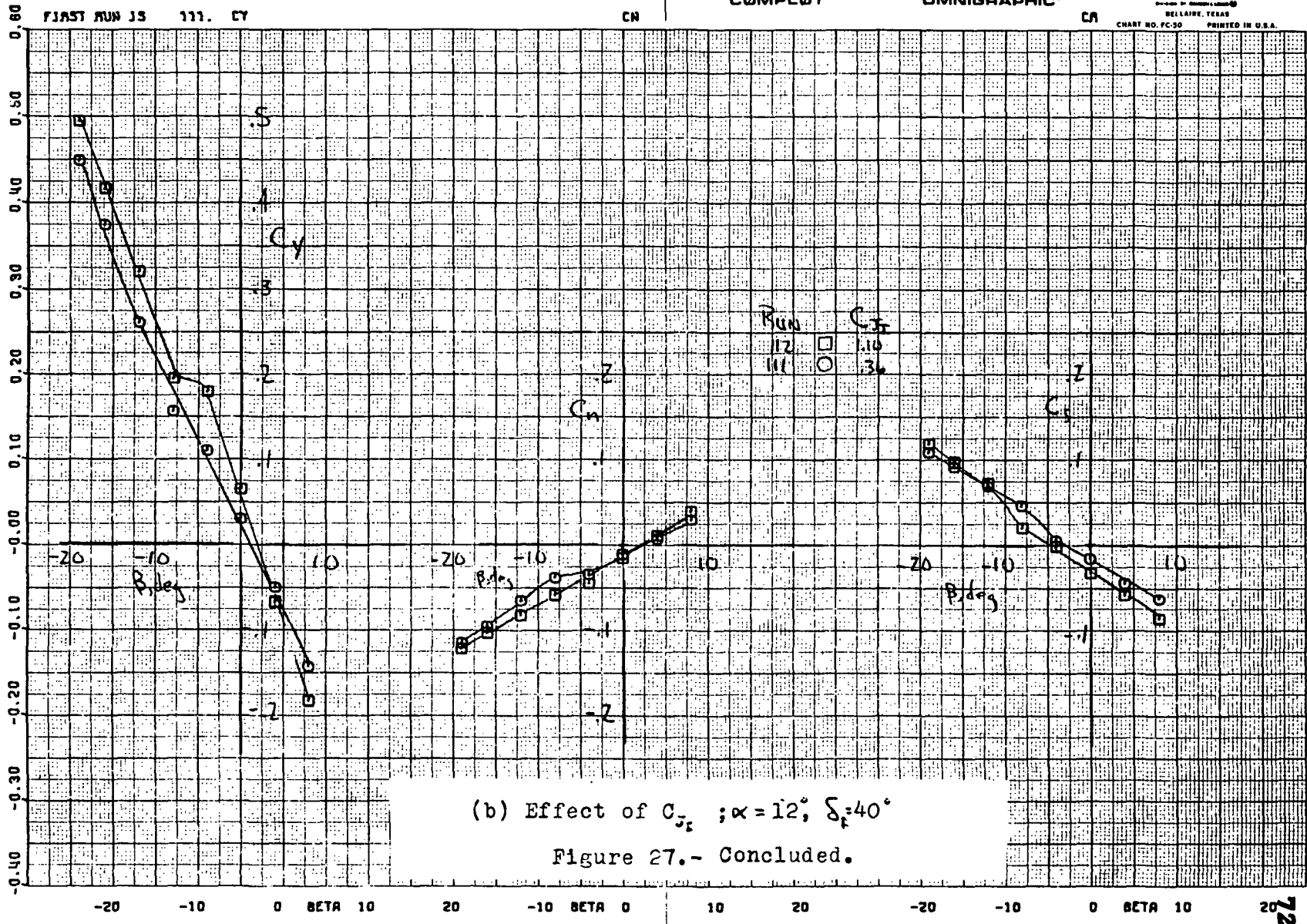
CN

COMPLØT

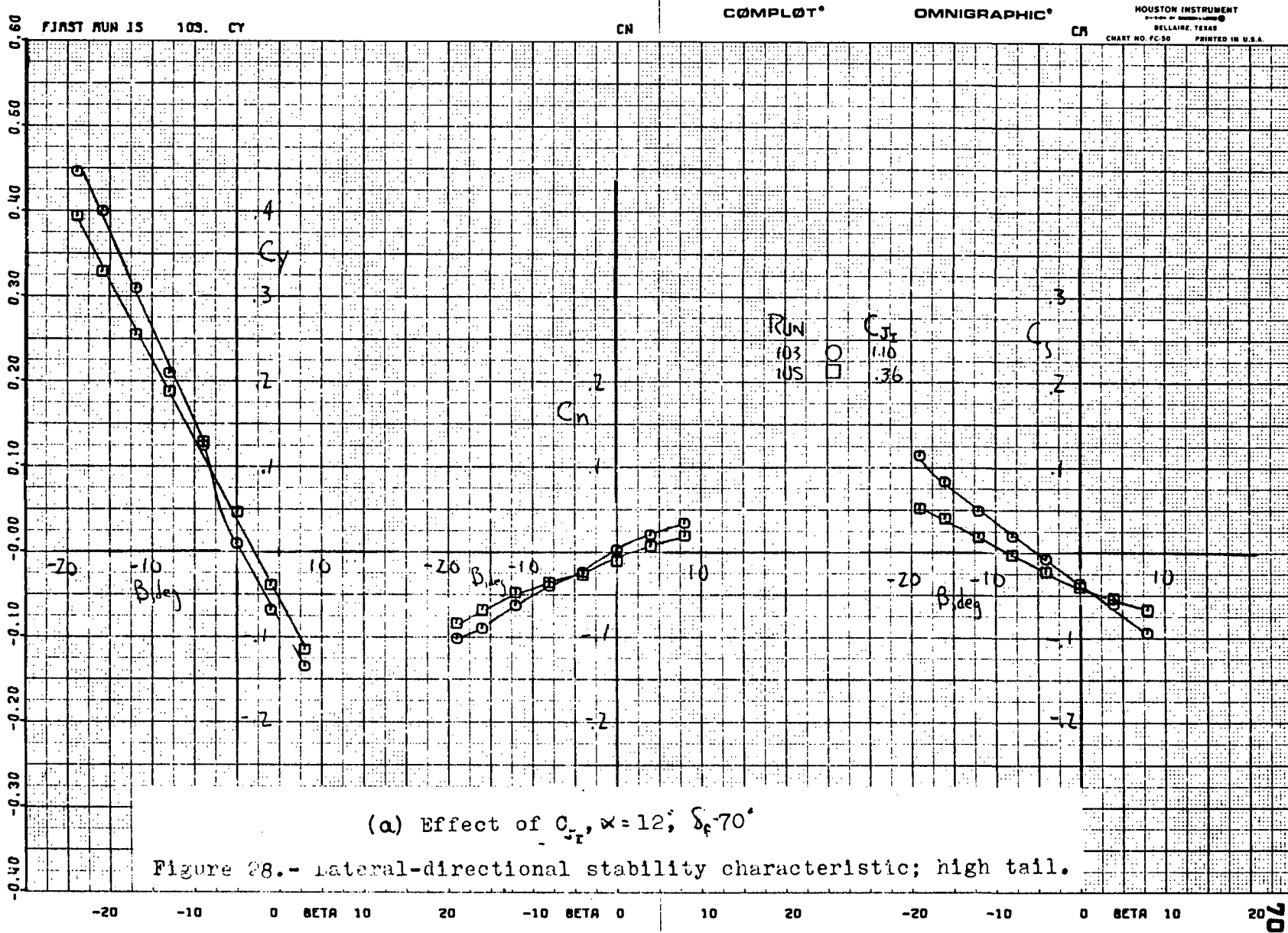
OMNIGRAPHIC

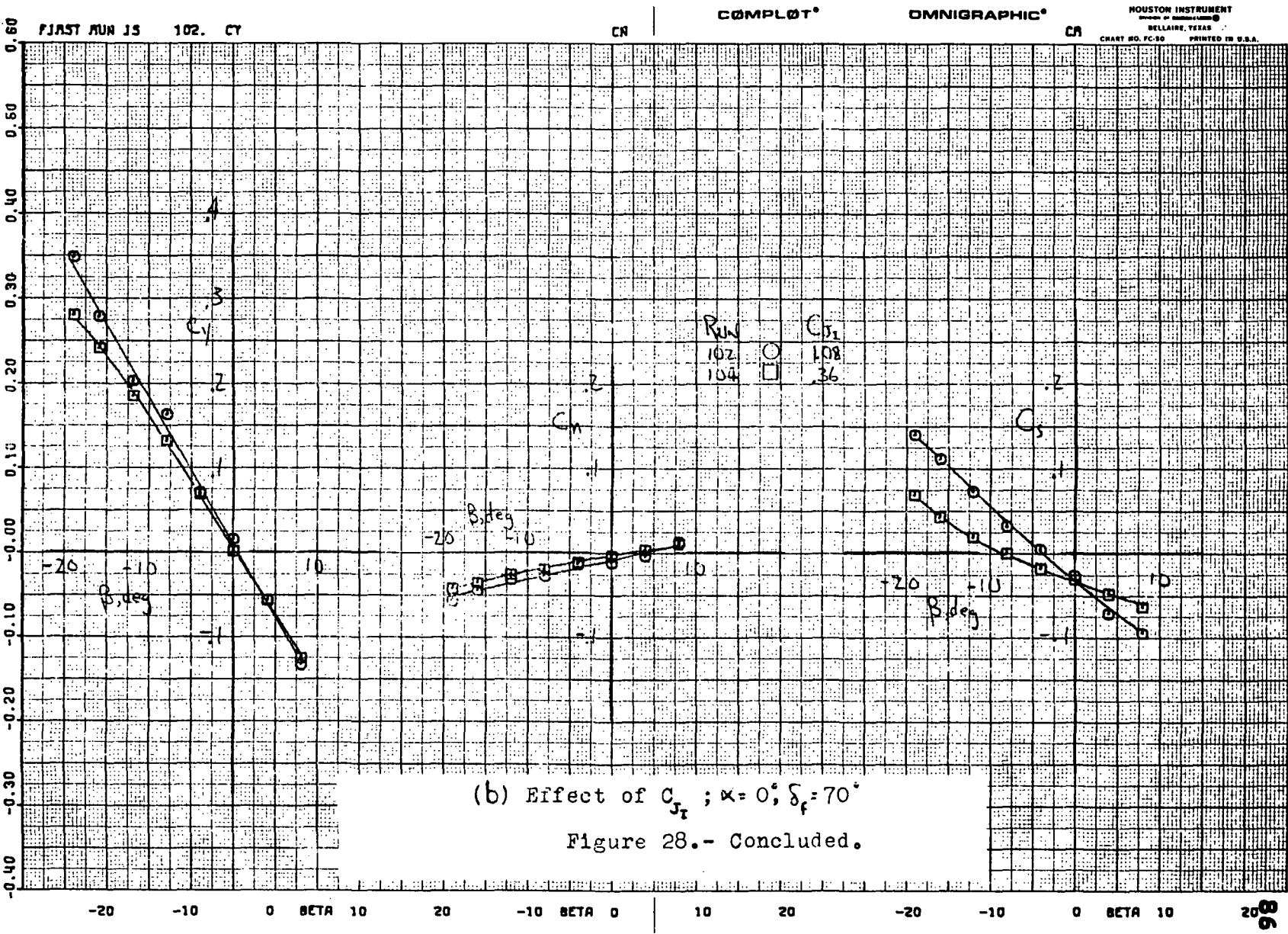
CN

HOUSTON INSTRUMENT  
BELLAIRE, TEXAS  
CHART NO. FC-50 PRINTED IN U.S.A.



117





118

216

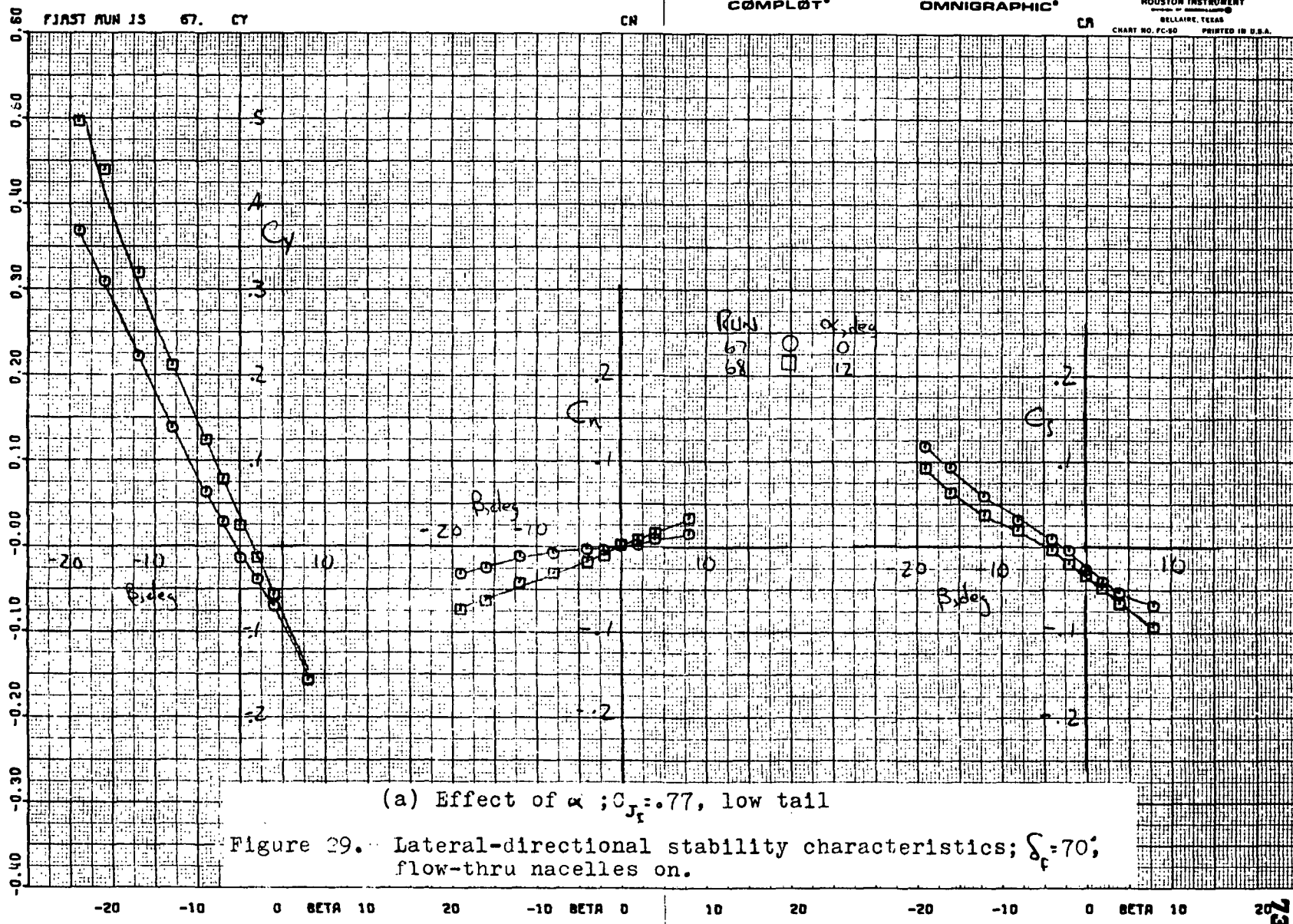
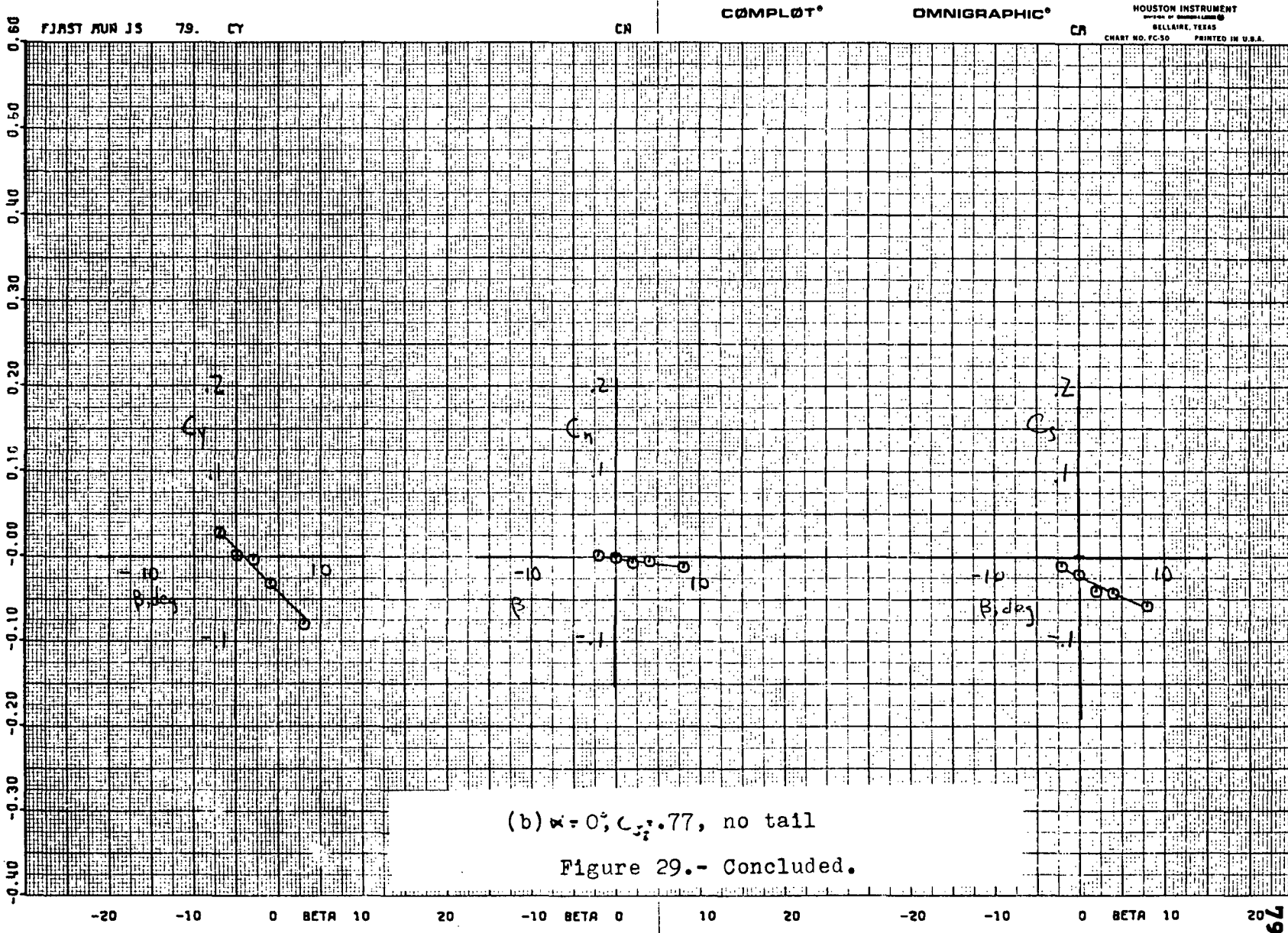


Figure 29. Lateral-directional stability characteristics;  $\delta_f=70^\circ$ ; flow-thru nacelles on.





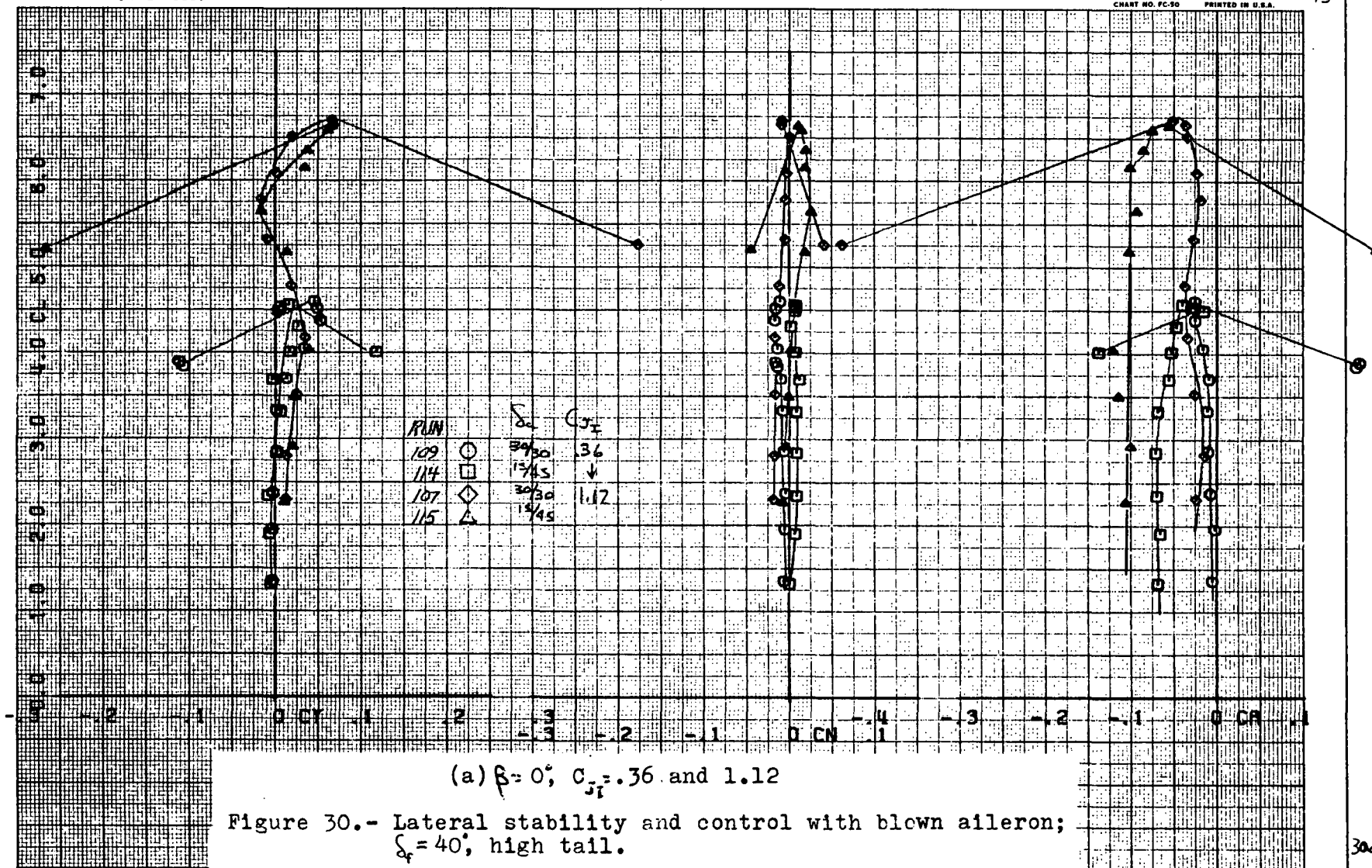
RUNS 109.

COMPLLOT

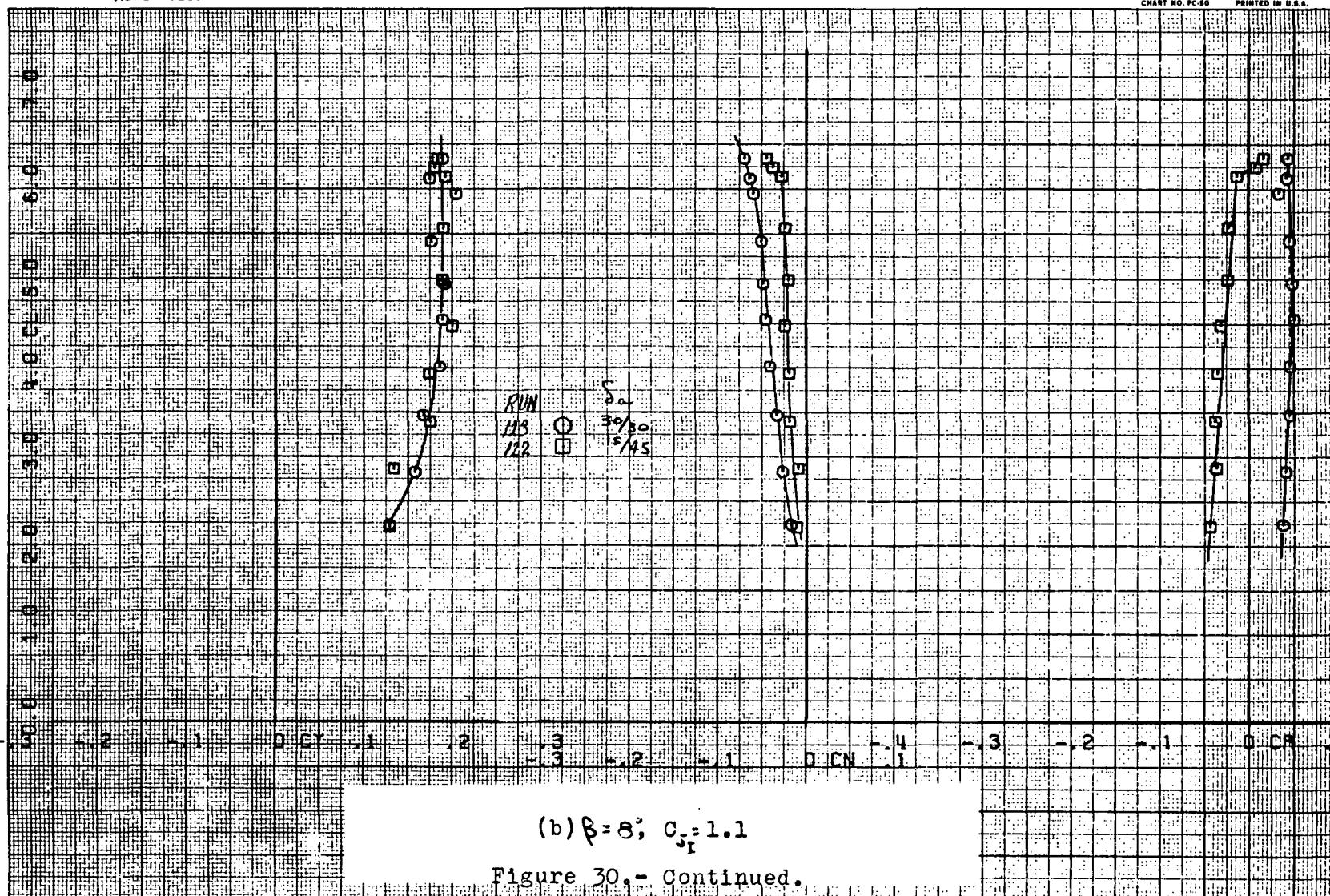
OMNIGRAPHIC

HOUSTON INSTRUMENT  
DIVISION OF HARRIS CORPORATION  
BELL LAIR, TEXAS  
CHART NO. FC-50 PRINTED IN U.S.A.

45



30a



(b)  $\beta = 8^\circ$ ,  $C_{J_i} = 1.1$

Figure 30.- Continued.



FIRST RUN 15 116. CY

CM

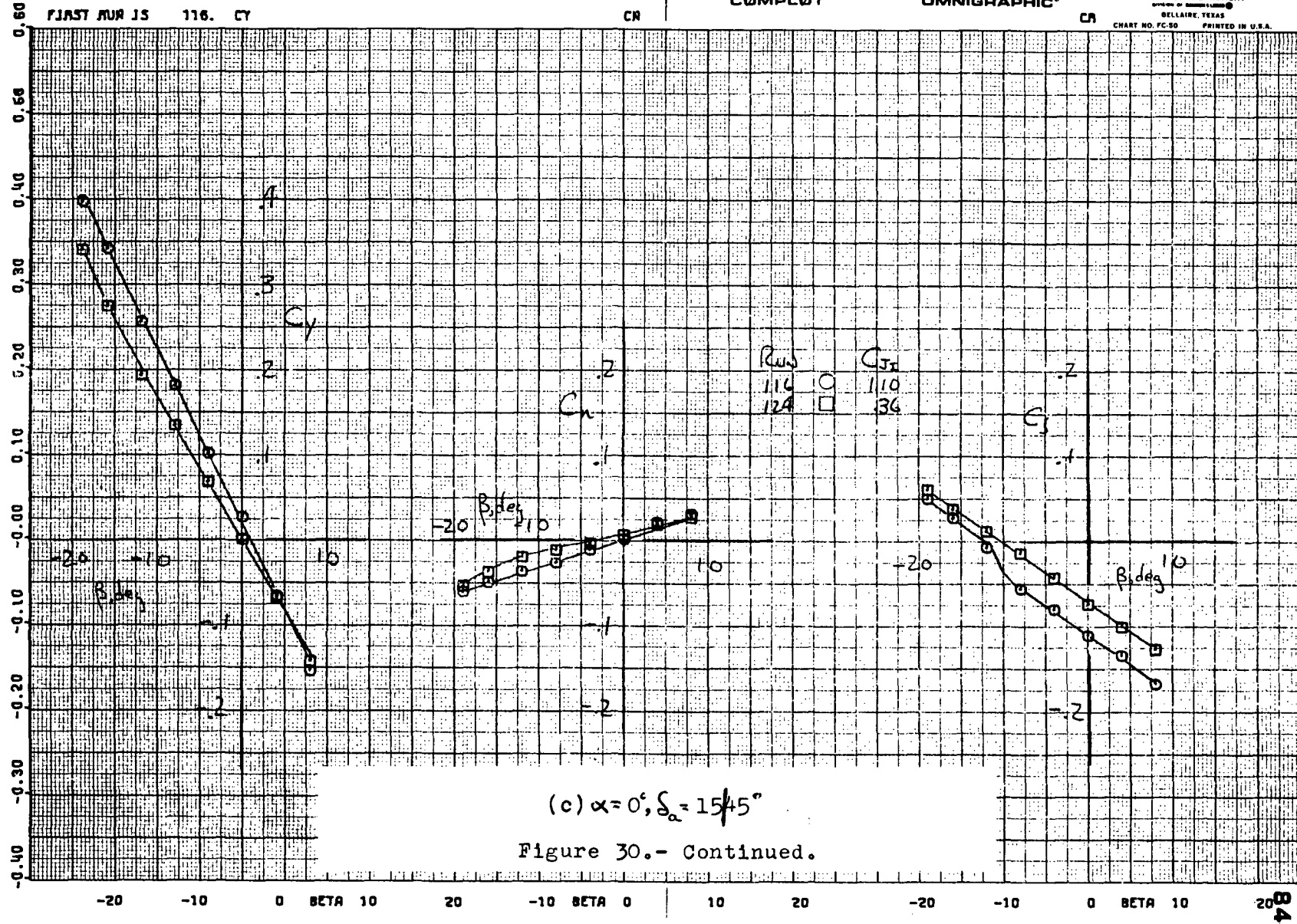
COMPLØT®

OMNIGRAPHIC®

CM

HOUSTON INSTRUMENT  
SHELLAIRE, TEXAS  
CHART NO. FC-50 PRINTED IN U.S.A.

47



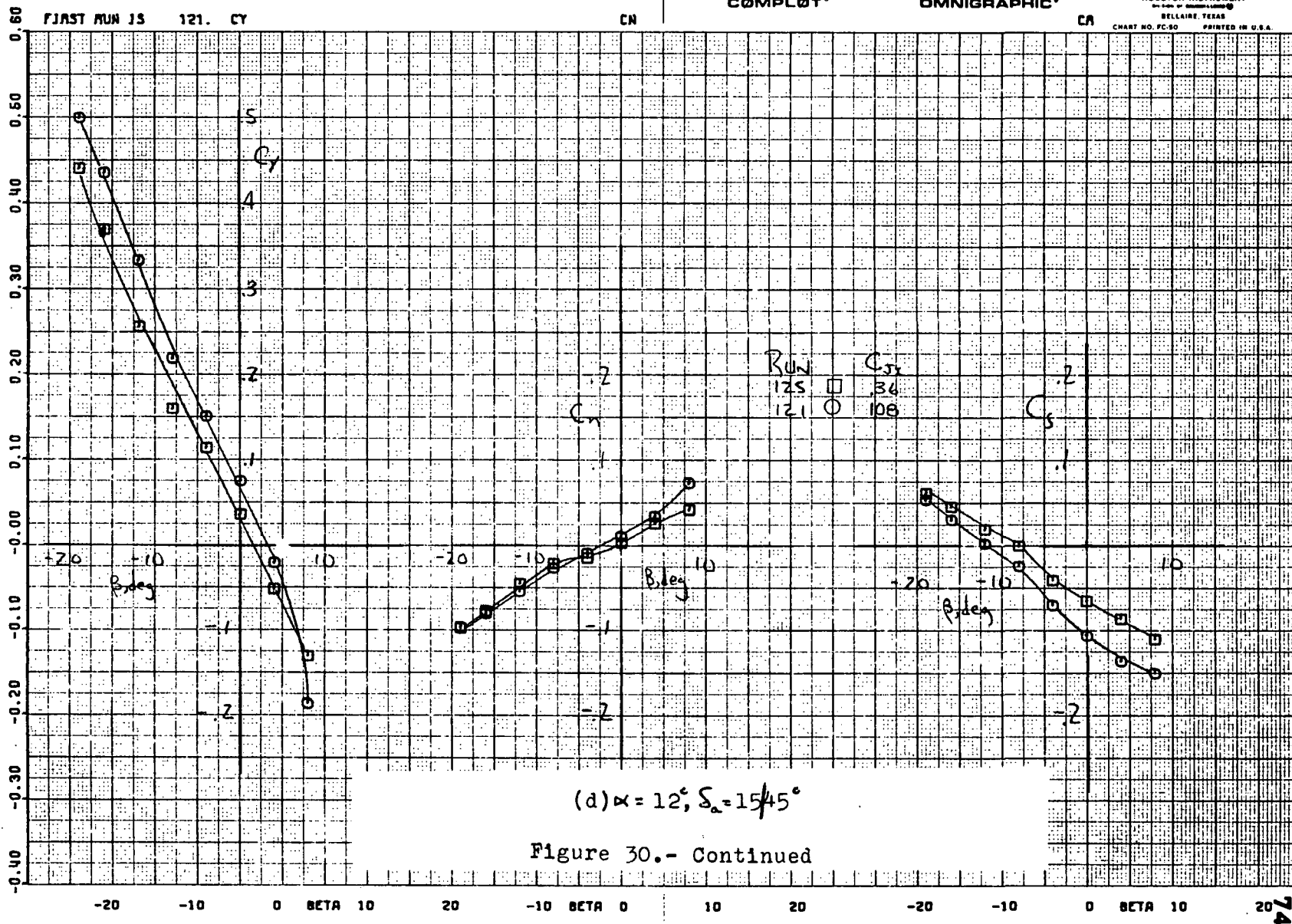
(c)  $\alpha = 0^\circ, \delta_\alpha = 15.45^\circ$

Figure 30.- Continued.

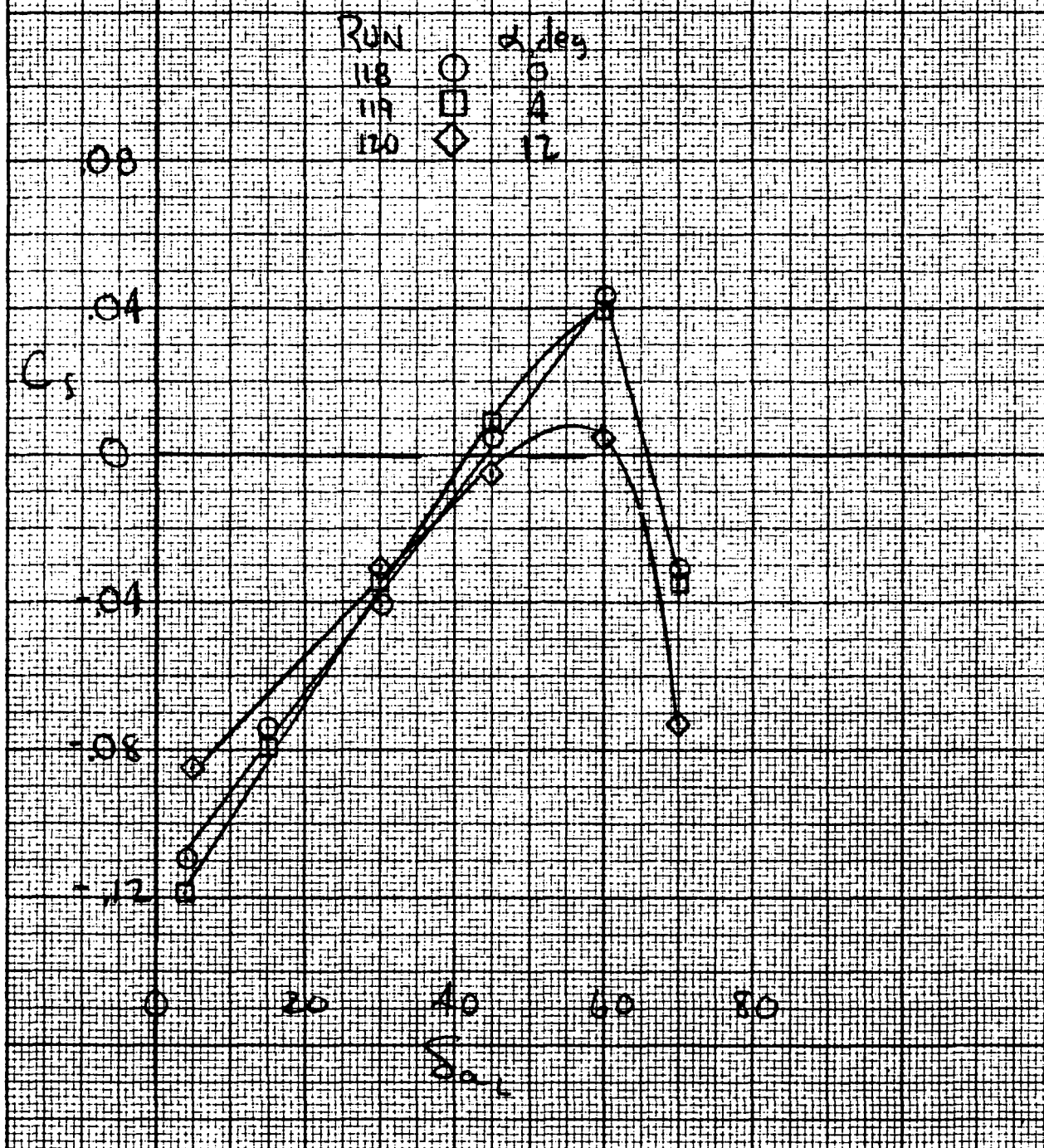
123

30c

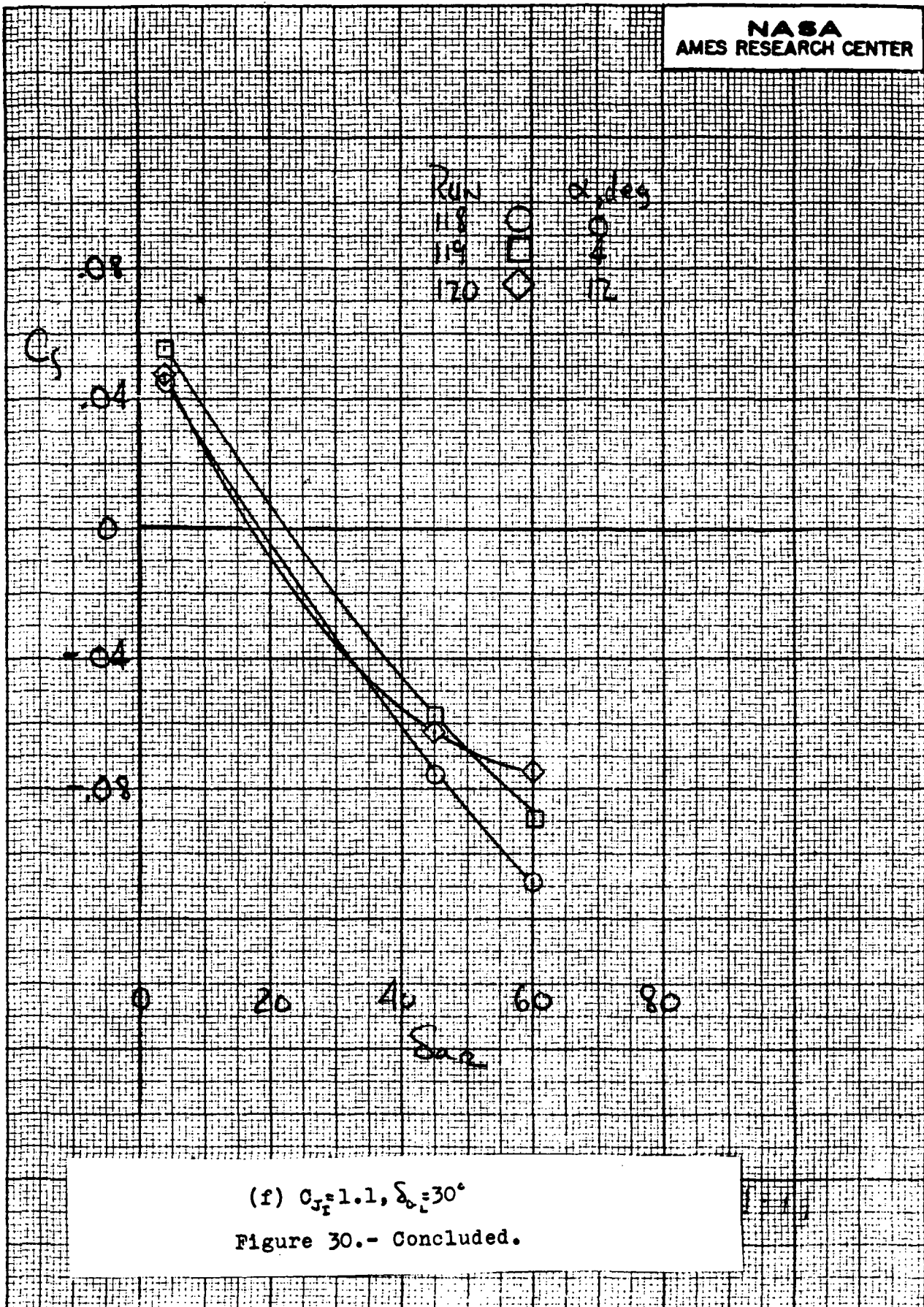
121



NASA  
AMES RESEARCH CENTER



(e)  $Q_{\infty} = 1.1, \delta_{a1} = 30^\circ$   
Figure 30.- Continued.



(f)  $C_{J_F} = 1.1$ ,  $\delta_{0_i} = 30^\circ$   
Figure 30.- Concluded.

RUN 100.

COMPL0T

OMNIGRAPHIC

HOUSTON INSTRUMENT  
BELLAIRE, TEXAS  
CHART NO. FC-50 PRINTED IN U.S.A.

49

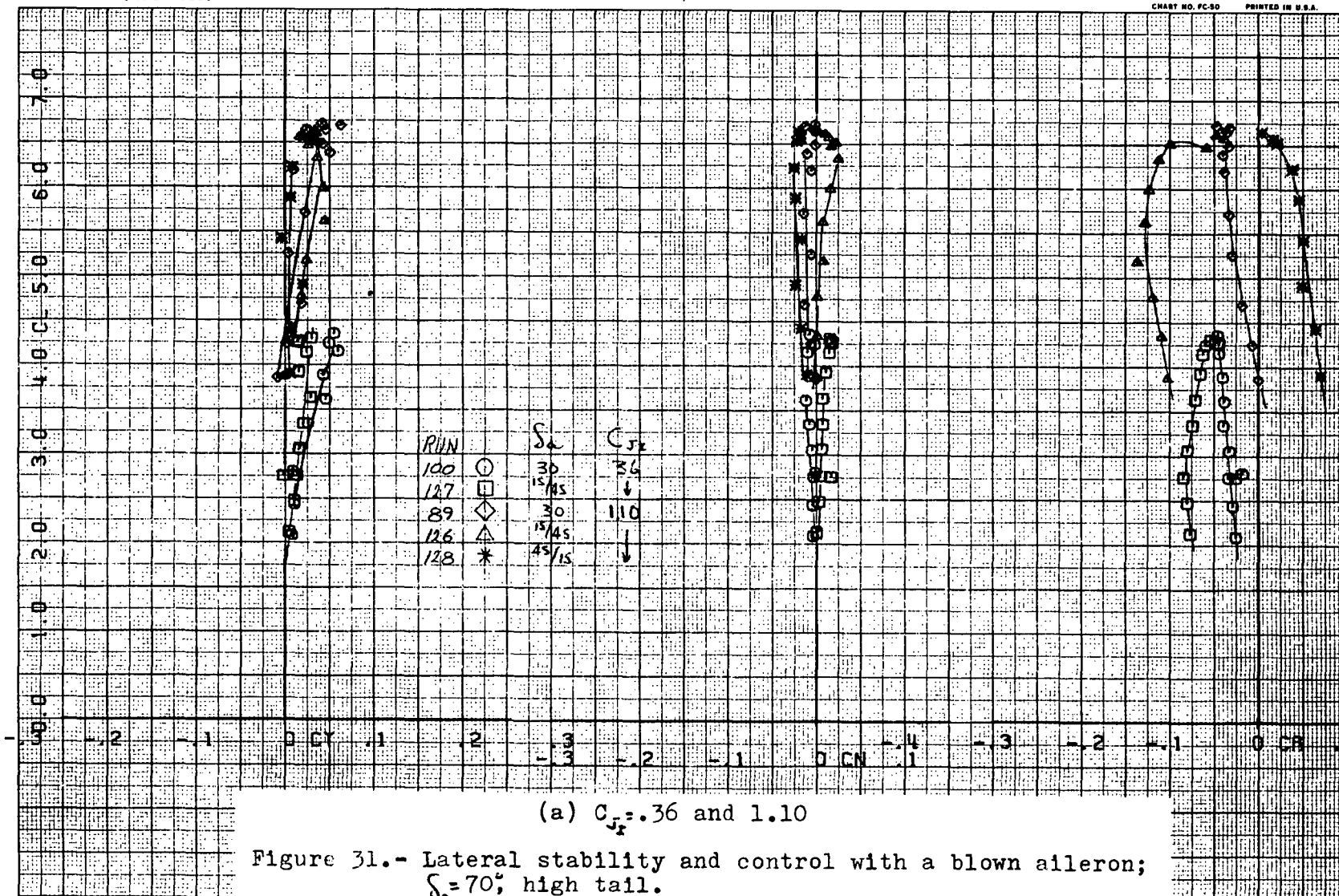
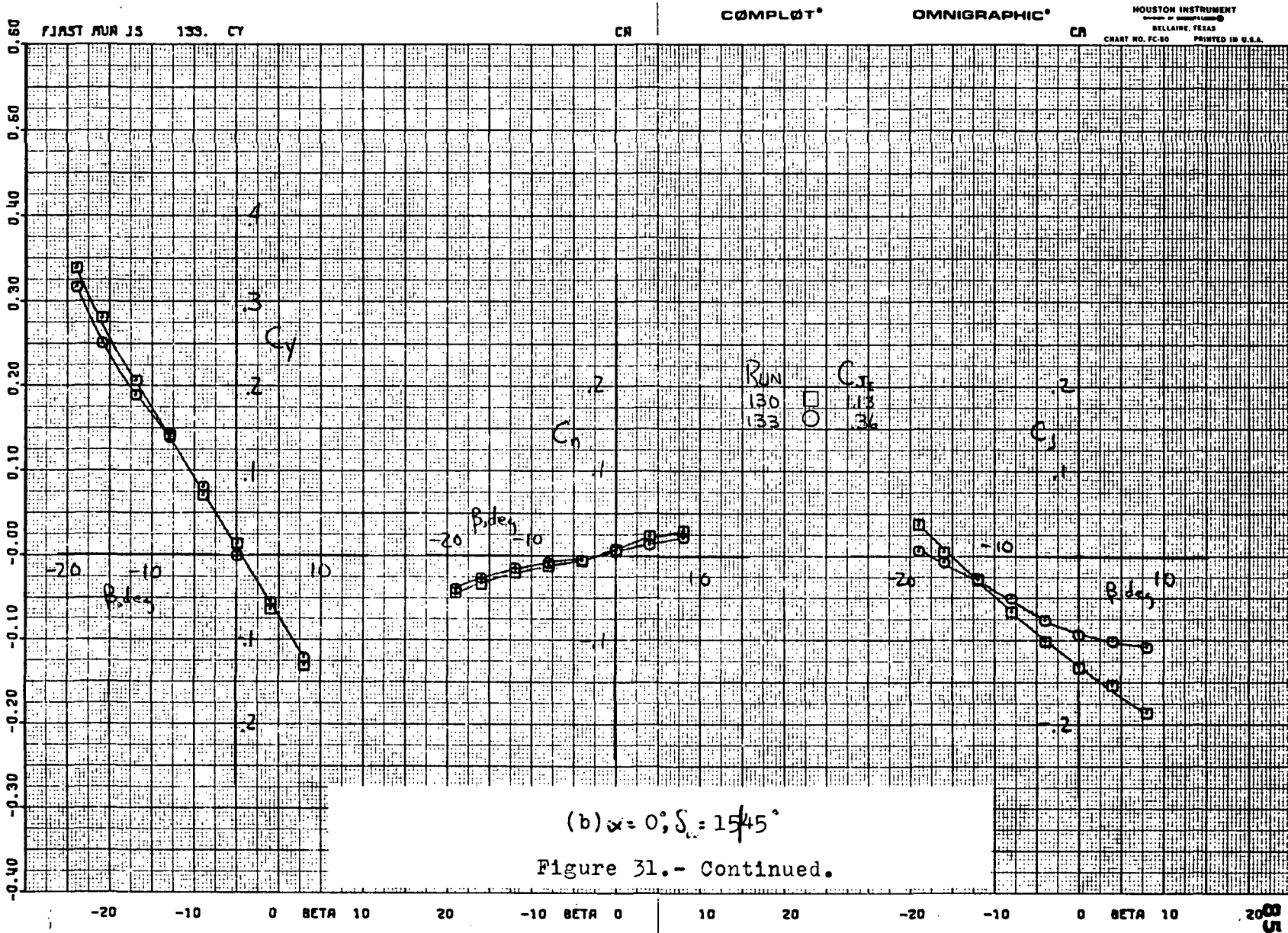


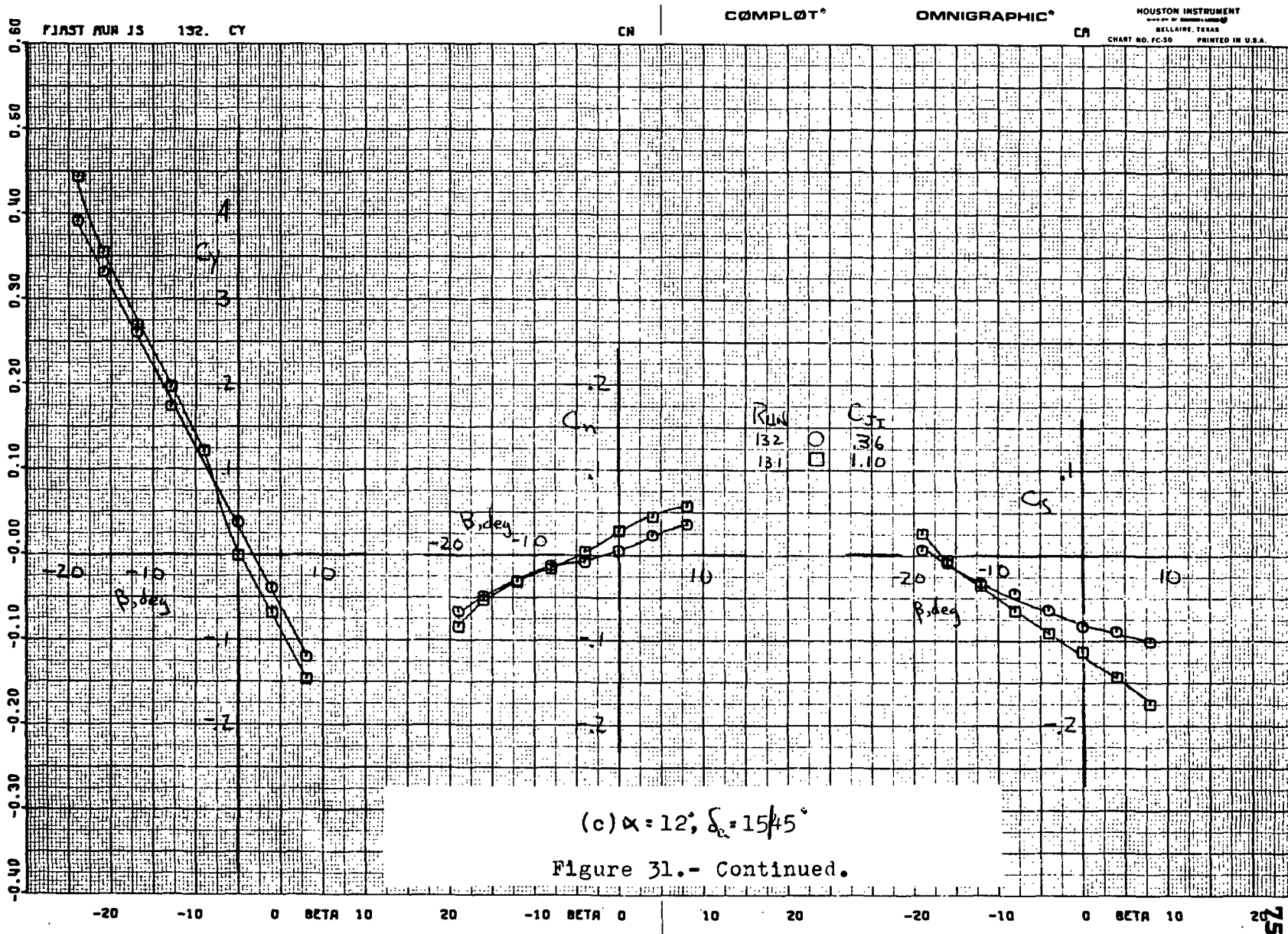
Figure 31.- Lateral stability and control with a blown aileron;  
 $S_f = 70^\circ$ ; high tail.





128

316



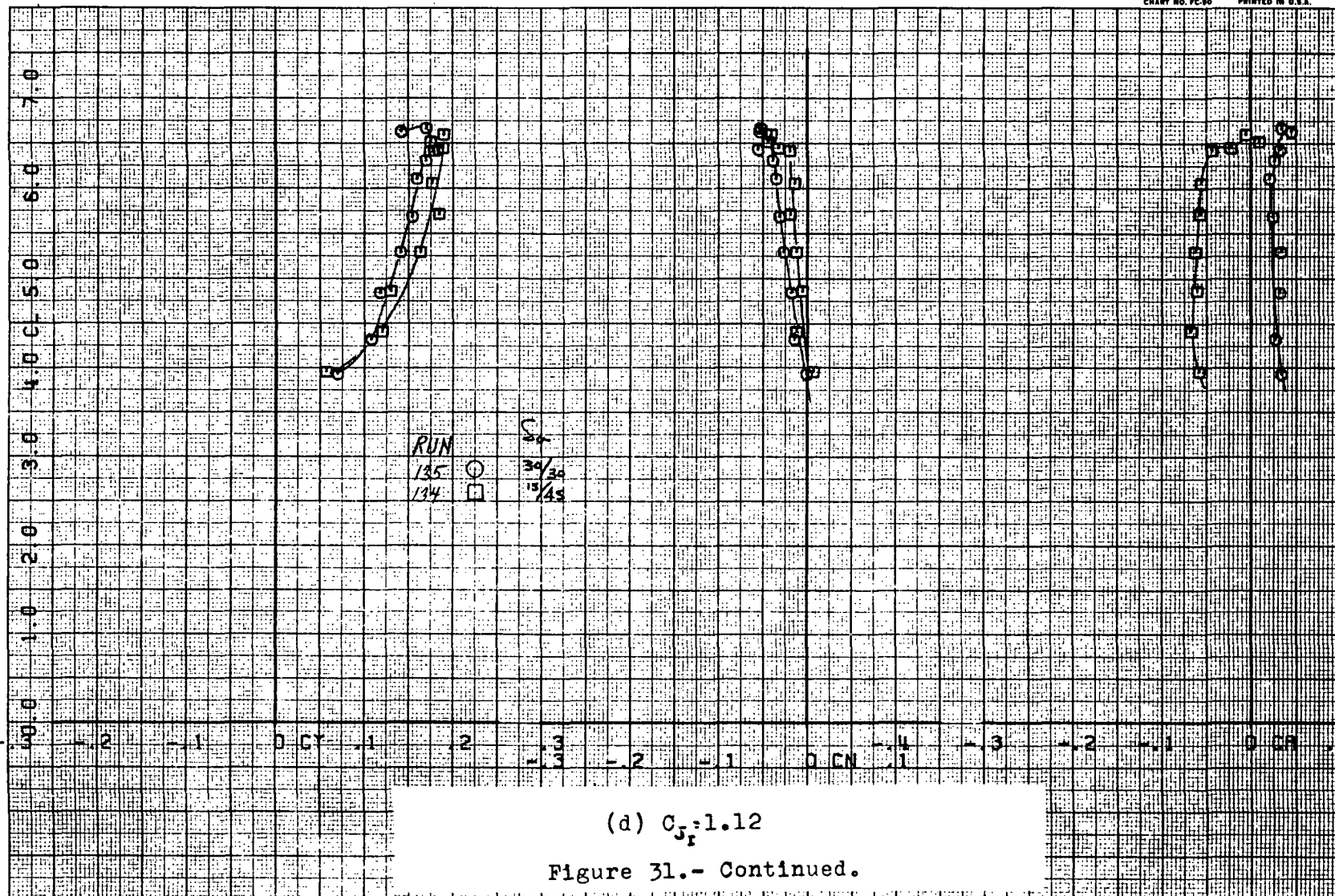
RUNS 135.

COMPLØT®

OMNIGRAPHIC®

HOUSTON INSTRUMENT  
DIVISION OF HUBBARD & PARSONS  
BELLARE, TEXAS  
CHART NO. FC-90 PRINTED IN U.S.A.

52



(d)  $C_{J_f} = 1.12$

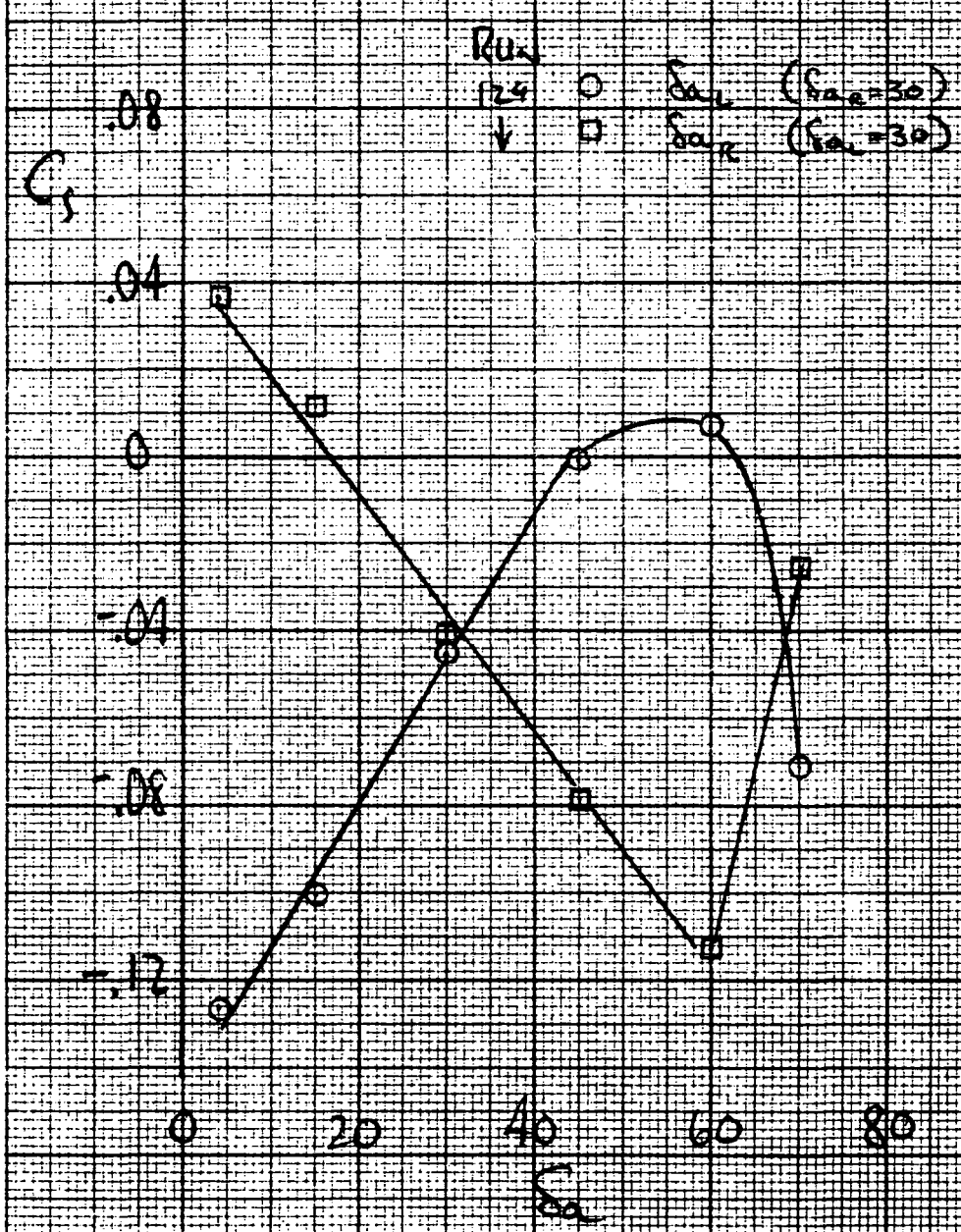
Figure 31.- Continued.

130

24

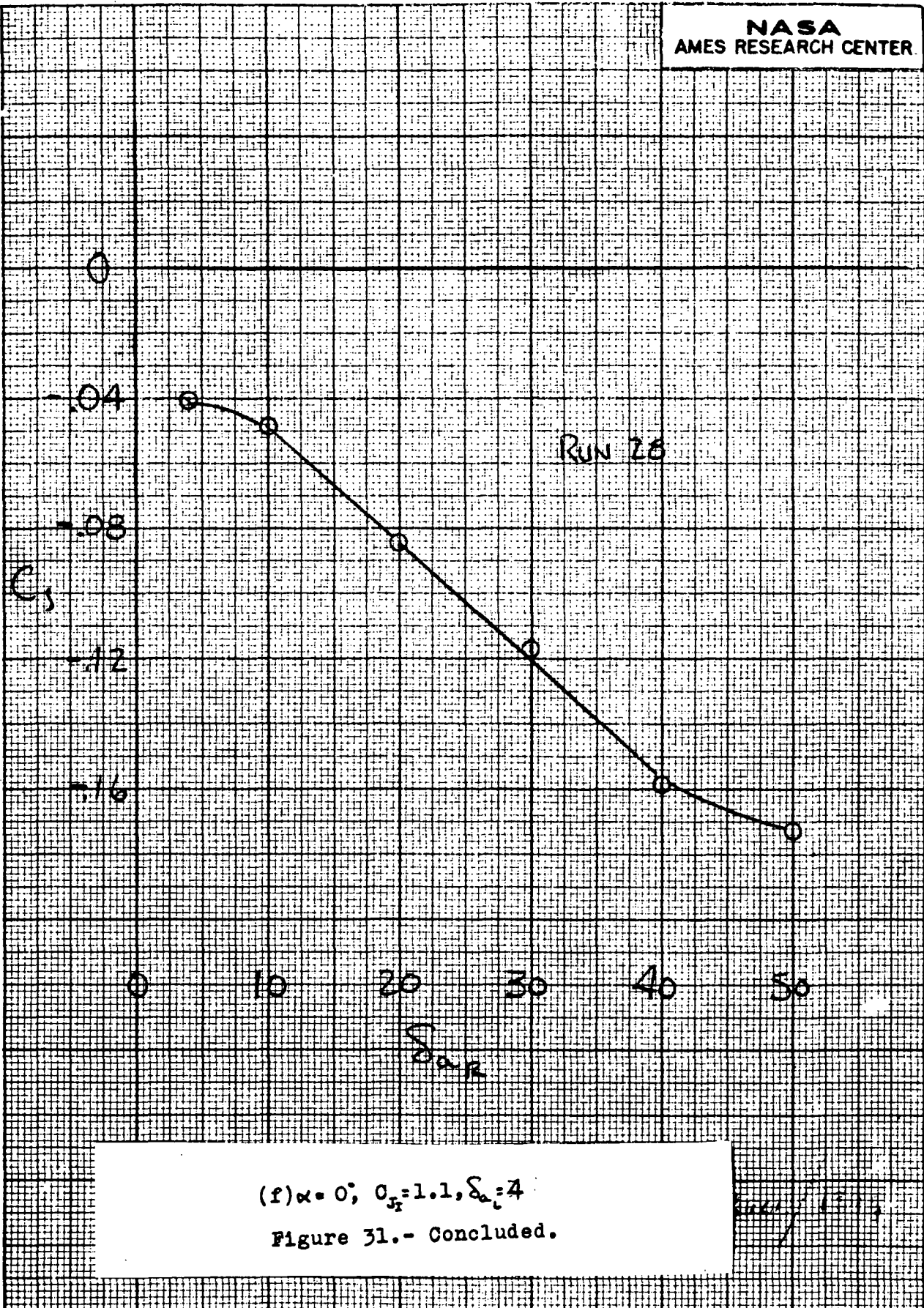
3d





(e)  $\alpha = 4^\circ$ ,  $C_{J_T} = 1.1$

Figure 31.- Continued.



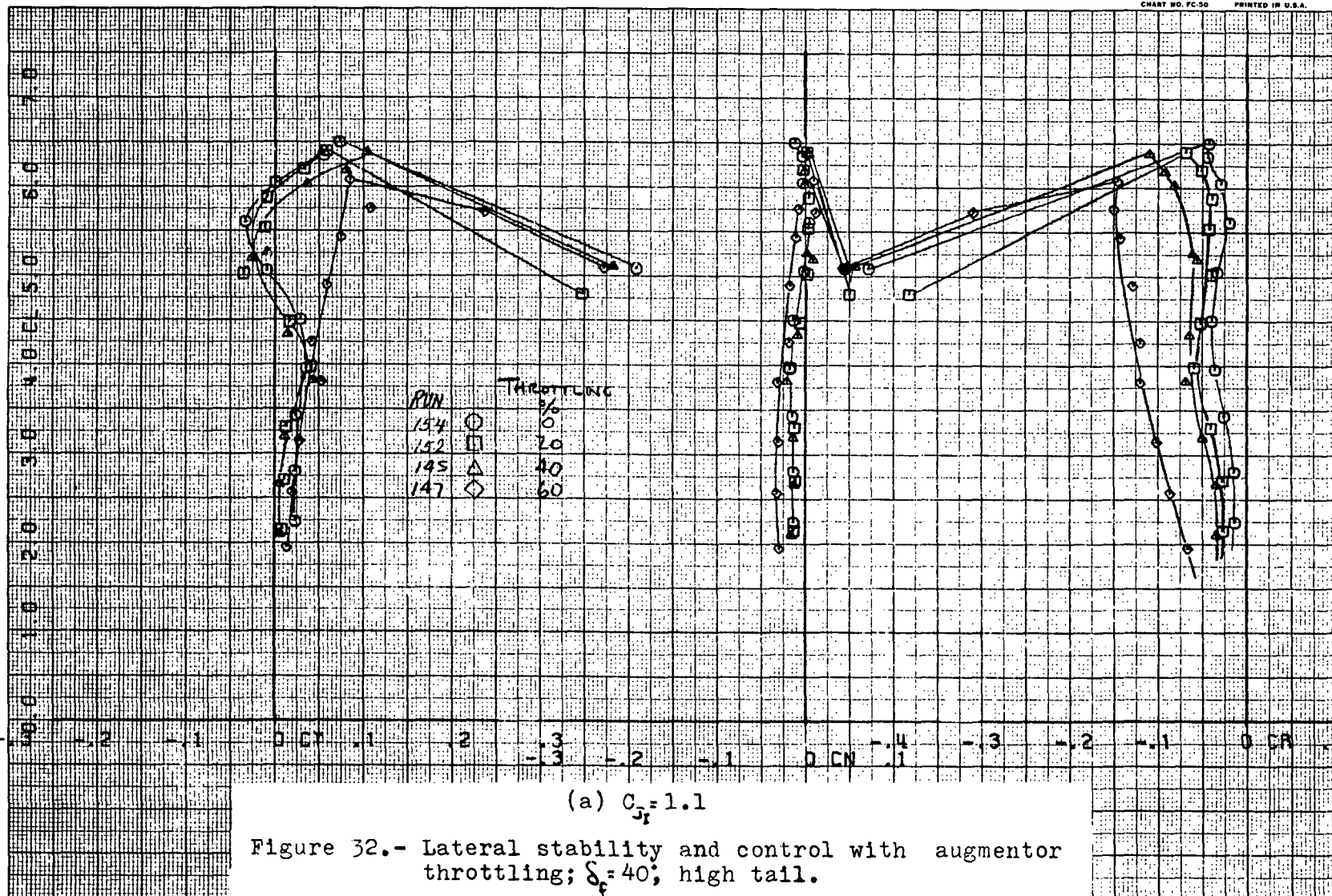
RUNS 154.

COMPLØT®

OMNIGRAPHIC®

HOUSTON INSTRUMENT  
DIVISION OF BELL & HOWELL  
BELLAIRE, TEXAS  
CHART NO. FC-50 PRINTED IN U.S.A.

60



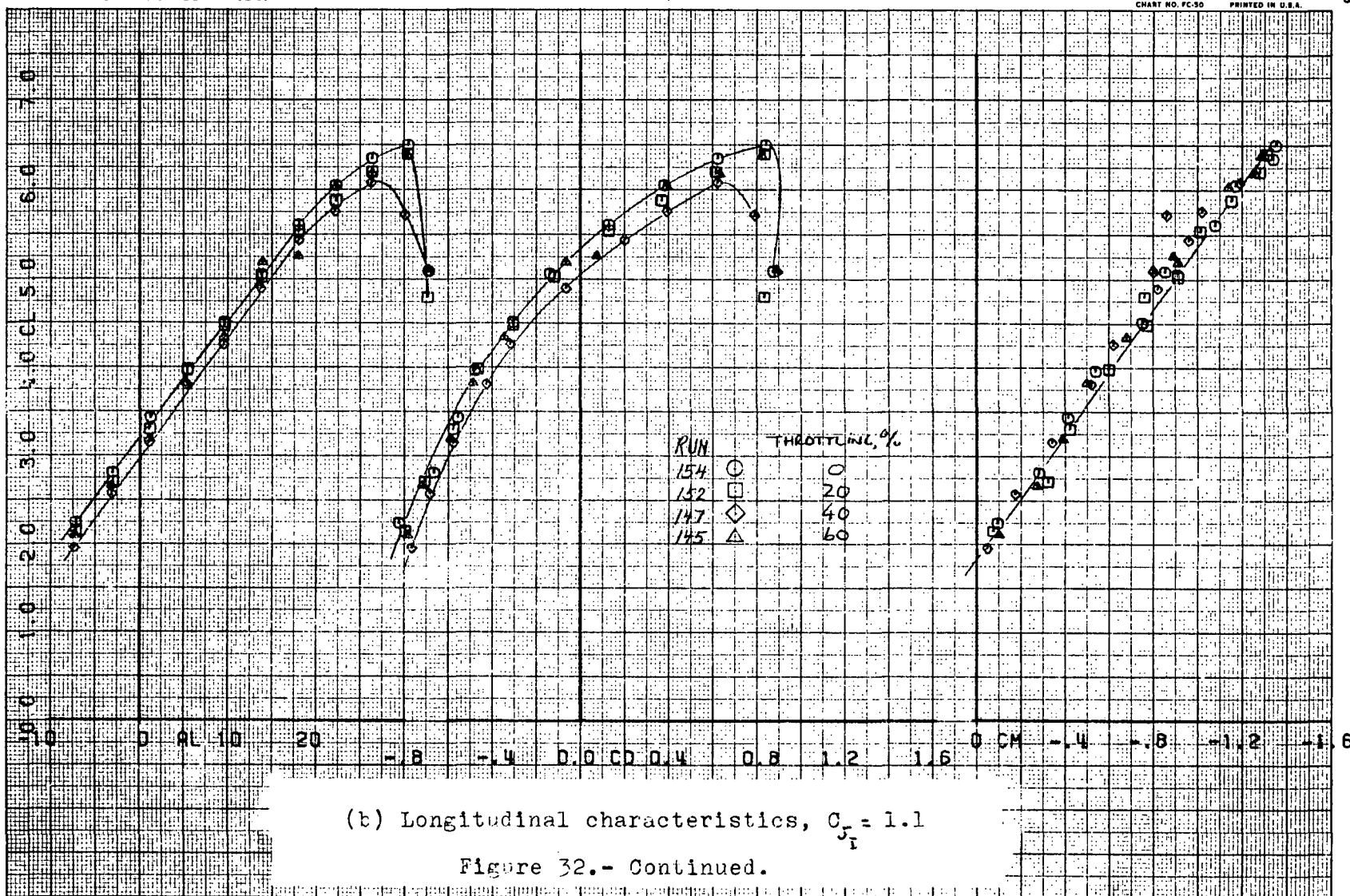
FAST RUN 15 154.

COMPLLOT®

OMNIGRAPHIC®

HOUSTON INSTRUMENT  
DALLAS, TEXAS  
CHART NO. FC-50 PRINTED IN U.S.A.

61



(b) Longitudinal characteristics,  $C_{J_1} = 1.1$

Figure 32.- Continued.

134

42

326

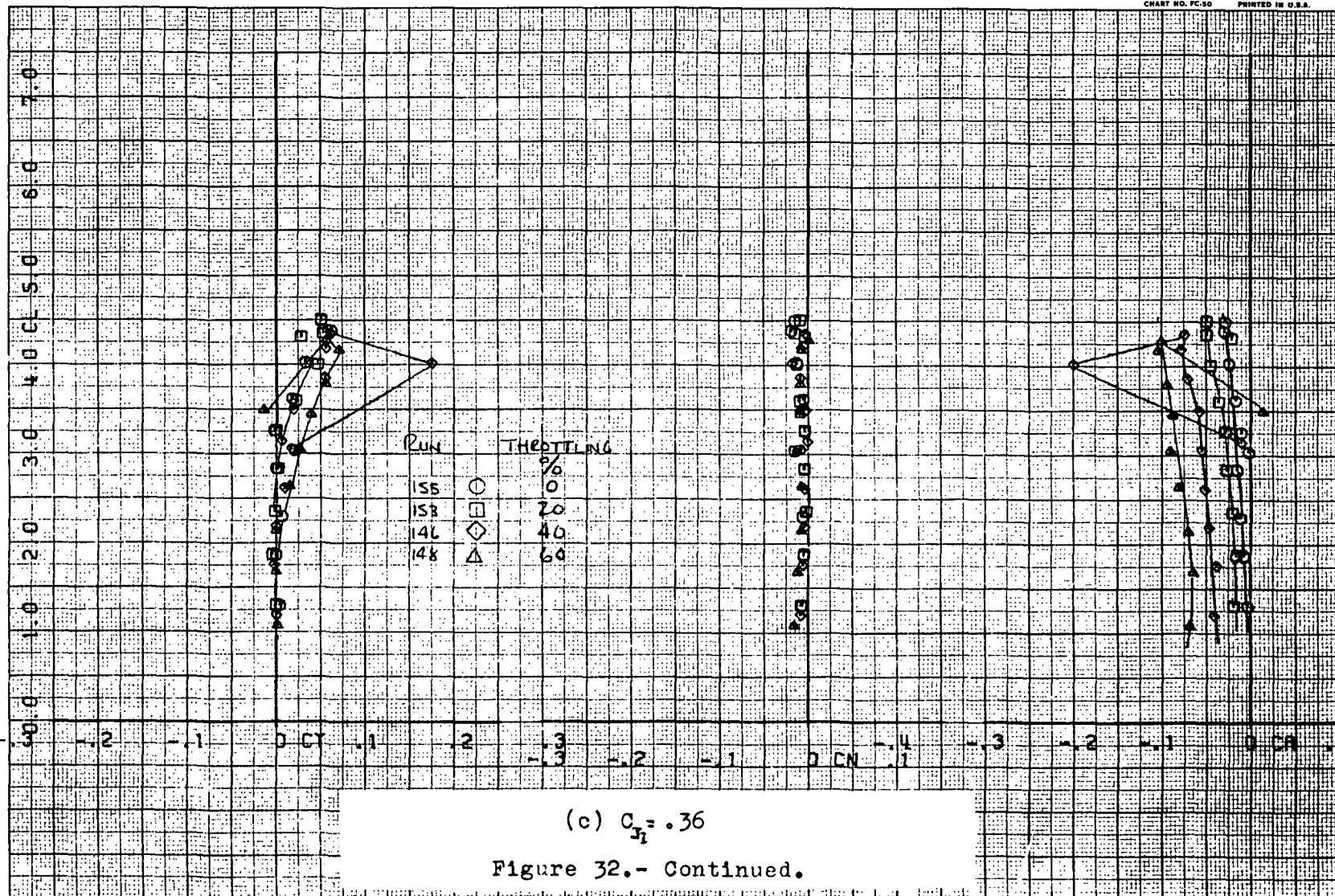
RUNS 155.

COMPLLOT®

OMNIGRAPHIC®

HOUSTON INSTRUMENT  
BELLAIRE, TEXAS  
CHART NO. FC-50 PRINTED IN U.S.A.

62



(c)  $C_{T1} = .36$

Figure 32.- Continued.

135

30

32c



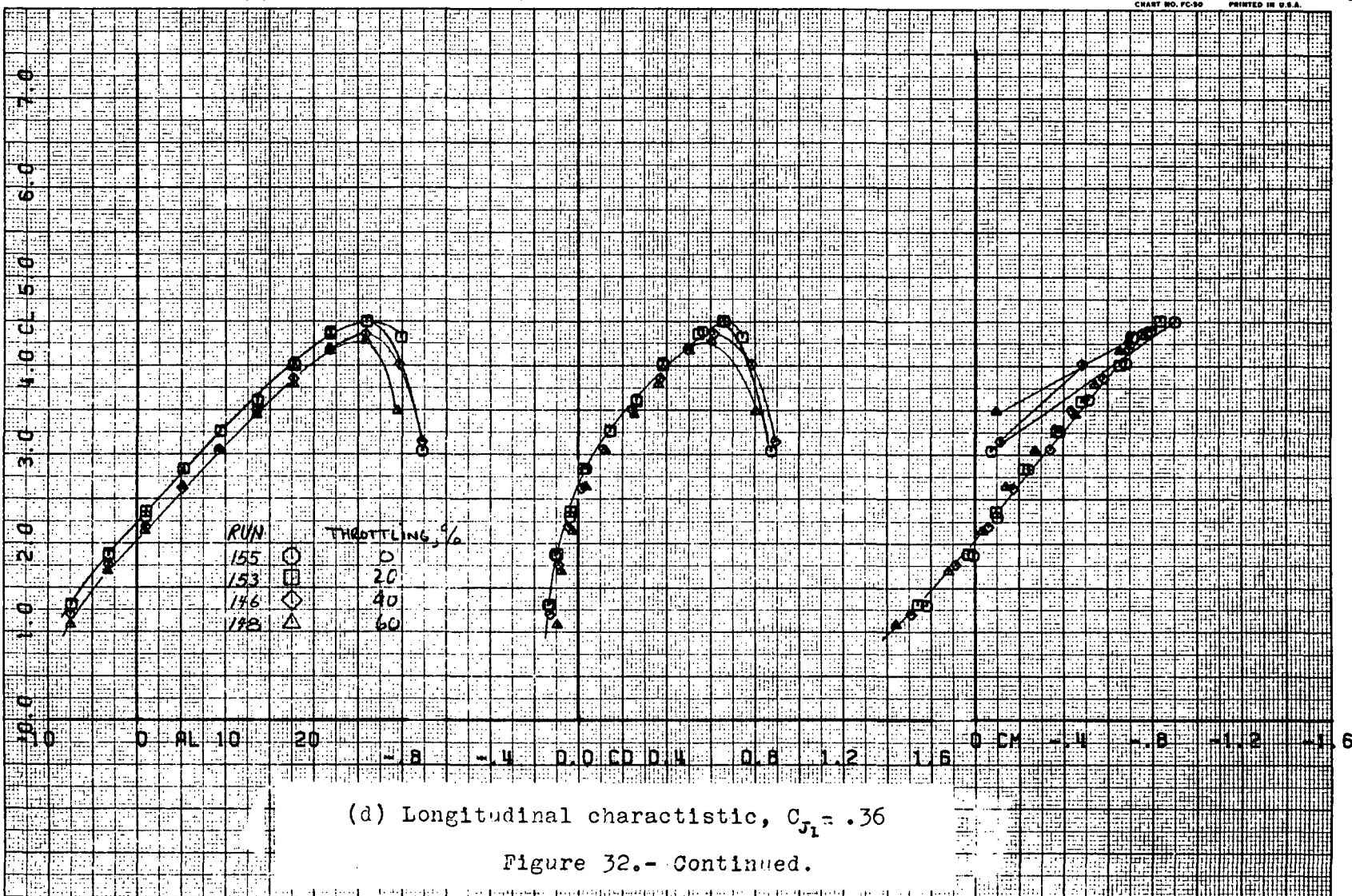
FAST RUN 15 155.

COMPLØT

OMNIGRAPHIC

HOUSTON INSTRUMENT  
DIVISION OF GENERAL ELECTRIC  
BELLAIRE, TEXAS  
CHART NO. PC-50 PRINTED IN U.S.A.

63



136

43

32d

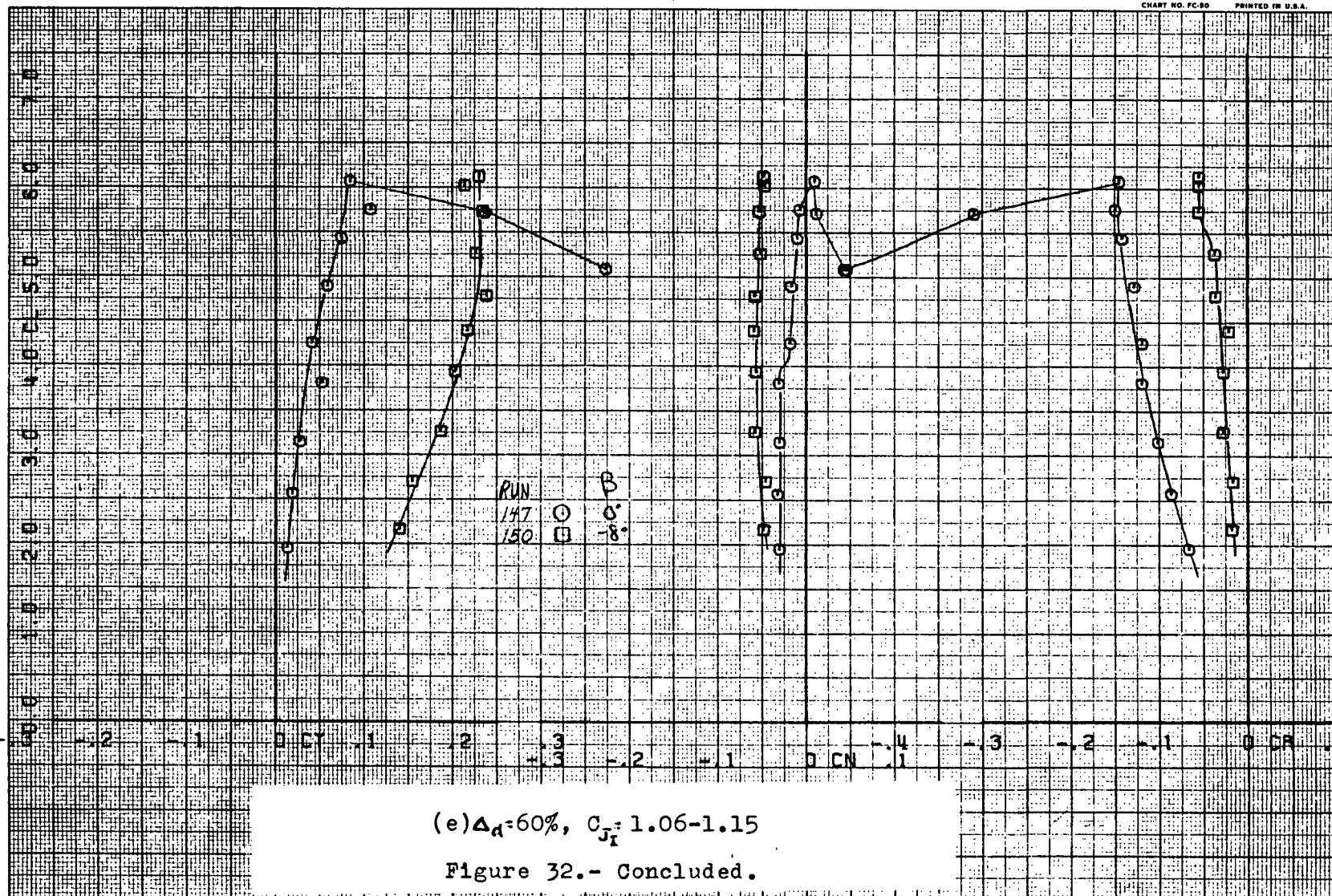
RUN 147.

COMPL0T®

OMNIGRAPHIC®

HOUSTON INSTRUMENT  
DIVISION OF BELL & HOWELL  
BELLAIRE, TEXAS  
CHART NO. FC-80 PRINTED IN U.S.A.

64



137

31

32e



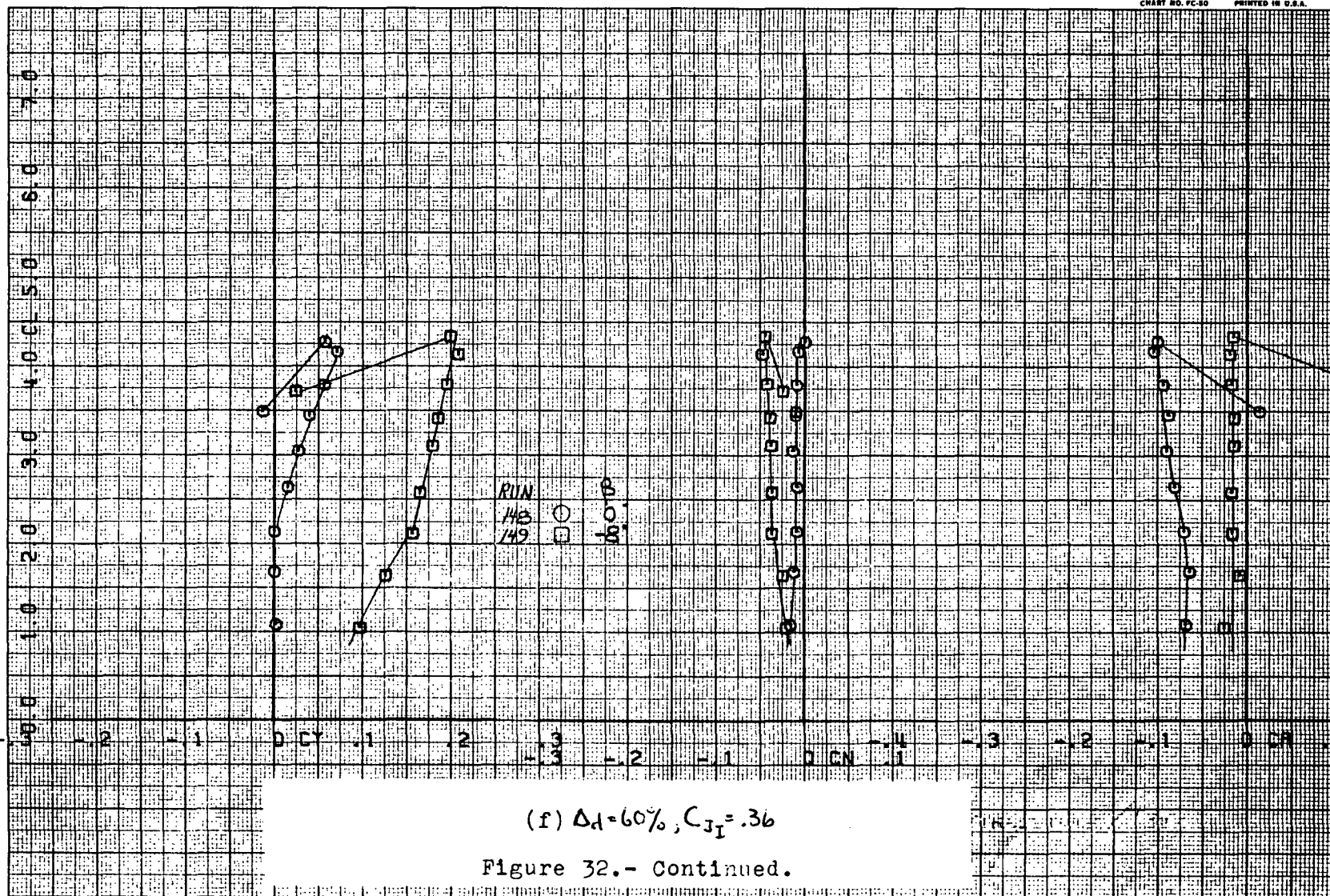
RUN 148.

COMPLØT®

OMNIGRAPHIC®

HOUSTON INSTRUMENT  
DIVISION OF ELECTRO-TECH  
BELLARE, TEXAS  
CHART NO. PC-50 PRINTED IN U.S.A.

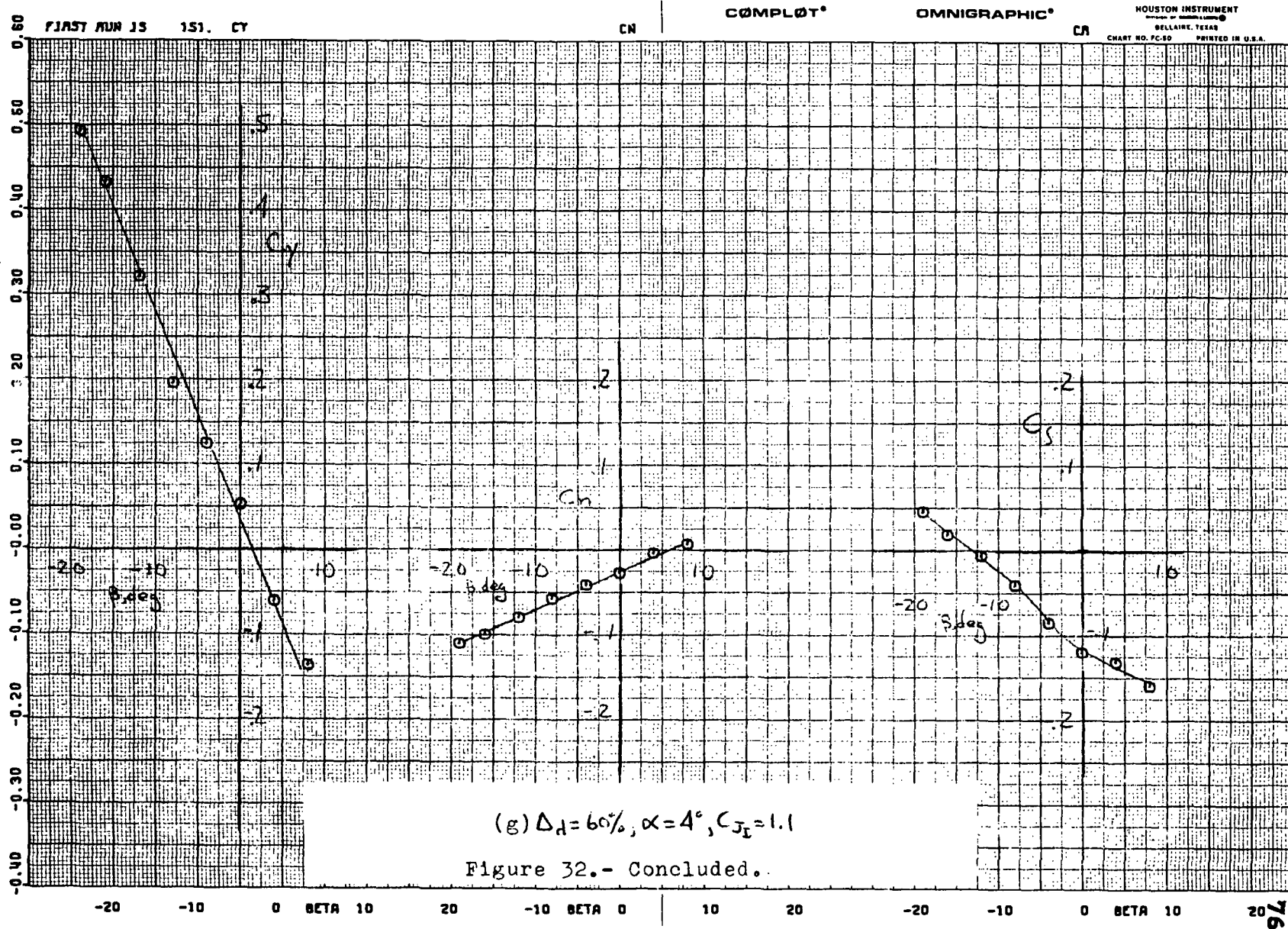
65

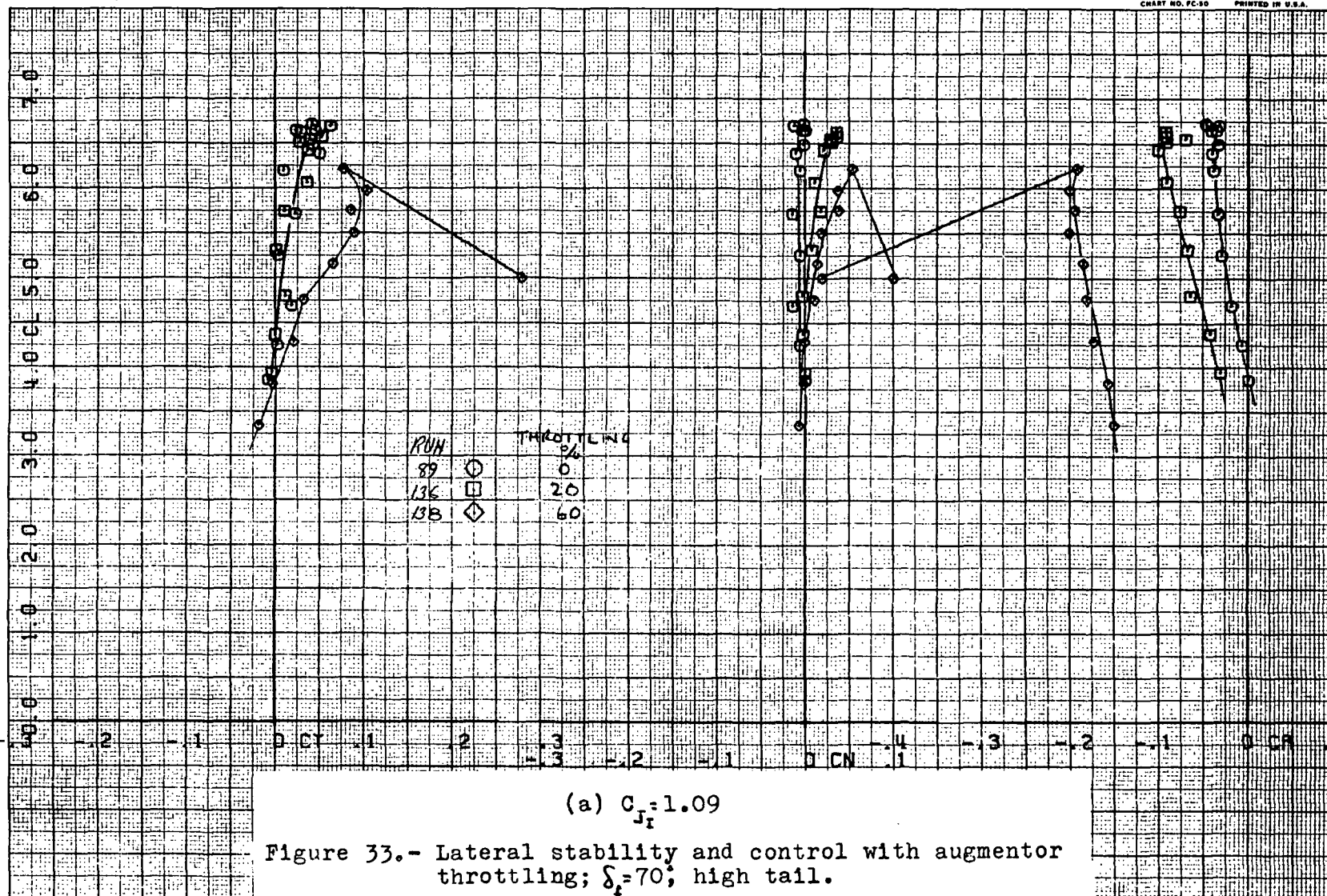


(f)  $\Delta d = 60\%$ ,  $C_{II} = .36$

138

32 32f



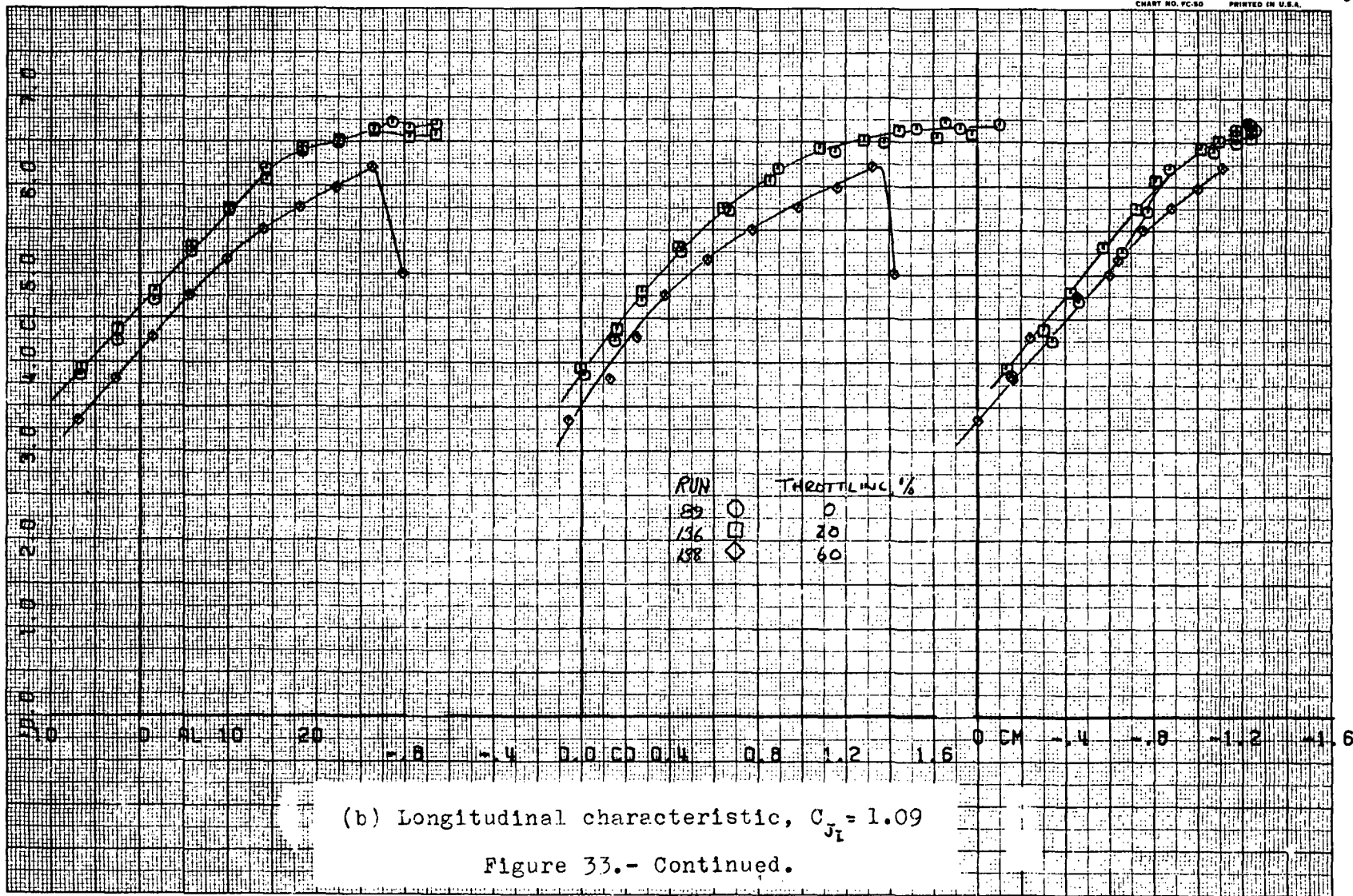


FIRST RUN 15 89.

COMPLØT®

OMNIGRAPHIC®

HOUSTON INSTRUMENT  
DIVISION OF HOUSTON LAMAR  
BELLAIRE, TEXAS  
CHART NO. PC-50 PRINTED IN U.S.A.



(b) Longitudinal characteristic,  $C_{J_1} = 1.09$

Figure 33.- Continued.

141

40

336

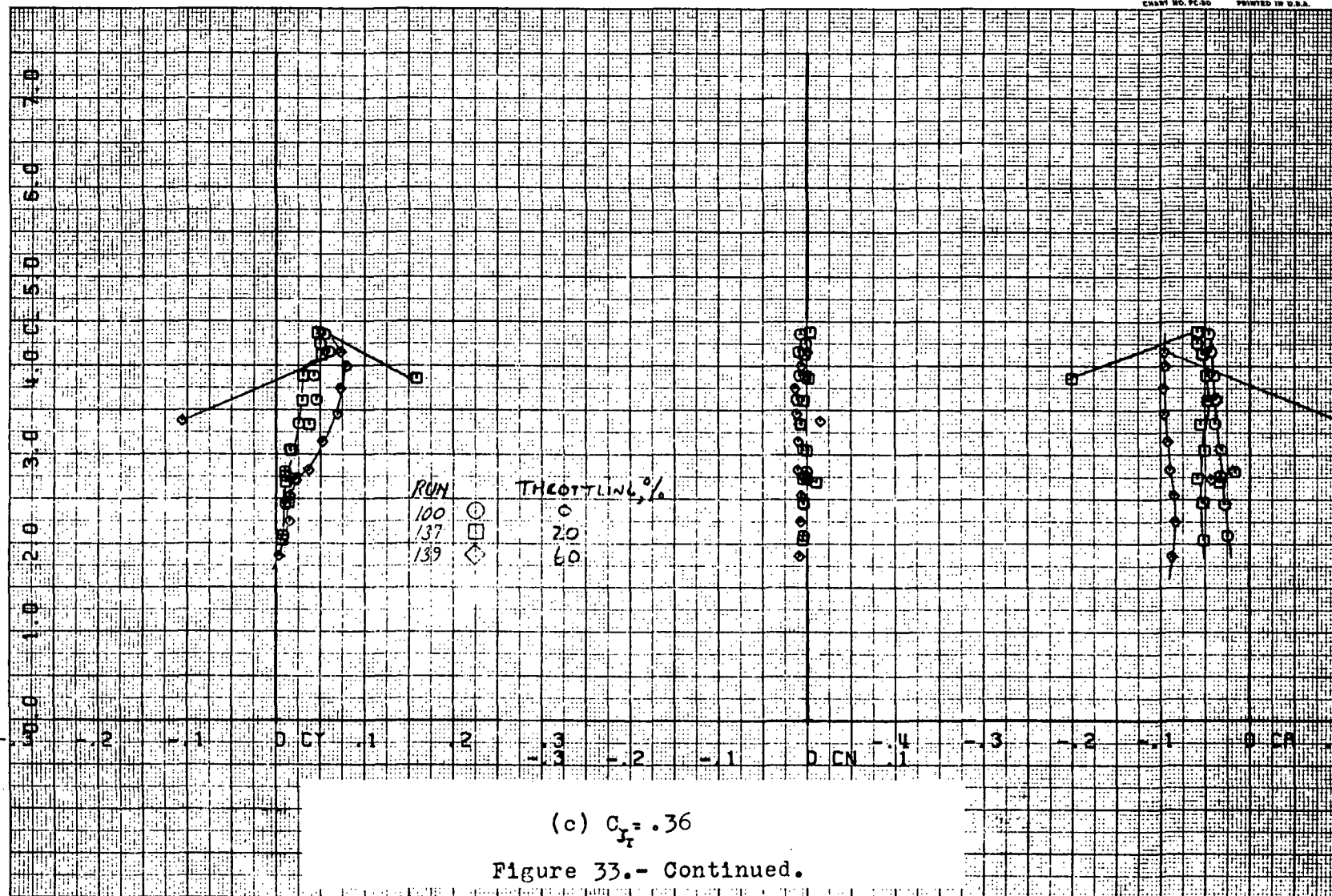
RUNS 100.

COMPLØT®

OMNIGRAPHIC®

HOUSTON INSTRUMENT  
DIVISION OF GENERAL ELECTRIC  
BELLAIRE, TEXAS  
CHART NO. PC-50 PRINTED IN U.S.A.

55



(c)  $C_T = .36$

Figure 33.- Continued.

142

26

33c



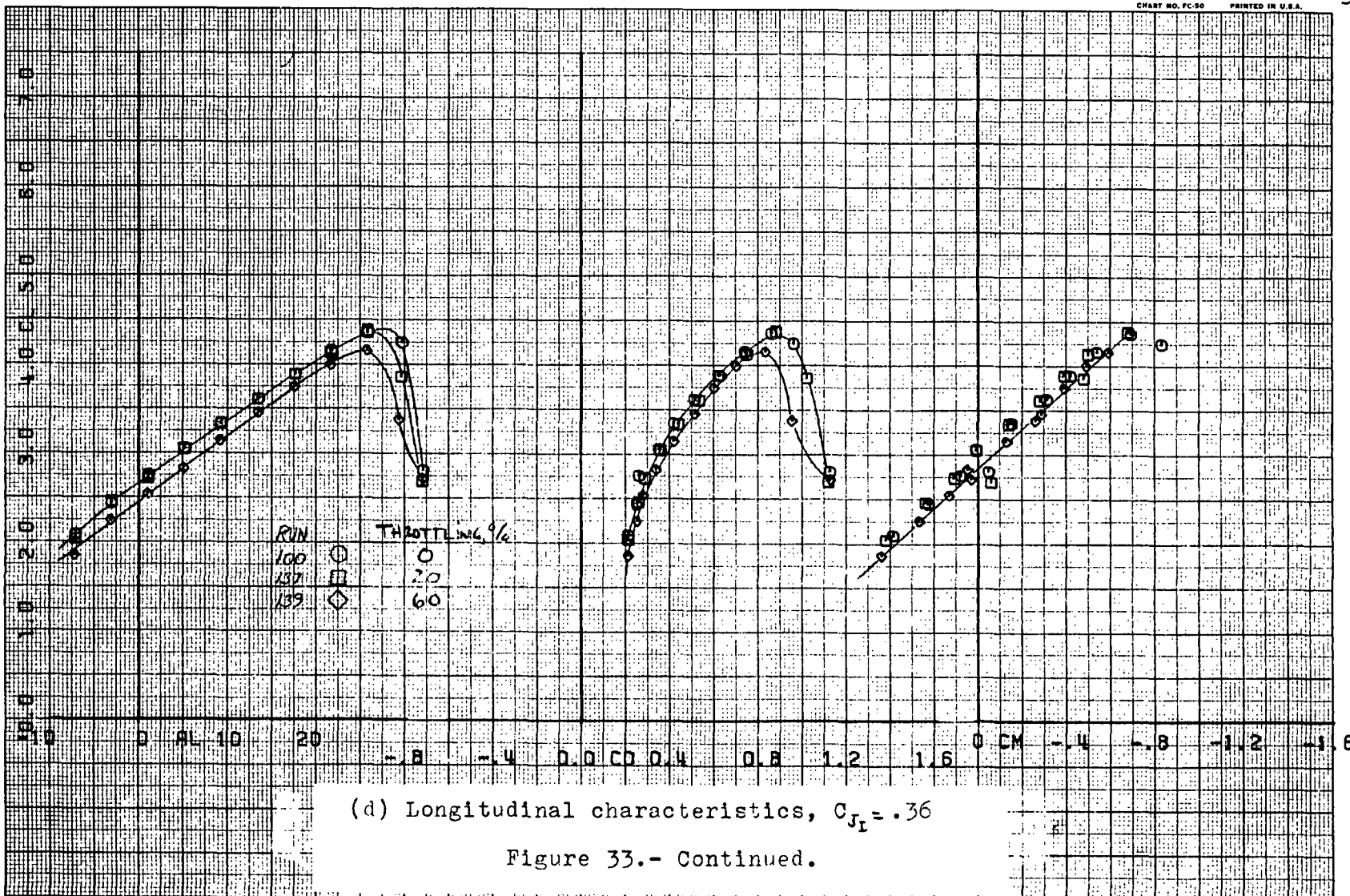
FAST RUN 15 100.

COMPL0T

OMNIGRAPHIC

HOUSTON INSTRUMENT  
DIVISION OF GENERAL ELECTRIC  
BELLAIRE, TEXAS  
CHART NO. FC-50 PRINTED IN U.S.A.

56



143

41

33d

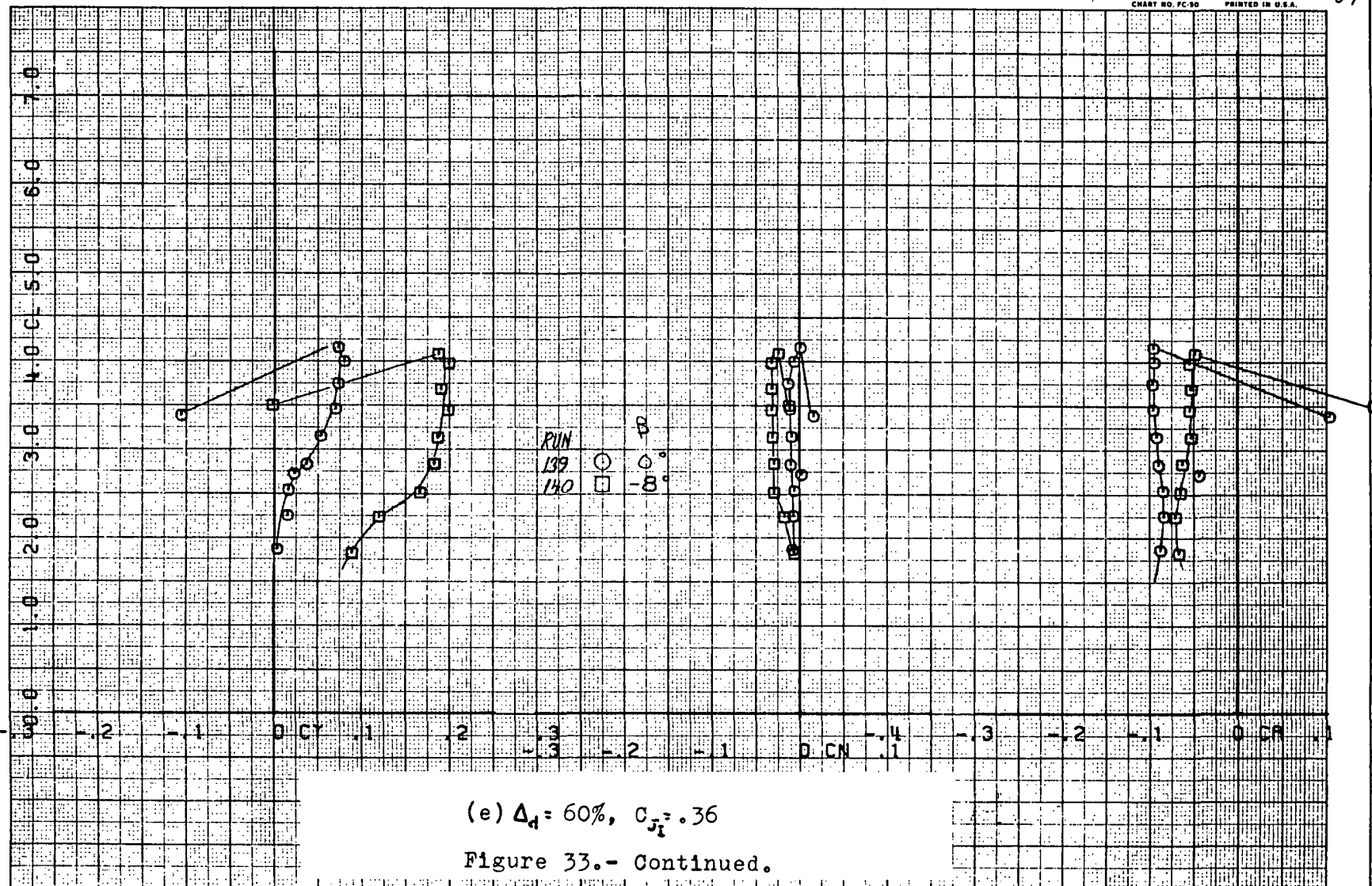
RUNS 139.

COMPLØT®

OMNIGRAPHIC®

HOUSTON INSTRUMENT  
DIV. OF HOUSTON LUMBER  
BELLAIRE, TEXAS  
CHART NO. FC-50 PRINTED IN U.S.A.

57



144

27 33e



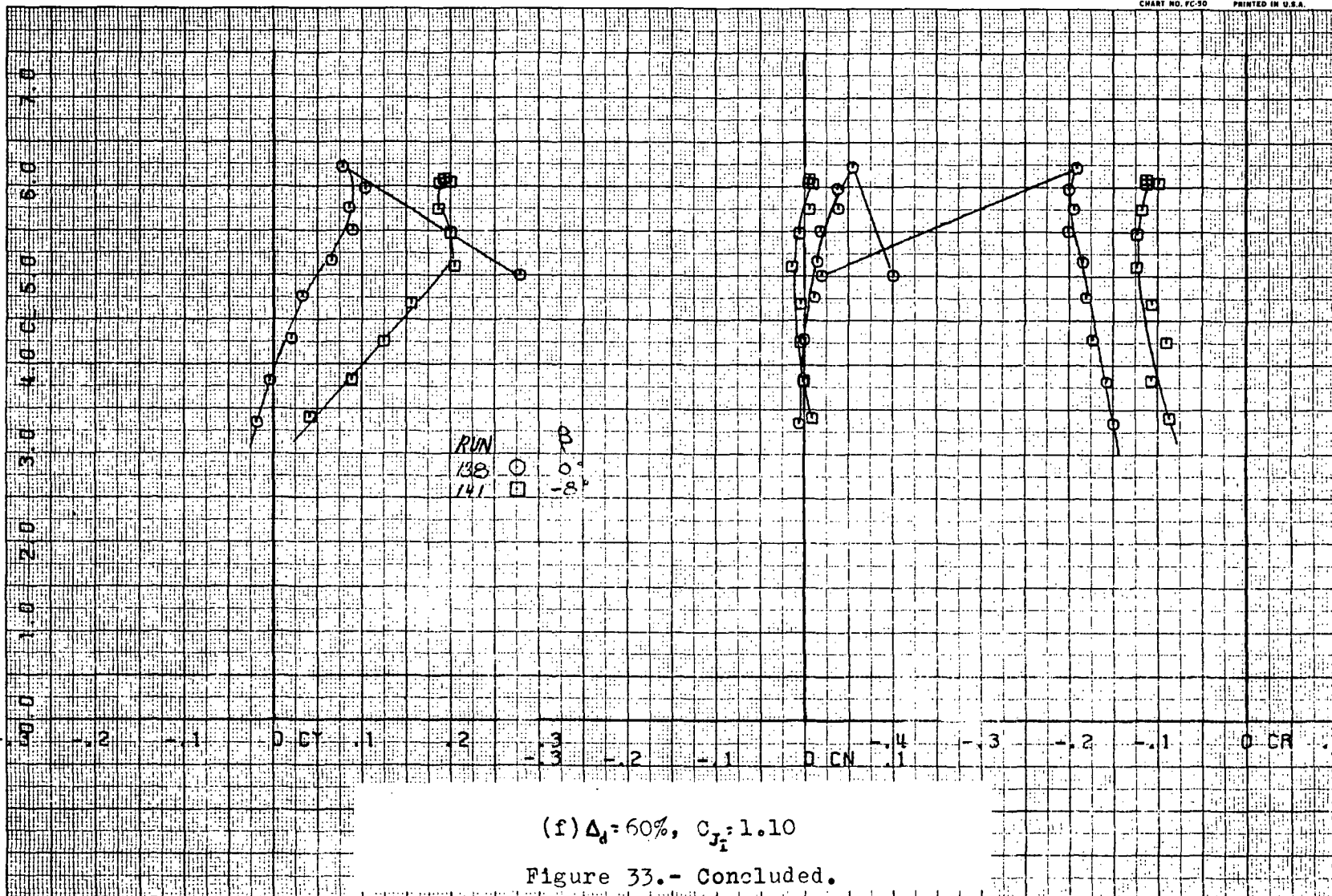
RUN 138.

COMPL0T®

OMNIGRAPHIC®

HOUSTON INSTRUMENT  
DIVISION OF HOUSTON ELECTRIC  
BELLAIRE, TEXAS  
CHART NO. FC-50 PRINTED IN U.S.A.

57



(f)  $\Delta_d = 60\%$ ,  $C_{j1} = 1.10$

Figure 33.- Concluded.

145

28

33f

RUN 156.

COMPLØT®

OMNIGRAPHIC®

HOUSTON INSTRUMENT  
BELL LAIRE, TEXAS  
CHART NO. PC-50 PRINTED IN U.S.A.

67

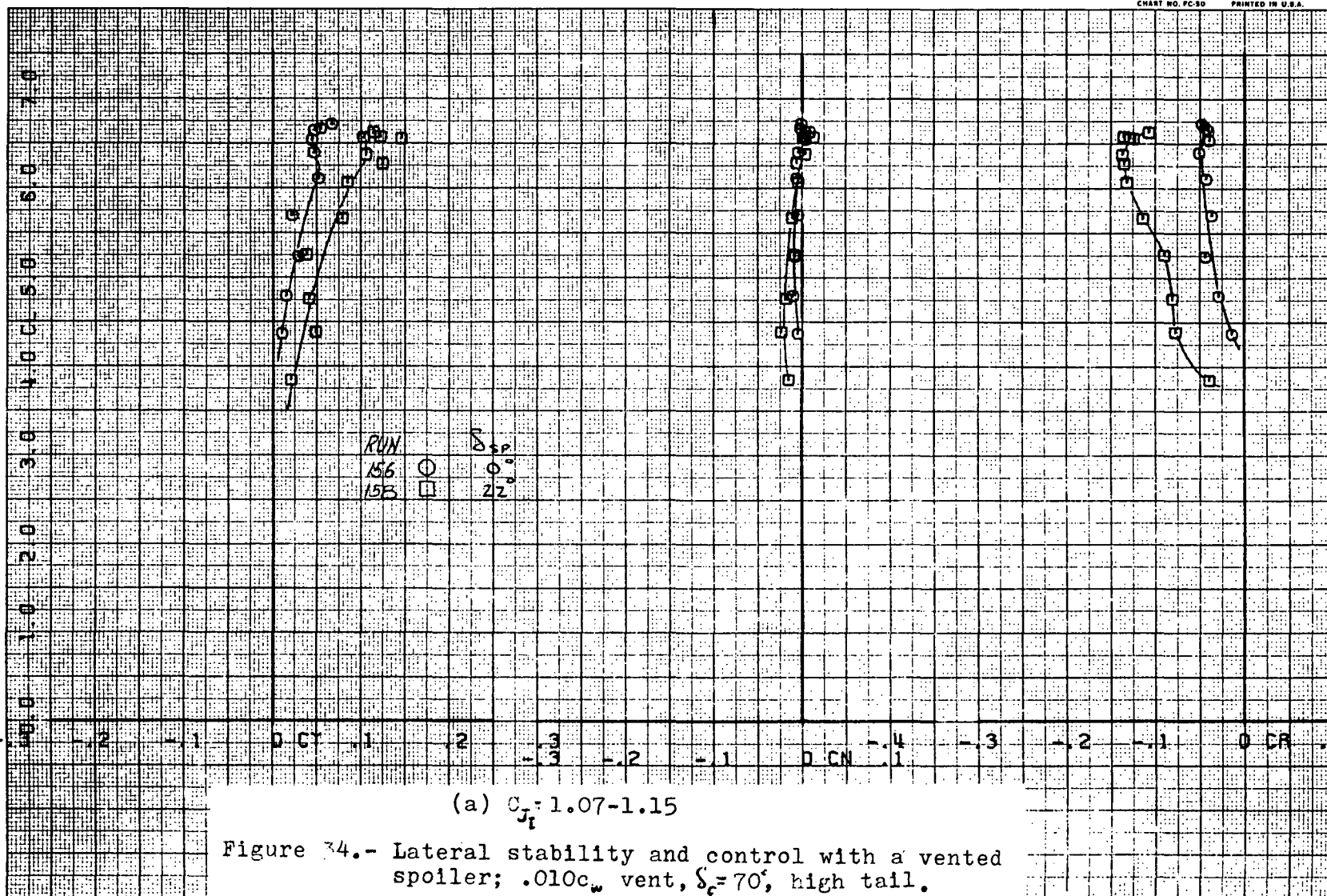


Figure 34.- Lateral stability and control with a vented spoiler; .010c<sub>w</sub> vent,  $\delta_c = 70^\circ$ , high tail.

146

33

34a

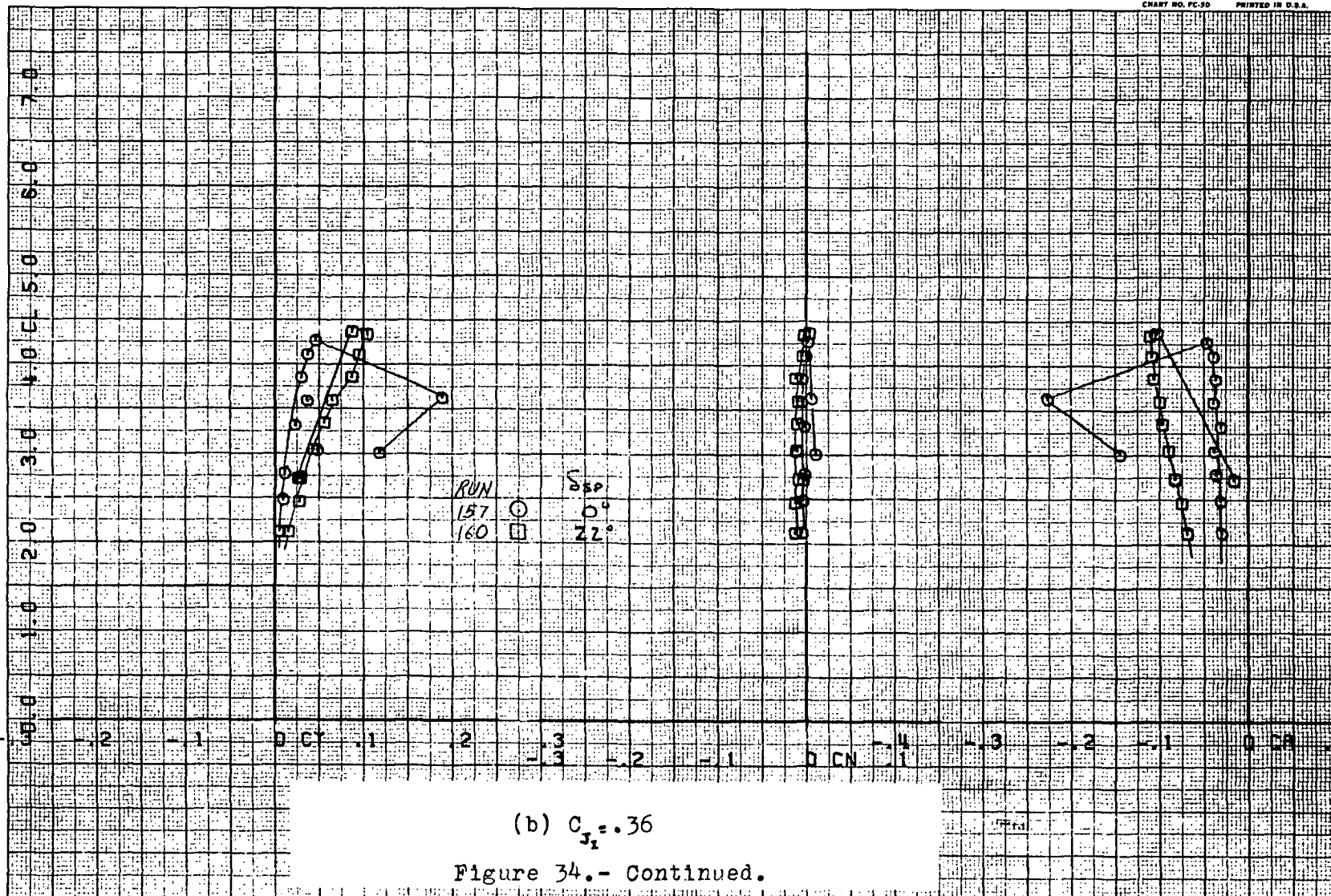
RUNS 157.

COMPL0T®

OMNIGRAPHIC®

HOUSTON INSTRUMENT  
CHART NO. FC-30 PRINTED IN U.S.A.

68

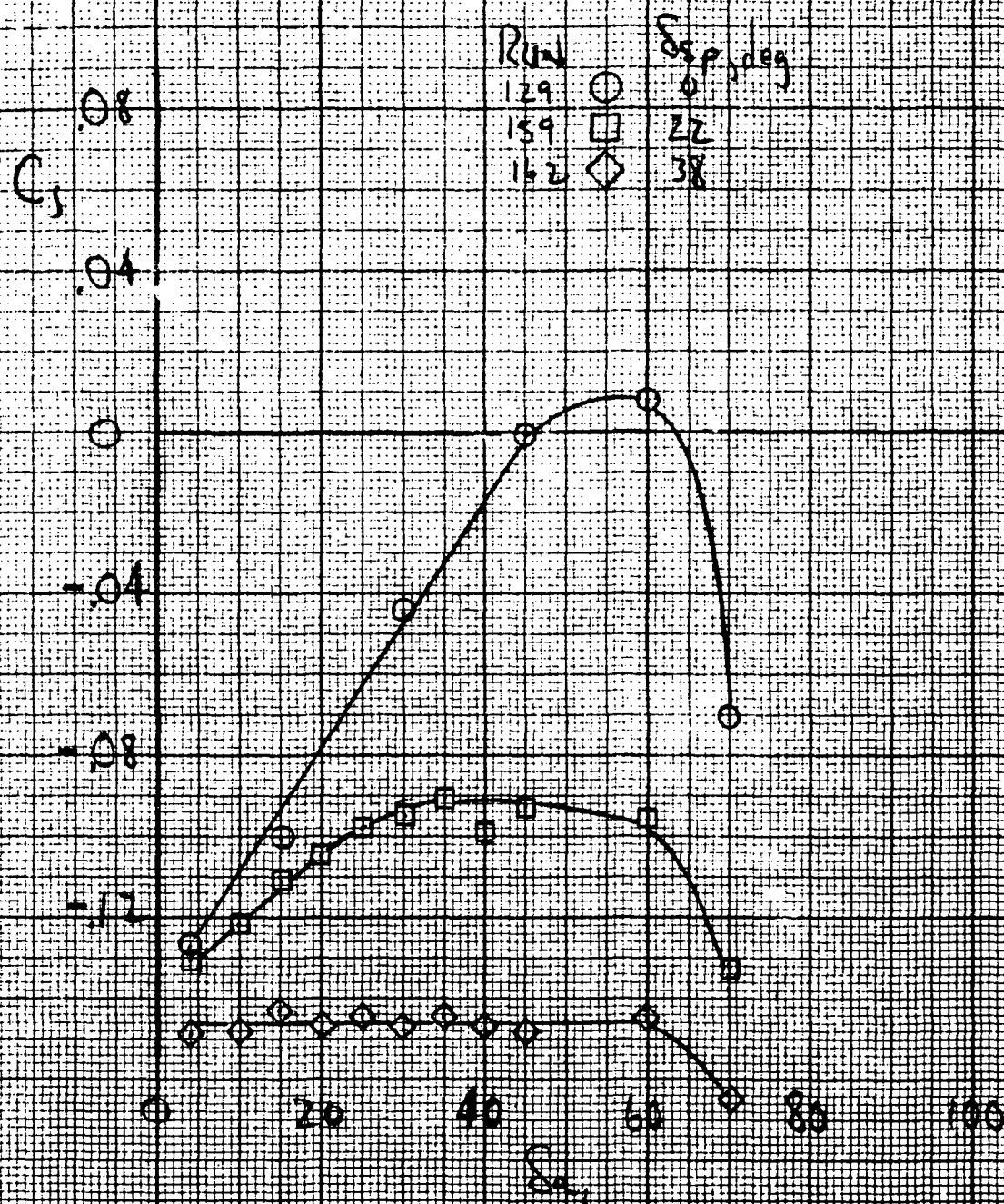


(b)  $C_{J1} = .36$   
Figure 34.- Continued.

147<

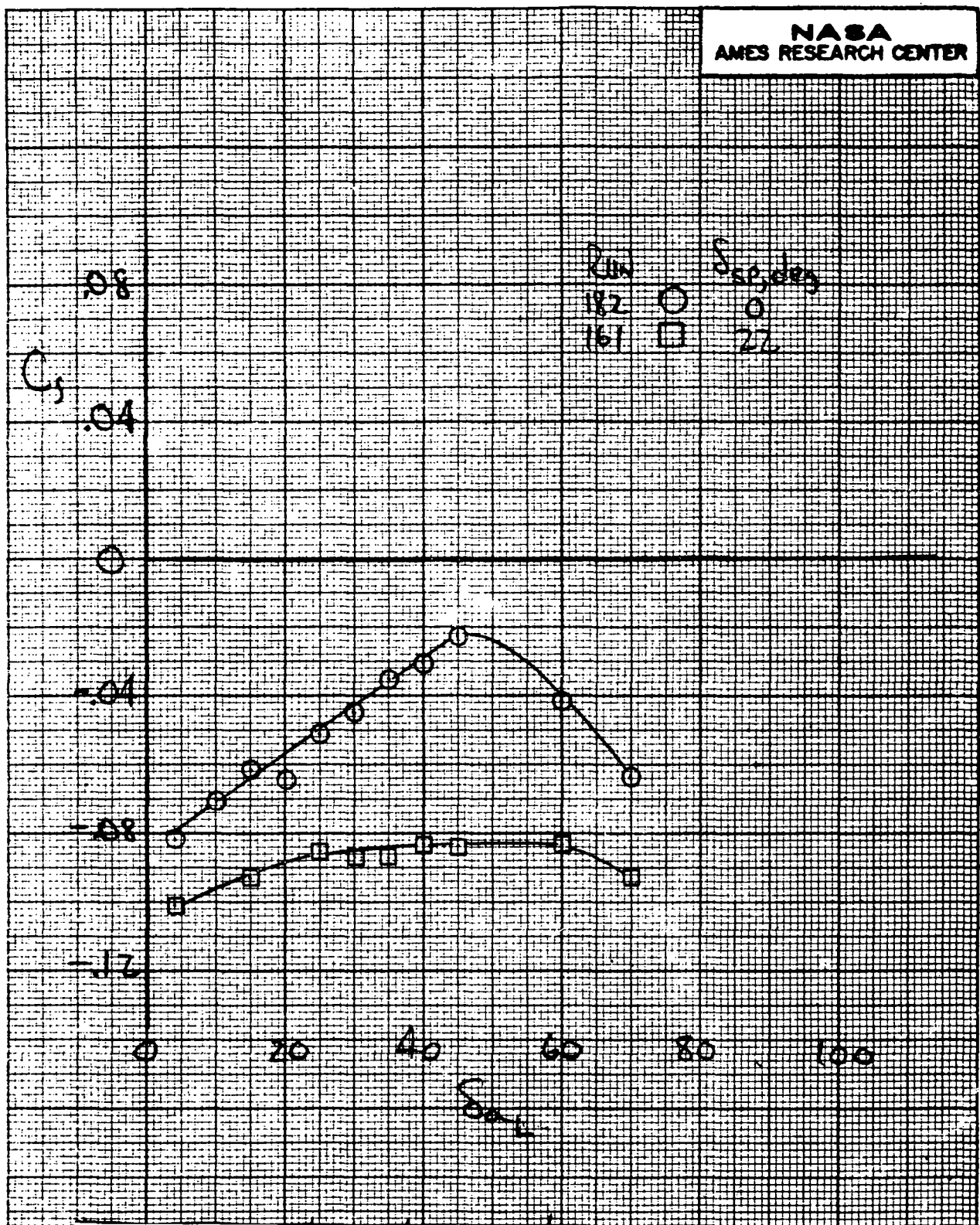
34

346



(c) Aileron control effectiveness;  $C_{x_1} = 1.1, \alpha = 4^\circ, S_{\alpha_2} = 30^\circ$

Figure 34.- Continued.



(d) Aileron control effectiveness;  $C_{x_1} = .4$ ,  $\alpha = 4^\circ$ ,  $S_{\alpha_2} = 30^\circ$

Figure 34.- Concluded.

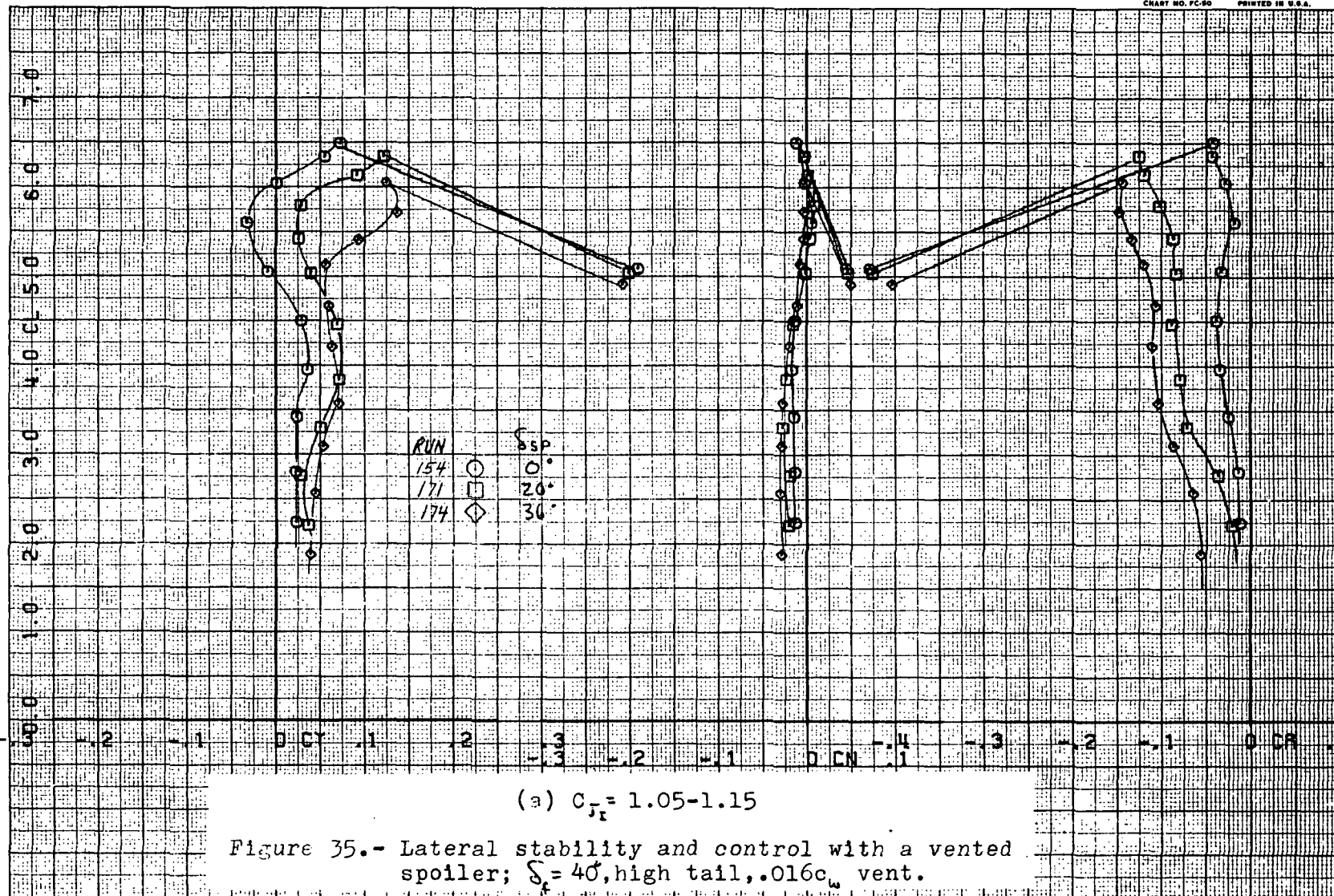


RUN 154.

COMPL0T°

OMNIGRAPHIC°

HOUSTON INSTRUMENT  
BELLARE, TEXAS  
CHART NO. FC-50 PRINTED IN U.S.A.



(a)  $C_{F_T} = 1.05-1.15$

Figure 35.- Lateral stability and control with a vented spoiler;  $S_f = 40^\circ$ , high tail, .016  $c_w$  vent.

150

37

35a

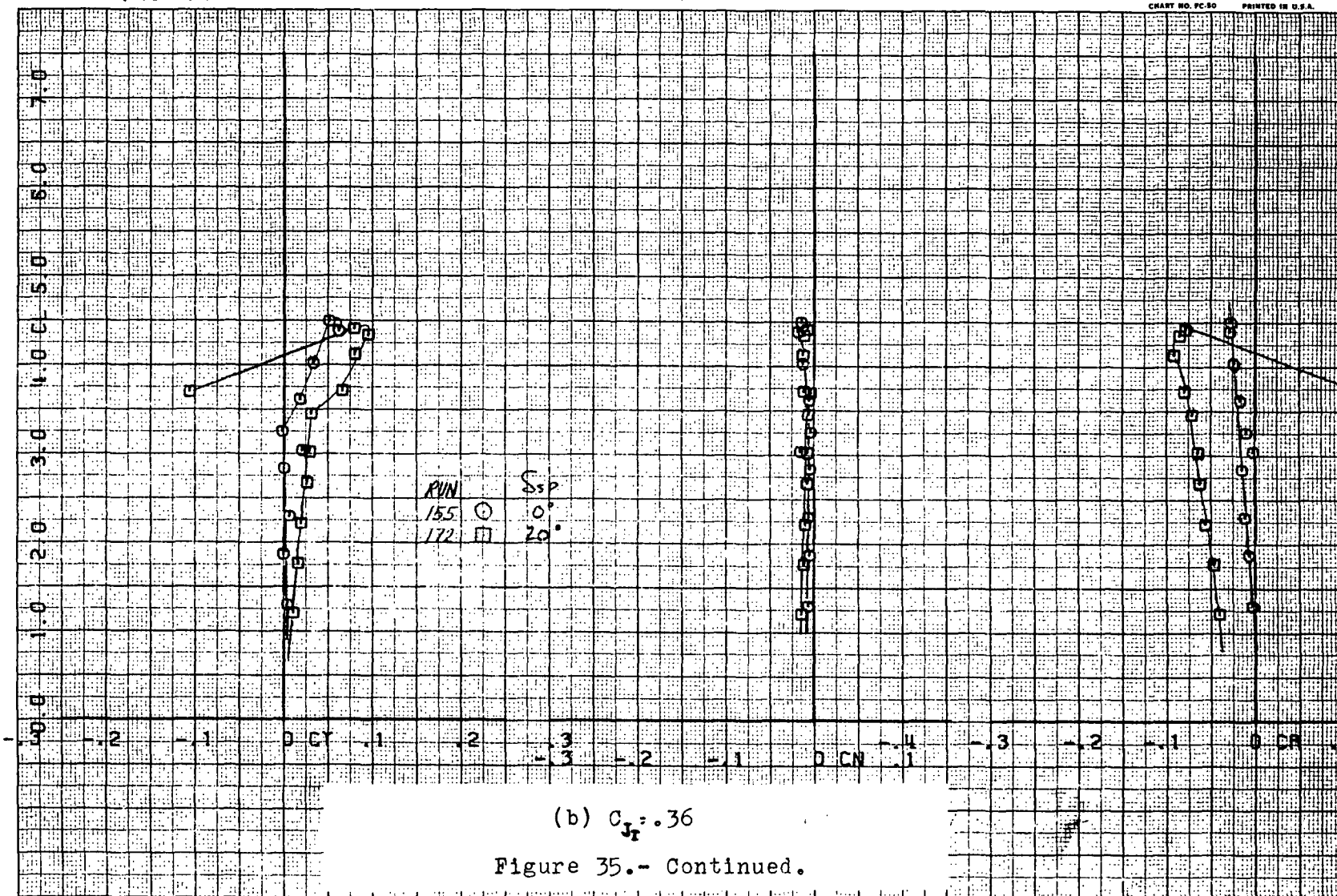
RUN 155.

COMPL0T°

OMNIGRAPHIC°

HOUSTON INSTRUMENT  
BELLARE, TEXAS  
CHART NO. PC-50 PRINTED IN U.S.A.

72



(b)  $C_{Jr} = .36$

Figure 35.- Continued.

151

38

356



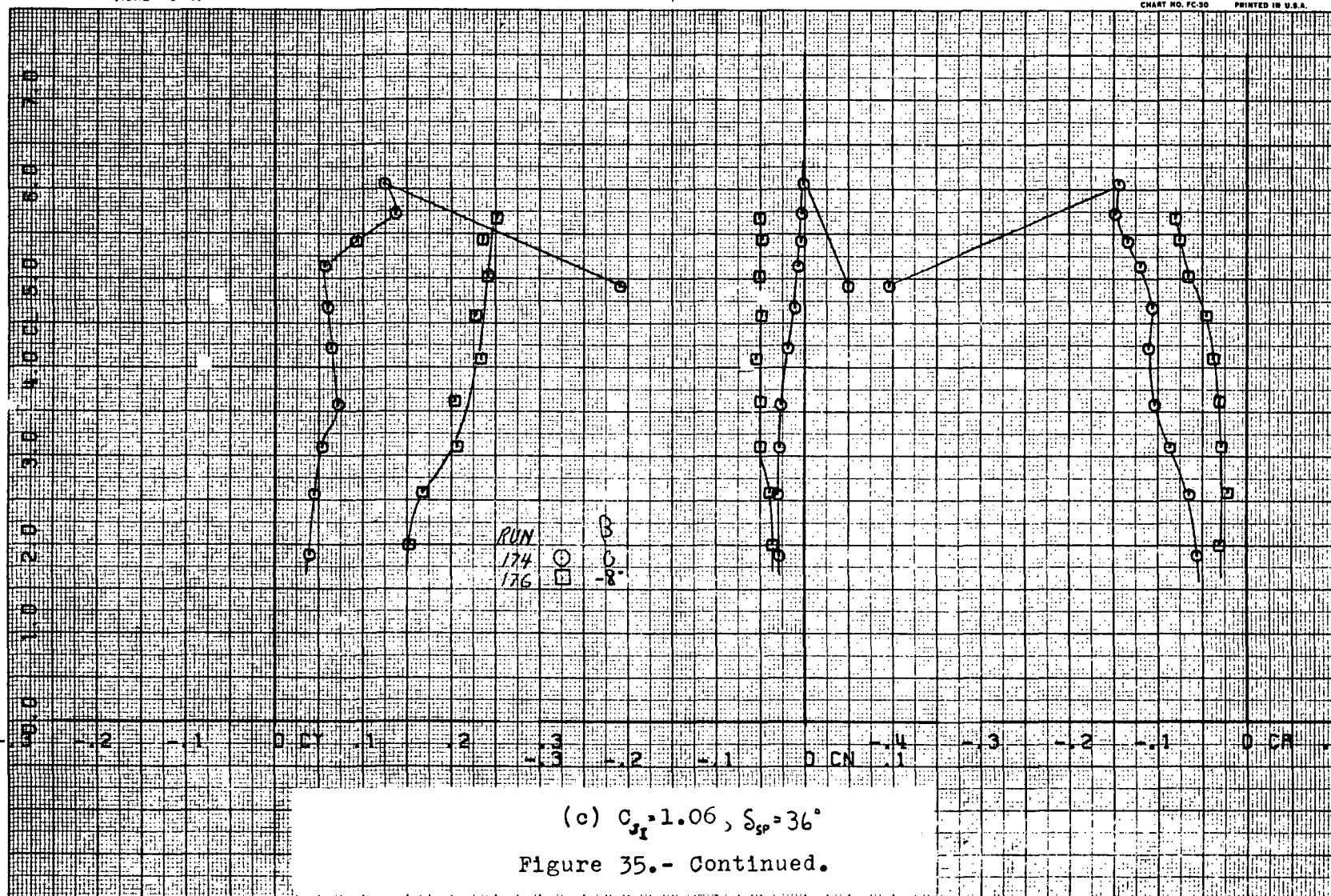
RUNS 174.

**CØMPLØT®**

**OMNIGRAPHIC®**

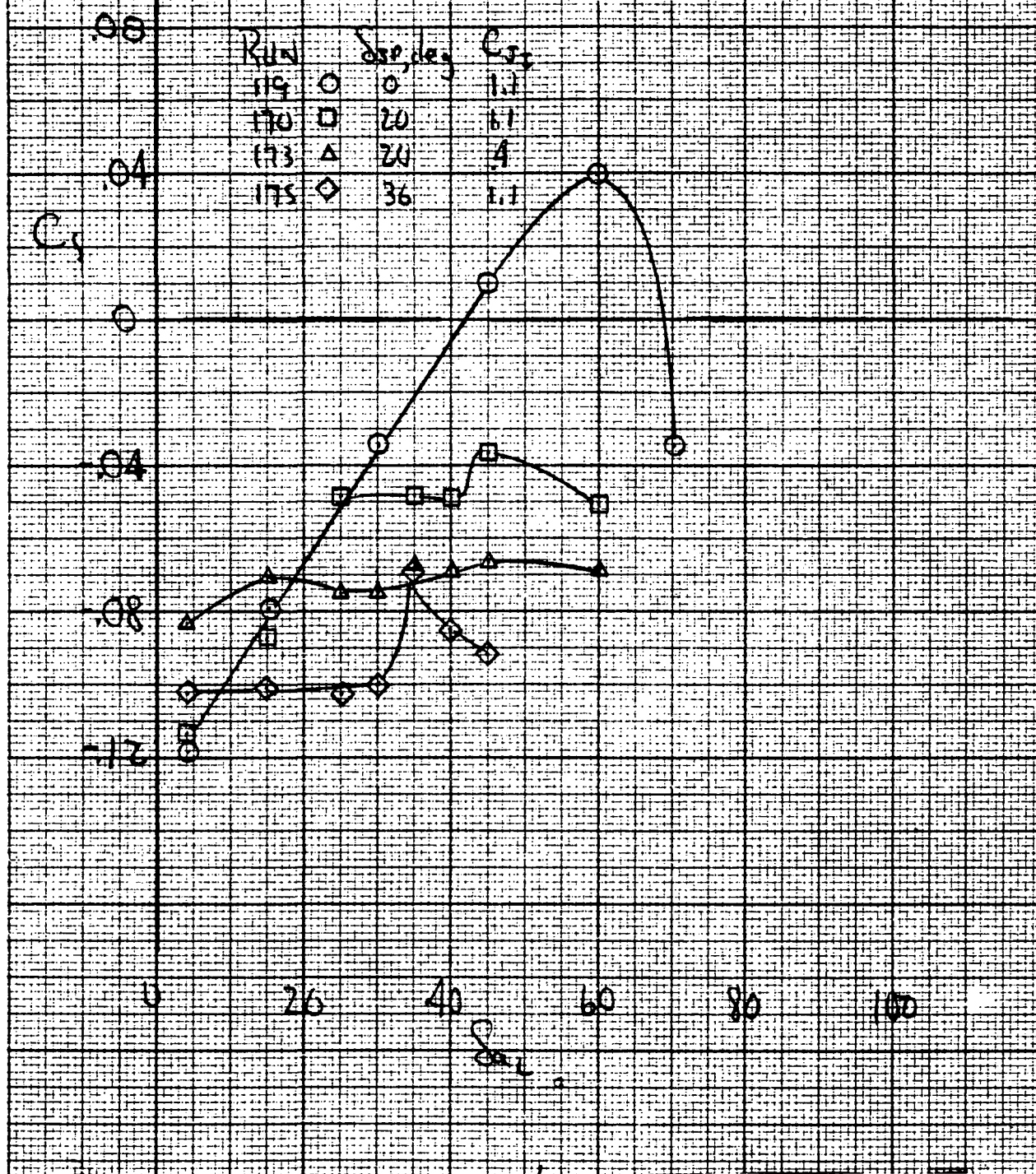
**HOUSTON INSTRUMENT**  
DIVISION OF CHRYSLER CREDIT CORPORATION  
BELLAIRE, TEXAS  
CHART NO. FC-30 PRINTED IN U.S.A.

73



35c

66



(d) Aileron control effectiveness;  $\alpha = 4^\circ$ ,  $S_w = 30^\circ$

Figure 35.- Concluded.

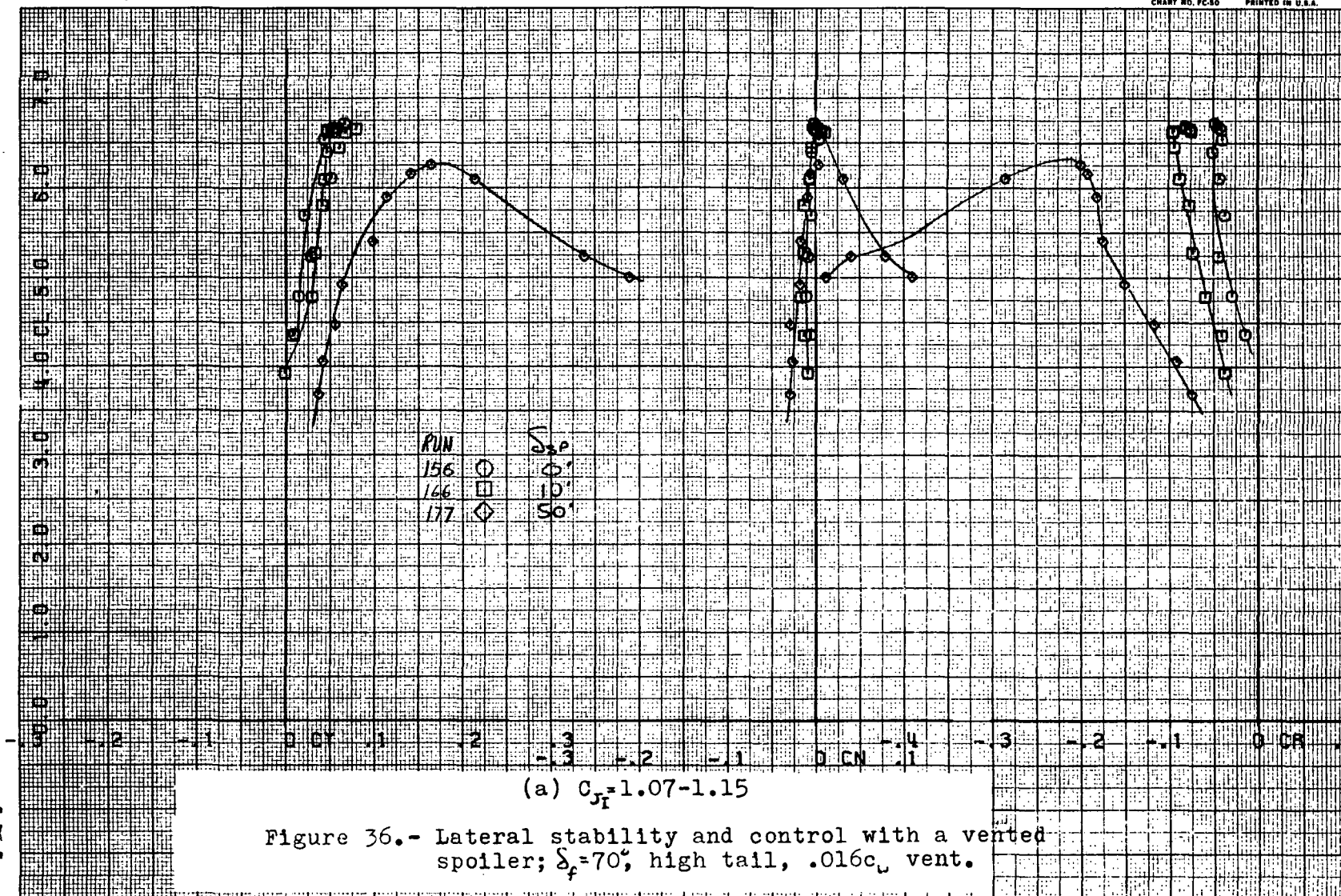
RUNS 156.

COMPLLOT®

OMNIGRAPHIC®

HOUSTON INSTRUMENT  
DIVISION OF GENERAL ELECTRIC  
BELL LAIR, TEXAS  
CHART NO. FC-50 PRINTED IN U.S.A.

69



154

35

36a

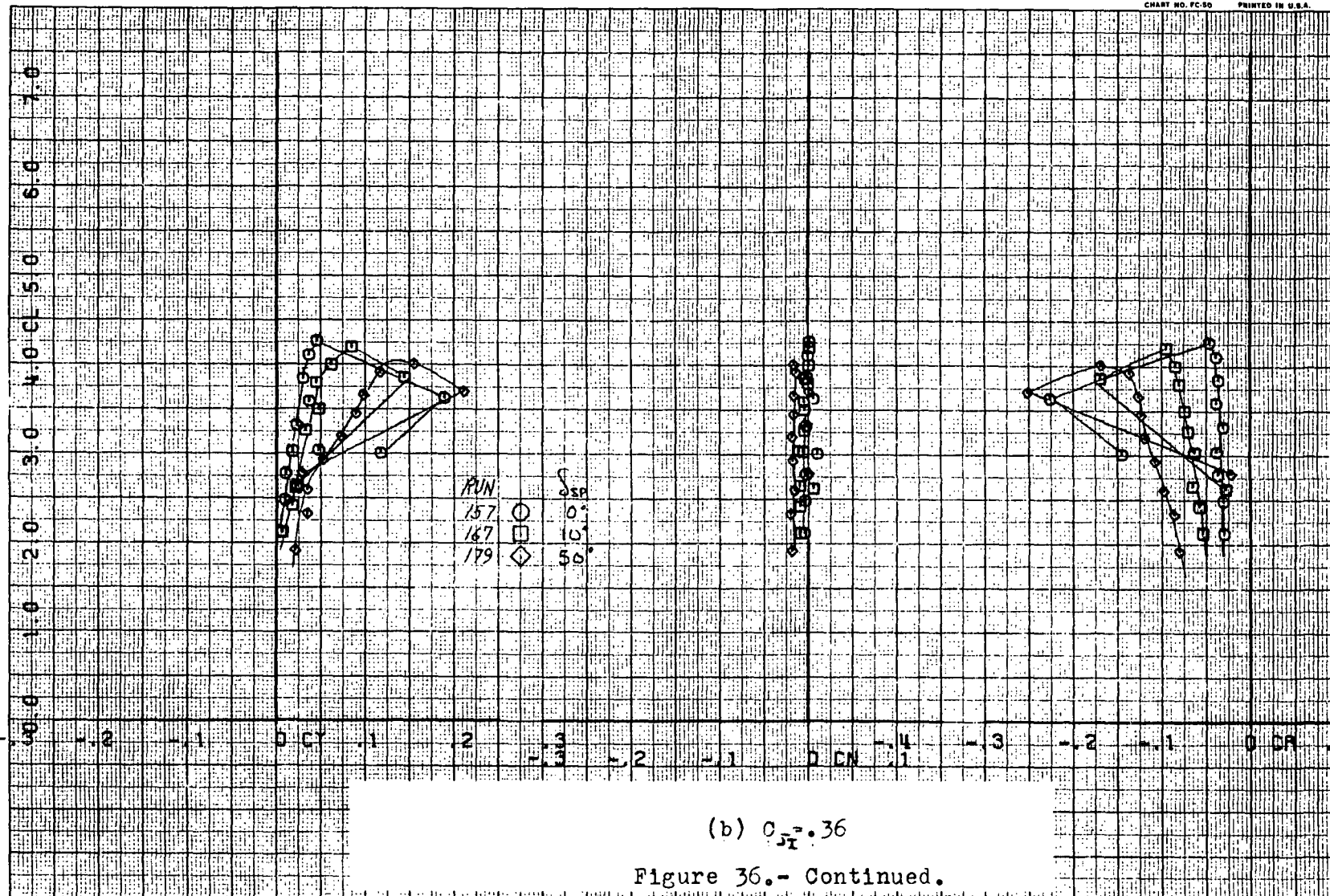
RUNS 157.

COMPLØT®

OMNIGRAPHIC®

HOUSTON INSTRUMENT  
DIVISION OF GENERAL ELECTRIC  
BELLAIRE, TEXAS  
CHART NO. FC-50 PRINTED IN U.S.A.

70



(b)  $C_{H1} = .36$

Figure 36.- Continued.

36 366

155

FJAST RUN 13 181. CT

CM

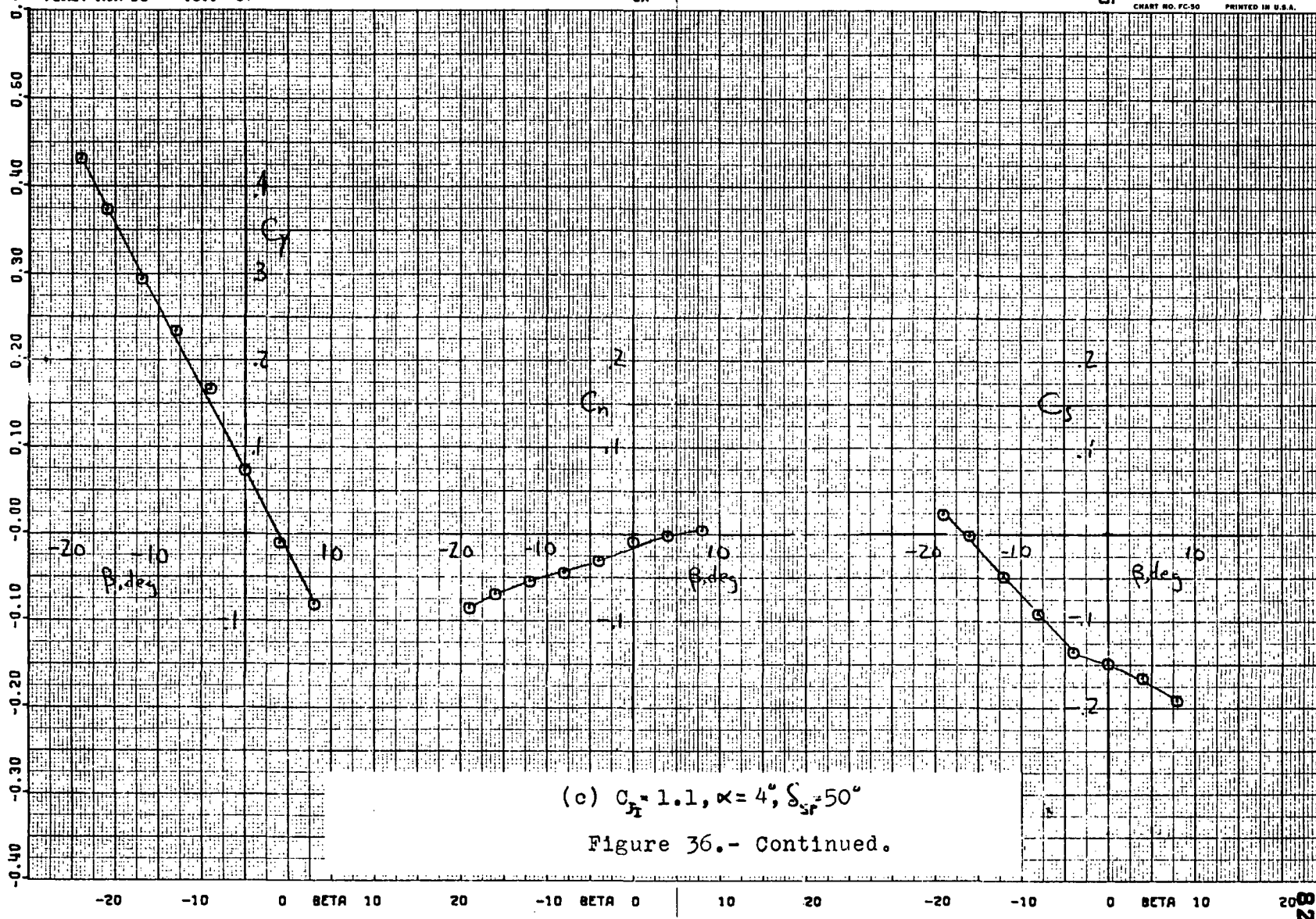
COMPLØT

OMNIGRAPHIC

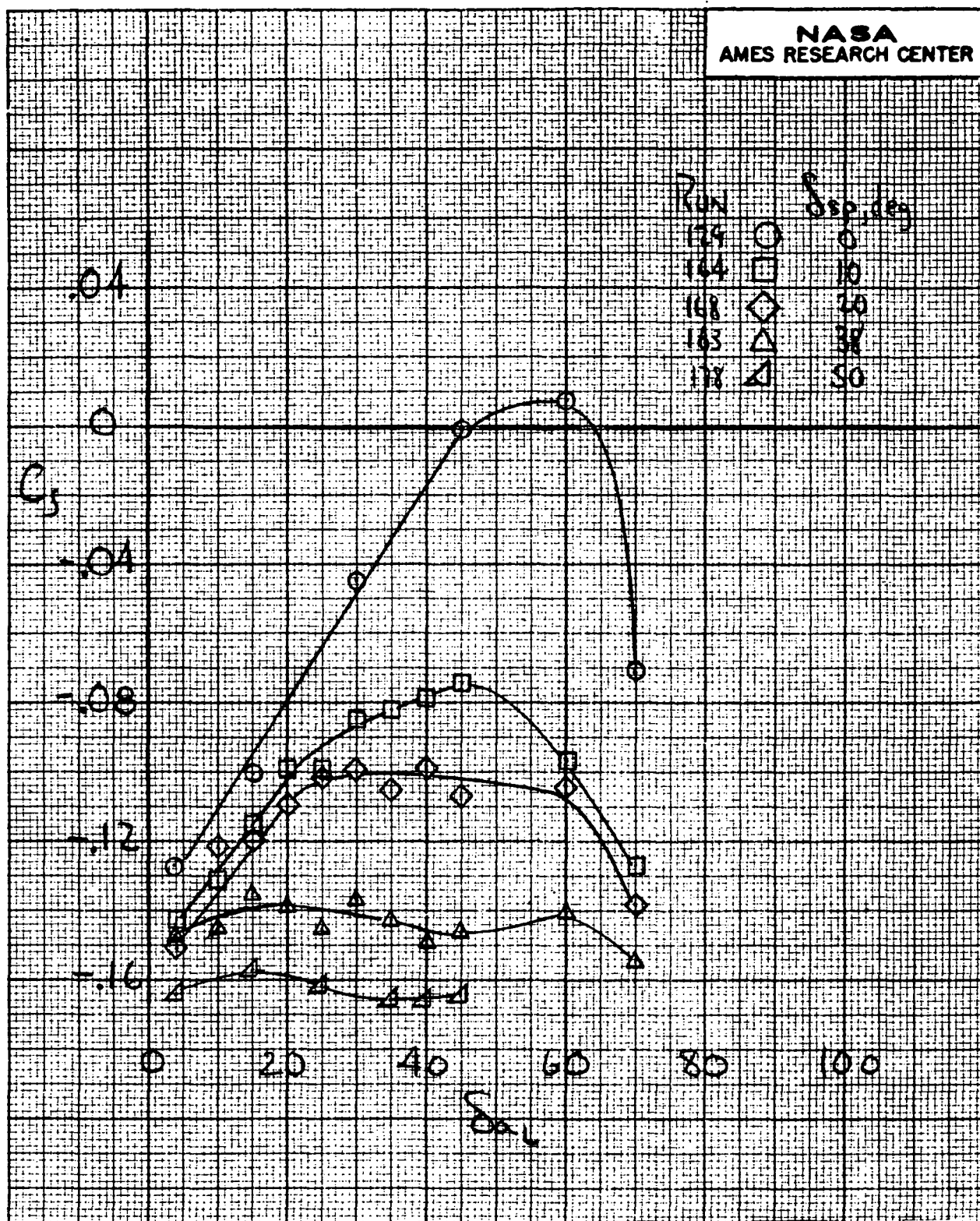
CM

HOUSTON INSTRUMENT  
DIVISION OF BELL & HOWELL  
BELL LAIR, TEXAS  
CHART NO. FC-50 PRINTED IN U.S.A.

74

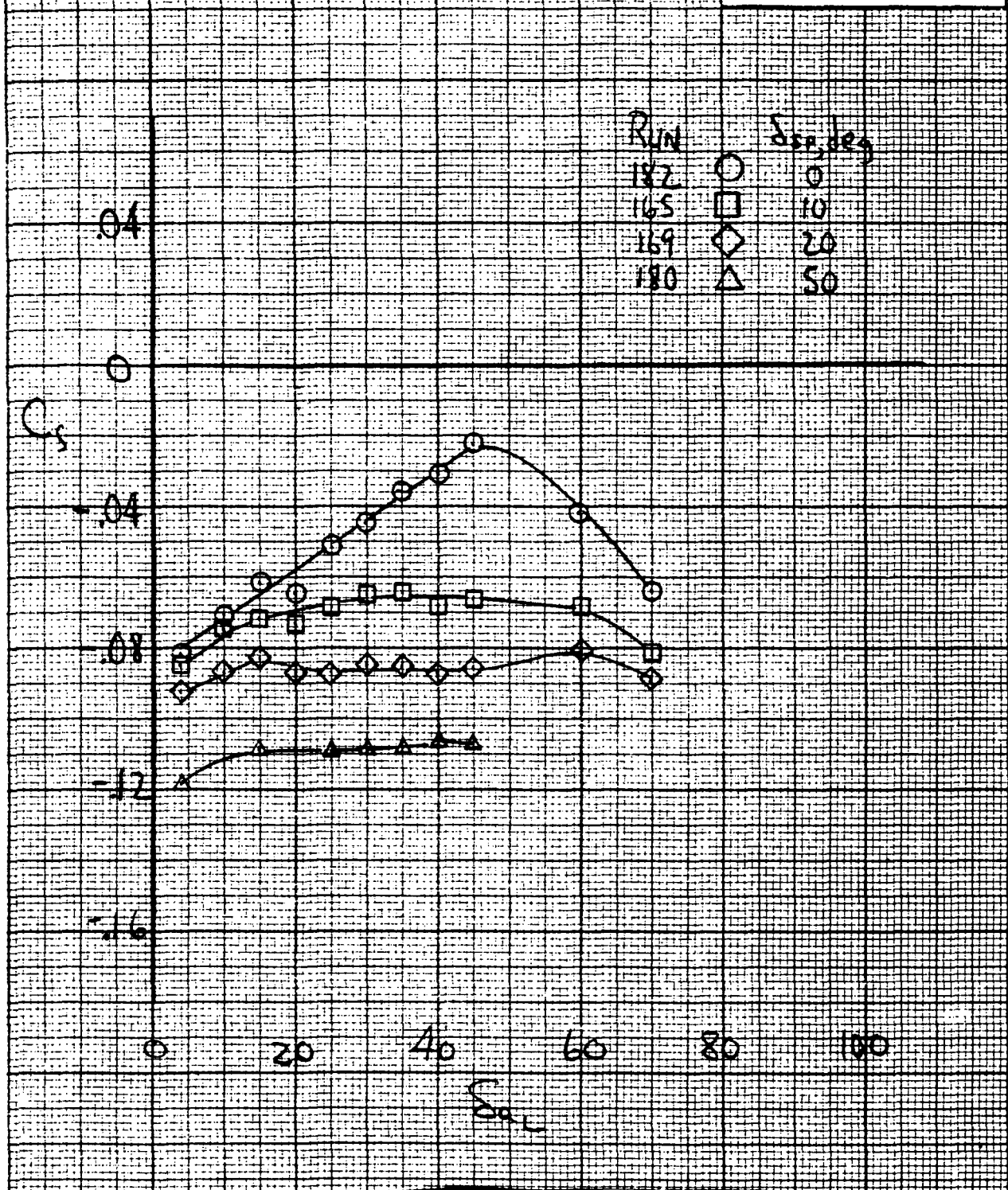






(d) Aileron control effectiveness;  $C_z=1.1, \alpha=4^\circ, \delta_{a_r}=30^\circ$

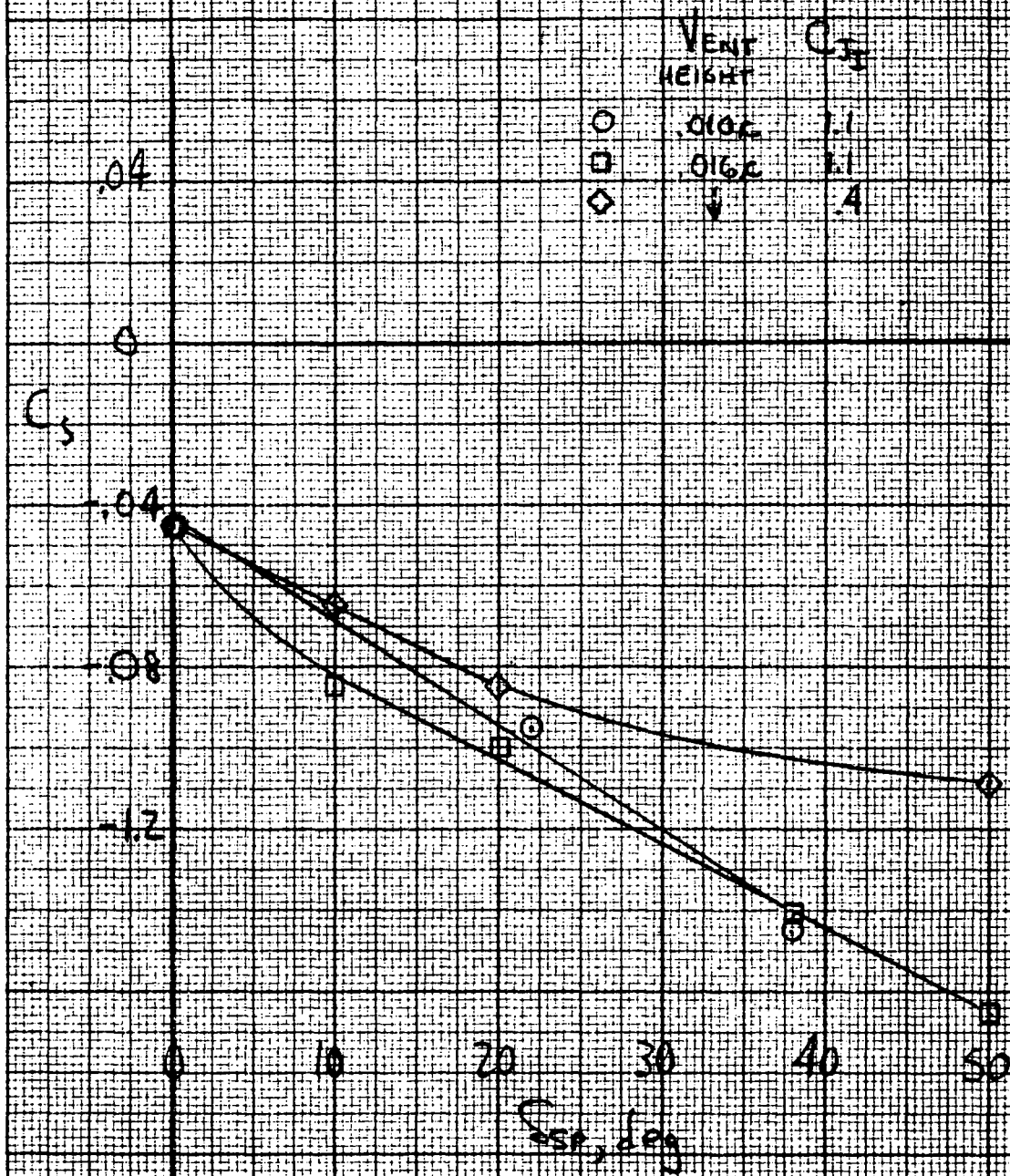
Figure 36.- Continued.



(e) Aileron control effectiveness;  $C_{x_T} = .4$ ,  $\alpha = 4^\circ$ ,  $S_{a_r} = 30^\circ$

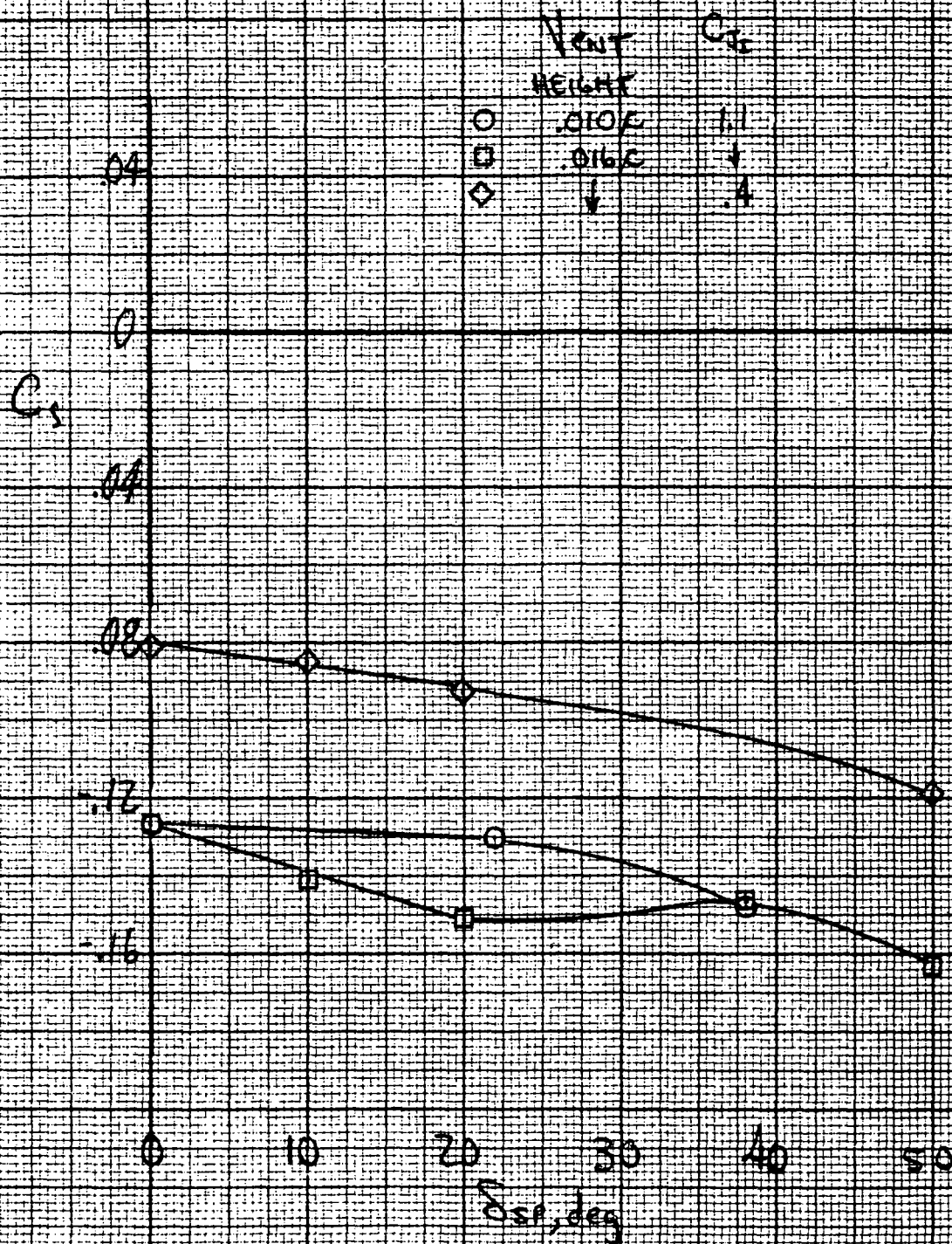
Figure 36.- Concluded.





(a)  $S_{\alpha} = 30^\circ$

Figure 37.- Spoiler control effectiveness;  $S_{\alpha} = 70^\circ$ ;  $\alpha = 4^\circ$ .



(b)  $\delta_a = 4/30^\circ$   
Figure 37.- Concluded.